Coastal Habitat Mapping and Monitoring Utilising Remote Sensing

Gwawr Angharad Jones

A thesis submitted in fulfilment of the requirements for the degree of Doctor of Philosophy

July 12, 2017

Aberystwyth University

Supervisors: Dr Peter Bunting, Clive Hurford and Professor Henry Lamb

Acknowledgements

This thesis would not have been possible without the constant guidance, support and enthusiasm of so many people it is hard to know where to start, but I will of course give it a go! First of all I would like to thank my supervisors, Pete Bunting, Clive Hurford and Henry Lamb for all their time and patience. Pete especially has been a rock and I wouldn't be at this point without the knowledge and skills he's passed on to me. Clive too has been instrumental in this project and I would like to thank him for taking the time to teach me and for always showing an interest with valued support. A special mention here to Richard Lucas who supported the work and helped establish the connection between NRW, making this research possible. Perhaps the greatest lesson they've all taught me is that there are opportunities in every obstacle no matter what life throws at you.

None of this work would have been possible without the continued guidance from many of the specialists at NRW who I accompanied on many a field trip. A massive thank you to Karen Wilkinson, Dan Guest, Julie Greer, Huw Green, Heather Lewis and Rhodri Dafydd who not only took the time to collect field data in all weathers (memories of one lightning storm in particular still terrifies me), but took an interest and guided me through the complex ecology of my study sites. A special mention to Dave Carrington from Bridgend County Borough Council for always welcoming me to Kenfig, for sharing his incredible knowledge of the site and for driving us around in the Landy of course! I value the knowledge they passed on to me but I also thank them for their friendliness.

I cannot forget my PhD colleagues and friends for making the whole experience a lot of fun. To Becky, Alisdair, Heather, Sarah, Nathan, Josh, Sizwe; we had great times and laughed a lot but we were always there for each other too. Thank you all for your support and I really do value your friendship. Thanks also to all the other students who helped me along the way, particularly with fieldwork. A special mention to Georgina for accompanying me on several trips to Kenfig, Alex for helping with the transition to QGIS, and Marie for always listening and giving excellent advice.

A huge thanks to my family and friends who have always been there and supported my life decisions no matter what. A special thank you to my youngest brother Meirion for coming along on a field trip, I laughed a lot that day! Nia, Iona, Einir, Bet, Dyl, Lleucu, Louise

and Llinos, I apologise for all the complaining and moaning over the last 4 years. Your continued support and friendship is extremely important to me. Diolch am bopeth!

Last, but not least, a huge thanks to my new colleagues at the Joint Nature Conservation Committee. Paul and Lawrence, or the EO Monitoring Applications Team as we are now known as, your understanding, guidance and constant support over the last year has really helped me through this writing stage. Many thanks for allowing me to focus on the PhD when I needed to the most.

Of great importance to the whole project are my co-funders Natural Resources Wales. Thank you for allowing this research to happen.

Abstract

Coastal habitats are highly sensitive to change and highly diverse. Degrading environmental conditions have led to a global decline in biodiversity through loss, modification and fragmentation of habitats, triggering an increased effort to conserve these ecosystems. Remote sensing is important tool for filling in critical information gaps for monitoring habitats, yet significant barriers exist for operational use within the ecological and conservation communities. Reporting on both extent and condition of habitats are critical to fulfil policy requirements, specifically the ECs Habitat's Directive. This study focuses on the use of Very High Resolution (VHR) optical imagery for retrieving parameters to identify associations that can separate habitat boundaries for extent mapping down to species level for indicators of condition, with a focus on operational use. The Earth Observation Data for Habitat Monitoring (EODHaM) system was implemented using Worldview-2 data from two periods (July and September), *in situ* data and local ecological knowledge for two sites in Wales, Kenfig Burrows SAC and Castlemartin SSSI. The system utilises the Food and Agricultural Organisation's (FAO) Land Cover Classification System (LCCS) but translations between land cover and habitat schemes are not straight forward and need special consideration that are likely to be site specific. Limitations within the rule-based method of the EODHaM system were identified and therefore augmented with machine learning based classification algorithms creating a hybrid method of classification generating accurate (>80% overall accuracy) baseline maps with a more automated and repeatable method. Quantitative methods of validation traditionally used within the remote sensing community do not consider spatial aspects of maps. Therefore, qualitative assessments carried out in the field were used in addition to error matrices, overall accuracy and the kappa coefficient. This required input from ecologists and site specialists, enhancing communication and understanding between the different communities. Generating baseline maps required significant amount of training data and updating baselines through change detection methods is recommended for monitoring. An automated, novel map-to-image change detection was therefore implemented. Natural and anthropogenic changes were successfully detected from Worldview-2 and Sentinel-2 data at Kenfig Burrows. An innovative component of this research was the development of methods, which were demonstrated to be transferable between both sites and increased understanding between remote sensing scientist and ecologist. Through this approach, a more operational method for monitoring site specific habitats through satellite data is proposed, with direct benefits for conservation, environment and policy.

List of Publications

Journal Articles

Lucas, R., Blonda, P., Bunting, P., Jones, G., Inglada, J., Arias, M., Kosmidou, V., Petrou, Z. I., Manakos, I., Adamo, M., 2015. The Earth Observation Data for Habitat Monitoring (EODHaM) system. International Journal of Applied Earth Observation and Geoinformation 37, pp. 17 - 28.

Reports

Lucas, R., Jones, G., Bunting, P., Kosmidou, V., Petrou, Z., Inglada, J., Adamo, M., Blonda, P., Mucher, S. and Arvor, D., 2013. Land cover and habitat classification from Earth Observation data: a new approach from BIOSOS.

Book Chapters

Jones, G,. Bunting, P., Hurford, C., in press. Mapping coastal habitats in Wales. In: The Roles of Remote Sensing in Nature Conservation: A practical guide and case studies. Springer Nature.

Abbreviations and Acronyms

ANN - Artificial Neural Networks

ANOVA - Analysis of Variance

AOD - Atmospheric Optical Depth

ARCSI - Atmospheric and Radiometric Correction of Satellite Imagery

ARD - Analysis Ready Data

AVHRR - Advanced Very High Resolution Radiometer

AVIRIS - Airborne Visible/Infrared Imaging Spectrometer

BNSC - British National Space Centre

CBD - Convention on Biological Diversity

CCW - Countryside Council for Wales

CLC - CORINE Land Cover

CORINE - Co-ordination of Information on the Environment

CVA - Change Vector Analysis

CVI - Chlorophyll Vegetation Index

DEM - Digital Elevation Model

DN - Digital Numbers

DOS - Dark Object Subtraction

EAGLE - EIONET Action Group on Land Monitoring in Europe

EIONET - European Environment Information and Observation Network

EO - Earth Observation

EODHaM - Earth Observation Data for Habitat Monitoring

ERF - Extremely Random Forest

ESA - European Space Agency

ETM+ - Enhanced Thematic Mapper Plus

EUNIS - European Nature Information System

FAO - Food and Agricultural Organisation

GCP - Ground Control Points

GDAL - Geospatial Data Abstraction Library

GEO - Group on Earth Observations

GEOBIA - Geographic Object-based Image Analysis

GEO BON - Group on Earth Observations Biodiversity Observation Network

GEOSS - Global Earth Observation System of Systems

GHC - General Habitat Categories

GIS - Geographical Information Systems

GLC - Global Land Cover

GPS - Global Positioning Systems

HR - High Resolution

ICA - Independent Components Analysis

IFOV - Instantaneous Field of View

IRS - Indian Remote Sensing

ISO - International Organisation for Standardisation

JNCC - Joint Nature Conservation Committee

LAI - Leaf Area Index

LCCS - Land Cover Classification System

LCML - Land Cover Metadata Language

LEDAPS - Landsat Ecosystem Disturbance Adaptive Processing System

LGAC - Landsat Global Archive Consolidation

LiDAR - Light Detection and Ranging

LPS - Leica Photogrammetry Suite

MERIS - Medium Resolution Imaging Spectrometer

MLC - Maximum Likelihood Classifier

MOD - Ministry of Defence

MODIS - Moderate Resolution Imaging Spectrometer

NASA - National Aeronautics and Space Administration

NCC - Nature Conservancy Council

NDVI - Normalised Difference Vegetation Index

NDWI - Normalised Difference Water Index

NIR - Near Infra-red

NNR - National Nature Reserve

NOAA - National Oceanic and Atmospheric Administration

NRW - Natural Resources Wales

NVC - National Vegetation Classification

OBIA - Object-based Image Analysis

PCA - Principal Components Analysis

PSRI - Plant Senescence Reflectance Index

RAT - Raster Attribute Table

RBF - Radial Basis Function

RF - Random Forest

RGB - Red, Green, Blue

RMSE - Root Square Mean Error

RPC - Rational Polynomial Coefficients

RSGISLib - Remote Sensing and Geographical Information Systems Library

SAC - Special Area of Conservation

SAR - Synthetic Aperture Radar

SPOT - Satellite Pour l'Observation de la Terre

SRTM - Shuttle Radar Topography Mission

SSSI - Sites of Special Scientific Interest

SVM - Support Vector Machine

SWIR - Short Wave Infra-red

TM - Thematic Mapper

UAV - Unmanned Aerial Vehicle

UK BAP - UK Biodiversity Action Plan

UK LCM - UK Land Cover Map

UNECD - United Nations Conference on Environment and Development

USGS - US Geological Survey

VHR - Very High Resolution

WBI - Water Band Index

WBP - Wales Biodiversity Plan

Table of Contents

List of Figures

List of Tables

Chapter 1

Introduction

Human activities have been changing the environment for hundreds of years (Stanners et al., 1995) and the growing global population has led to the expansion of urbanisation and agricultural activity (European Environment Agency, 2010). Ultimately, natural resources have been exploited for human needs at the expense of degrading environmental conditions leading to declines in global biodiversity through loss, modification and fragmentation of habitats (Foley, 2005; Pimm and Raven, 2000). A combination of these processes affect the environment on all scales from local to a global level and can impact biodiversity in a negative manner. This increases the need for comprehensive mapping and monitoring of our environment to underpin policies which, in turn provide protection. Coastal habitats, which are highly sensitive to changes in our climate (Hallegatte, 2009), are critical for a wide range of biodiversity, but are at risk from rising sea levels; this has triggered an increased effort to conserve these ecosystems. With its capacity to fill important information gaps, remote sensing is being seen as an important tool for monitoring changes in these habitats, but better and more consistent methodologies are required to encourage operational use. This research will demonstrate the importance of remote sensing in moving forward with an emphasis on operational use and a focus on a

range of coastal habitats.

1.1 Biodiversity Policies and Strategies

National and international agencies have been driven to take policy measures to protect landscapes and habitats after recognising the impact of land use and change. The United Nations Conference on Environment and Development (UNECD) in Rio de Janeiro in 1992 led to the Rio Declaration, which recognised that the only way to progress socially and economically was to protect the environment. Many vital documents resulted from UNECD such as Agenda 21 and the Convention on Biological Diversity (CBD) (United Nations, 1992). Their objectives are to improve the conservation of biological diversity and the CBD set a target to significantly reduce the current rate of biodiversity loss by 2010 (Balmford et al., 2005). This led to many strategies across Europe, the UK response being the Biodiversity Action Plan (UK BAP). However, the target of halting biodiversity loss by 2010 was not reached (European Environment Agency, 2010), so this resulted in a new strategy by the CBD and Europe's own new EU Biodiversity Strategy 2011-2020.

In Europe, the need to protect the environment was recognised in 1979 resulting in the Convention on the Conservation of European Wildlife and Natural Habitats (1979) which was adopted in Bern, Switzerland. One of the objectives is to ensure conservation and protection of wild plant and animal species, and their natural habitats. The European community implements the Bern Convention by means of Council Directive 79/409/EEC on the Conservation of Wild Birds (EC Birds Directive, 1979), and Council Directive 92/43/EEC on the Conservation of Natural Habitats and of Wild Fauna and Flora (EC Habitats Directive, 1992). The UK government transposed the Bern Convention into national law by means of the Wildlife and Countryside Act 1981 (UK Parliament, 1981),

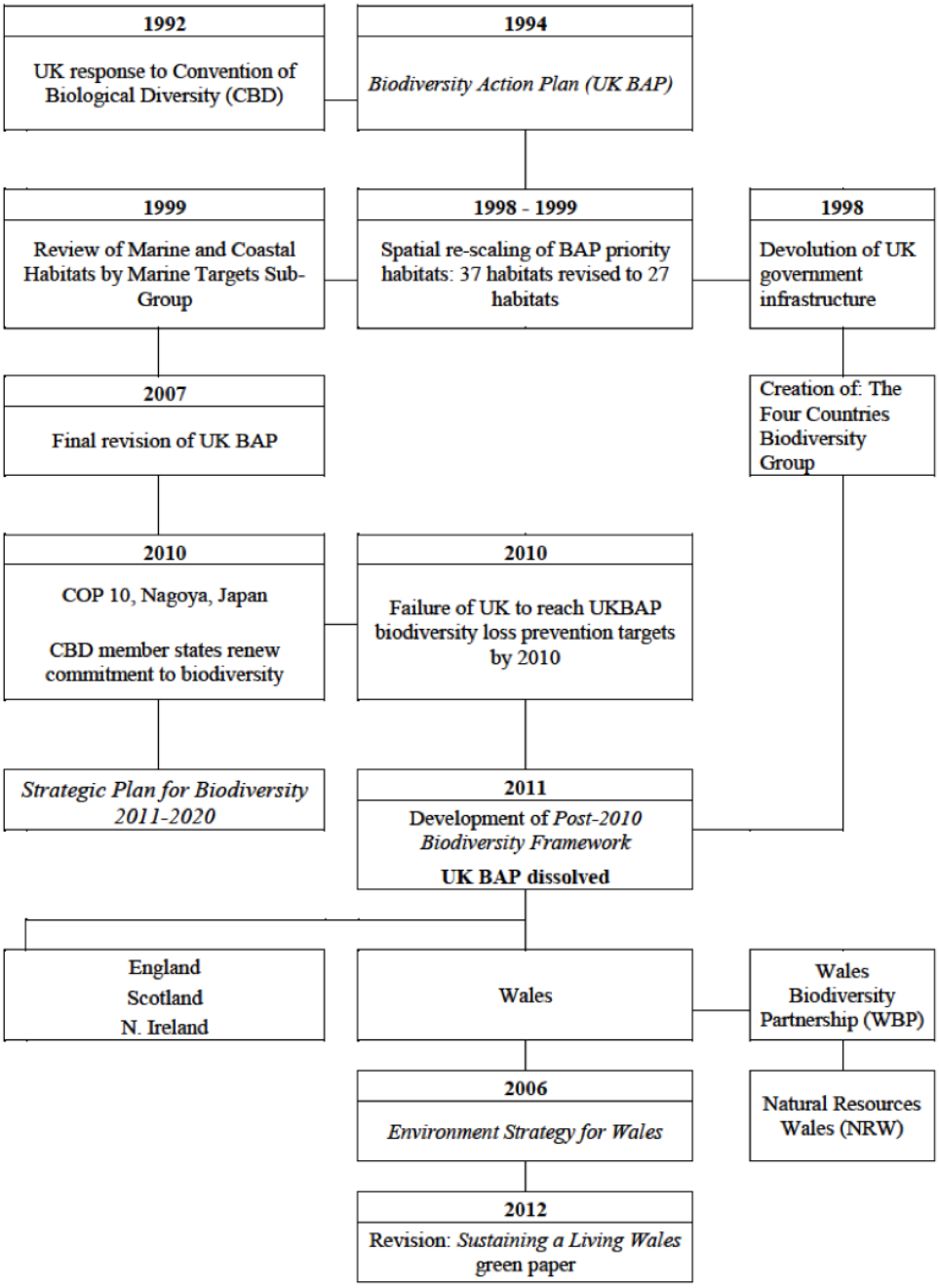

Figure 1.1: Timeline of UK biodiversity policy development with a focus on Wales (Ettrich, 2013).

and The Conservation Regulations 1994 (Statutory Instrument 2716, 1994).

Figure 1.1 shows that in the UK, failure to reach biodiversity loss prevention targets by 2010 led to the Post-2010 Biodiversity Framework which replaces UK BAP. Following the devolution of the UK in 1998, the four countries are considered independently within the framework. In Wales, the Welsh Biodiversity Partnership (WBD) provide the leadership for biodiversity action priorities, with support from Natural Resources Wales (NRW), formerly Countryside Council of Wales (CCW), Welsh Government and the Wildlife Trust Wales. The 'Environment Strategy for Wales' (National Assembly for Wales, 2006) outlines the challenges and priorities that are supported in order to achieve UK, European and Global legislation on preventing biodiversity loss.

1.2 Conservation in Wales

The UK supports a wide variety of species and habitats which are managed by designated areas of protection. Special Areas of Conservation (SACs), have European significance as they were created under the EC Habitats Directive (1992) and they form part of a large European ecological network called Natura 2000 (Ostermann, 1998). Within SACs the extent and condition of the featured habitats need to be monitored so that policies and strategies can be formed to maintain and enhance biodiversity (Bunce et al., 2008). Sites that have national importance are protected as Sites of Special Scientific Interest (SSSIs) (Figure 1.2).

The authority responsible for reporting on environmental legislation in Wales is NRW (formerly the CCW, Environment Agency Wales and Forestry Commission Wales) and every six years, Member states of the European Union are required by Article 17 of the Directive to report on conservation status of Annex 1 habitats and Annex II species (as listed in the Habitats Directive) on the Natura 2000 sites and beyond (JNCC, 2006). The

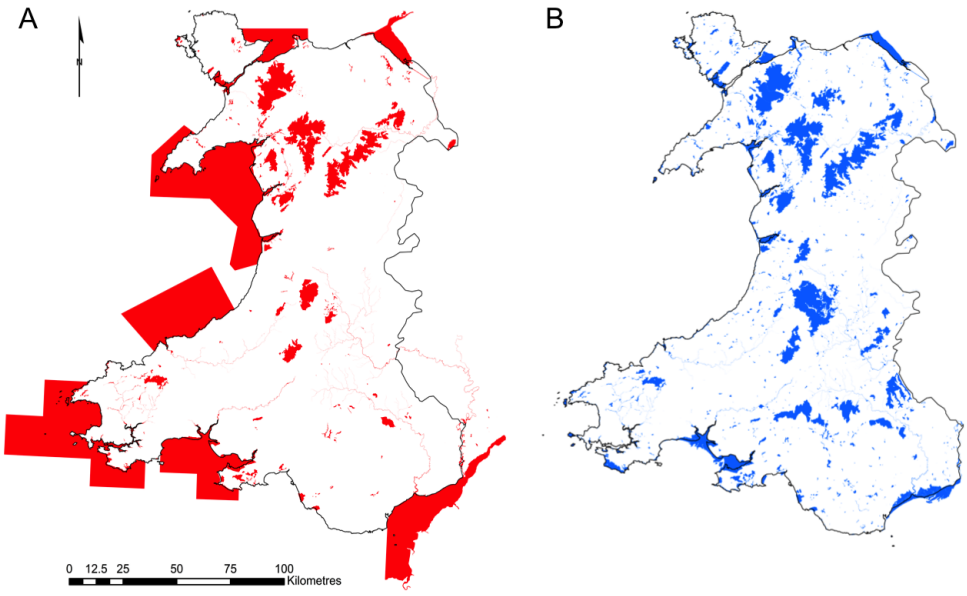

Figure 1.2: Designated A:Special Areas of Conservation and B: Special Sites of Scientific Interest in Wales (CCW, 2013).

conservation status of a natural or semi-natural habitat is defined as:

> *(e)"the sum of the influences acting on it and its typical species that may affect its long-term natural distribution, structure and functions as well as the long term survival of its typical species";(i) "the sum of the influences acting on the species that may affect the long-term distribution and abundance of its populations"*

(Article 1 (e) and 1 (i), EC Habitat's EC Habitats Directive (1992)).

Although, Wales is considered independently within national legislation, the reports collated with those from the other home nations and submitted to Europe as the UK level. Since the EC Habitats Directive (1992) came into force in 1994, three UK reports have been submitted. The first of which focused on the designation of SACs while the latter two provided assessment of conservation status for all 167 habitats and species protected by EU legislation and monitored in the UK. Some Annex I habitats are thriving but in

over 50% of occurrences they are declining and in poor condition. This means that action is essential but current methods of assessments are difficult as field surveys take time and repeatability is costly.

The Natura 2000 programme aims to identify those pressures on habitats that are most likely to lead to a decline in condition and an unfavourable status. Once identified, a plan can be adopted to target and mitigate the risk, improve the current condition of these features and protect them for the future. This programme will be used in Wales to inform the Wales Prioritised Action Framework which was formed to achieve the EU's new 2020 Biodiversity Strategy. This work will require better methods to condition map and monitor the features on the sites, and to monitor the surrounding landscapes to identify any external pressures on the protected sites.

1.3 Surveillance and Monitoring of Habitats

The habitats listed in the EC Habitats Directive, or Annex I habitats, are prioritised for conservation across Europe and therefore, are the main habitats of interest in this research project. Specifically, the Habitats Directive seeks to maintain favourable conservation status (as quoted earlier), which requires information on surveillance and monitoring through time. For example, the location and extent of these habitats are essential as a start point. Table 1.1 describes the measures currently used in habitat surveillance and monitoring. As the location of habitats is already known through the SAC and SSSIs networks (Figure 1.2), this measure is excluded.

Reporting obligations are in place to assess the effectiveness of policies and their implementation, but there are gaps in current evidence information. Although this reporting period is currently in its fourth phase, there is still a need for accurate mapped inventories showing the extent of Annex I habitats using methods that are more consistent so they can

Table 1.1: Description of measures used in habitat surveillance and monitoring (adapted from Medcalf et al. (2011)).

Measure	Description	Comment
Extent	This is the spatial expression of a particular habitat. It includes its bio-geographical range and how it interacts with the surrounding land.	Natural habitats rarely have "hard" boundaries and often merge into adjoining habitats through an area known as an ecotone. Some habitats must be surrounded by other complimentary habitats in order to survive, therefore extent is taken to encompass this range of features.
Condition	Condition is an assessment of how close a habitat is to its ideal fully functioning state. A habitat in poor condition does not have all the necessary components to function in ecological terms, or these components are in less than ideal numbers or proportions.	Condition of habitat has been described in detail by Common Standards Monitoring in the UK (JNCC). For each habitat species indicative of good condition and poorer condition are recorded, along with other features such as wetness and bare ground. In many cases negative indicator species and features can be easier to detect, therefore a lack of these can be taken as a proxy for the habitat being in good condition.

be regularly updated. Repeatable measures that contribute to establishing the condition and change in condition of habitats are also needed. Table 1.2 provides a summary of the nature and characteristics of these known gaps in evidence needed to support reporting obligations.

Table 1.2: Summary of known current gaps in provision (adapted from Medcalf et al. (2011)).

Measure	Nature and characteristics of gaps in provision
Extent	lack of consistent quality and repeatable survey information; limited accurate evidence of baseline extent of features at site-level; lack of sufficient detailed information to feed into habitat system conversion tools.
Condition	insufficient knowledge of condition outwith statutory sites; few proxy measures in existence that do not require fieldwork.
Change	insufficient information on change in extent available; limited availability of established methods to measure change; potential future natural range of habitats is not well understood.

1.4 Current Earth Observation Systems

The Group on Earth Observations (GEO), which was formed in 2002, recognised that international collaboration on Earth Observation (EO) was essential, and aims to improve policy decisions by coordinating strategies among participating governments and organisations. A central part of GEO's mission is to build the Global Earth Observation System

of Systems (GEOSS), which is a set of independent EO systems that interact and provide access to data for a broad range of users. These links aim to strengthen the monitoring of our environment by enhancing our understanding of Earth processes and predictive capabilities to underpin decisions made for policy and action. In 2016, the UK formed a network called UKGEOS, which aims to continue interaction with the global network and capitalise on new sensors called the Sentinels, which are currently being launched by the European Space Agency (ESA).

In terms of monitoring biodiversity, a separate network with links to GEO was formed in 2008, this was called the Group on Earth Observations Biodiversity Observation Network (GEO BON). This network recognised a need for better integration between multiple types of data for monitoring, from remotely sensed data to ground sourced field data. The vision includes a global biodiversity observation network that contributes to effective management policies for biodiversity and ecosystem services. The current lack of integration affects the work of a wide range of users from policy makers to conservation managers therefore, impeding progress and the capacity to assess the effectiveness of their actions. Despite the real progress being made with these initiatives and the complexities of our environment, evidence gaps still exist in location, extent and condition of habitats (Medcalf et al., 2011).

One way to ensure that these observation networks improve is to examine and integrate increasingly sophisticated systems such as very high resolution (VHR) remote sensing satellite systems. In Europe, two European Framework (FP7) projects were funded to develop EO systems for monitoring Natura 2000 sites, which are the ‘multi-scale service for monitoring Natura 2000 habitats of European community interest’ (MS.MONINA), and the ‘biodiversity multi-source monitoring system: from space to species (BIOSOS). This research project is based on, and will use, the EO Data for Habitat Monitoring (EODHaM) system developed by the BIOSOS project. The system is designed to integrate

multi-image data and expert knowledge sourced from ecologists, conservation managers and remote sensing experts to generate useful mapping and provide a baseline for monitoring (Lucas et al., 2015). The system will be outlined in detail in Chapter 6.

1.5 Why Remote Sensing?

Remote sensing can become an essential tool for evaluating the implementation of environmental policies (Mayer and Lopez, 2011), for assessing the extent and condition of habitats, and for quantifying losses, degradation or recovery associated with events and processes (Nagendra et al., 2013). Today, a broad variety of data is available from different sensors, ranging from multi-resolution optical imagery, to radar and Light Detection and Ranging (LiDAR) products (Corbane et al., 2015). Specifically, progressive improvements have been made in spatial, temporal and spectral resolution in satellite remote sensing, which creates opportunities to improve consistency which is currently lacking in monitoring systems. However, the uptake of remote sensing in ecological applications, particularly in detailed conservation status assessments such as required by the EC Habitat Directive is still rarely exploited (Borre et al., 2011).

Advanced methodologies to handle remote sensing data include classification and derived biophysical parameters, however the problems that exist in current surveys, particularly in terms of complexity in definitions and classification systems apply here too. The connection between remote sensing scientists and ecologists needs to strengthen to provide the detailed information required by conservation managers and policy makers. The first step to improvement is a better understanding of some of the associations derived from remote sensing data therefore, remote sensing techniques need to be further developed and tailored for identification and monitoring of habitats and their subsequent conservation status (Medcalf et al., 2011).

The EODHaM system in particular, has developed remote sensing techniques that produce detailed habitat maps from VHR EO data. In the process, progress was made on integrating in situ data from conservation managers in addition to work on nomenclature required for transitions between classification systems (Kosmidou et al., 2014). The flexibility of the system means that there is potential for adaption as more advanced techniques become available.

As collaboration increases, it is evident that remote sensing will not have all the answers but where information cannot be directly used for evidence, it can help by targeting field work. This reduces cost and increases efficiency in addition to providing information on areas that are vast or difficult to access. Forming baselines is key to any monitoring process where change is measured, and remote sensing can play a key role in establishing these baselines (Charnock, 2016).

1.6 Aims and Objectives

1.6.1 Aim

The aim of this study is to explore remote sensing techniques for monitoring coastal Annex I habitats in Wales. The development of methods that will form the basis of operational approaches is largely the motivation behind this research. The study focuses on the use of VHR optical imagery for retrieving parameters to identify associations that can separate habitat boundaries for extent mapping down to species level for indicators of condition.

1.6.2 Objectives

1. Review current land cover and habitat classification systems and asses their suitability for determining Annex I habitat definitions, focusing on their retrieval from EO data and associated parameters.

2. Implement and evaluate the EODHaM system for mapping Annex I habitats utilising Worldview-2 data from two periods (July and September), in situ data and local ecological knowledge from ecologists, conservation and site managers.

3. Develop and adapt the EODHaM system by integrating more advanced remote sensing techniques such as machine learning to aid automation and operational use, and generate a baseline map of Annex I habitats, including mapping down to species level for proxies of condition.

4. Explore the use of automated change detection techniques, specifically a map-to-image method to identify any changes in habitat extent and generate an updated Annex I habitat map.

1.6.3 Thesis Outline

Introduction

The policy relevance for this research and its importance and scalability to the global stage is described. The gaps in national monitoring systems are identified and the potential use of remote sensing for filling these gaps is introduced. Outlines aims and objectives.

Literature Review

This chapter provides an overview on past and current methods of habitat and land cover mapping, background on remote sensing of vegetation and issues with the uptake of remote sensing data in operational techniques for monitoring. Issues of scale are outlined and a review of research and methods available for habitat mapping with remote sensing is included.

Study Site

A full description of study sites, including presence of flora and fauna of importance and management regimes.

Data Collection and Processing

All processing of data is explained, including pre-processing of imagery, calculation of derived parameters and preparation of field data for analysis.

Habitat Definitions and Classification Schemes

A review on current habitats and where they fit within numerous classification schemes that are currently in use. Additionally, an evaluation of how depicting these schemes using EO data is included.

Classification of Broad Habitats

A background on the EODHaM system is provided before the system is implemented for all study sites. A more automated and statistically robust method of threshold derivation

is used for use within the rule-base classification method. An evaluation of output maps and suitability of the system to produce detailed information is performed.

Classification of Annex I Habitats

A review of remote sensing methods is carried out before implementing more advanced classification techniques for detailed habitat mapping. An Annex I habitat map and species level map to determine condition is created and assessed for accuracy at each site.

Change Detection

A review of change detection techniques is carried out before implementing a map-to-image automated method for change analysis at Kenfig only. Worldview-2 data acquired two years after the data used for baseline mapping is analysed in addition to Sentinel-2 data. A critical evaluation of spatial scales needed for change detection is included.

Conclusions

The ability of methods used throughout this research to perform as an operational system is discussed. Further work and application to policy, national and international monitoring schemes is included.

Chapter 2

Literature Review

This chapter will provide a review of the literature on habitat mapping and remote sensing of vegetation. The definitions used are as follows:

1. Land Cover observed biophysical description of the Earth's surface (Di Gregorio and Jansen, 2000);

2. Natural habitats are terrestrial or aquatic areas distinguished by geographic, abiotic and biotic features, whether entirely natural or semi-natural (Convention on the Conservation of European Wildlife and Natural Habitats, 1979);

3. Earth Observation (EO) is the interpretation and understanding of measurements made by airborne or satellite-borne instruments of electromagnetic radiation reflected from or emitted by objects on the Earth's surface by using remote sensing technologies (Paul and Magaly, 2011). Thus, the purely visual interpretation of analogue or digital images is excluded in this context (Corbane et al., 2015);

4. Spatial resolution (grain) is defined as very high resolution (VHR) $<$3m; high resolution (HR) 3-30m; medium resolution 30-300m; low resolution $>$300m (ESA, 2016).

2.1 Habitat and Land Cover Mapping

Recognising the extent and distribution of land elements has a high significance in terms of monitoring and management for conservation purposes. Organisations such as the Ordnance Survey provide some details in regard to land cover but the Land Utilisation Surveys in the 1930s (Stamp, 1934) and 1950s (Coleman, 1961) were the first to address the need for a land use map to monitor change. In the 1980s, the government funded a project called "Monitoring Landscape Change" (Hunting Surveys and Consultants, 1986) which used aerial photography from different snapshots through time to estimate the extent of land cover and identify landscape change. However, inconsistencies apply to most available datasets in the UK, rendering precise repeat surveys impossible and making it difficult to firstly map land cover effectively, before monitoring changes through time is possible.

The Nature Conservancy Council (NCC) recognised the need for a standardised mapping programme and in the 1980s developed a system called "Phase 1 mapping" (Unit, 1990) which included the identification of sites for increased protection (Howard et al., 2003). Its purpose was to gather information about the location, distribution and extent of wild plants and animals, and natural and semi-natural habitats. A Phase 1 Habitat Survey was conducted in Wales between 1987 and 1997 (Howe et al., 2005) where over 80% of the land was surveyed to obtain information about the extent and distribution of natural and semi-natural habitats for developing wildlife conservation initiatives.

Cherrill and McClean (1999) and Stevens et al. (2004) both studied the reliability and repeatability of the Phase 1 survey conducted in Wales. Two basic types of error were identified including the misclassification of vegetation types and spatial displacement between boundaries of classes. These are difficult to distinguish from each other as georeferencing errors can be mistaken for classification errors. Quality assurance and control are subjec-

tive as the experience and expertise of the surveyors can vary and create inconsistencies in the survey data. Standardised methods and habitat definitions are therefore essential not only in the Phase 1 approach but in ecological projects generally, and can be encouraged through quality assurance measures (Unit, 1990). Very little would be gained from repeating the Phase 1 survey of Wales using the Phase 1 method, so it is therefore very unlikely to be repeated in the near future. However its products are still being used today to support management in planning decisions and policy. The Phase 1 survey was also laborious work in terms of time and cost, and similar to the previous surveys mentioned above, would prove difficult to repeat future surveys of this nature.

These difficulties are still recognised and apply to all survey methods, as the identification of Annex 1 habitats in the field is not always straightforward either. The problems here can lie in the identification of some of the habitats which then leads to difficulties when selecting sites and assessing the national list of proposed sites. Poorly defined habitats that sometimes overlap are the main source of error, which leads to differences in interpretation between countries or even regions (Evans, 2006, 2010). As mentioned previously, this increases demand for a consistent recognition system that prevents the most obvious errors and introduces consistency (Bunce et al., 2012). This topic is discussed in more detail in Chapter 5.

2.2 Remote Sensing of Vegetation

2.2.1 Spectral Reflectance of Vegetation

Different land surfaces have characteristic reflectance responses across the visible light spectrum, near infrared (NIR) and short wave infrared (SWIR) wavelengths. The understanding of spectral reflectance curves allows remote sensing the ability to differentiate

between different types of vegetation that is not always possible by naked eye. The typical reflectance of green vegetation is shown in Figure 2.1.

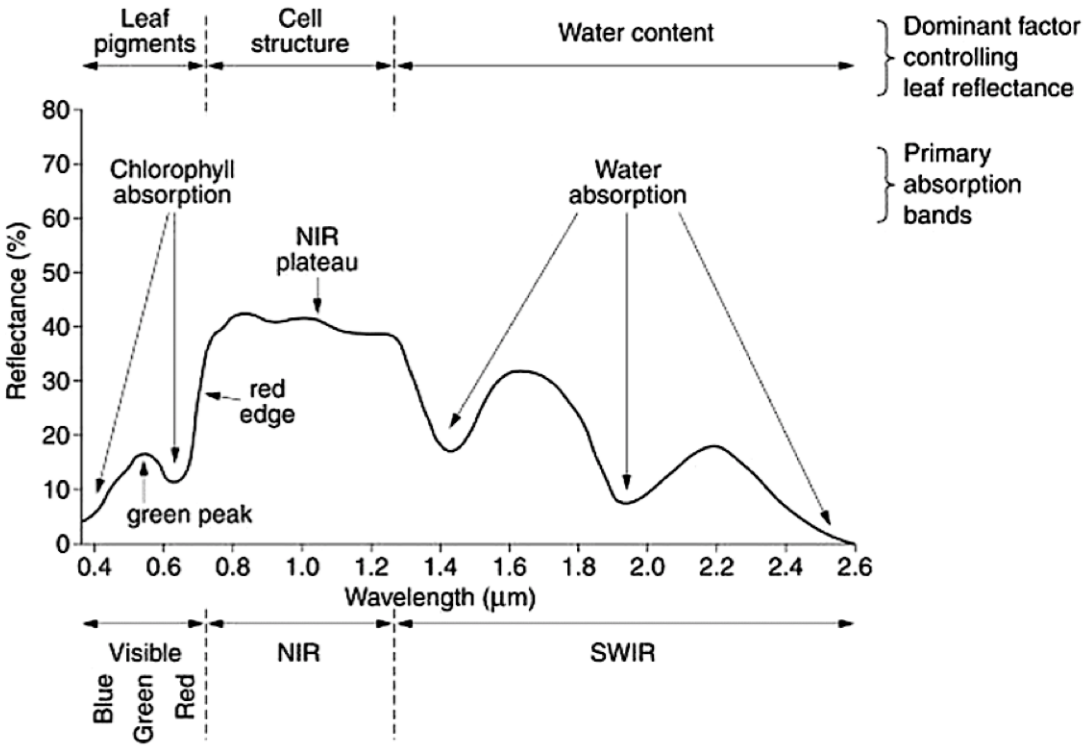

Figure 2.1: Spectral reflectance of vegetation (re-drawn from (Elachi and Van Zyl, 2006)).

As illustrated, there are certain factors that control the sensitivity of leaf reflectance, from pigments such as chlorophyll a and b, and carotenoids, to the internal cell structure of leaves which affects reflectance in the NIR wavelengths. In the SWIR wavelengths reflectance is dominated by liquid water absorption and also weakly affected by absorption due to other biochemical components (Gao and Goetz, 1994). The NIR and SWIR wavelength regions are also linked with canopy structure, which applies to grasslands and shrubs as well as forestry.

According to Asner (1998), vegetation spectral reflectance is primarily a function of optical properties of tissue, leaf, woody stems and litter, canopy biophysical properties and soil reflectance. Asner et al. (1998) also incorporate illumination conditions and view-

ing geometry but as these are mostly eliminated through image pre-processing techniques such as atmospheric correction and standardisation of data capture, the other factors become key in identifying spectral reflectance of different vegetation types.

2.2.2 Spectral Bands and Indices

One of the leading methods for extracting vegetation abundance from measures of radiance are vegetation indices. Early remote sensing studies have utilised these indices such as the Normalised Difference Vegetation Index (NDVI) to measure vegetation from remote sensing data (Baret et al., 1989). The NDVI has shown sensitivity to the productivity of vegetation with values ranging from -1 to +1 where vegetation is normally equal to NDVI values of greater than 0.3 (Gao, 1996). However, there is evidence that the NDVI is affected by soil reflectance and its known to be saturated when applied to images with a Leaf Area Index (LAI) of 3 or greater, therefore it is not always comparable across a heterogeneous image (Major et al., 1990; Elvidge and Lyon, 1985; Todd and Hoffer, 1998). Regardless, NDVI does show a correlation with vegetation abundance and other ecological parameters such as fraction of photosynthetic radiation. Numerous other vegetation indices with varying complexities have been developed using the same wavelength regions during the past 20 years but are not used as extensively as the NDVI (Gao, 1996).

As the high water content of vegetation dominates the spectral reflectance of vegetation in the NIR regions of the electromagnetic spectrum, indices based on the water absorption bands are expected to have a preferential sensitivity to canopy structure (Sims and Gamon, 2003). One of these indices is the Normalised Difference Water Index (NDWI), which is less sensitive to atmospheric effects in comparison with NDVI. However, similar to the NDVI, the NDWI does not completely remove the background soil reflectance effects

(Gao, 1996). Another index is the Water Band Index (WBI) (Peñuelas et al., 1993) which has been used to successfully distinguish different species with varying water fluxes (Qiu et al., 2007; Serrano et al., 2000). WBI responses vary with vegetation type and physiological status making it a useful index for vegetation mapping (Fuentes et al., 2001).

A particular advantage of remote sensing is that data of the same wavelength regions can be acquired on a repetitive basis and consistently compared. This allows data capture in different seasons which is particularly useful for discriminating between vegetation types that differ across the seasons. Indices such as the Plant Senescence Reflectance Index (PSRI) have been developed to capture these differences, particularly as non-photosynthetic vegetation such as stems and litter are described as a function of the spectral reflectance of green vegetation. During senescence, plant tissues undergo remarkable changes in colour as a result of changes in the content of and proportions between individual pigments (Chichester and Nakayama, 1965; Knee, 1988; Buchanan-Wollaston, 1997). This makes the application of non-destructive reflectance spectroscopy very attractive for assessing the physiological state of plants and monitoring of senescence-induced events in vegetation very attractive (Guyot et al., 1990; Merzlyak et al., 1999; Sims and Gamon, 2002).

2.3 Uptake of Remote Sensing Data

Satellite data are currently underused within the ecological monitoring communities, and especially by those looking to track biodiversity. Currently, the acceptance of aerial photography to aid monitoring is widely accepted and has been routinely used for decades, but there is still a barrier to the uptake of remotely sensed data. Many monitoring activities are rooted in policies and actions provided by government, which have been aware of satellite data, particularly Landsat sensors, since at least the 1980s. The NCC, an in-

dependent government advisory body in the UK, undertook a comparison of field survey techniques, aerial photography and satellite imagery as far back as 1990 (Table 2.1). This identified advantages and disadvantages of each method.

However, even with major advances in the latter column of Table 2.1, no move has been made to routinely adapt actions and integrate remote sensing data into policy and beyond. Leidner et al. (2012) focused on three factors that have an impact on the uptake of remote sensing data for understanding changes in biodiversity:

1. Data continuity
2. Data affordability
3. Data access

2.3.1 Data Continuity

Satellite remote sensing products can provide long-term archives of consistent data, which is one of the key advantages of using remotely sensed data over more traditional field survey methods mentioned in Section 2.1. Multi-decadal, continuous EO data is only available from a small number of satellite systems, both of which were launched and operated by the USA. They are components of the Landsat program, which is jointly operated by the U.S Geological Survey (USGS) and National Aeronautics and Space Administration (NASA), and the Advanced Very High Resolution Radiometer (AVHRR) which is operated by the U.S National Oceanic and Atmospheric Administration (NOAA). Although other platforms exist and provide complementary information, none have operated and provided such consistent time series data for as long as Landsat (four decades) and AVHRR (three decades).

The key factor in the uptake of these satellite systems for various monitoring programs

Table 2.1: Comparison of Phase 1 survey with remote sensing (Unit, 1990).

Phase 1 Survey	**Aerial Photography**	**Satellite Imagery**
Complete ground cover possible; not limited availability of other data	Complete cover exists for 1940s; cover good for 1970s but incomplete for other dates; quality variable	Frequent complete cover exists since 1982 for Landsat TM, but cloud obscures many images
Direct recording in the field	Relies on tone and pattern of spectral reflectance	Relies on spectral reflectance in a more limited range of tones, but images have greater contrast than for aerial photography
Accuracy depends on skill of field surveyors; few problems of interpretation	Image accurate but interpretation variable and often difficult	Image accurate; interpretation by specialists essential
Can be used to standardise other methods	Should be calibrated by field survey	Should be calibrated by field survey
No sophisticated or expensive equipment	Needs complicated and expensive equipment	Needs complicated and expensive equipment
Yields complete set of Phase I habitat categories	Yields limited set of habitat categories	Yields limited set of habitat categories
Yields maps, descriptive notes and statistical data	Can yield maps and statistical data	Can yield maps and statistical data
Gives information on dominant and other plant species	Little species information	Very little species information
Gives information on canopy and ground layer	Information on canopy only (unless repeated at different seasons)	Information on canopy only (unless repeated at different seasons)
Data gathering slow, interpretation rapid	Data gathering quick, but interpretation laborious	Data gathering quick, interpretation potentially very fast if fully automated
Target notes give site-related information on species, communities, management threats, etc for a large number of sites	Site-related information limited; no target notes	Site-related information limited; no target notes
Can be used for conservation evaluation	Limited use for conservation evaluation	Limited use for conservation evaluation

beyond biodiversity, such as land use and weather forecasting, is the fact that they are supported and funded by government. This was not always the case, and during the 1990s the Landsat program was privately funded, which resulted in a vast amount of Landsat scenes being captured and stored beyond the U.S, and which now reside outside the central USGS central archive. Consequently, the USGS has begun a Landsat Global Archive Consolidation (LGAC) program which aims to transform all scenes received from international ground stations to a common format, updating the global central archive (Wulder et al., 2012). This project aims to finish updating the archive by 2018, meaning users need only go to one central archive for all the global Landsat data, and they can be confident that the formats are consistent, hence removing some of the barriers to user uptake.

Data continuity requires synergies between long-term records of imagery and additional satellite systems at a global scale (Turner et al., 2015). USGS and NASA launched the Landsat Data Continuity Mission, known as Landsat 8 in February 2013, ensuring the longevity of the Landsat program for years to come. ESA and the European Commission began a very ambitious mission within the Copernicus Programme, initiating a series of dual satellite constellations known as the Sentinels. So far, both Synthetic Aperture Radar (SAR) satellites, known as Sentinel-1, and the optical satellite known as Sentinel-2 have been successfully launched. The Sentinel-2 mission will provide medium spatial resolution imagery from 10 m to 60 m of global land surfaces and coastal waters every 5 days once the second satellite is fully operational in the summer of 2017. This sensor is highly comparable with Landsat but will have a higher revisit time (currently Landsat has global coverage every 16 days) (Berger et al., 2012; Drusch et al., 2012). Together with Landsat, there is potential to observe any area of our planet every two to three days, and as the Sentinels are funded by several governments from the EU, the likelihood of inclusion in policies is highly likely, especially those concerning the environment.

2.3.2 Data Affordability

Conservation is chronically underfunded (McCarthy et al., 2012), and the cost of satellite imagery until very recently contributed to the continuous barrier of uptake in the ecological community. In 2008, the USGS began providing open access to all Landsat imagery, i.e. the newly acquired images as they are ingested from Landsat 8 and the entire archive dating back to 1972. This means that the archive is available for download free at the point of use from the internet (Belward et al., 2008). This policy shift resulted in a dramatic increase in the distribution of images as seen in Figure 2.2, meaning that the investment from the US Government is returned in research and application based services around the globe (Raunikar et al., 2013). Turner et al. (2015) states that roughly 10% of the publications for 2013 found in a Web of Science search on "Landsat" also contained the terms "biodiversity", "biological diversity", or "conservation", which means that these communities are important users of these satellite images.

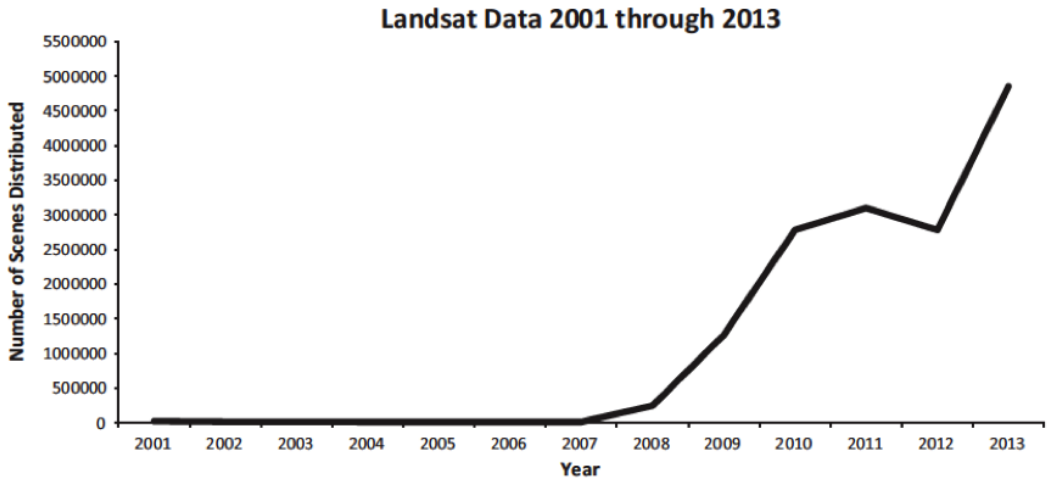

Figure 2.2: The number of Landsat scenes distributed per year. From December 2008, when all Landsat data in the USGS archive were made freely available, the number of scenes distributed sees a sharp increase. In November 2011, Landsat 5 acquisition were suspended due to degradation of the instruments, which almost certainly accounts for the dip in 2012 (Turner et al., 2015).

Governments across Europe will see a similar benefits by ensuring that all of the medium resolution satellite data acquired on a frequent basis by the Sentinels missions are distributed free of charge.

2.3.3 Data Access

Data access in this context refers to the ability of end users to discover, retrieve, and manipulate the data to extract information from satellite images (Turner et al., 2015). In terms of discovering and retrieving data, the internet provides a platform for making satellite datasets globally available. However, with the limited data distribution strategies, tools and technical capacity of end users, effective access continues to be limited and is restricted to users with no experience in handling satellite imagery. Although strategies are in place to help resolve this issue with the LGAC program aiming to provide a central platform for all Landsat data when complete, and the Scientific Hub developed by ESA for the dissemination of the Sentinels data (ESA, 2016). Another consideration of general access to archives is the increasing popularity of cloud platforms with both Google and Amazon hosting public datasets of Landsat and Sentinel-2 on their individual platforms (Google Cloud Platform, 2016; Amazon Cloud Platform, 2016).

One of the main barriers to uptake of satellite imagery is the fact that raw imagery distributed by providers still require further processing before end users can use these data for analyses. These pre-processing steps typically involve orthorectification and atmospheric correction which require specialist skills that are often beyond the capabilities of users in the conservation and biodiversity communities. The need for consistent, centralised access to higher level products is gradually being recognised within the remote sensing community. Projects such as Landsat Ecosystem Disturbance Adaptive Processing System (LEDAPS) are running to provide a higher level product for the Landsat archive

(Vermote and Saleous, 2007). However, the confidence in such products are still relatively low due to the data culture of remote sensing analysts preferring to pre-process these data individually with no universal standard for the processes. Until these issues are addressed, data access is likely to remain a barrier to the widespread uptake of satellite imagery.

Turner et al. (2015) states that increased access to pre-processed and value-added data would allow greater use of satellite imagery by those in the ecological community with limited technical remote sensing skills. The development of user-friendly, intuitive, and centralised data portals, which fill the semantic, technological and technical gaps that exist between data providers and data users, would significantly increase the use of remote sensing and help close the gaps. This would be particularly true if guidance was provided on the most appropriate datasets to use according to the need.

2.4 Issues of Scale

All observations depend on the scale of study. The most prevalent, and most discussed aspect is spatial scale, which comprises of two major components, extent and grain (Kotliar and Wiens, 1990; Forrnan, 1995). Extent refers to the spatial size of the study area and this project focuses on SACs and SSSIs on the coast of Wales. The larger site has a maximum area of 4 km^2 making the extent of the study areas relatively small. The level of information that can be maintained at this extent, given constraints on time, effort and cost is relatively high.

The grain refers to the resolution of remote sensor at the size of the smallest unit or pixels. Within this aspect there are several types or resolution to consider:

- Spatial

- Spectral
- Temporal
- Radiometric

The amount of information that can be retrieved, on numbers of habitat types critically depends on these factors above (Nagendra, 2001). To understand the smallest unit it is necessary to explain how the information is captured. The most common kind of scanner used to collect electromagnetic radiation, especially on space-borne platforms are push-broom scanners where an array of solid-state charge-coupled devices sees a single point on the scan line (Figure 2.3). The instantaneous field of view (IFOV) is the angle which incident energy is focused on the detector. The resulting ground resolution cells are called pixels (Lillesand et al., 2004). The main focus of this study is optical sensors but other types of sensors are available such as SAR and LiDAR, which are all complementary to optical sensors (Strittholt et al., 2007).

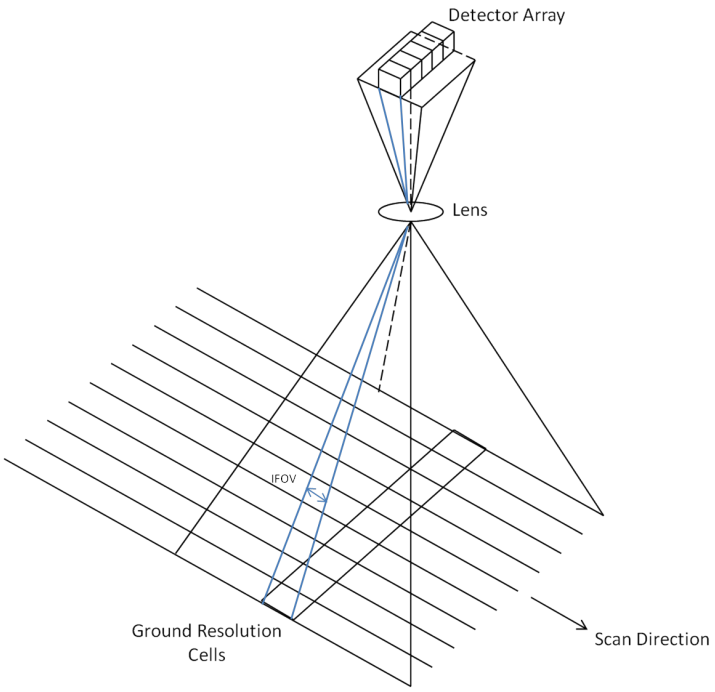

Figure 2.3: Pushbroom Scanner System Operation (Image adapted from (Sabins, 2007)).

The signal attributed to any given pixel arises as a result of contributions not only from the field of view corresponding to that pixel but also includes contributions that properly belong to neighbouring pixels. In other words the pixel intensities are not independent but there is autocorrelation among them (Cracknell, 1998). No pixel, however small it might be, represents completely homogeneous characteristics (Cracknell, 1998; Somers et al., 2011). The measured signal from the sensor therefore, always results from the interactions of electromagnetic radiation with multiple constituents within each pixel (Keshava and Mustard, 2002). It is therefore important to consider each aspect of scale before deciding which sensor and method is most appropriate for specific applications.

However, scale is not the only issue, as there are a multitude of sensor types available that provide different scales of coverage, which is also important to be aware of when deciding applicability of sensors. Figure 2.4 provides an insight into the power of remote sensing and collection of in situ measurements in a biodiversity context. Although, some references will be made to imagery acquired by aircraft in this review, at the beginning of this research project, the technologies surrounding the use of Unmanned Aerial Vehicles (UAVs) were less stable and accessible (Turner, 2014), and it was therefore not considered for operational use and is absent from this section. These data were, however, available and used as an additional form of validation in this project. The recent increase in the availability of UAVs and their ability to carry different sensor arrays means that UAV imagery is likely to form a fundamental component of ecological surveys and monitoring in the future.

2.4.1 Spatial Resolution

In the ecological community, there is a broad assumption that the higher the spatial resolution the better, which usually results in ordering VHR data whenever costs permit and

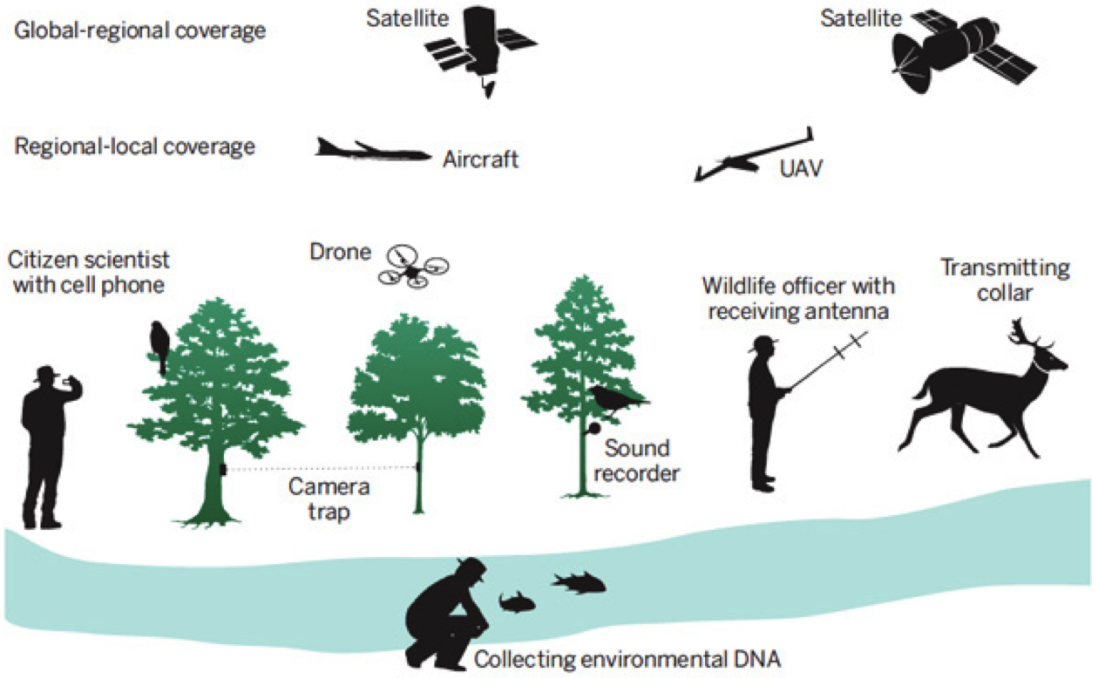

Figure 2.4: Sensor Power: Networking satellite and airborne remote sensing with in situ sensing allowing many elements of biodiversity to be tracked over time (Turner, 2014).

data coverage is available (Nagendra and Rocchini, 2008). However, it is important to note that the spatial scale is dependent on distribution and the heterogeneity of the species and habitat being monitored, and is greatly affected by the application or operational activity. Therefore it is critical that pixel sizes reflect the chosen operational scale. For example, within a highly diverse tropical forest, individual trees need to be covered by more than a single pixel to reduce adjacency effects from neighbouring trees or other species for tree species discrimination, making the likely pixel size needed very fine ($<$2 m). For managed temperate forests with more homogeneous stands a pixel size of 30 to 250 m may be more suitable since coarser resolution reduces the within class variability of the spectral signature which leads to an increased inter-class separability (Gosh et al., 2014).

In many cases, the use of high (10 m) to medium (30 m) spatial resolution data may be

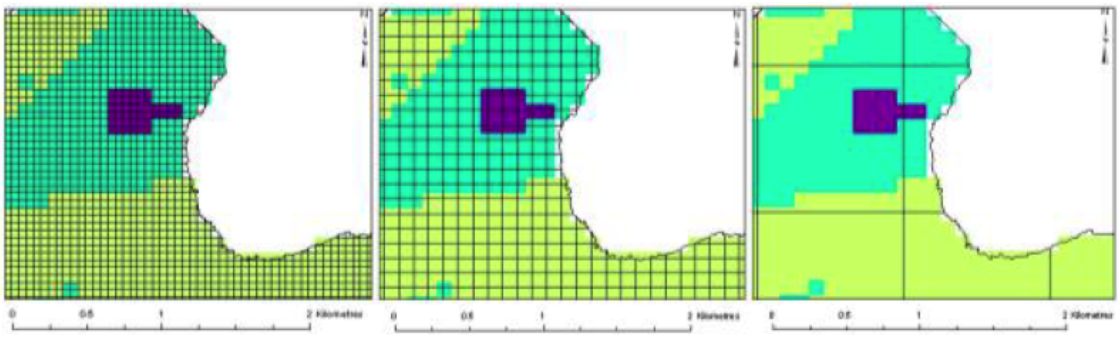

Figure 2.5: Diagrammatic representation of the effect of pixel size on habitat feature recognition (Medcalf et al., 2011).

sufficient to capture broad extent and spatial patterns of habitats (Nagendra et al., 2013). In Wales, the update of the national Phase 1 habitat map used remote sensors with these spatial resolutions, such as Satellite Pour l'Observation de la Terre (SPOT) and Indian Remote Sensing (IRS) satellites, successfully at broad habitat scales (Lucas et al., 2007, 2011). While several other studies have used Landsat Thematic Mapper (TM) for a wide range of habitat mapping (Varela et al., 2008; Pôças et al., 2011).

While the use of VHR may be preferred by ecologists, there are trade-offs in increasing the spatial resolution to levels that are much finer than the operational scale. Shadows caused by tall objects in the landscape such as buildings or tree canopies can decrease classification accuracies (Fuller, 2005; Nagendra et al., 2010b,a), which can be compensated for with image analysis techniques such as segmentation or adding a shadow class to the classification scheme (Sawaya et al., 2003; Förster and Kleinschmit, 2008; Mücher, 2011). However, other researchers have successfully produced habitat maps at finer operational scale with VHR regardless, such as bogs (Bock et al., 2005a; Charnock, 2016) and ecotones and mosaic areas of acid grassland, scattered bracken and acid flushes (Comber et al., 2010).

Although there is a wide range of remotely sensed data available at a wide range of spatial scales, most habitat mapping is carried out using additional ancillary datasets which

also vary in spatial scale. For example, ancillary datasets on site conditions for the local scale typical of Natura 2000 habitats in Europe very from 1:25,000 to 1:50,000 (e.g. some soil maps) to 1:1,000 to 1:5,000 for some field generated habitat maps and Digital Elevation Models (DEMs) (Nagendra et al., 2013; Weiers et al., 2004; Förster and Kleinschmit, 2008; Lucas et al., 2011). Regardless, ancillary datasets such as altitude, slope and soil type have proved incredibly useful for classifying habitat types that have distinct and defined state factors or clear boundaries such as grassland and agriculture, and can greatly increase classification accuracy (Bock et al., 2005b; Lucas et al., 2007; Förster and Kleinschmit, 2008).

2.4.2 Spectral Resolution

A key factor of remote sensing data is its ability to acquire information beyond the visible wavelengths. Therefore, spectral resolution refers to the number of bands across the electromagnetic spectrum from which a sensor acquires information. The most common term to describe satellite platforms is multispectral as they acquire information in the visible, NIR, SWIR and thermal portions of the spectrum in relatively broad bands (see Figure 2.6). Hyperspectral sensors are also available where these bands are much narrower and can amount to hundreds within the same portion of the spectrum.

The first spaceborne hyperspectral sensor, Hyperion, provides data at 30m spatial resolution but with 196 bands and Thenkabail et al. (2004) found that it significantly outperformed a number of other optical sensors from Landsat to IKONOS, especially in the shortwave infrared portion of the spectrum. Hyperspectral sensors are more popular on airborne platforms however, with several studies using NASA's Airborne Visible/Infrared Imaging Spectrometer (AVIRIS) for monitoring research (Turner et al., 2003; Papeş et al., 2010; Schmidtlein and Sassin, 2004). Another advantage of airborne hyperspectral sen-

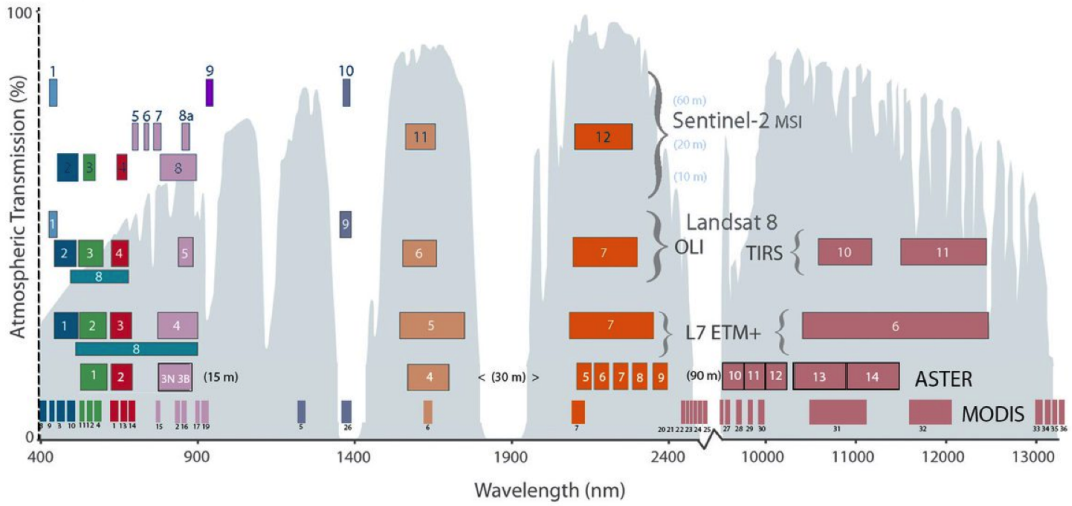

Figure 2.6: Band comparison of multiple sensors across the electromagnetic spectrum (USGS, 2016).

sors is their drastically increased spatial resolution, for example AVIRIS captures data at the 2x2m pixel level. However, airborne data is not routinely acquired and can be particularly expensive to task if integrating into a monitoring system: the cost will always be an important factor for ecological monitoring.

Trade-offs between spatial and spectral resolution can therefore be problematic. For example, Gao (1999) found that Landsat data at 30m spatial resolution was more useful than SPOT data at 10m spatial resolution for discriminating mangrove forests in New Zealand because of the greater spectral resolution and the inclusion of the thermal infrared bands. However, recent VHR satellites such as Worldview-2 and Worldview-3 are beginning to combine high spatial with a higher spectral resolution in the same platform (Nagendra and Rocchini, 2008), opening up more opportunities for habitat mapping and monitoring from remotely sensed data.

2.4.3 Temporal Resolution

Increasing temporal resolution can facilitate the accurate delineation of spectrally similar habitats in areas with seasonal environmental fluctuations, particularly if images are selected during the periods that emphasise any phenological differences (Nagendra, 2001; Nagendra et al., 2013). de Colstoun et al. (2003) found that the discrimination of 11 different land cover types in a recreational park in the USA increased substantially when using multi-season Landsat Enhanced Thematic Mapper Plus (ETM+) imagery.

Changes in the spatial and temporal patterns of vegetation can be used to support the detection of habitat modification and landscape change (Garbulsky et al., 2004). The National Park network in Spain used the NDVI derived from NOAA/AVHRR to assess changes in photosynthetic activity between 1982 and 2006, with the contrast between growing and non-growing seasons increasing over the period (Alcaraz-Segura et al., 2009). Although the coarse spatial resolution (typical of the high temporal resolution sensors required for detailed phenological studies) is not appropriate for the local scale monitoring of individual habitat patches. These products may however, provide early warning of regional scale ecological change and support decisions on the allocations of further resources for more detailed spatial assessments (Nagendra et al., 2013).

2.4.4 Radiometric Resolution

Radiometric resolution refers to colour depth and should be considered when selecting remote sensing data for habitat mapping. A fine radiometric resolution means that the sensor is more sensitive to detecting small differences in reflected or emitted electromagnetic energy (Lillesand et al., 2004). For example, Rama Rao et al. (2007) observed a small but definite increase in classification accuracy when a simulated 12-bit IRS LISS 3 dataset

was used instead of the original 7-bit dataset. Legleiter et al. (2002) also found a slight improvement of the overall accuracy in the classification of stream habitats when using data of a higher radiometric resolution, although this was secondary to the improvement delivered by increase in spectral and spatial resolution (Nagendra et al., 2013).

2.5 Habitat Mapping with Remote Sensing

Remote sensing has enormous potential as a source of information on landscape patterns, habitats and dominant species (Bock et al., 2005b). Many advantages of remote sensing data for improving the efficiency for habitat mapping and monitoring have already been discussed, and similar to the advantages mentioned in (Alexandridis et al., 2009), can be summarised as:

- HR coverage of large areas at low cost;
- Observation at several non-visible wavelengths of the spectrum;
- More consistent processing across a study area.

Mapping of broad habitat types as generic land cover classes is a common practice using remote sensing and is done on a very coarse scale (Wulder et al., 2004). At a global scale, land cover mapping has been accomplished by utilising the Moderate Resolution Imaging Spectroradiometer (MODIS) satellite at 500m resolution (Friedl et al., 2010), while country and regional level land cover classifications have been accomplished using medium resolution sensors. The two main types of satellite imagery at this resolution, which are more commonly used in ecological remote sensing are the Landsat images and the SPOT system neither of which, with resolutions of 30 m and 10 m respectively, are capable of providing the quality needed for the whole range of habitats mapped (Unit, 1990). This is particularly true if also trying to detect components associated with habitat

condition, always a requirement for conservation management and reporting.

The first satellite-derived pixel-based land cover map was generated using Landsat TM in 1990 as part of the United Kingdom Land Cover Map (UK LCM) (Fuller et al., 1994). Another map was generated in 2000 using an object-based approach (Fuller et al., 2002) but these maps have been used reluctantly by the ecological community due to, mainly, low resolutions and inaccuracies, but also due to the lack of understanding amongst users of the limitations of remote sensing. The updating of the Phase 1 survey in Wales in 2010 (Lucas et al., 2011) also used EO data in the form of SPOT-5, ASTER and IRS time-series as a repeat survey was deemed unlikely. However, many of the previous problems still existed even with higher resolutions and better accuracies. On the other hand, this study created the first national habitat map (as opposed to land cover) generated through the implementation of EO data, and can potentially be adapted to allow continual monitoring of the extent and condition of habitats (Lucas et al., 2011).

The prospect of monitoring vegetation phenology from EO platforms is also a key area of interest when discussing the use of EO data and habitat monitoring. With the emergence of long time data records from sensors it is now possible to observe variations in phenological parameters, such as length of the growing season. Visible changes in vegetation phenology may be important indicators of climactic change, as phenology responds to the effect of several physiological and biogeochemical factors of the ecosystem (Menzel, 2002). For example, time-series NDVI data have been used to indicate changes in LAI globally, with these reflecting human-induced and natural events and processes, including those related to climactic fluctuation (Liu et al., 2010). Phenology is also important for estimating biological productivity, understanding land-atmosphere interactions and the management of vegetative resources (Lieth, 1971; Taylor Jr, 1974; Sarmiento and Monasterio, 1983). Therefore, it is a key factor in mapping to the species level using EO data and also essential for monitoring change. Additionally, timing the acquisition of

remotely sensed datasets to coincide with critical phenological stages of flowering or leaf senescence is very important when mapping invasive species (He et al., 2011).

It is also important to have well designed programmes of field data collection that maximise the use of data for remote sensing interpretation and conservation assessments. *In situ* field sampling networks therefore, need to be designed in combination with remote sensing using, for instance, stratified sampling designs to carefully assess species distributions across different habitat types and enhance interpretative power (Nagendra, 2001). Unless the spatial grain, extent and timing of remote sensing data *in situ* data and models are well matched, the robustness of conclusions on management effectiveness, and the interpretive power of the analytical techniques used, will be limited. Remote sensing interpretation needs to be grounded in field data, as this is critical for effective adaptive management and monitoring (Nagendra et al., 2013).

2.5.1 Protected Area Mapping and Monitoring

Over the last few years, it has been recognised that remote sensing is an essential tool for evaluating the implementation of environmental policies (Mayer and Lopez, 2011), and several European projects and numerous scientific studies have addressed the issue of mapping and monitoring protected habitats via remote sensing for derivation of conservation status. The translation of these scientific studies to operational use is less common, and the multitude of sensors and applied methods available have impeded on feasibility in this context (Corbane et al., 2015). In the UK, some innovative work has been done to address this problem in the form of the Crick Framework. Figure 2.7 shows the tier system designed to group habitats into classes based on the feasibility of remote sensing techniques to provide the right kind of information.

Table 2.2 summarises the use of remote sensing for protected area mapping and monitor-

Figure 2.7: The Crick Framework tier system (Medcalf et al., 2011).

ing in relation to information needed to report on conservation status. The vast majority of the studies mentioned have used Landsat TM/ETM+ images which proves that this sensor really has been the workhorse of land cover monitoring, and should continue to do so with an invaluable historical record that now covers four decades (Nagendra et al., 2013). Techniques have also improved and by combining these data with ancillary data or active sensors, more detailed land cover boundaries are possible at higher accuracies (Kasischke et al., 1997; Dobson et al., 1992; Hatunen et al., 2008; Ali et al., 2013; Bargiel, 2013), especially when mapping less complex habitat mosaics (Lengyel et al., 2008).

In recent years, VHR datasets have been increasing in popularity as more habitat categories can often be resolved, but the lack of shortwave-infrared band in these datasets has significantly hampered their potential for monitoring complex environments. However, sensor such as Worldview-2 and Worldview-3, with additional coastal, yellow, red edge and near infrared bands is anticipated to provide benefits over other VHR sensors such as IKONOS, Quickbird and GeoEye. Techniques and software for processing these data,

Table 2.2: Summary of active and passive remote sensing data useful for protected area monitoring (adapted from Nagendra et al. (2013) and Corbane et al. (2015)).

Sensor	Habitat mapping and change detection	Assessing habitat degradation	Biodiversity assessment	Tracking pressures and threats
Coarse spatial resolution (e.g., MODIS, AVHRR)	Only useful in landscapes with large vegetation patches (Carrão et al., 2008) including ancillary data (Friedl et al., 2010)	Near-real time alerts of deforestation in threatened forests (e.g., Amazon; (Joseph et al., 2011); Mapping overall changes in photosynthetic activity to provide early warnings or regional ecological and climate change (Liu et al., 2010) (Alcaraz-Segura et al., 2009)	Not very useful	Tracking fires and changes in overall photosynthetic activity (Boyd et al., 2002); (Lentile et al., 2006); (Alcaraz-Segura et al., 2009)
Medium to high spatial resolution (e.g., Landsat SPOT, Sentinel-2)	Captures broad extent and spatial patterns of habitats (de Colstoun et al., 2003); (Lucas et al., 2007); (Varela et al., 2008); (Pôças et al., 2011) With multi-seasonal imagery for forests (Foody and Hill, 1996); grasslands (Price et al., 2002); heathlands (Morán-Ordóñez et al., 2012);	Broad scale loss and degradation of habitats (e.g., semi-arid vegetation) degraded through desertification); useful for habitat suitability models (Muldavin et al., 2001); (Tong et al., 2004; Ingram et al., 2005); (Théau et al., 2005)	Indicators of overall species richness and diversity (Feeley et al., 2005); (Gillespie, 2005; Torres et al., 2010) (Costanza et al., 2011)	Identifying disturbances in protected areas (e.g., urbanisation, fire, agriculture, alien species) (Asner et al., 2004); (DeFries et al., 2005; Nunes et al., 2005); (Blanco et al., 2009)
High temporal resolution data (multi-season data or images corresponding to specific seasons)	Separation of habitat types spectrally similar in single date imagery (Lucas et al., 2007, 2011)	Intra-annual variances in retrieved measures of biophysical properties (e.g., productivity; (Rouget et al., 2006)	Information on invasive species and other species of interest (e.g., using images acquired corresponding to critical phenological stages of flowering or leaf senescence (Everitt et al., 2005); (Ramsey III et al., 2005); (He et al., 2011)	Detection of specific events (e.g., selective logging, fires) achieved through greater frequency of observation (Nagendra et al., 2013)
Very high spatial resolution (e.g., IKONOS, Quickbird, Worldview-2)	Mapping successional fine-scale homogeneous habitat, ecotones and mosaic areas (Bock et al., 2005b; Comber et al., 2010), but with challenges of mixed pixel and object shadowing	Identifying fine scale degradation in forests (Souza et al., 2003)	Indicators of overall species richness and diversity (Kumar et al., 2009) (Hall et al., 2012); Delineation of tree crowns to species level (Everitt et al., 2005; Somodi et al., 2012). Problems of mixed pixels and shadowing (Fuller, 2005; Lucas et al., 2008)	Detection of fine-scale disturbances (e.g., pollution, tree falls, pest attacks; (Asner et al., 2002); (Fuller, 2006; Lee et al., 2010)
Hyperspectral (e.g., ASTER, HyMap, AVIRIS, Hyperion)	Distinguishing habitat types in low-contrast environments, and identifying forest successional classes (Papeş et al., 2010); (Thenkabail et al., 2004; Oldeland et al., 2010);	Assessment of habitat stress based on changes in chemical composition of foliage, which can be related to parameters such as nutrient deficiency and changes in soil (Townsend et al., 2008); (Joseph et al., 2011)	Differentiation of plant communities that are specifically similar (Ishii et al., 2009); (Ghiyamat and Shafri, 2010; Ward et al., 2013); (Sluiter and Pebesma, 2010)	Identifying disturbances (e.g., pest attacks that lead to changes in foliage colour, and fine-scale modification in grass biomass due to disturbances in grazing (Breyer, 2009)
Active remote sensing data (e.g., SAR LiDAR)	Discriminating structurally complex habitats (e.g., forests) based on 3D structure, either alone or in combination with optical remote sensing (Treuhaft et al., 2004; Rahman and Sumantyo, 2010) (Karjalainen et al., 2008; Zhu et al., 2012)	Monitoring habitat degradation, including within canopy (Kuplich, 2006; Hyde et al., 2006); (Waser et al., 2008; Graf et al., 2009)	Floral and faunal diversity in habitats with complex three-dimensional structure (Asner et al., 2008; Koch, 2010); (Vauhkonen et al., 2010)	Detecting dead standing trees, patterns of clearing and damage caused by fire (Siegert et al., 2001); (Lucas et al., 2008)

in addition to SAR and LiDAR data, are also likely to become more available in future years, and the increase in open source material will benefit many managers of protected areas in countries where funding is more limited (Nagendra et al., 2013). However, it is recognised that more effort should be put into developing a coherent and operational method which produces most, or all, relevant parameters to assess conservation status in a single workflow (Corbane et al., 2015).

For VHR imagery is the use of object based image analysis (OBIA) is generally considered the standard approach to image classification (Nagendra et al., 2013; Lucas et al., 2015). The disadvantages of a VHR spatial resolution is that the imagery can be noisy and image segmentation to generate objects is seen as a way to combat this issue. As many image segmentation techniques generate objects based on homogeneous spectral values of pixels based on the assumption that landscape features have similar spectral properties, the method works well in many studies that delineate land cover features (Blaschke et al., 2001). However, when trying to validate boundaries of objects generated from EO data, especially for ecological purposes where ecotones are important features in the landscape, generating objects at an appropriate scale for mapping that also represents the area of interest appropriately is particularly difficult. Another feature in complex landscapes are mosaic structures of habitats, which are also common but just as difficult to capture within object boundaries generated from EO data. For this reason, it was decided that the minimum mapping unit available, which are pixels, will be used in this study.

2.5.2 Annex I Habitat Mapping and Monitoring

The use of remote sensing for providing some of the information required for reporting on Article 17 of the Habitat's Directive (Griffiths et al., 1997) is still very limited in an operational sense (Borre et al., 2011). For the 2007 report, 18 out of 25 member states

indicated having used remote sensing data, in conjunction with other methods. This relates to estimating the area of 130 different habitat types in 382 habitat conservation status assessments (14% of all habitat assessments). Experts in Belgium, Ireland, Luxembourg, Spain and Sweden confirm that the use of remote sensing data was largely due to visual interpretation of red, green and blue (RGB), and occasionally infrared, images (Trullén and Alonso, 2007; Skånes et al., 2007), but information on the use of remote sensing from other member states is hard to come by. Borre et al. (2011) assumes that, as the use of aerial photography is widely integrated into vegetation and habitat mapping, the same situation applies to many other member states.

Table 2.3 shows the results of entries in the 'methods used' field, which is required when writing the report for Article 17. The administrations generally considered ground survey to deliver good or moderate quality data, while remote sensing was seen as moderately reliable, which suggests that nature conservation bodies have less confidence in remote sensing than in field work (Borre et al., 2011). However, what is considered remote sensing in this section is mostly visual interpretation of RGB images only, and this view is limited to this method and does not apply to remote sensing as defined in this chapter. It is also interesting to note that most studies that propose advanced semi-automated or automated remote sensing methods also emphasise the need for *in situ* data, while others state the need to integrate expert knowledge into workflows. It is likely, therefore, that any operational system in the future will include elements of all three methods outlined in Table 2.3.

2.6 Conclusions

Data continuity, affordability and access are no longer barriers to the uptake of remote sensing in ecological communities with open access and government funded infrastruc-

Table 2.3: Contingency table of methods used and perceived data quality for habitat area estimation, as reported by member states in the Article 17 reporting on habitat conservation status in 2007 (Convention on the Conservation of European Wildlife and Natural Habitats, 1979).

Used method	Quality of data			
	Good	Moderate	Poor	Total
Ground survey	421	415	72	908
Remote sensing	27	236	31	294
Expert opinion	22	407	457	886
Total	470	1058	560	2088

ture for EO. However, conservation organisations that do not necessarily have the skill force for handling EO data yet, are presented with maps, often of land cover, which do not adequately represent the habitats of importance to biodiversity. While a large number of maps exist at various scales, these are often of limited utility and hence may not be adopted. Furthermore, many maps are also generated once, with no capacity for updates and, where different sensor data are used for classification, inconsistencies occur hence the detection of changes is often problematic (Borre et al., in press). The development of habitat and species monitoring that facilitates routine mapping and monitoring is therefore essential for operational purposes (Lucas et al., 2011; Nagendra et al., 2013).

Issues of scale will always exist and better decisions need to be made regarding spatial and operational scale in accord with the requirements of the project before making intelligent decisions on the kind of EO data that is appropriate. Although high to medium resolution sensors such as Landsat and Sentinel-2 are set to continue to be the workforce in environmental monitoring, the increased spectral resolution of Worldview-2, with the VHR resolution is deemed to be the most appropriate sensor for mapping at the spatial scale of this project.

In conclusion, remote sensing can play a key role in characterising and mapping habitat within and surrounding protected areas and ultimately assisting their management. These data can be used to inform on changes in the landscape which may have an adverse impact

on biodiversity but also allow for long term restoration of habitats (e.g. through replanting, establishment of corridors and/or promotion of regeneration) and protection from adverse effects of factors such as climate change (Jones et al., 2009). Most importantly, however, these data can provide managers of protected areas with spatial and temporal information on the extent and condition of habitats and influence their response to change over varying time scales.

The use of remote sensing need to be made standard practice which has not happened yet despite all the ongoing advancement in this area and much discussion on its utility. The technical challenges faced by managers is clearly a barrier still, but the answer lies in better integration between the *in situ* data and expert knowledge provided by local ecologists and the technical expertise of remote sensing analysts. There is, therefore, a need for ecologists, conservation biologists, policy makers, protected area managers, conservation consultants and practitioners to be provided with a basic technical understanding of remote sensing. This would allow the conservationists to interact with remote sensing analysts and clarify their requirements before being advised on the most appropriate images and data interpretation processes to meet their monitoring and planning requirements (Nagendra et al., 2013). From the conservationists' perspective, the repeatability of the remote sensing protocols on the same site (i.e. pre-processing standards) and the transferability of these protocols to other sites (amount of site specific training data needed) are key considerations (Borre et al., in press), and knowing this will help focus the research in remote sensing projects.

Chapter 3

Study Sites

3.1 The Welsh Coastline

Coastal and near shore environments contain a wide range of habitats that are often characterised by high biodiversity, including rocky cliffs, shore platforms, sandy beaches, dunes, salt marshes and mudflats. Wales has a total coastline length of approximately 1,600km (Brazier et al., 2007). Geologically, north and west Wales are mostly composed of relatively hard rocks such as slates, mudstones and sandstones, while south and south-east Wales is dominated by softer rocks such as shales, coal measures and limestone (Webb et al., 2010). The Welsh coastline supports a wealth of habitats and c.70% is protected by environmental or conservation designations (Williams and Davies, 2001). This study focuses on a sand dune ecosystem in south east Wales, called Kenfig Burrows, and a section of the rocky cliff formation situated on the Pembrokeshire coast near Castlemartin.

3.2 Kenfig

3.2.1 Sand Dune Systems

Sand dune systems are an important component of the Welsh coastal landscape but the total sand dune resource in Wales has experienced long-term decline and fragmentation as a result of urban and industrial development, golf course construction, caravan park development and planting of coniferous plantations (Pye and Blott, 2009). Sand dune stabilisation and the decline of important pioneer habitats is not unique to Wales, many dune systems across western Europe have experienced reductions in dune mobility and in the extent of bare sand over the past 60 years. The stabilisation of dunes by successional processes has reached such extremes that the proportion of bare sand has fallen below 5% in many systems (Webb et al., 2010). Concerns about the negative impact of this trend on biodiversity are justified by the disappearance of some rare species entirely from several dune systems, including those bordering the Bristol Channel (Provoost et al., 2011).

The most important factors influencing the dynamism of sand dune systems are wind energy, sand availability and the degree of vegetation cover. There are several other factors that influence vegetation cover in particular, from climactic, such as temperature and rainfall, to human intervention such as grazing pressure, physical disturbances by trampling or other activities and management measures. The mobility of sand is determined by a balance between a number of drivers outlined in Table 3.1. This balancing act naturally changes over time, where systems go through episodes of mobility and stabilisation (Webb et al., 2010).

Recent UK climate change projections state that it is highly unlikely that the climatic conditions needed to reverse the stabilisation trend will occur naturally for the foreseeable future. Instead they are more likely to aid dune stabilisation with climate warming and

Table 3.1: Measures of dune mobility and stability drivers (Webb et al., 2010).

Dune Mobility Drivers	Dune Stability Drivers
High wind speeds	Low wind speeds
Low rainfall	High rainfall
High rates of evaporation	Low rates of evaporation
Short growing season	Long growing season
Nutrient deficiency which limits plant growth	Nutrient excess which promotes plant growth
Large source of available sand	Small source of available sand
Coastal erosion and frontal dune blowout development	Coastal progradation and new foredune ridge development
High grazing pressure	Low grazing pressure
High visitor pressure	Low visitor pressure
Lack of dune stabilisation measures	Effective dune stabilisation measure

an increase in rainfall promoting vegetation growth. Increasing levels of rain will also reduce the potential for windblown sand. Therefore, conservation managers are faced with a difficult choice. Either do nothing and allow the negative impacts on biodiversity to continue, or intervene and attempt to reverse the trend (Pye and Blott, 2009).

3.2.2 Site Description

Kenfig Burrows is located between Port Talbot and Porthcawl on the south east side of Swansea Bay (Figure 3.1). The water table within the dune system at Kenfig is relatively high and significant areas of dune slacks are flooded during the winter months. For this reason, the wet slacks here support a notably rich flora. The mean monthly rainfall in coastal areas in south Wales is approximately 120mm between October and January, falling to 60 mm between April and July. Mean monthly temperatures (and evaporation) reach a minimum of about 8°C in January and February and a maximum of 21°C in July and August (Figure 3.2).

The site is approximately 4 km long and 2 km wide, totalling over 600 ha. Approximately

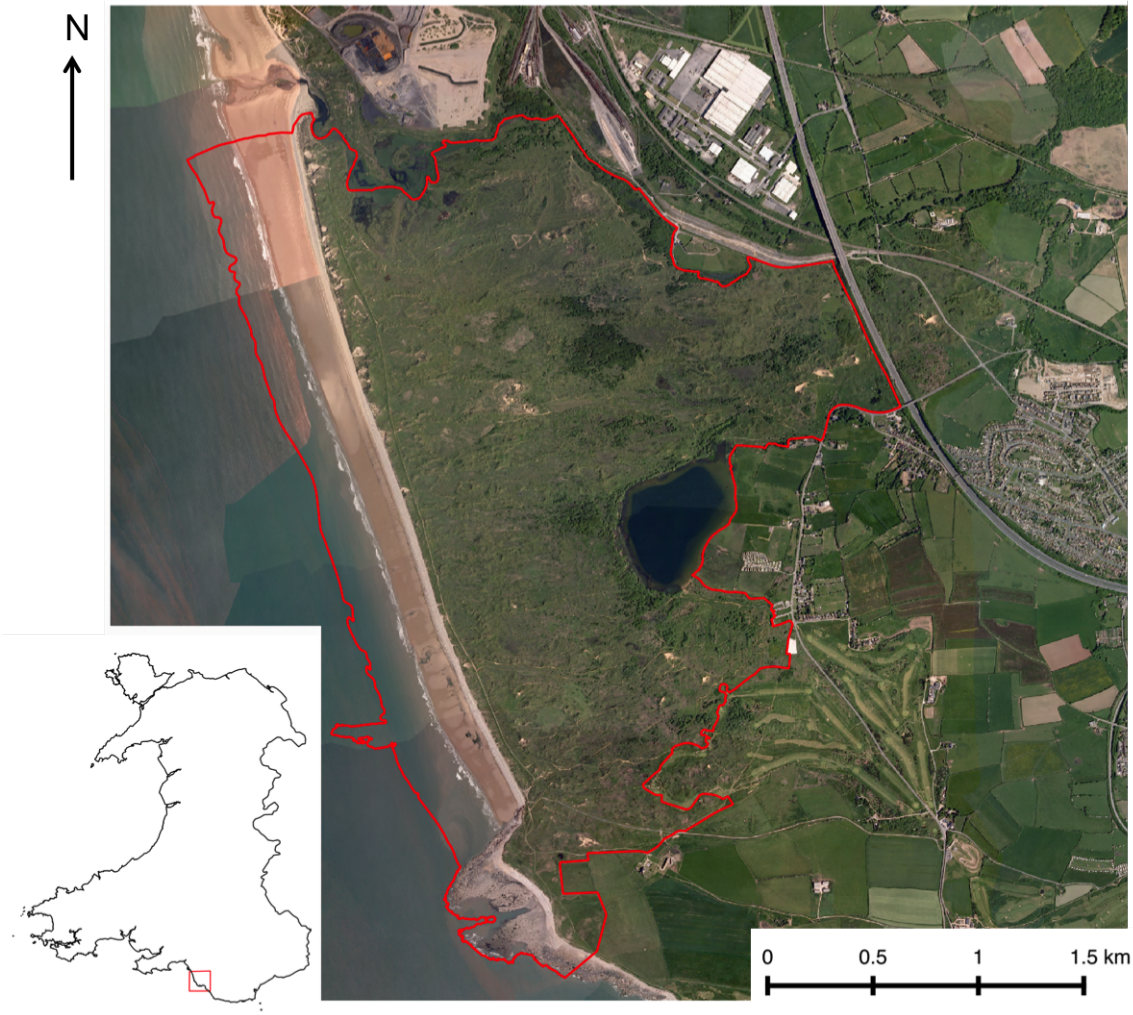

Figure 3.1: Location of Kenfig Burrows site and aerial photography of the site acquired in 2006 before any major management measures were performed. The extent (in red) is the SAC boundary. Note the near absence of bare sand.

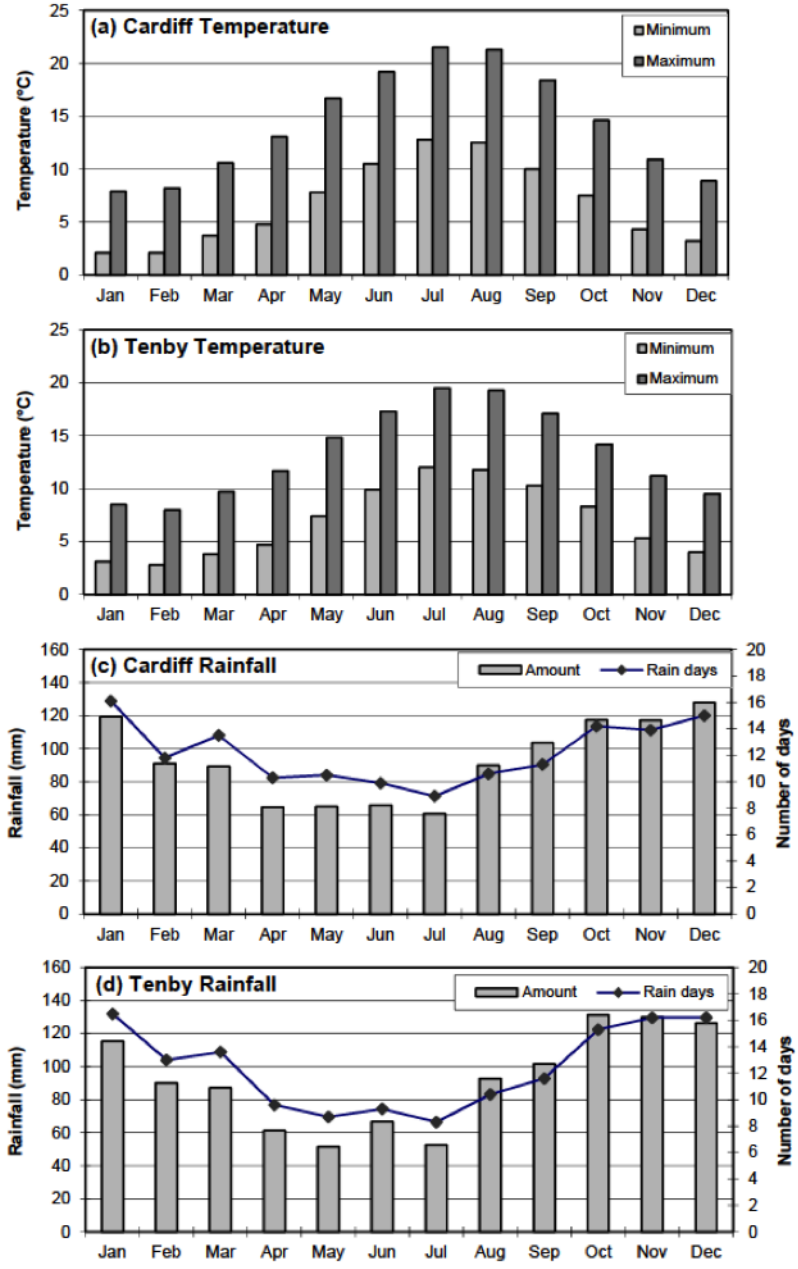

Figure 3.2: Average monthly minimum and maximum temperature for the period 1971-2000 at: (a) Cardiff and (b) Tenby. Average monthly rainfall and number of rain days for the period 1971-2000 at (c) Cardiff and (d) Tenby. Data source:Met Office. (Pye and Saye, 2005).

57% of the site comprises sand dunes, supporting a broad range of plant community types. Natural processes largely govern the dune areas, which grade from shifting embryonic dunes with an abundance of bare sand to a more fixed stable dune community. This range of communities includes a high proportion of sparsely vegetated and open dune slacks or wet hollows. The condition of these habitats depend on a number of factors including the periodicity of inundation, nutrient status of the aquatic system and quantity of water, as well as the management regime (CCW, 2013a).

3.2.3 Habitats and Site Designations

The site has been designated for various reasons under different legislations. Kenfig has both National Nature Reserve (NNR) and SSSI status and therefore has legal requirements for monitoring conservation values under the UK's Wildlife and Countryside Act. The site is also a SAC and is part of the Natura 2000 programme which has legal requirements under the EC's Habitats Directive (Convention on the Conservation of European Wildlife and Natural Habitats, 1979). The site is currently managed by Bridgend Borough Council on behalf of Natural Resources Wales.

Table 3.2: Designated special features for Kenfig (CCW, 2013a).

Designation	Feature
SAC Annex I habitats that are primary reason for the selection of this site	2130 Fixed dunes with herbaceous vegetation ('grey dunes'); 2170 Dunes with *Salix repens ssp. argentea (Salicion arenariae)*; 2190 Humid dune slacks; 3140 Hard oligo-mesotrophic waters with benthic vegetation *Chara spp.*
Annex I habitats present as a qualifying feature, but not primary reason for selection of this site	1330 Atlantic salt meadows *(Glauco-Puccinellietalia maritimae)*
Annex II species that are a primary reason for the selection of this site	1395 Petalwort *Petalophyllum ralfsii*; 1903 Fen orchid *Liparis loeselii*

Table 3.2 shows all the habitats that are responsible for the site's designation as a SAC. One of the main reasons for its designation is the presence of a relatively rare habitat on a UK and European scale, particularly the successionally younger phases of humid dune slack development, which are typical of more mobile dune systems. Kenfig is therefore, one of the most important sites in the UK of the humid dune slacks (2190) habitat and it now hosts the entire UK population of the sand dune variety of fen orchid *Liparis loeselii var. ovata* (the sand dune form) (Pye and Blott, 2011). The site is also an important site for the petalwort *Petalophyllum ralfsii*, which also prefers the successionally young dune slack habitat (Figure 3.3).

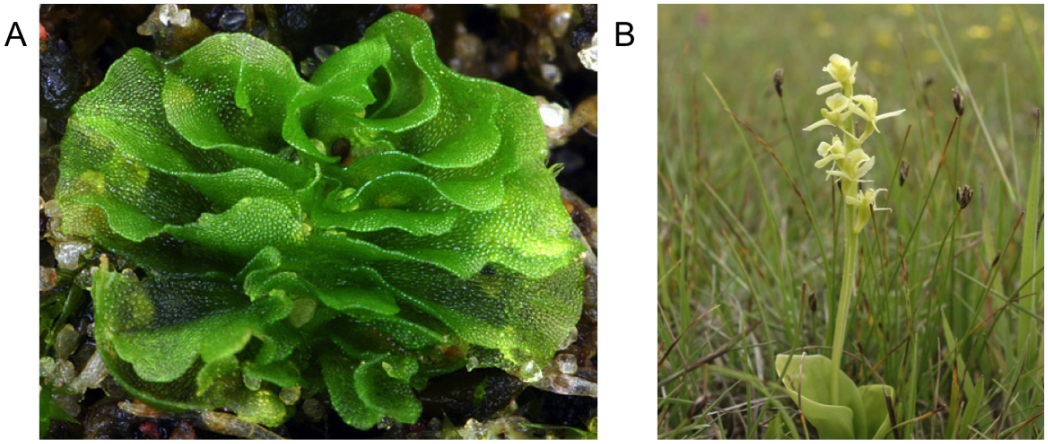

Figure 3.3: Annex II species present at Kenfig. A) petalwort *Petalophyllum ralfsii*; B) fen orchid *Liparis loeselii*.

Figure 3.4 shows the distribution of habitats according to the Phase 1 map of Wales. This map makes no reference to Annex I habitats but it does provide a rough idea of the location and extent of habitats such as the humid dune slacks. Some of the Annex I habitats are difficult to separate, notably the 'humid dune slacks' and 'dunes with *Salix repens ssp. argentea*' habitats. For this reason they are lumped together for practical conservation and monitoring purposes at Kenfig (CCW, 2013a). The humid dune slack habitat includes both successionally young, species-rich and mature slacks, while the dunes with *Salix repens spp, argentea* equate to drier areas of mature dune slacks, including the so-called

'hedgehog dunes'.

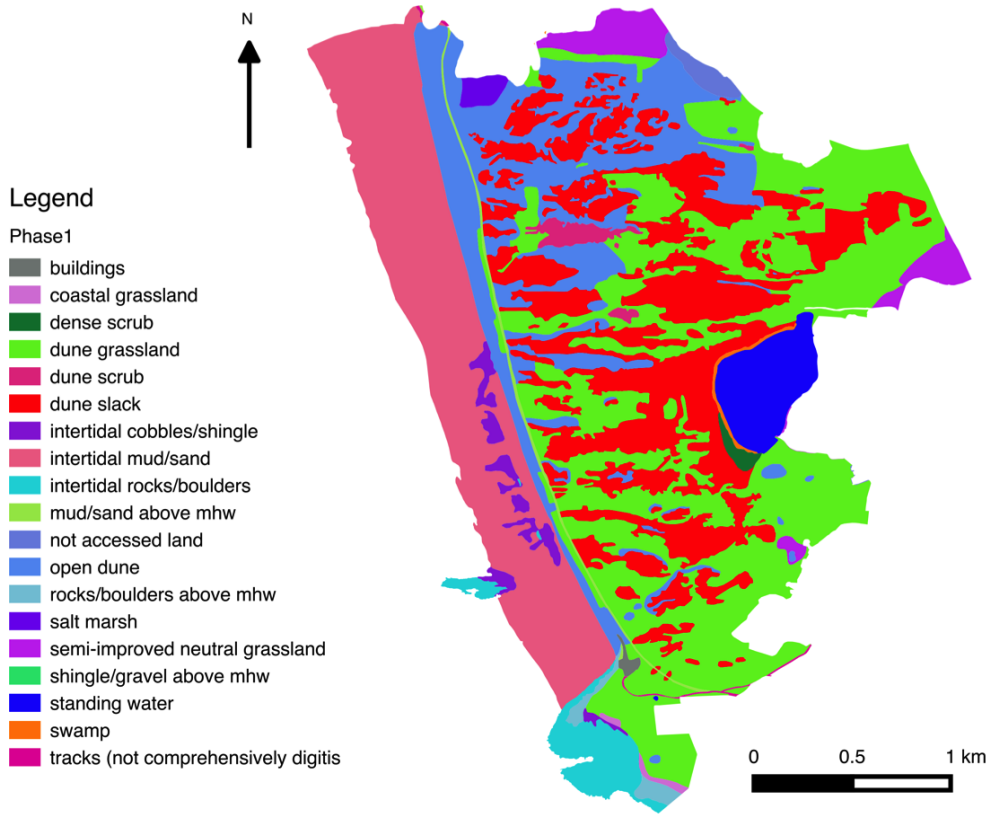

Figure 3.4: Phase 1 map of Kenfig. Data distributed by NRW.

For conservation management and monitoring purposes, the Humid Dune Slack habitat can be split into four recognisable successional phases: embryo slack, successionally-young slack, orchid-rich slack and mature slack. Embryo slack is characterised by >25% bare sand with clonal patches of *Salix repens*, and the presence of *Carex arenaria*, *Sagina nodosa* and *Juncus articulates*. Successionally-young slack is characterised by the presence of 5%-25% open sand and thalloid liverworts, and a suite of stress tolerating species (Grime et al., 2014) including *Equisetum variegatum*, *Carex viridula* and *Eleocharis quinqueflora*. Orchid-rich slack is characterised by a species-rich closed sward typically with several species of orchid well represented, including *Epipactis palustris*, *Dactylorhiza incarnata* and *Dactylorhiza praetermissa*. Mature slack vegetation is typically species-poor

and dominated by *Salix repens*, *Carex nigra*, *Calamagrostis epigejos*, *Juncus* spp, or any combination of these (CCW, 2013a).

The fixed dunes habitat class also follows a successional sequence from successionally young through to mature. The successionally-young grassland is declining as a consequence of successional processes and is characterised by bare sand and/or the moss Tortulla ruraliformis, and the presence of a suite of stress tolerating species including *Thymus polytrichus*, *Phleum arenarium*, *Anthyllis vulneraria* and *Viola tricolor*. The more species rich closed swards are characterised by species such as *Lotus corniculatus*, *Ranunculus bulbosa* and *Trifolium arvense*. This species-rich grassland then succeeds to species-poor rank grassland typically dominated by *Arrhenatherum elatius* and/or Dactylis glomerata. A number of negative indicator species have been identified as early warnings of key factors such as overgrazing, over-stabilisation or eutrophication: these include *Rosa pimpinellifolia* >50cm in height, *Chamerion angustifolium* and *Heracleum sphondylium* (CCW, 2013a).

3.2.4 History of Change

Limited changes have occurred to the position of the coastline at Kenfig since 1876, although there is a slow long-term trend of erosion (Pye and Saye, 2005). However, dramatic changes have been witnessed inland particularly with the extent of bare sand. Figure 3.5 shows the amount of bare sand present at Kenfig during the 1940s. Analysis from Ettrich (2013), who used Landsat data from the 1970s onwards to track changes in bare sand, also shows the rate at which dune stabilisation occurred at Kenfig in that period. The dunes were fairly stable in the south of the site for some time before the 1970s but a large proportion in the north still showed a vast extent of bare sand. This is evident in the type of vegetation present on these respective areas. Areas of new sand accumulation

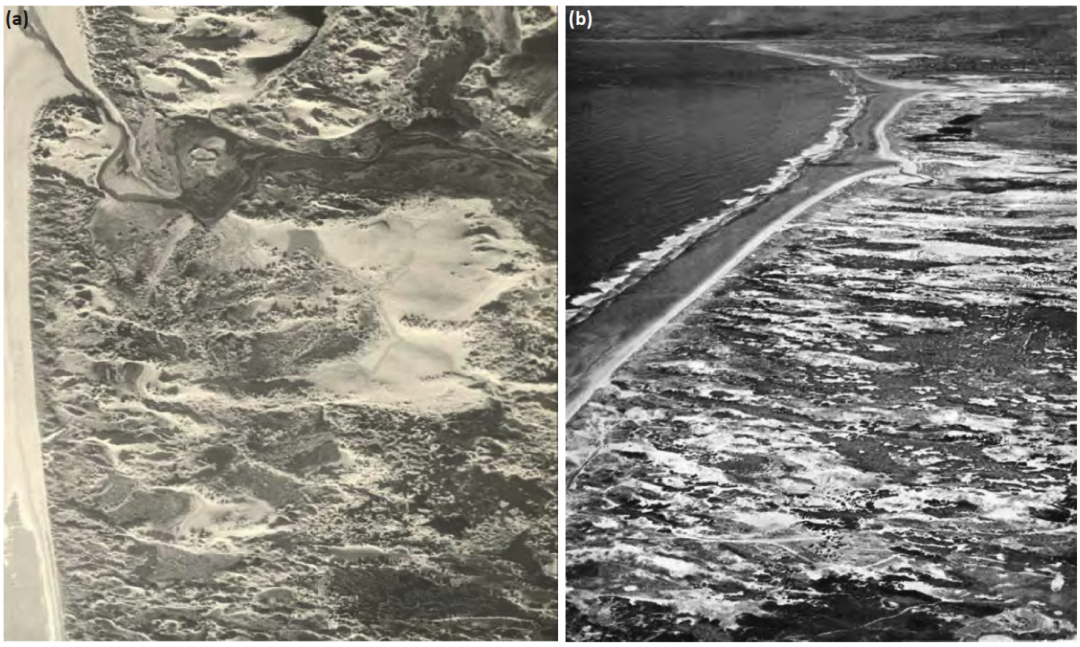

Figure 3.5: Historical air photographs of Kenfig Burrows: (a) vertical photograph of the northern end of the system, showing a large area of bare sand near the outlet of the Afon Cynffig, taken in 1946; (b) oblique photograph, looking north-west, taken in 1948 (Steers, 1946). At this time, virtually all of the vegetation on the site would have been considered to be in the successionally-young stages of development.

are largely vegetated by marram communities, which is characterised as one of the early stages of stabilisation in sand dune systems. In the south, more stable sand dunes are dominated by *Festuca* grassland with extensive dry *Salix*, *Calluna* and *Salix*-dominated slacks (Hurford, 2006).

3.2.5 Management

The development of thick grass swards and scrub presents an increasing problem at Kenfig and there is a serious risk to the condition and even the existence of many designated habitats and species (Webb et al., 2010). For example, at Kenfig, where c.25% of the UK population of the fen orchid *Liparis loeselii* (and 100% of the dune variety) resides, there

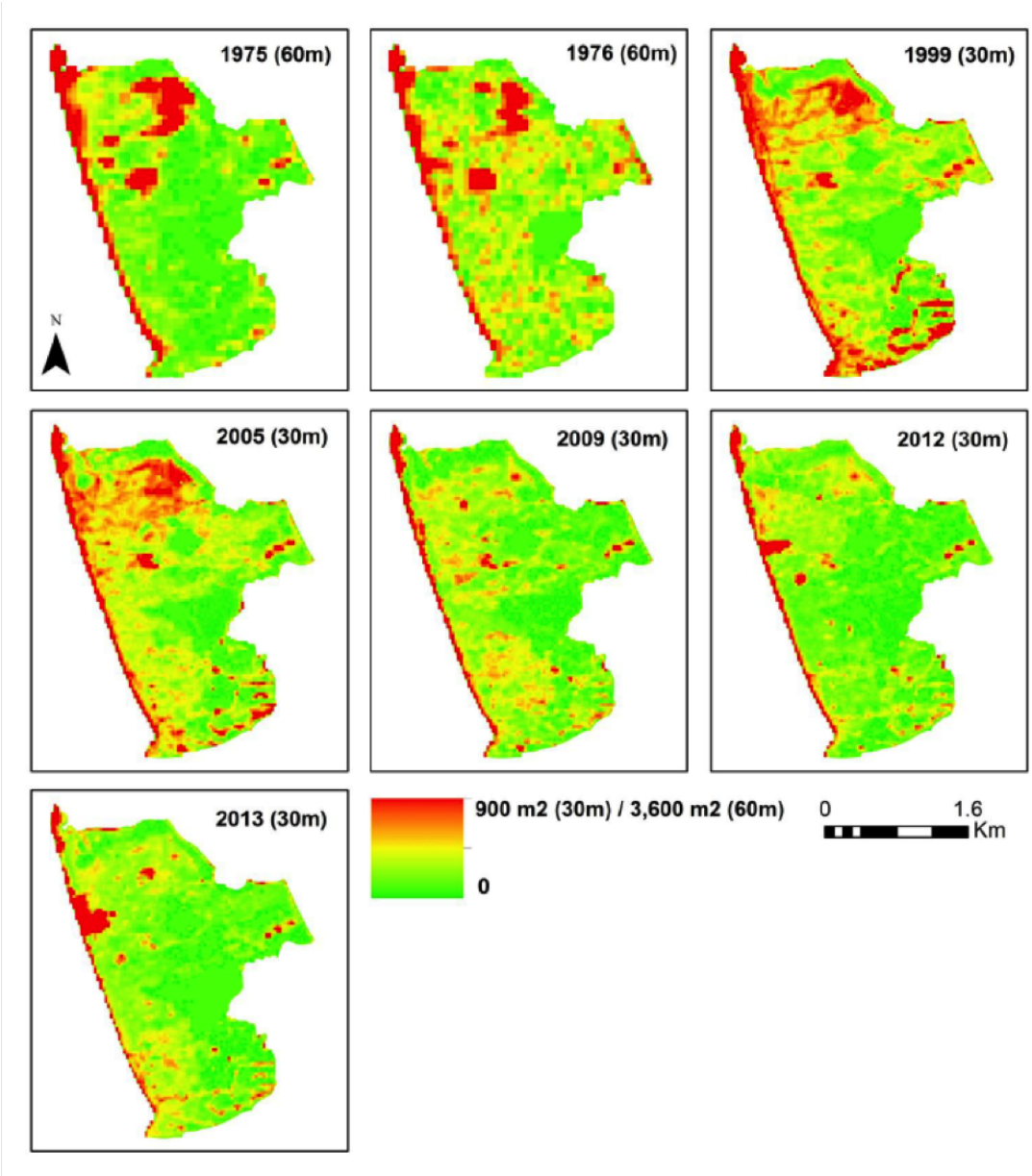

Figure 3.6: Change in bare sand abundance 1975 to 2013. Spatial resolution of Landsat images in brackets (Ettrich, 2013).

has been a marked reduction in its population numbers, despite management interventions such as stock grazing, mowing and excavation of artificial scrapes. Kenfig has a rich history of management interventions over the past couple of decades to try and reverse the stabilisation of the sand dune system (Table 3.3).

Table 3.3: Biodiversity management at Kenfig Burrows (Adapted from Ettrich (2013)).

Practice	Initiation Year	Source	Effect
Slack Mowing	1994	Rhind and Jones (1999)	Increase in the number of fen orchids
Sand rejuvenation of Sker Beach	2000	Ltd (2000)	No expected formation of embryo dunes
Scrub control	2000	Kenfig Website (2013)	Reduction of Sea Buckthorn
Creation of bare sand areas	2001	Kenfig Website (2013)	Re-establishment of petalwort
Increased intensity of grazing	2006	Pye and Blott (2011)	Limited success resulting in a massive decline of fen orchid population
Artificial enlargement of blowouts	2010	Pye and Blott (2011)	Limited success
Creation of sand corridor	2012	Pye and Blott (2011)	Limited success
Artificial enlargement of blowouts	2013		Unknown

Slack mowing, managed by Bridgend Borough Council, combined with stock grazing occurs on a regular cycle at Kenfig. The blowout enlargements and rejuvenation areas at Kenfig are trial management interventions that have the potential to improve the mobility of sand at Kenfig, though any sand movement to date has been local in nature. The fen orchid restoration scrapes have been mores successful in recreating successionally-young humid dune slack vegetation at Kenfig, and c.15% of these had been recolonised by fen orchids at the time of writing. These scrapes are unlikely to increase sand mobility of the site, but they do provide more opportunities for the spread of the stress tolerating species associated with the successionally-young slack habitats. Increased grazing intensity simulated the building of a 3.7 km fence in the north of the site, which excludes areas of the dune system. However, this has had a negligible impact on the availability of bare sand (Pye and Blott, 2011).

3.3 Castlemartin

3.3.1 Site Description

Castlemartin is located on the coast of south Pembrokeshire (Figure 3.7). The area is very exposed and consists of a broad expanse of rolling lowland grassland and heathlands adjoining coastal cliffs. The Ministry of Defence (MOD) currently manages a large proportion of the site and this MOD land is used for both live firing and dry military training. The climate of the area is fairly similar to that described for Kenfig (Figure 3.2). The site is approximately 8 km long but very narrow. Semi natural habitats on site include dry heath, sea cliff vegetation, rocky and sandy shores. The area supports numerous birds including peregrine falcon *Falco peregrinus*, chough *Pyrrhocorax pyrrhocorax* and skylark *Alauda arvensis*, and is home to the largest sea bird colonies on the mainland of south west Britain. Other important species include greater horseshoe bat *Rhinolophus ferrumequinum*, marsh fritillary *Euphydryas aurinia*and other rare invertebrates (Pembrokeshire National Park, 2011). Castlemartin is also a site of geological importance with distinctive coastal platforms averaging 50m above sea level developed on carboniferous limestone. Some of those characteristic geomorphological features include caves, stacks and arches (Figure 3.8).

3.3.2 Habitat and Site Designations

Castlemartin is part of several designated areas. The Limestone Coast of South West Wales SAC comprises a series of SSSIs stretching from Castlemartin at the western end of southern Pembrokeshire to the Bishopston Valley on the south east coast of Gower. Some of the SSSIs that underpin the SAC have management units that extend beyond the

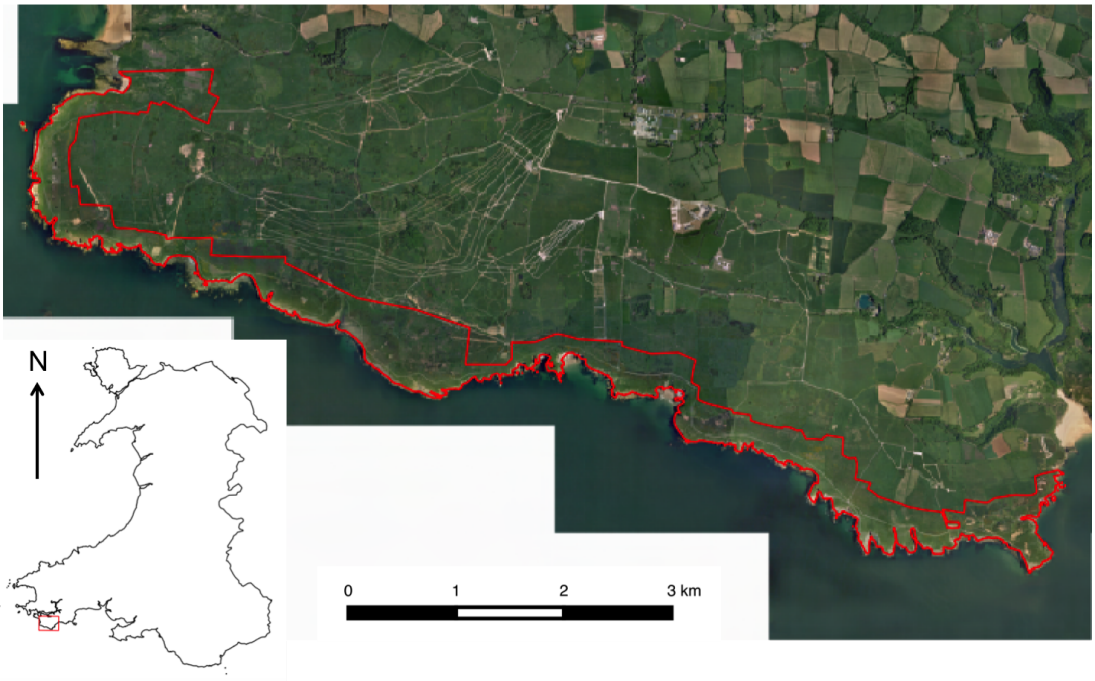

Figure 3.7: Location of Castlemartin site and aerial photography of the site acquired in 2006. The extent (in red) is the SAC boundary.

boundaries of the SAC, and Castlemartin SSSI is one of them (CCW, 2013b). For this project, only the SAC area of Castlemartin SSSI is studied. The area is also part of the Pembrokeshire Coast National Park.

Table 3.4 shows all of the Annex I habitats that are protected by the site's designation as a SAC. The main reason is the presence of all the component habitats that form the Annex I habitat, 1230 Vegetated sea cliffs of the Atlantic and Baltic coasts, all of which must meet the definition for favourable status before the whole conservation feature can be reported as favourable. These habitats include maritime grassland and maritime heath. The maritime grasslands range from short open swards with occasional areas of bare ground to taller, more closed swards where *Festuca rubra* can form tussocks. Some of the abundant species in these communities include *Armeria maritima*, *Scilla verna* and *Plantago maritima*. Maritime heath occurs in exposed locations as stands of low, wind-pruned heath dominated by *Calluna vulgaris* and *Erica cinerea*. Species such as *Scilla*

Figure 3.8: Pictures of some of the geological features present along the Castlemartin coastline.

Table 3.4: Designated special features for the Castlemartin component of the SAC (CCW, 2013b).

Designation	Feature
SAC Annex I habitats that are primary reason for the selection of this site	1230 Vegetated sea cliffs of the Atlantic and Baltic coasts;
Annex I habitats present as a qualifying feature, but not primary reason for selection of this site	4030 European dry heaths; 6210 Semi-natural dry grasslands and scrubland facies: on calcareous substrates (*Festuco-Brometalia*)

verna, *Polygala spp.*, *Viola lactea* and *Carex spp.* are present in stands of the maritime heath (CCW, 2013b).

In comparison to the maritime heath habitat, the Annex I habitat 4030 European dry heath will be dominated by Erica cinerea, Ulex europaeus or by Ulex gallii or co-dominated by two or more of these; in contrast Ulex ssp. should not be present in maritime heath (CCW, 2013b). The Annex I habitat 6210 Semi-natural grasslands and scrubland facies on calcareous substrates (*Festuco-Brometalia*) is referable to the National Vegetation Classification (NVC) communities *Festuca - Avenula* grassland (CG2) and *Festuca - Hieracium - Thymus* grasslands (CG7). These grasslands mainly occur on shallow soils overlaying

areas of limestone bedrock (CCW, 2013b), and the extent of these communities can be seen in Figure 3.9.

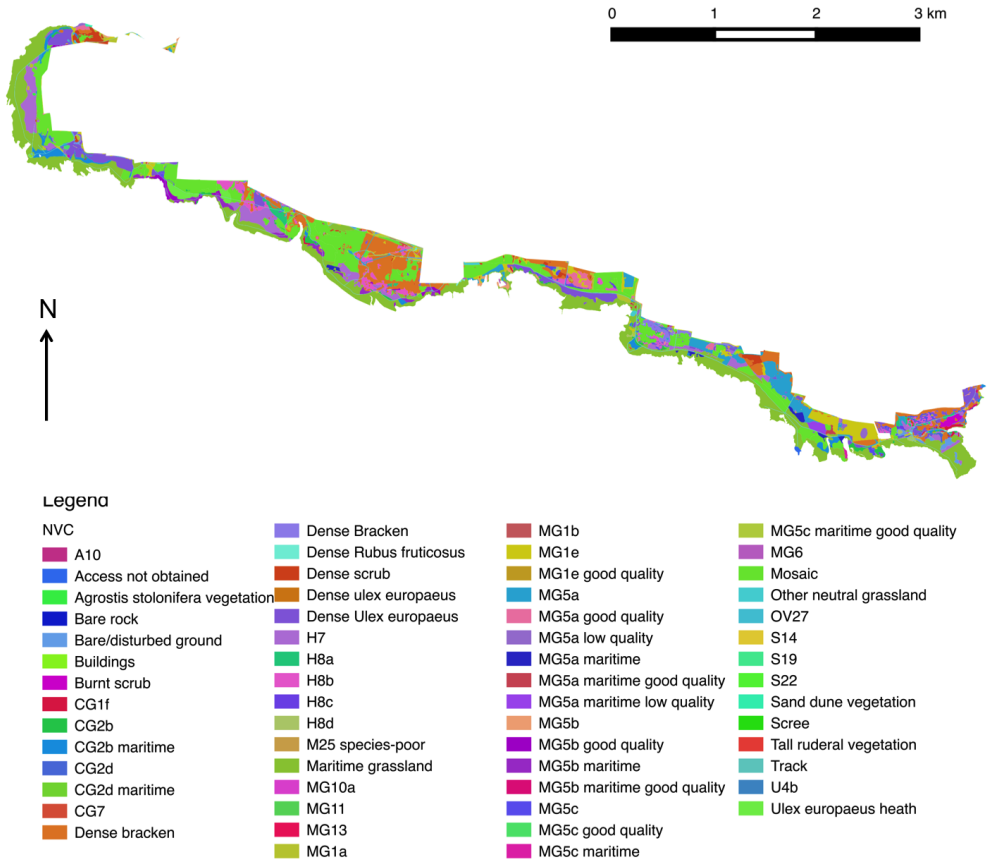

Figure 3.9: NVC map of Castlemartin. Data distributed by NRW.

3.3.3 Management

As stated previously, the Castlemartin component of the SAC is managed mostly by the MOD. Military activities such as changes in target, bunker, road or radar locations tend to lead towards excessive erosion that could cause localised damage to all of the habitats of interest for this study. However, a number of localised scrapes created in the past by the military for training purposes have led to the creation of young pioneer heath, resulting in more diverse patches of heathland habitat that can support scarce species. The more

exposed, seaward areas of maritime grassland and heath are mainly maintained by natural environmental factors including exposure to salt spray, thin soils and climatic extremes. Further inland, both heathland and grassland habitats are maintained by traditional grazing practices. Without an appropriate grazing regime of winter sheep and cattle grazing for instance, these areas would become rank and turn to gorse scrub. Another factor that needs to be managed is the almost annual occurrence of, accidental and uncontrolled fires. These fires can affect sections of the dry heath and scrub and any other habitats that border the burnt areas. This can lead to long-term damage, nutrient enrichment and an increase in the dominance of rank grasses or bracken (CCW, 2013b).

Chapter 4

Data Collection and Pre-Processing

4.1 Satellite Remote Sensing Data

One of the many advantages of using satellite imagery for mapping and monitoring is the possibility of acquiring data regularly with similar sensor specifications. Regularly acquiring imagery allows a monitoring system to be created, as the repeatability of surveys is often deemed problematic, rendering many data acquisition methods unsuitable. With a range of VHR (<2m resolution) satellites now available, the level of detail seen from space is becoming more suitable for mapping and monitoring habitats at finer scales e.g. Annex I habitats.

The satellite chosen for this study was Worldview-2 launched in 2009. It has 8 spectral bands at a spatial resolution of 2m and a panchromatic band at a spatial resolution of 0.46m (Figure 4.1). In addition to the red, green, blue and NIR bands there are four additional bands that have been created to support specific applications. The coastal band (400-450nm), yellow band (585-625nm), red edge band (705-745nm) and the NIR2 band (860-1040nm) all support vegetation identification and analysis. For example, the red

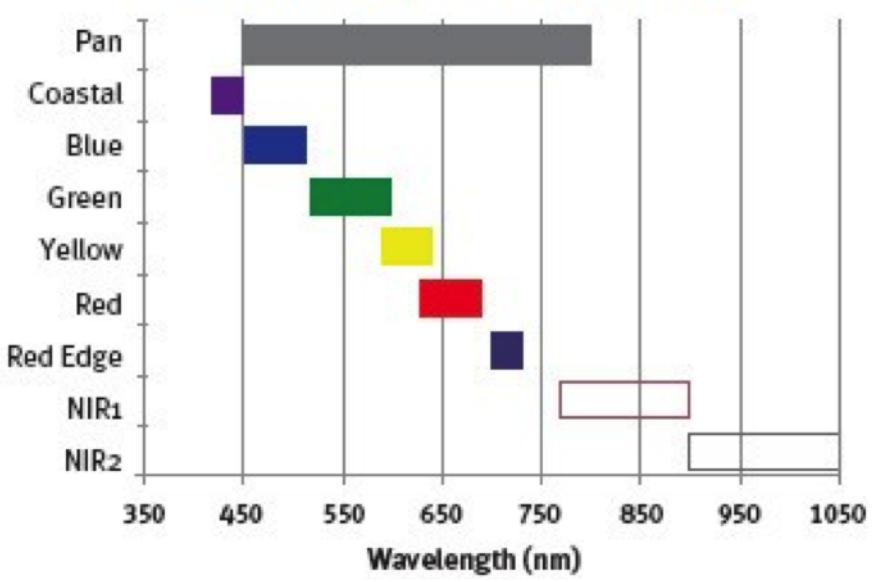

Figure 4.1: Spectral bands available in Worldview-2 imagery (Digital Globe, 2009).

edge band aids in the analysis of vegetation condition as that region of the wavelength is directly related to plant health through chlorophyll production (Horler et al., 1983). It can revisit any site location within one day and is capable of capturing 975,000 km squared per day (Digital Globe, 2009).

4.1.1 Tasking Imagery

Worldview-2 allows users to task an image acquisition by setting the area of interest (minimum of 10km x 10km) and the time window for image capture. The minimum recommendation for time window duration is 6 to 8 weeks, to ensure a cloud free acquisition. If there is less than 15 % cloud cover then the acquisition is considered successful. Archived imagery is also available however, for this study, all imagery acquired was tasked to ensure that the range of seasonal information was captured for all sites. Lucas et al. (2015) states that at least two images are needed either before the peak flush of vegetation (pre), at peak flush (peak), or after peak flush (post). The pre, peak and post terms applied from

now on will be a reference to the vegetative stage at the time of image acquisition. Table 4.1 shows the details of successful image acquisition for all sites. The cloud does not cover any of the area of interest within the Kenfig 2014 image.

Table 4.1: List of successful image acquisitions for all study sites.

Site	Date	Cloud Cover (%)
Castlemartin	22nd July 2012 (peak)	0
	22nd of September 2012 (post)	0
Kenfig	22nd July 2012 (peak)	0
	22nd of September (post)	0
	4th June 2014 (peak)	5

4.1.2 Pre-Processing of Satellite Imagery

Before satellite imagery can be used for classification a range of pre-processing techniques need to be applied. Satellite measurements vary due to a number of factors, including variations in illumination and viewing geometry, clouds and atmospheric conditions, variations in the pixel footprint, sensor noise, and influence of various meteorological events like snowfall, rain and haze. If these components can be corrected then the likelihood of precise replication for future monitoring events are increased greatly (Eklundh et al., 2011). Different techniques are available and need to be applied depending on the nature and objectives of the project.

Orthorectification

Orthorectification is the process that corrects optical remote sensing data for topographic relief and systematic sensor and platform-induced geometry errors (Leprince et al., 2007). These artefacts can be seen in raw imagery (Figure 4.2) where in this instance the viewing angle of the sensor are different resulting in distortions. This procedure provides imagery

that is resampled to true geometry and generates uniformity in scale allowing direct comparisons between various datasets, including imagery acquired at different dates, making it one of the most important pre-processing steps for application orientated evaluations such as classification (Reinartz et al., 2011).

Figure 4.2: Subset of raw Worldview-2 imagery.

To achieve orthorectification, a sensor model or geometric model is applied where a mathematical relationship relates object positions (*X, Y, Z*) to their corresponding two-dimensional (2D) image positions (*x, y*). Numerous sensor models are available from 2D polynomial functions to 3D rational functions (Tao and Hu, 2001; Fraser and Yamakawa, 2004; Fraser et al., 2006), but the most commonly used model for VHR imagery is terrain-independent 3D rational functions with vendor image support data (Aguilar et al., 2008). The third-order rational polynomial coefficients or RPCs, which are required to use this

model, are distributed by the image vendor for VHR sensors such as Worldview-2.

In addition to the RPCs, a high resolution and precise digital elevation model (DEM) is required to achieve high geometric accuracy (Toutin, 2004). DEMs such as the Shuttle Radar Topography Mission (SRTM) (NASA Jet Propulsion Laboratory, 2014) are used in orthrectification procedures but a resolution of 30m is not sufficient for VHR imagery. LiDAR data can derive high accuracy and resolution DEMs offering advantages over traditional methods (Liu et al., 2007). The Environment Agency Geomatics Group flies airborne LiDAR producing precise elevation data regularly in England and Wales (Environment Agency Geomatics Group, 2013). The data used for orthorectification is shown in Table 4.2.

Table 4.2: Dates of LiDAR data used for orthorectification (Data provided by Environment Agency Geomatics Group (2013))

Site	Date Flown	Resolution (m)
Castlemartin	27-28th April 2006	2
Kenfig	26-27th February 2006	2

Another requirement for the process is ground control points (GCPs) to achieve high absolute geometric accuracies. Although, VHR satellites claim to reach accuracies of approximately 3m root mean square errors (RMSE) without using GCPs there is still a need for ground control information to reach lower RMSE values (Reinartz et al., 2011). GCPs can be obtained by several means e.g. measuring points such as road junctions in situ with GPS or in aerial photography. A more automated method is to use previously orthorectified satellite imagery as reference images (Jacobsen, 2005), which has been shown to be very precise with low RMSE values (Müller et al., 2007).

All Worldview-2 images were orthorectified using the Leica Photogrammetry Suite (LPS) in Erdas IMAGINE 2013 software where 3D rational function with Worldview-2 RPC was selected as the sensor model. The reference coordinate system was set to British National Grid and imagery was resampled using bilinear interpolation. This procedure

has corrected the sensor displacements viewed in Figure 4.2 (Figure 4.3).

Figure 4.3: Subset of orthorectified Worldview-2 imagery.

GCPs were selected after the initial resampling using the AutoSync tool where automatic tie points were generated based on 3 manually selected GCPs. The reference image in this case was one of the resampled Worldview-2 images so that all imagery would co-register with each other. The number of GCPs used and RMSE values are shown in Table (4.3).

Radiometric Correction

As satellite sensors record pixel values in Digital Numbers (DN) ranging from 0 - 255 a radiometric correction needs to be applied to convert DNs into radiance values. All

Table 4.3: Reference image, GCPs and RMSE values for correcting Worldview-2 images.

Site	Resampled Image	Reference Image	Number of GCPs	RMSE (m)
Castlemartin	July 2012 Multispectral	September 2012 Multispectral	366	1.13
	July 2012 Panchromatic		1639	5.87
	September 2012 Panchromatic		1687	5.63
Kenfig	July 2012 Multispectral	September 2012 Multispectral	339	1.01
	July 2012 Panchromatic		1911	5
	September 2012 Panchromatic		1989	4.89
	June 2014 Multispectral		245	1.11
	June 2014 Panchromatic		1856	5.47

Worldview-2 products are delivered as radiometrically corrected image pixels where their values are a function of how much spectral radiance enters the telescope aperture at an altitude of 770 km and the instrument conversion of that radiation into a digital signal. This is unique to Worldview-2 therefore, to allow direct comparison with other sensors, image pixels need to be converted into top-of-atmosphere spectral radiance using the following equation (Updike and Comp, 2010):

$$L_{\lambda Pixel,Band} = \frac{K_{Band} \times q_{Pixel,Band}}{\Delta\lambda_{Band}} \tag{4.1}$$

where:

$L_{\lambda Pixel,Band}$ is top-of-atmosphere spectral radiance image pixels $[W - m^{-2} - sr^{-1} - \mu m^{-1}]$

K_{Band} is the absolute radiometric calibration factor for a given band $[W - m^{-2} -$

$sr^{-1} - count^{-1}]$

$q_{Pixel,Band}$ are radiometrically corrected image pixels [counts]

$\Delta\lambda_{Band}$ is the effective bandwidth for a given band [μm]

The absolute calibration factor is located in the metadata file for each image and the effective bandwidths for each Worldview-2 band is listed in Table 4.4.

Table 4.4: Worldview-2 Effective Bandwidths.

Spectral Band	Effective Bandwidth, $\Delta\lambda$ [μm]
Coastal	47.3
Blue	54.3
Green	63.0
Yellow	37.4
Red	57.4
Red Edge	39.3
NIR1	98.9
NIR2	99.6

Atmospheric Correction

All imagery was corrected to surface reflectance using open source software Atmospheric and Radiometric Correction of Satellite Imagery (ARCSI) that utilises Py6S (Vermote et al., 1997). The model requires data on the Aerosol Optical Depth (AOD) at the time of image acquisition to ensure that the model simulates accurate conditions within the Earth's atmosphere at that time. This data was acquired as visibility from the Met Office weather station data. For Castlemartin the closest station to the study area was Orielton while the closest station to Kenfig is St Athan (Figure 4.4). Table 4.5 shows the visibility values acquired from weather station data at the date and time of image acquisition.

Figure 4.4: Map of operational weather stations in Wales.

Table 4.5: Visibility data to use within ARCSI for atmospheric correction of imagery to surface reflectance.

Site	Image Acquisition Date and Time	Visibility (km)
Castlemartin	11.50am 22nd July 2012	20
	3.54pm 22nd September 2012	10
Kenfig	11.50am 22nd July 2012	35
	3.36pm 22nd September 2012	35
	2.20pm 4th June 2014	30

4.1.3 Vegetation Indices

Several indices are available within the literature that can be calculated to aid interpretation of biophysical parameters on the ground. Table 4.6 shows all the indices calculated in this study.

Table 4.6: Table of vegetation indices calculated for this study.

Index	Abbreviation	Specific Formula	Reference
Anthocyanin Reflectance Index	ARI	$\frac{1}{Green} - \frac{1}{Red}$	Gitelson et al. (2001)
Blue-wide Dynamic Range Vegetation Index	BWDRVI	$\frac{0.1 \times NIR2 - Coastal}{0.1 \times NIR2 + Coastal}$	Hancock (2006)
Browning Reflectance Index	BRI	$\frac{\frac{1}{Green} - \frac{1}{Red}}{NIR2}$	Merzlyak et al. (2003)
Canopy Chlorophyll Content Index	CCCI	$\frac{\frac{NIR2 - rededge}{NIR2 + rededge}}{\frac{NIR2 - Red}{NIR2 + Red}}$	Pinter Jr et al. (2003) Barnes et al. (2000)
Chlorophyll Green	ChlGreen	$\frac{NIR1}{Green}^{-1}$	Gitelson et al. (2006)
Chlorophyll Index Green	CIgreen	$\frac{NIR2}{Green} - 1$	Hunt Jr. et al. (2013) Ahamed et al. (2011)
Chlorophyll Index Red Edge 710	CIrededge710	$\frac{Panchromatic}{RedEdge} - 1$	Wu et al. (2009)
Chlorophyll Index Red Edge	CIrededge	$\frac{NIR2}{RedEdge} - 1$	Hunt Jr. et al. (2013) Ahamed et al. (2011)
Chlorophyll Red Edge	Chlrededge	$(\frac{NIR1}{RedEdge})^{-1}$	Gitelson et al. (2006)
Chlorophyll Vegetation Index	CVI	$NIR2 \times \frac{Red}{Green^2}$	Hunt Jr. et al. (2013)
Coloration Index	CI	$\frac{Red - Coastal}{Red}$	Hunt Jr. et al. (2013) Ahamed et al. (2011)
Datt 1	Datt1	$\frac{NIR1 - RedEdge}{NIR1 - Red}$	Le Maire et al. (2004) Datt (1999)
Datt 4	Datt4	$\frac{Red}{Green \times RedEdge}$	Datt (1998)
Datt 6	Datt6	$\frac{NIR2}{Green \times RedEdge}$	Datt (1998)
Difference 678/500	D678_500	$Red - Blue$	Merzlyak et al. (1999)
Difference 800/550	D800_550	$NIR1 - Green$	Le Maire et al. (2004)
Difference 800/680	D800_680	$NIR1 - Red$	Jordan (1969)
Green Difference Vegetation Index	GDVI	$NIR2 - Green$	Gitelson et al. (2002)
Green Atmospherically Resistant Vegetation Index	GARI	$\frac{NIR2 - Green - Coastal - Red}{NIR2 - Green + Coastal - Red}$	Gitelson et al. (1996)
Green Leaf Index	GLI	$\frac{2 \times Green - Red - Coastal}{2 \times Green + Red + Coastal}$	Gobron et al. (2000)
Green Normalised Difference Vegetation Index	GNDVI	$\frac{NIR2 - Green}{NIR2 + Green}$	Lymburner et al. (2000)
Green-Blue NDVI	GBNDVI	$\frac{NIR2 - Green + Coastal}{NIR2 + Green + Coastal}$	Wang et al. (2007b)
Green-Red NDVI	GRNDVI	$\frac{NIR2 - Green + Red}{NIR2 + Green + Red}$	Wang et al. (2007b)
Infrared Percentage Vegetation Index	IPVI	$\frac{NIR2}{\frac{NIR2 + Red}{2}} \times ((\frac{Red - Green}{Red + Green}) + 1)$	Kooistra et al. (2003)
Intensity	I	$(\frac{1}{30.5}) \times Red + Green + Coastal$	Escadafal et al. (1994)
Leaf Chlorophyll Index	LCI	$\frac{NIR1 - RedEdge}{NIR1 + Red}$	Pu et al. (2008)
Maccioni	Maccioni	$\frac{NIR1 - RedEdge}{NIR1 - Red}$	Maccioni et al. (2001)
MERIS Terrestrial Chlorophyll Index	MTCI	$\frac{Panchromatic - RedEdge}{RedEdge - Red}$	Dash and Curran (2004)
mND680	mND680	$\frac{NIR1 - Red}{NIR1 + Red - 2 \times Coastal}$	Sims and Gamon (2002)
Modified NDVI	mNDVI	$\frac{NIR1 - Red}{NIR1 + Red - 2 \times Coastal}$	Huete et al. (1997)
Modified Normalised Difference 750/705	MND750_705	$\frac{Panchromatic - RedEdge}{Panchromatic + RedEdge - 2 \times Coastal}$	Apan et al. (2003)
Modified Simple Ratio	mSR	$\frac{NIR1 - Coastal}{Red - Coastal}$	Kooistra et al. (2003)
Modified Simple Ratio 705/445	MSR705_445	$\frac{Panchromatic - Coastal}{RedEdge - Coastal}$	Sims and Gamon (2002)
Double Difference Index	DDn	$2 \times RedEdge - Panchromatic - Panchromatic$	Main et al. (2011)
Norm G	NormG	$\frac{Green}{NIR2 + Red + Green}$	
Norm Red	NormRed	$\frac{Red}{NIR2 + Red + Green}$	

Photochemical Reflectance Index	PRI	$\frac{Green-Panchromatic}{Green+Panchromatic}$	Zarco-Tejada et al. (2001)
Plant Pigment Ratio	PPR	$\frac{Green-Coastal}{Green+Coastal}$	Metternicht (2003)
Physiological Reflectance Index	ND550_531	$\frac{Panchromatic-Green}{Panchromatic+Green}$	Zarco-Tejada et al. (2001)
Photosynthetic Vigour Ratio	PVR	$\frac{Green-Red}{Green+Red}$	Metternicht (2003)
Normalised Pigment Chlorophyll Index	NPCI	$\frac{Red-Coastal}{Red+Coastal}$	Aparicio et al. (2004)
Red Edge NDVI	reNDVI	$\frac{Panchromatic-RedEdge}{Panchromatic+RedEdge}$	Ahamed et al. (2011)
Normalised Difference 750/650	ND750_680	$\frac{Panchromatic-Red}{Panchromatic+Red}$	Richardson et al. (2002)
Normalised Difference 790/670	ND790_670	$\frac{NIR1-Red}{NIR1+Red}$	Barnes et al. (2000)
Normalised Difference Red Edge Index	NDRE	$\frac{NIR1-RedEdge}{NIR1+RedEdge}$	Herrmann et al. (2010)
Green NDVI Hyper	GNDVIhyper	$\frac{NIR1-Green}{NIR1+Green}$	Gitelson et al. (2001)
Pigment Specific Normalised Difference C2	PSNDc1	$\frac{NIR1-Blue}{NIR1+Blue}$	Blackburn (1998)
Pigment Specific Normlised Difference B2	PSNDb2	$\frac{NIR1-Panchromatic}{NIR1+Panchromatic}$	Blackburn (1998)
Normalised Difference 900/680	ND900_680	$\frac{NIR2-Red}{NIR2+Red}$	Underwood et al. (2003)
Normalised Difference Chlorophyll	NDchl	$\frac{NIR2-RedEdge}{NIR2+RedEdge}$	Le Maire et al. (2008)
Normalised Green Red Difference Index	NGRDI	$\frac{Green-Red}{Green+Red}$	Zarco-Tejada et al. (2001)
Blue Normalised Difference Vegetation Index	BNDVI	$\frac{NIR2-Coastal}{NIR2+Coastal}$	Yang et al. (2004)
Normalised Difference Vegetation Index	NDVI	$\frac{NIR1-Red}{NIR1+Red}$	Baret et al. (1989)
Redness Index	RI	$\frac{Red-Green}{Red+Green}$	Escadafal (1993)
Normalised Difference Red Edge Red	NDVIrededge	$\frac{RedEdge-Red}{RedEdge+Red}$	Ehammer et al. (2010)
Panchromatic NDVI	PNDVI	$\frac{NIR2-(Green+Red+Coastal)}{NIR2+(Green+Red+Coastal}$	Wang et al. (2007b)
Plant Senescence Reflectance Index	PSRI	$\frac{Red-Blue}{RedEdge}$	Merzlyak et al. (1999)
Red - Blue NDVI	RBNDVI	$\frac{NIR2-(Red+Coastal)}{NIR2+(Red+Coastal)}$	Wang et al. (2007b)
Simple Ratio	SRPanC	$\frac{Pan}{Coastal}$	
	SRPanB	$\frac{Panchromatic}{Blue}$	
	SRPanG	$\frac{Panchromatic}{Green}$	
	SRPanY	$\frac{Panchromatic}{Yellow}$	
	SRPanR	$\frac{Panchromatic}{Red}$	
	SRPanRE	$\frac{Panchromatic}{RedEdge}$	
	SRPanNIR1	$\frac{Panchromatic}{NIR1}$	
	SRPanNIR2	$\frac{Panchromatic}{NIR2}$	
	SRCPan	$\frac{Coastal}{Panchromatic}$	
	SRCB	$\frac{Coastal}{Blue}$	
	SRCG	$\frac{Coastal}{Green}$	
	SRCY	$\frac{Coastal}{Yellow}$	
	SRCR	$\frac{Coastal}{Red}$	
	SRCNIR2	$\frac{Coastal}{NIR2}$	
	SRBPan	$\frac{Blue}{Panchromatic}$	
	SRBC	$\frac{Blue}{Coastal}$	
	SRBG	$\frac{Blue}{Green}$	
	SRBY	$\frac{Blue}{Yellow}$	
	SRBR	$\frac{Blue}{Red}$	
	SRBRE	$\frac{Blue}{RedEdge}$	
	SRBNIR1	$\frac{Blue}{NIR1}$	
	SRBNIR2	$\frac{Blue}{NIR2}$	

Simple Ratio	SRGPan	$\frac{Green}{Panchromatic}$	
	SRGC	$\frac{Green}{Coastal}$	
	SRGB	$\frac{Green}{Blue}$	
	SRGY	$\frac{Green}{Yellow}$	
	SRGR	$\frac{Green}{Red}$	
	SRGRE	$\frac{Green}{RedEdge}$	
	SRGNIR1	$\frac{Green}{NIR1}$	
	SRGNIR2	$\frac{Green}{NIR2}$	
	SRYPan	$\frac{Yellow}{Panchromatic}$	
	SRYC	$\frac{Yellow}{Coastal}$	
	SRYB	$\frac{Yellow}{Blue}$	
	SRYG	$\frac{Yellow}{Green}$	
	SRYR	$\frac{Yellow}{Red}$	
	SRYRE	$\frac{Yellow}{RedEdge}$	
	SRYNIR1	$\frac{Yellow}{NIR1}$	
	SRYNIR2	$\frac{Yellow}{NIR2}$	
	SRRPan	$\frac{Red}{Panchromatic}$	
	SRRC	$\frac{Red}{Coastal}$	
	SRRB	$\frac{Red}{Blue}$	
	SRRG	$\frac{Red}{Green}$	
	SRRRE	$\frac{Red}{RedEdge}$	
	SRRNIR1	$\frac{Red}{NIR1}$	
	SRRNIR2	$\frac{Red}{NIR2}$	
	SREPan	$\frac{RedEdge}{Panchromatic}$	
	SREC	$\frac{RedEdge}{Coastal}$	
	SREB	$\frac{RedEdge}{Blue}$	
	SREG	$\frac{RedEdge}{Green}$	
	SREY	$\frac{RedEdge}{Yellow}$	
	SRER	$\frac{RedEdge}{Red}$	
	SRENIR1	$\frac{RedEdge}{NIR1}$	
	SRENIR2	$\frac{RedEdge}{NIR2}$	
	SRNIR1Pan	$\frac{NIR1}{Panchromatic}$	
	SRNIR1C	$\frac{NIR1}{Coastal}$	
	SRNIR1B	$\frac{NIR1}{Blue}$	
	SRNIR1G	$\frac{NIR1}{Green}$	
	SRNIR1Y	$\frac{NIR1}{Yellow}$	
	SRNIR1R	$\frac{NIR1}{Red}$	
	SRNIR1RE	$\frac{NIR1}{RedEdge}$	
	SRNIR1NIR2	$\frac{NIR1}{NIR2}$	
	SRNIR2Pan	$\frac{NIR2}{Panchromatic}$	
	SRNIR2C	$\frac{NIR2}{Coastal}$	
	SRNIR2B	$\frac{NIR2}{Blue}$	
	SRNIR2G	$\frac{NIR2}{Green}$	
	SRNIR2Y	$\frac{NIR2}{Yellow}$	
	SRNIR2R	$\frac{NIR2}{Red}$	

Simple Ratio	SRNIR2RE	$\frac{NIR2}{RedEdge}$	
	SRNIR2NIR1	$\frac{NIR2}{NIR1}$	
Water Band Index	WBI	$\frac{Blue}{NIR1}$	Lucas et al. (2012)
Red Edge Position Index	REP	$RedEdge - (NIR2 - Red)$	Lucas et al. (2012)
Forest Discrimination Index	FDI	$NIR1 - (RedEdge + Coastal)$	Lucas et al. (2012)
Woody Index	Woody	$\frac{Blue-Green}{Blue+Green}$	Lucas et al. (2012)
Near Infra-Red Difference	DiffNIR	$NIR1 - NIR2$	Lucas et al. (2012)
Normalised Difference Water Index	NDWI	$\frac{Green-NIR1}{Green+NIR1}$	Gao (1996)
Peak Post Difference NDVI	peakpostNDVIDiff	$peakNDVI - postNDVI$	Lucas et al. (2012)

4.2 Airborne Data

4.2.1 LiDAR

As previously stated, LiDAR data was also acquired from the Environment Agency Geomatics Group (Table 4.2). The data was downloaded as a processed product in the form of a Digital Terrain Model (DTM). For Kenfig, the 2006 acquisitions are used in the initial mapping analysis (Chapter 6) and a more up to date acquisition (January 2014) was used in conjuncture with the 2014 Worldview-2 image to monitor change at the site. The later acquisition at Kenfig was flown at a higher resolution of 1m.

4.2.2 Unmanned Aerial Vehicle (UAV) Imagery

Imagery at a very high resolution (5cm) was available in the visible portion of the electromagnetic spectrum at one site, Kenfig. Processing included mosaicking the image tiles together to provide a complete picture of the site to aid interpretation. A spatial reference is then applied to the resultant mosaic, The image was acquired in 2012 at low cost and is used for generating more generic class points such as bare sand, trees and bracken. These points are then in putted into the analysis for spatially separating point data into training and accuracy datasets (see section 4.3.2).

4.3 Fieldwork

4.3.1 GPS Point Collection

Decision support tools used for vegetation management require accurate information on the spatial array of different plant communities' location. Since 2000, when the signal errors that were reduced intentionally by the US Department of Defence was disabled (Hulbert and French, 2001), the use of Global Positioning Systems (GPS) have greatly improved in precision and accuracy. This allows GPS points to be collected at an accuracy of 1m or less. Figure 4.5 shows the method in the field to collecting point data used to train and validate EO data.

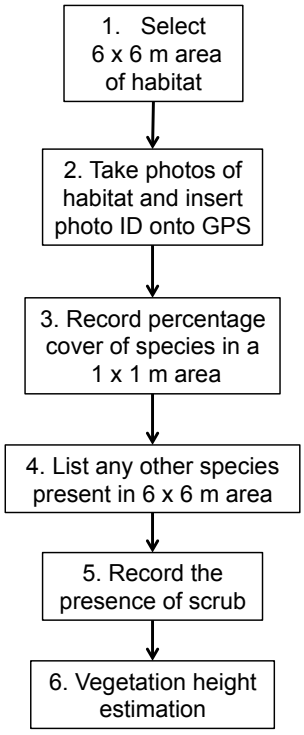

Figure 4.5: The process to collecting information for each point in the field.

The habitat area needs to be 6x6m in order to account for inaccuracies introduced when

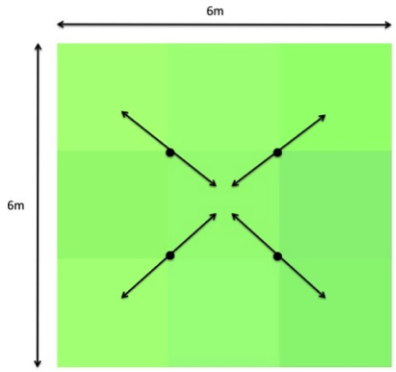

Figure 4.6: The effect of GPS accuracy on validating pixels.

collecting GPS points. Figure 4.6 shows how the location of the point within a pixel can affect which pixel the point is actually referring to. However, it is taken into account when habitats of interest do not cover this area due to the mosaic nature of vegetation and difficulties in defining extents with set boundaries.

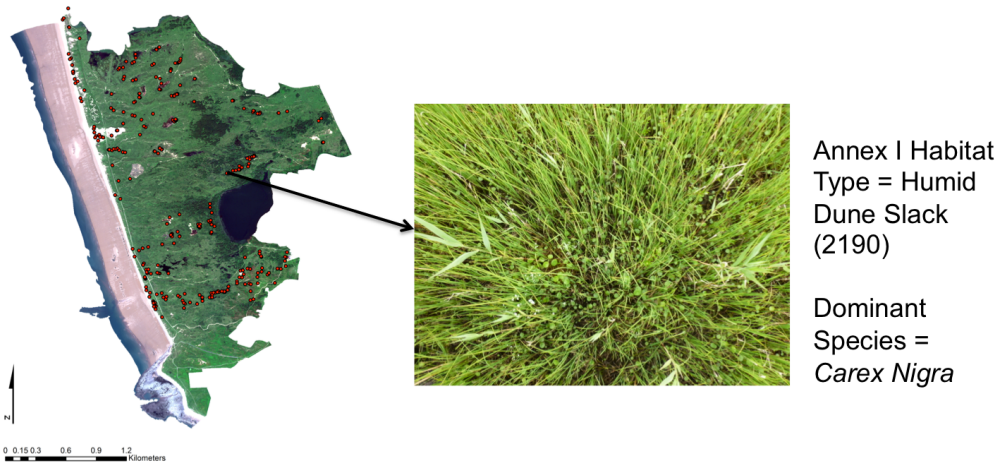

Figure 4.7: Example of the information collated into a Geographical Information System (GIS) to aid interpretation.

4.3.2 Spatially separating points into training and accuracy

In order to train and validate EO data the GPS points were separated into a training set and accuracy set. To avoid clustering of points from a single area into one set, point selection was based on spatial location in addition to class. A sampling grid was created using Remote Sensing and Geographical Information System Library (RSGISLib) at different resolutions (5m, 10m, 15m, 20m) that comprised of two values (1 for training and 1 for accuracy) and the resolution that split the classes evenly was chosen. Table 4.7 shows the resolutions chosen for each class while Figures 4.8 and 4.9 shows the final distribution of training and accuracy points for both study sites.

Table 4.7: Table of sampling grid resolutions chosen for allocating points into a training or accuracy dataset. Class is related to Annex I habitats with other classes present on site categorised as broad habitat or land cover from the Land Cover Classification System (LCCS). Sampling grids were chosen based on the number of points, with the closest to equality selected for each.

Site	Class	Sampling Grid Resolution (m)	Number of Training Points	Number of Accuracy Points
Castlemartin	Bare Ground	15	4	2
	European dry heath (4030)	5	6	5
	Semi-natural dry grasslands and scrubland facies on calcareous substrates (6210)	5	12	11
	Other Grassland	10	4	4
	Vegetated Sea Cliffs (1230)	5	49	50
	Scrub	5	7	5
	Bracken	10	10	10
Kenfig	Bare Ground	20	3	3
	Dunes with Salix repens ssp argentea (2170)	20	12	11
	Fixed coastal dunes with herbaceous vegetation (grey dunes) - (2130)	15	42	40
	Humid dune slack (2190)	20	84	78
	Bracken	10	36	36
	Shifting dunes along the shoreline with Ammophila arenaria (white dunes) - (2120)	20	2	1
	Trees	20	4	3
	Water	10	19	22

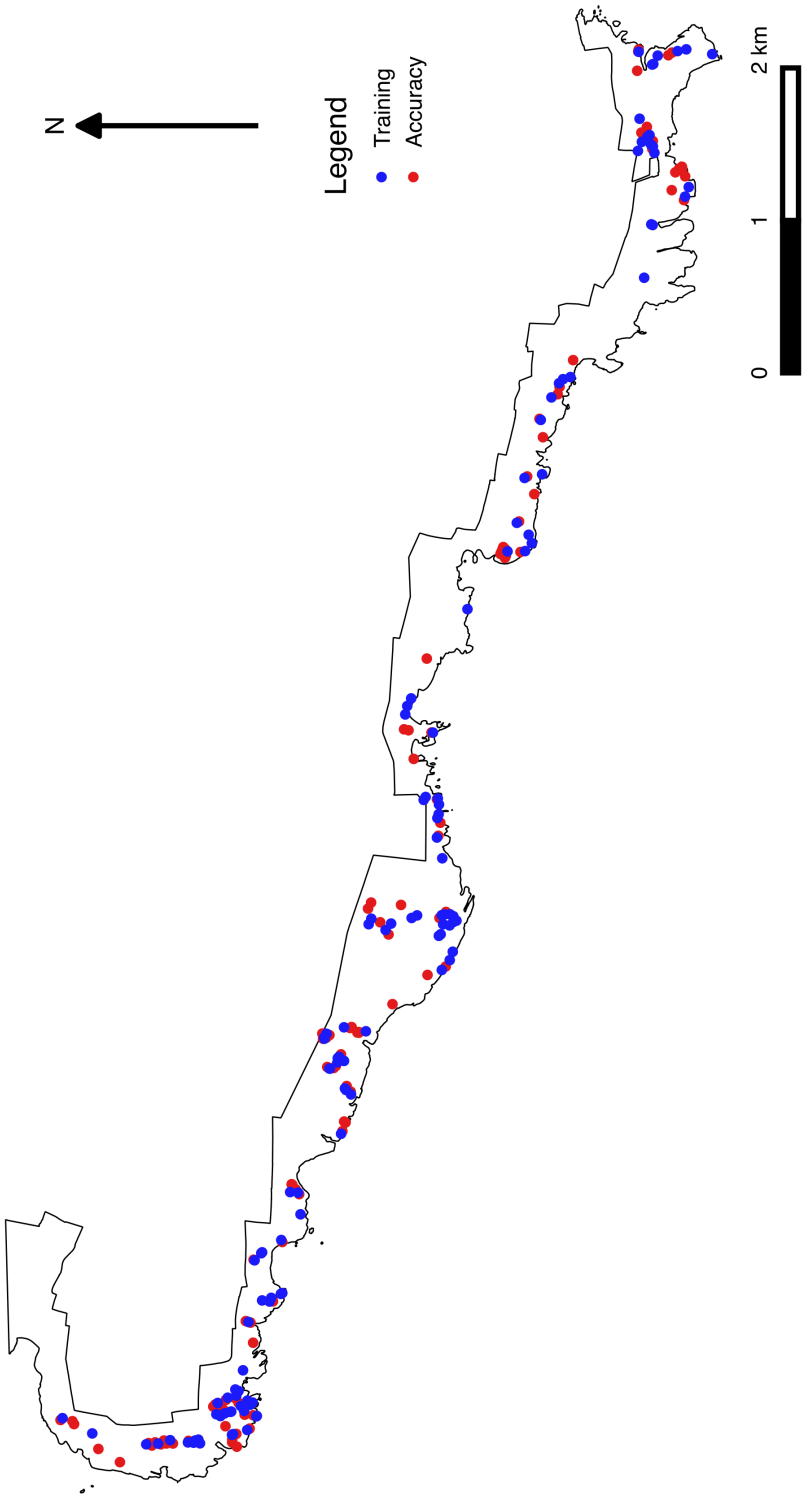

Figure 4.8: Allocation of GPS points to training and accuracy datasets at Castlemartin.

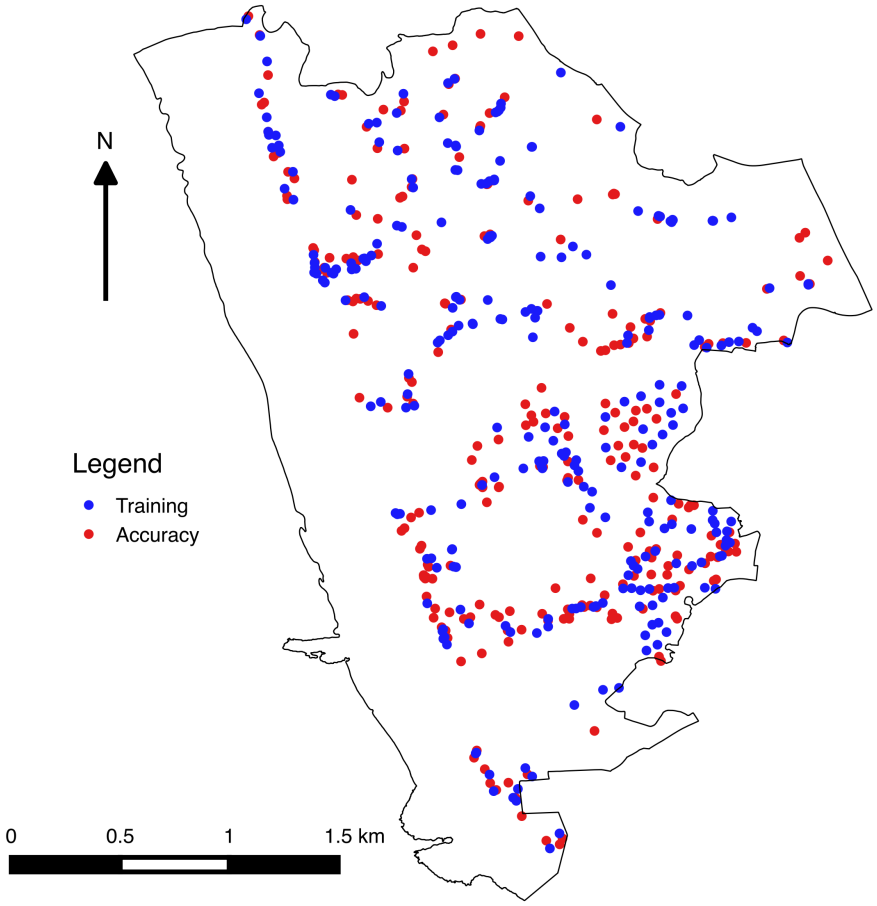

Figure 4.9: Allocation of GPS points to training and accuracy datasets at Kenfig.

Chapter 5

Habitat Definitions and Classification Schemes

5.1 Introduction

Action needed for conserving biodiversity has been recognised globally and has resulted in the urgency of developing more frequent and regular updates on land cover and habitat information (Schmeller, 2008). Organisations at national, regional and global scales have responded by producing an increased number of datasets using different classification schemes, which has resulted in incompatibility across a wide range of applications (Herold et al., 2006). This chapter will explore some of these classification schemes at a wide range of scales before moving on to explore some of the difficulties of defining the Annex I habitats of interest in this study on the ground and translating those to remote sensing techniques.

5.2 Overview to Classification Schemes

The harmonisation of classification schemes is important for moving forward, particularly if EO data is to be routinely used for mapping and monitoring approaches. The potential for EO data for biodiversity monitoring has been widely recognised (Nagendra, 2001; Turner et al., 2003; Mücher, 2011), however, there is no systematic protocol for this kind of monitoring at any scale (Buchanan et al., 2009). This will provide a background on the classification schemes used from global to national scales, and will highlight the differences between products created while utilising them. The classification schemes that were designed to standardise mapping procedures will also be described. The standardisation of approaches not only aids policy and decision makers, but also helps with the acceptance of schemes across borders and continents.

5.2.1 Global Scale

Global land cover (GLC) datasets, before the advancement of remote sensing over the last couple of decades, were based on pre-existing maps and atlases compiled from ground surveys, national mapping programs, and highly generalised biogeographic maps (Matthews, 1983; Olson, 1982; Wilson and Henderson-Sellers, 1985). The first phase of GLC products derived from remote sensing were created using AVHRR at coarse spatial resolutions of 1km and above including products created by the University of Maryland and IGBP DISCover project (DeFries et al., 1995; DeFries and Townshend, 1994; Hansen et al., 2000; Loveland et al., 2000; Stone et al., 1994; Townshend, 1994). As higher resolution satellite sensors were launched, there was a focus on developing improved GLC products with the generation of GLC2000 produced from SPOT VEGETATION (Bartholomé and Belward, 2005), the MODIS Collection 4 Land Cover Product (Friedl et al., 2002), the

MODIS Collection 4 Vegetation Continuous Fields product (Hansen et al., 2002), and the GlobeCover product produced using data from Medium Resolution Imaging Spectrometer (MERIS) (Arino, 2010). There are also ongoing projects to develop global products derived from Landsat data at 30m resolution e.g, (Giri et al., 2013; Chen et al., 2015; Gong et al., 2013).

Table 5.1 lists the classification scheme used in current GLC datasets. They are often selected without considering their quality and suitability for applications (Verburg et al., 2011) and one of the key issues is lack of inter-comparability where class definition contributes along with scale, method and validation (Jung et al., 2006; Herold et al., 2008). Efforts have been made to standardise land cover characterisation and the use of the Land Cover Classification System (LCCS) is one of these. The LCCS (Di Gregorio and Jansen, 2000) has been developed by the Food and Agriculture Organisation (FAO) as a comprehensive and standardised classification system designed for mapping purposes, which is independent of scale (Mora et al., 2014). The hierarchical nature of the system allows a dynamic creation of classes without users having to conform to a set, pre-defined list of class definitions, which combats some of the heterogeneity issues of land cover mapping on a global scale. Some GLC products already use this classification system, the latest version (Land Cover Metadata Language (LCML - LCCS v.3)) is a proposed standard by the International Organisation for Standardisation (ISO) under the reference ISO 19144-1 (Mora et al., 2014).

Little effort has been spent on generating habitat maps at a global scale, particularly from remote sensing, as habitat definitions rely on species composition and can include multiple types of land cover within a single habitat. However, the framework for habitat monitoring needs to be consistent in contrasting landscapes and applicable globally, as with land cover classification (Kosmidou et al., 2014). Habitat is a widely used term but its definition and concept remains diverse and ambiguous, complicating its consistency

Table 5.1: List of classes used in schemes for several global land cover products.

IGBP Classes	UMD Classes	LAI/FPAR	BGC	PFT	GLC2000 Classes
Evergreen needleleaf forest	Evergreen needleleaf forest	Evergreen needleleaf forests	Evergreen needleleaf vegetation	Evergreen needleleaf tree	Tree Cover, needle-leaved, evergreen
Deciduous needleleaf forest	Deciduous needleleaf forest	Deciduous needleleaf forests	Deciduous needleleaf vegetation	Needleleaf deciduous tree	Tree Cover, needle-leaved, deciduous
Evergreen broadleaf forest	Evergreen broadleaf forest	Evergreen broadleaf forests	Evergreen broadleaf vegetation	Broadleaf evergreen tree	Tree Cover, broadleaved, evergreen
Deciduous broadleaf forest	Deciduous broadleaf forest	Deciduous broadleaf forests	Deciduous broadleaf vegetation	Broadleaf deciduous tree	Tree Cover, broadleaved, deciduous, closed
Mixed forests	Mixed forest				Tree Cover, mixed leaf type
					Tree Cover, broadleaved, deciduous, closed
					Tree Cover, regularly flooded, fresh water
					Tree Cover, regularly flooded, saline water
Woody savannas	Woody savannas	Savanna			Mosaic: Tree Cover / Other natural vegetation
Savannas	Savannas	Savanna			
Grasslands	Grassland	Grasse/cereal crops	Annual grass vegetation	Grass	Herbaceous Cover, closed-open
					Sparse Herbaceous or sparse Shrub Cover
Closed shrublands	Closed shrublands	Shrublands		Shrub	
Open shrublands	Open shrublands	Shrublands		Shrub	
					Shrub Cover, closed-open, evergreen
					Shrub Cover, closed-open, deciduous
Croplands	Croplands	Broadleaf crops	Annual broadleaf vegetation	Cereal crop	Cultivated and managed areas
Cropland/natural vegetation mosaics				Broadleaf crop	Mosaic: Cropland/Tree Cover/ Other natural veg
Permanent wetlands					Mosaic: Cropland / Shrub or Grass Cover
Urban and built-up land	Urban and built-up land	Urban	Urban	Urban	Regularly flooded Shrub and/or Herbaceous Cover
Barren or sparsely vegetated	Barren or sparsely vegetated	Unvegetated	Unvegetated	Barren or sparsely vegetated	Artificial surfaces and associated areas
Water	Water	Water	Water	Water	Bare Areas
Permanent snow and ice				Snow and ice	Water Bodies (natural and artificial)
					Snow and Ice (natural and artificial)
					Burnt area

for monitoring purposes (Bunce et al., 2013). There is one classification scheme that has attempted to address the problem of habitats at a global scale, General Habitat Categories (GHCs). It has been tested throughout Europe (Bunce et al., 2005, 2006, 2008, 2011) and is based on the ecological refinement of the land cover categorisation used in LCCS (Bunce et al., 2011). This is the first instance where a translation from land cover to habitats has been attempted, and as both schemes rely heavily on lifeforms, height and cover as criteria, they aid the links between products created from remote sensing data and in situ observations (Kosmidou et al., 2014). Furthermore, studies have extracted Annex I habitats from GHC nomenclature demonstrating it's usefulness for harmonisation across habitat schemes and for fulfilling policy requirements (Adamo et al., 2014).

5.2.2 Pan European Scale

In Europe, the need to establish harmonised nomenclatures and methodologies across the region was recognised in the 1980s, where the European Commission implemented the CORINE programme (Co-ordination of Information on the Environment). CORINE Land Cover (CLC) uses a bottom-up approach where national teams are producing the maps of their own countries which is then integrated into the European level database managed by the European Environment Agency. There have been 4 iterations of CLC since 1990 where Landsat data has been the main source of information until 2006 where higher resolution satellite sensors where utilised (SPOT 4-5, IRS LISS III and Rapid Eye (2012 only)). The nomenclature is hierarchical and has remained relatively stable since CORINE's inception. Any enhancements, which improve some class definitions, as higher resolution information becomes available from satellites, are kept comparable over time thanks to the hierarchy. Many countries still use this dataset for multiple applications as their only source of land cover information, however, it does not capture the required detailed information on habitats as stated by the EC Habitat's directive. This translation into habitat maps is very important for conservation applications as habitats provide

a better link to flora and fauna species providing significant indicators for biodiversity monitoring (Bunce et al., 2012).

To provide the nomenclature needed for characterising European habitats, the European Nature Information System (EUNIS) was developed. The EUNIS habitat classification is a common reporting language on habitat types at European level and originated from several other initiatives, including the CORINE biotopes (Devillers et al., 1991), CLC nomenclature (Bossard et al., 2000) and Annex I. This classification scheme does not produce any datasets and maps like CORINE but does provide a comprehensive habitat definition list to facilitate the harmonised description and collection of data across Europe (Davies et al., 2004). Work has also been done to cross reference the EUNIS habitat classification with the CLC nomenclature so that habitats can be derived from CLC products using these pan European schemes. However, its use is seen more commonly in marine ecosystem applications and is not widely used for terrestrial applications, as national schemes are deemed better suited.

In 2014, it was recognised that creating new classification schemes was not going to fix the issue of transparency between schemes and nomenclatures especially as the uptake of new schemes such as the GHC proved low in popularity. The response was the formation of the EAGLE group, also referred to as the European environment information and observation network (EIONET) Action Group on Land monitoring in Europe. The group recognised that many existing classification systems address a specific theme, policy or thematic focus and that there was a lot of overlap, particularly between land cover and land use categories. Shortcomings in the existing CLC nomenclature were also recognised including the advancement of technologies such as satellite imagery pushing for more evolved thematic requirements and political reporting obligations. A problem with definitions was also targeted as an issue, as individual countries across different biogeographical regions interpret classes differently (Figure 5.1).

The EAGLE concept aims to bridge these issues by creating a tool for analytic decom-

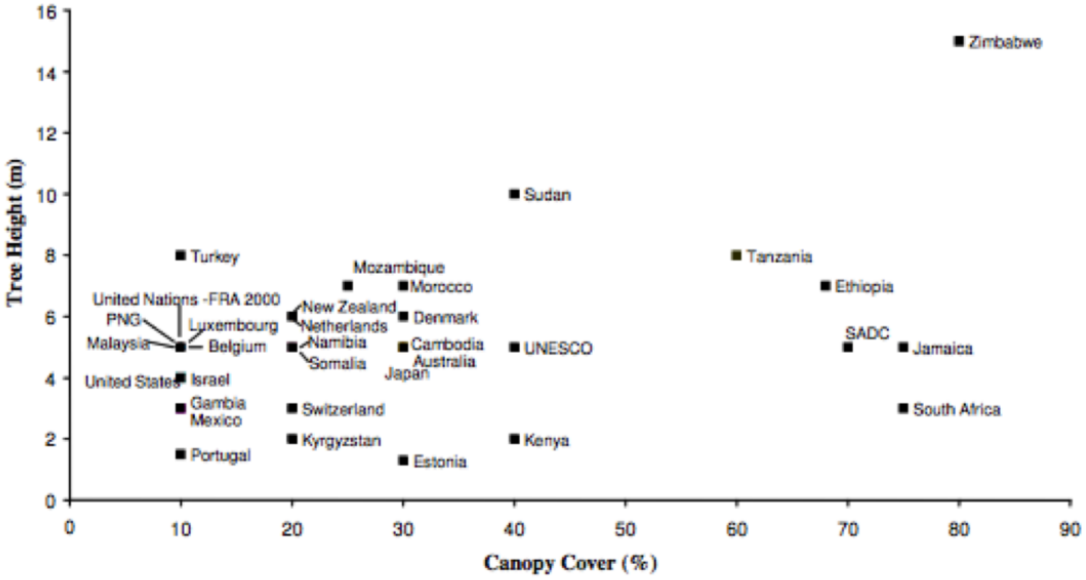

Figure 5.1: An example of the physical requirements of a forest class. Note most countries have additional characteristics for the definition of forest (Comber et al., 2005).

position of class definitions and for semantic translation between recent or future nomenclatures. The purpose is to harmonise future European land monitoring systems, and this includes information on habitats amongst all the land cover and land use nomenclatures, from European scale down to National level (Arnold et al., 2013). Use cases include decomposing GHCs by expression through the EAGLE model elements, which makes the concept relevant for other types of monitoring beyond land cover and land use. This tool allows for the interpretation and definitions of classes and categories across all scales, but it can also be used as a tool to decide on which nomenclature is the most appropriate for specific applications depending on types of data available. For example, if VHR EO data is available for habitat mapping, then the chance of mapping detailed habitat extent is much higher and a classification scheme which describes broad categories would not be suitable. However, the problem remains, in that national partners in such European scale approaches still face difficulty in uptake if they are not part of policy requirements,

particularly when there is a wide range of classification schemes to choose from.

5.2.3 National Level Scale - UK

The UK has a long heritage in the development and application of land cover mapping approaches based on EO data dating back to 1990. The UK LCM was a product created under the Countryside Survey, which was the national land monitoring scheme in the UK with a habitat focus. There have been three iterations of the land cover product since. Each has been criticised for inconsistencies over time (Smith, 2014), similarly to other land cover products of regional and global scales. The product has its own classification scheme, which changed slightly with each iteration as each map was generated as a stand-alone product using different methods, making it difficult to monitor changes over time.

The UK also has a rich heritage of classification schemes specifically for habitat inventories and surveys. Two of these have been in existence since the 1970s (Phase 1 and NVC) while another (UK BAP) was generated in response to the CBD which the UK signed up to in 1992. All three were created with UK specific habitats and plant communities in mind, instead of trying to fit British habitats into other regional or global scale classification schemes. It is no wonder that the uptake of harmonised classification schemes at pan European scales is not popular with field ecologists as familiarity with national schemes purposefully built for UK ecology makes more sense. The reluctance to conform to international classifications is not helpful at the global scale either, as some features that are deemed important are not necessarily considered with the same significance outside of the UK.

While the UK BAP scheme, which was set up to help achieve biodiversity targets for 2012 is no longer specifically relevant due to policy updates, Phase 1 and NVC are still

very popular classification schemes in the UK. The original Phase 1 habitat maps were first created over a period of 30 years with extensive fieldwork all over the UK. The field survey technique provided a standardised system to record semi-natural vegetation in the field and was not designed for use with remote sensing. However, an updated version of the Wales Phase 1 habitat map was created using EO data from 2000-2009 (Lucas et al., 2011). The NVC is what most academic botanist follow in the UK after many years of training. However, many ecologists believe that the latest categories to be characterised were done in haste revealing inconsistencies with the vegetation characteristics, particularly within sand dune and saltmarsh communities (Williams, 2006). As NVC maps are typically created by ground surveys, they are often of limited extent and are not updated on a regular enough basis for use by land managers and conservation practitioners. Studies have also been unsuccessful at mapping NVC communities with EO systems (Shanmugam et al., 2003), as many of the communities are differentiated by associate species that are usually undetectable by EO data.

5.3 Annex I Habitat Types

This section will discuss the definition of the main Annex I Habitat types in relation to the classification schemes mentioned above. Consideration will also be given to mapping these habitats with remote sensing, including feasibility and likelihood of class separation from other surrounding habitat types.

5.3.1 Humid Dune Slacks 2190

Habitat Definition

Humid dune slacks appear as flat valleys in dune systems and they represent the wetland component as they are formed where the underlying water table reaches the surface (Fig-

ure 5.2). A particular distinguishing feature is a seasonally fluctuating water table, which usually reaches a maximum in winter, where most slacks will be under water, and drops in the summer. The nutrient levels of the slacks are low and the range of communities found is considerable depending on dune structure and successional stage.

Figure 5.2: Humid Dune Slack at Kenfig Burrows SAC.

European vegetation classifications recognise a succession of slack types from bare damp sand to wet slacks dominated by trees and shrubs. While humid dune slacks include creeping willow, the Annex I type excludes those sites where the species is dominant and is associated with Yorkshire-fog *Holcus lanatus* and at times with the bryophytes *Campylium stellatum* and *Calliergon cuspidatum*. A further community is typified by silverweed *Potentilla anserina* and common sedge *Carex nigra* (JNCC, 2007d).

In the UK the predominant NVC types that are included in the 2190 habitat definition include:

- SD13 *Sagina nodosa - Bryum pseudotriquetrum* dune-slack community
- SD14 *Salix repens - Campylium stellatum* dune-slack community
- SD15 *Salix repens - Calliergon cuspidatum* dune-slack community
- SD17 *Potentilla anserina - Carex nigra* dune-slack community

The SD16 NVC community (drier slacks) represents the habitat type 2170 dunes with *Salix repens* ssp. *argentea (salicion arenariae)* (JNCC, 2007c). Table 5.2 show the sub-types related to this habitat and in many cases the translation from Annex I to EUNIS and CORINE is much wider in comparison to the NVCs where the translation is narrower.

Table 5.2: Main sub-types of humid dune slack identified in the EUNIS and CORINE biotopes classifications and the EU Interpretation Manual.

EUNIS (moist wet dune slacks)	CORINE (humid dune slacks)	EU Interpretation Manual (humid dune slacks)
Dune slack pools	Dune slack pools	Freshwater aquatic communities of permanent dune slack water bodies
Dune slack pioneer swards	Dune slack pioneer swards	Pioneer formations of humid sand and dune pool fringes, on soils with low salinity
Dune slack fens	Dune slack fens	Calcareous and, occasionally acidic fen communities, often invaded by *Salix repens* occupying the wettest parts of dune slacks
Dune slack grassland and heaths	Dune slack grasslands	Humid grasslands and rushbeds of dune slacks, also often with creeping willows (*Salix rosmarinifolia, S.arenaria*)
Dune slack reedbeds, sedgebeds and canebeds	Dune slack reedbeds and sedgebeds	Reedbeds, tall-sedge communities and canebeds of dune slacks
Wet dune slacks; dominated by shrubs or trees		

Without the disturbance of grazing, or damage caused by anaerobic conditions in very wet slacks, the biomass increases, organic matter accumulates and the nutrient status (particularly nitrogen and phosphorus) of the soil increases. This results in increasing dominance of tall grasses and shrubs, including *Calamagrostis epigejos*) (wood small-reed) and *Salix*

repens, and the decline of the typical slack specialist of the species-rich phase, which is important for several associated species (JNCC, 2007-1). *Salix repens* is commonly found in dune slack vegetation and the boundaries between humid dune slacks and habitat type 2170 dunes with *Salix repens* ssp. *argentea* are often difficult to define on the ground. Dunes with *Salix repens* often mark the mature phase of calcareous dune slacks (the SD16 community in the UK National Vegetation Classification), and are reported separately in the UK. A range of other wetland types, especially swamp, mire and tall herb fen community, occur within the slacks on some dune systems, including Kenfig. Additionally, dune slack habitats do not always fit to the definition of 2190 humid dune slacks and can range from temporary water bodies to mature wetland communities lying within the larger dune systems (Houston, 2008).

Mapping with Remote Sensing

There are clearly several key features that define this habitat from an ecological sense, but contextually there are some features that will stand out in remote sensing data that will be able to separate this habitat from its surroundings. The key definition is that humid dune slacks are always relatively flat and are surrounded by dunes that have a higher slope value. With a high resolution DEM, where derivatives such as slope can be calculated, the boundaries of this habitat should be fairly straightforward to distinguish. The difficulty in separating the types of slack that are defined in the Annex I habitat with those that are not will be more challenging from EO, however, if an original slack boundary is formed from a DEM, then differences such as the type of dominant lifeform on a slack (woody in the case of *salix repens* and herbaceous for grassy slacks) should be separable. For example, some of the EUNIS classes such as dune slack reedbeds and sedgebeds can be recognised by tall emergent vegetation, which will have a different spectral response to dune slack pioneer swards, which will be short in height and have very little vegetation.

However, some of the NVC types will not be separable from EO (SD14 and SD15) as they are separated by mosses that exist below a canopy of *salix repens* and are most likely not visible from above.

These assumptions are based on the availability of VHR as it is expected that many of the slack features on sites will be too small for separation between neighbouring habitats in medium resolution imagery such as Landsat. The fact that humid dune slacks flood most winters also needs to be considered when handling EO data, as the slacks will need to be water free for the habitat types to be separated. The issue of related habitats, particularly an Annex I habitat (2170) also needs to be considered. As this habitat is located on the fringes of humid dune slacks and dunes and is mostly dominant with *salix repens*, then the suggestion is that the class should initially be included in the slack boundary class, and separated using measures of wetness (such as Normalised Difference Wetness Index) to distinguish drier stands of *salix repens.*

5.3.2 Fixed coastal dunes with herbaceous vegetation ("grey dunes") 2130

Habitat Definition

Fixed and semi-fixed dunes can be found on the dune ridges between the dune slacks that occupy a zone behind mobile dunes, usually dominated by marram *Ammophilla arenaria* (JNCC, 2007b).

In the UK the semi-fixed and fixed dune vegetation corresponds to the following NVC types:

- SD7 *Ammophila arenaria - Festuca rubra* semi-fixed dune community

Figure 5.3: Fixed dune grassland at Kenfig Burrows SAC.

- SD8 *Festuca rubra - Galium verum* fixed dune grassland
- SD9a *Ammophila arenaria - Arrhenatherum elatius* dune grassland, typical sub-community pp
- SD9b *Ammophila arenaria - Arrhenathrum elatius* dune grassland, *Geranium sanguineum* sub-community
- SD19 *Phleum arenarium - Arenaria serpyllifolia* dune annual community

Fixed dunes are an extremely complex habitat type and for the purposes of the Habitats Directive and the herbaceous vegetation of fixed dunes in the UK exhibit considerable variation. Of particular importance are Atlantic dune (*Mesobromion*) grasslands. As with 2110 Embryonic shifting dunes and 2120 Shifting dunes along the shoreline with *Ammophila arenaria*, this Annex I habitat type is widely distributed around the coats of the UK and are a major component of many sand dune systems.

Table 5.3: Main sub-types of fixed dune grassland identified in the EUNIS and CORINE biotopes classifications.

EUNIS (Coastal stable dune grassland dunes)	CORINE (Grey dunes)
Northern fixed grey dunes	Northern Atlantic grey dunes
Biscay fixed grey dunes	Biscay grey dunes
Mediterranean-Atlantic fixed grey dunes	Ibero-Mediterranean grey dunes
East Mediterranean fixed grey dunes	East Mediterranean fixed dunes
Atlantic dune Mesobromium grassland	Atlantic dune Mesobromium grasslands
Atlantic dune thermophile fringes	Atlantic dune thermophile fringes
Dune fine-grass annual communities	Dune fine-grass annual communities

Mapping with Remote Sensing

As with slacks, the main feature that will help distinguish fixed dune grassland from it is surroundings is the assumption that dunes have a higher slope value. However, there is also the issue of separating this habitat with Annex I habitat 2120 - shifting dunes. It is expected that more bare sand will be visible in the latter habitat, which will be spectrally distinct from remotely sensed data, but areas where *Ammophila arenaria* is dominant could present some confusion. The EUNIS sub-types seem to be differentiated by bio-geographical regions and are therefore not relevant for separation in this study as most of the habitats of interest are Atlantic dunes. When it comes to separating sub classes within fixed dune grassland of the NVC types from EO, the chances of separation are low unless there is one dominant species present that has a distinguishable feature, for example the presence of bracken. However, it is seen as feasible to map the Annex I habitat by process of elimination, i.e. its surrounding landscape is mapped first leaving out features that correspond with fixed dune grassland.

5.3.3 Semi-natural dry grasslands and scrubland facies: on calcareous substrates (*Festuco-Brometalia*) 6210

Habitat Definition

These grasslands are found on thin, well-drained, lime-rich soils associated with chalk and limestone. They occur predominantly at low to moderate altitudes in England and Wales. This Annex I category includes various forms of calcareous grassland referable in European terms to the *Mesobromion* and *Xerobromion* alliances. All forms of *Festuco-Brometalia* grassland compromise mixtures of grasses and herbs, in which there is at least a moderate representation of clacicolous species (Calaciura and Spinelli, 2008). The main sub-types of these grasslands in the UK correspond to the following NVC types:

- CG1 *Festuca ovina - Carlina vulgaris* grassland
- CG2 *Festuca ovina - Avenula pratensis* grassland
- CG3 *Bromus erectus* grassland
- CG4 *Brachypodium pinnatum* grassland
- CG5 *Bromus erectuc - Brachypodium pinnatum* grassland
- CG6 *Avenula pubescens* grassland
- CG7 *Festuca ovina - Hieracium pilosella - Thymus praecox/pulegioides* grassland
- CG8 *Sesleria albicans - Scabiosa columbaria* grassland
- CG9 *Sesleria albicans - Galium sterneri* grassland

In the field there was confusion between the distinction of limestone grassland and calcareous grassland types. The guidelines in the NVC state a number of species that should

be present. The problem with this is that many of these species must also be present for maritime grassland habitat. For continuity purposes, it was decided to adopt the classes used during a local monitoring project that used the presence or absence of *Carex flacca* to define these habitats. The problem with this is that there are only certain times of the year when this species is distinct within the habitat in addition to all the other species that need to be present in both grassland habitats. The limestone grassland at Castlemartin also supports the largest colony of the Annex II listed butterfly *Eurodryas aurinia* in Wales, with Devils-bit scabious *Succisa pratensis* (the foodplant for the larvae) occurring in large stands.

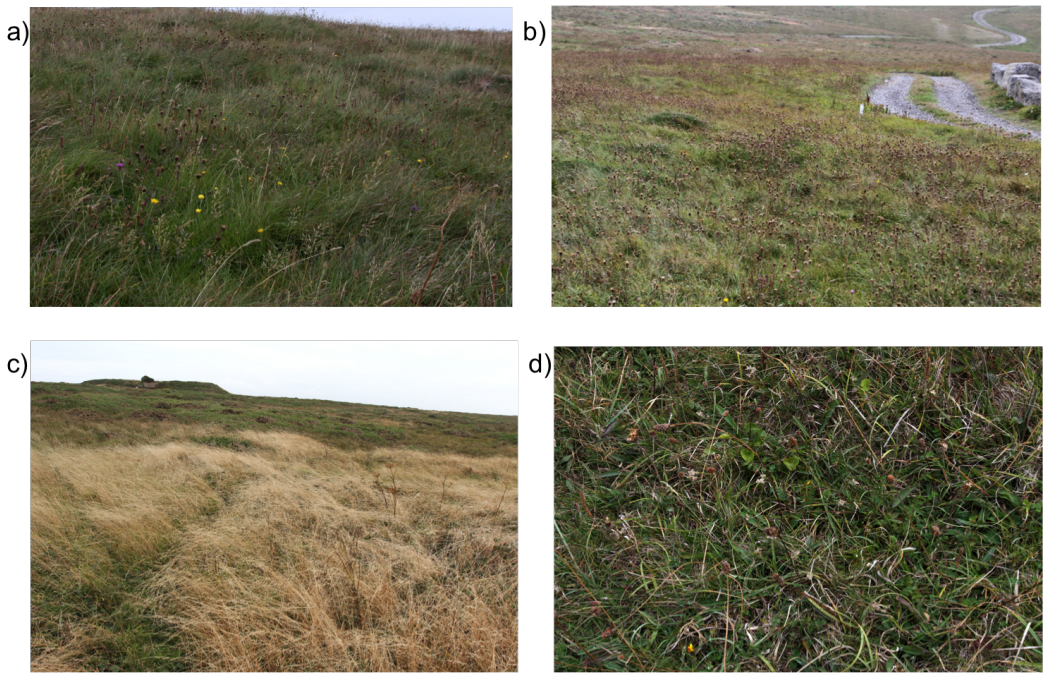

Figure 5.4: a) and b) limestone grassland; c) rank grassland - not Annex I type; d) short species rich limestone grassland.

Mapping with Remote Sensing

As with fixed dune grassland, mapping the different types of grassland will be more challenging using remote sensing. However, as seen in Figure 5.4, the visual differences

between the limestone grassland types that form the Annex I habitat and the rank grassland suggest that separation is possible. The differences in height and structure will affect the spectral response, but separation will still require as many training points as possible.

5.3.4 Vegetated sea cliffs of the Atlantic and Baltic coasts 1230

Habitat Definition

Vegetated sea cliffs are steep slopes fringing hard or soft coasts, created by past or present marine erosion, and supporting a wide diversity of vegetation types with variable maritime influences. The vegetation of sea cliffs in the UK includes 12 maritime cliff NVC types, although the range of vegetation types present is much broader. Cliff-top heath vegetation is included in the Annex I definition, and comprises maritime heath communities referable to NVC types H7 *Calluna vulgaris - Scilla verna* heath and H8d *Calluna vulgaris - Ulex gallii* heath *S. verna* sub-community. Cliff-top heath vegetation may extend landward into non-maritime zones, where it is considered as part of Annex I type H4030 European dry heaths (JNCC, 2007a). The main sub-types in the UK correspond to the following NVC types:

- MC1 *Crithium maritimum - Spergulatia rupicola* maritime rock-crevice community
- MC2 *Armeria maritima - Liguticum scoticum* maritime rock-crevie community
- MC3 *Rhodiola rosea - Armeria maritima* maritime cliff-ledge community
- MC4 *Brassica oleracea* maritime cliff-ledge community
- MC5 *Armeria maritima - Cerastium diffudum* ssp. *diffusum* maritime therophyte community

- MC6 *Atriplex prostrata - Beta vulgaris* ssp. *maritima* sea-bird cliff community
- MC7 *Stellaria media - Rumex acetosa* sea-bird cliff community
- MC8 *Festuca rubra - Armeria maritima* maritime grassland
- MC9 *Festuca rubra - Holcus lanatus* maritime grassland
- MC10 *Festuca rubra - Plantago* ssp. maritime grassland
- MC11 *Festuca rubra - Daucus carota* ssp. *gummifer* maritime grassland
- MC12 *Festuca rubra - Hyacinthoides non-scripta* maritime bluebell community
- H7 *Calluna vulgaris - Scilla verna* heath
- H8d *Calluna vulagris - Ulex gallii* heath *S.verna* sub community

Mapping with Remote Sensing

There are several aspects of this habitat's definition to consider here in context with mapping with remote sensing. This Annex I type includes different land covers within its definition that guarantees some aspects of the habitat can be separated. These will be the short maritime grassland that includes some bare ground and the pioneer heath class, which will have a lot of bare ground. Figure 5.5 demonstrates the differences between these classes. As with all grasslands mentioned so far, separation from other grassland types will prove difficult from remote sensing but here another challenge is presented in the form of differentiating maritime grassland from maritime heath. The latter will include woody vegetation, but enough training data will need to be acquired to secure a high chance of separation. Another problem is the presence of mosaic areas, and the question of scale. With 2 m VHR there is a good chance of separating mosaic vegetation depending on size of patches and if pixel based analysis is preserved. Once objects are

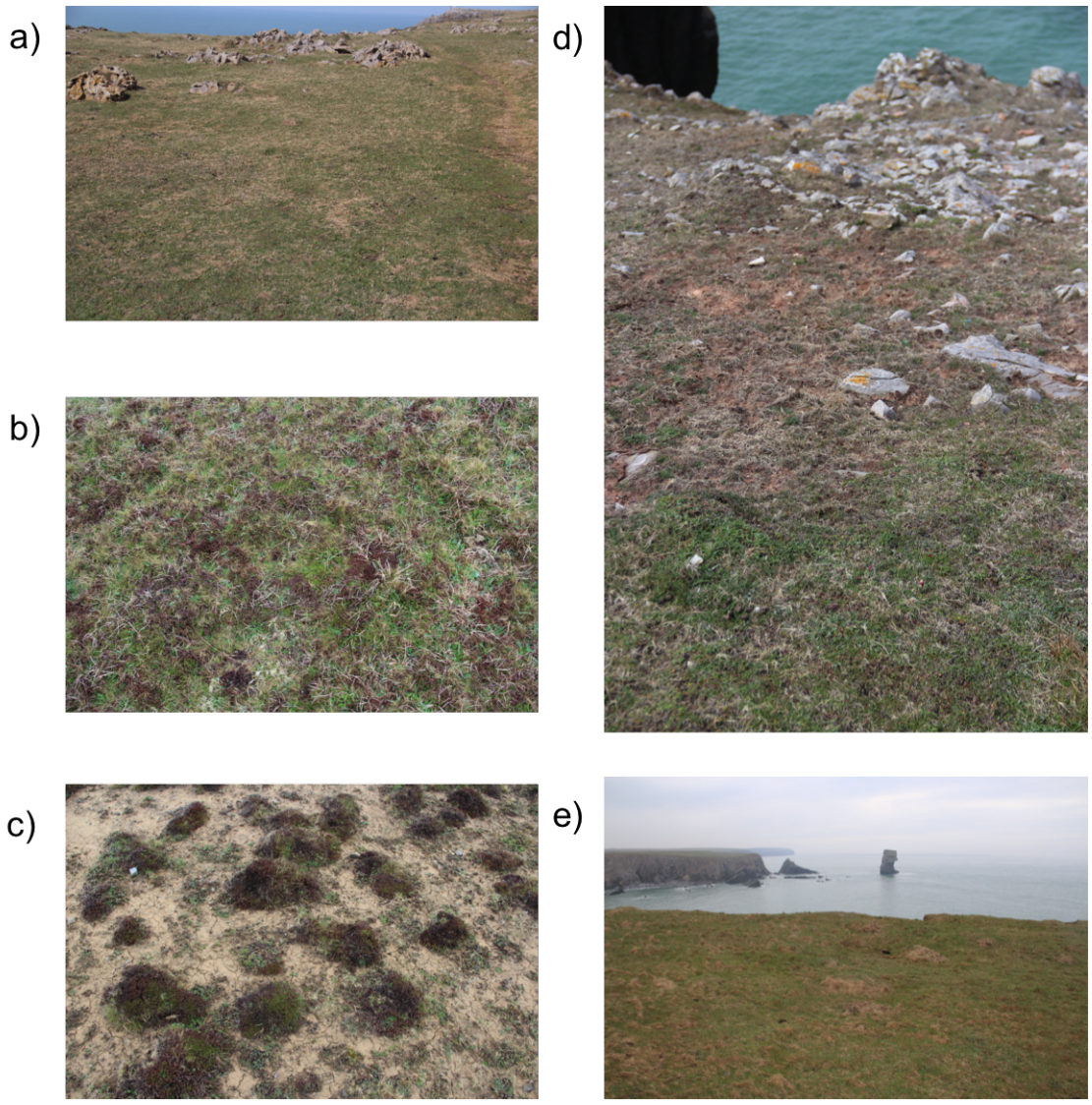

Figure 5.5: a), d) and e) maritime grassland; b) maritime heath; c) pioneer heath.

created, this patterning will be lost. It is inevitable that some patches will be too small and it is likely that those areas will be mapped as the most dominant feature.

5.4 Conclusions

A couple of key conclusions have been reached during the synthesis of the various classification schemes. First, it is evident that the problem of standardisation and harmonisation has been recognised as an issue at all scales and steps have been taken to try and tackle the issue. New classification schemes have been devised, like the LCCS, which can incorporate changes in scale as well as tackling the nomenclature needed for different applications. However, creating a new scheme for every new policy that comes around is not cost effective and does not solve problems in using datasets for change detection and comparison. The EAGLE concept has tried to combat that issue by providing a platform for translating definitions.

The second conclusion is that although land cover and habitat are related in many ways, especially when considering mapping and monitoring applications that utilise EO, there are key differences that need to be recognised, in particular the ability of a habitat to encompass more than one land cover type (e.g. bare ground and vegetative cover). This is the key reason why there are no products that emulate a habitat map like there are products created for land cover, and while there are some maps in existence that claim to be habitat maps, they are in fact land cover maps. This is also the reason why translating from one classification scheme to another is difficult when moving from a land cover dominated scheme to a habitat focused scheme and vice versa.

The uptake of different classification schemes in individual countries, especially new schemes is incredibly difficult to sell as local classification schemes are built specifically to the vegetation communities that exist in that country. This is true in countries such as

the UK, where the NVC scheme is still the most widely used and field ecologists try to fit and translate NVC categories into schemes like Annex I because of familiarity. There are problems with doing this in the field that can generate lengthy discussions on habitat definitions. If approaches of mapping and monitoring using EO are to be built operationally, then this way of thinking and working will have to adapt as some of the Annex I habitat definitions are possible to classify using EO while some of the NVC categories related to them are not.

Chapter 6

Classification of Broad Habitats

6.1 Introduction

Land use and increasing anthropogenic pressures remains a significant driver of land cover change and habitat degradation, which is of concern for maintaining biodiversity. The need to halt potential losses of biodiversity has been recognised for decades and many monitoring schemes have been initiated in response to EU nature directives, primarily focusing on the quantity and quality of habitats at the global, regional, national and landscape levels. In Europe, the Natura 2000 network was established to connect relevant designated sites across participating member states on a regional habitat scale to aid the fulfilments of the EC's habitats directive. However, mapping and monitoring methods still vary greatly across countries making it difficult to quantify the extent and condition of these habitats at an international level. Remote sensing technologies are increasingly recognised as a key approach for obtaining information on habitat extent and condition as the range and modes of data are vast and available at different spatial resolutions and temporal frequencies. This chapter provides a description of the method used to delineate

broad habitat types from EO data at two study locations, both of which have international significance.

6.2 Background: Sensors and Techniques

6.2.1 Aerial Optical Imagery

One of the oldest forms of remote sensing imagery is that acquired by aerial photography, which has traditionally been used as a basis for field mapping but can also be used for validating maps generated from other EO data sources (Adam et al., 2009). The very high spatial resolution of the dataset enables analysis of greater detail in comparison to any spatial resolutions acquired by spaceborne imagery, and can be used to identify and delineate plant assemblages at the physiognomic or formation levels (Howard et al., 1970). Many studies have demonstrated habitat maps based on the combination of aerial photography and a GIS where classes were digitised based on differences in colour and texture visible in the imagery with accuracies over 85% (Plieninger, 2006; Higinbotham et al., 2004; Zharikov et al., 2005). Harvey and Hill (2001) stated that the use of aerial photography over multispectral spaceborne data was clearly superior for mapping vegetation communities.

One of the most common limitations of most studies is the difficulty presented with co-registration of imagery and the correction for different environmental and atmospheric conditions at the time of image acquisition (Shanmugam and Barnsley, 2002; Zharikov et al., 2005). Many studies (Seher and Tueller, 1973; Shima et al., 1976; Lehmann and Lachavanne, 1997; Howland et al., 1980) have also questioned the feasibility of aerial optical imagery for mapping and monitoring on a continuous scale, as it is non-automated, making it time-consuming and costly to process. Some countries, such as Wales, fly na-

tional coverage of aerial photography, which is considered a valuable resource. However, most countries cannot afford to acquire or process data on such a scale which means this level of detail is only applicable when and where it is acquired.

The lack of spectral resolution of aerial photography is another major limiting factor for its application in vegetation mapping (Yang, 2007). Other airborne sensors available include the acquisition of hyperspectral data. Many studies (Wang et al., 2007a; Shanmugam et al., 2003; Thackrah et al., 2004; Schmidt and Skidmore, 2003; Lucas et al., 2002; Belluco et al., 2006; Vahtmäe et al., 2006; Heiden et al., 2007) have demonstrated that classifications based on high spectral resolution airborne data tend to provide the best results with accuracies as high as 92% overall accuracy stated. The capability of hyperspectral remote sensing to identify dominant plant species (Hestir et al., 2008; Oldeland et al., 2010) and chlorophyll contents (Blackburn and Steele, 1999; Zhang et al., 2008; Atzberger et al., 2010) is a clear advantage over other data sources because of its greater spectral range. The effectiveness of hyperspectral data in discriminating vegetation species is, however, questioned when considering the high correlation between species of similar biochemical and biophysical properties which are in turn directly influenced by environmental factors. The unique spectral signature based on species might not be as effective especially considering the variations within species relating to age, micro-climate, soil, topography and stresses (Price, 1994). Another limitation, similar to aerial photography, is that hyperspectral imagery is expensive to acquire and time-consuming to process, even over small areas (Adam et al., 2010) questioning its suitability for long-term monitoring priorities.

6.2.2 Optical Spaceborne Imagery

Optical spaceborne imagery is a key source of land cover information that is routinely used for resource management and monitoring programs (Bartholomé and Belward, 2005; Büttner et al., 2004; Fuller et al., 2002). The key advantage of satellite imagery is the

repeatability of data acquisition at frequent intervals and its ability to provide information at different scales (Roy and Tomar, 2000; Amarnath et al., 2003; Kerr and Ostrovsky, 2003; Rouget, 2003), which is of high significance for timely and cost-effective habitat monitoring (Fassnacht et al., 2006). The most popular sensor for ecological applications such as vegetation and habitat mapping is Landsat as it offers over 40 years of imagery with spectral measurements in all major portions of the electromagnetic spectrum (visible, near-infrared, and shortwave-infrared) (Cohen and Goward, 2004). Several studies have stated that the broader spectral range of Landsat increases mapping abilities in comparison to other sensors with greater spatial resolution such as SPOT (Harvey and Hill, 2001; Baker et al., 2006; Civco, 1989; Hewitt, 1990; Bolstad and Lillesand, 1992). However, the moderate resolution (30 m) of Landsat data is deemed suitable for coarse descriptive level mapping only (Malthus and Mumby, 2003).

The launch of commercial satellites IKONOS and Quickbird in 1999 and 2001 respectively improved abilities to classify vegetation at spatial scales previously only attainable from aerial photography (Turner et al., 2003). The VHR of these satellites is providing the means for more accurate change detection in ecosystem health, productivity and habitat quality (Klemas, 2011). Studies have successfully utilised Quickbird to map *Trapa natans*, *Phragmites australis* and *Lythrum salicaria* communities (Laba et al., 2008), salt-marsh vegetation (Belluco et al., 2006) and for monitoring bog vegetation (Harris and Bryant, 2009). While Anderson et al. (2004) successfully characterised *Juncus* communities using IKONOS imagery. These sensors however, are limited to four spectral bands (blue, green, red and near infrared) and it was not until the launch of Worldview-2 in 2009, which had an additional four bands (coastal, yellow, red edge and another near infrared band), that the potential of VHR sensors to map natural vegetation communities was unlocked. Worldview-2 has been used to assess fine-scale plant species diversity in grassland (Dalmayne et al., 2013), identify natural vegetation formations in dune and marsh

systems (Rapinel et al., 2014), and several studies estimated forest biomass and structural parameters (Eckert, 2012; Mutanga et al., 2012; Ozdemir and Karnieli, 2011).

6.2.3 Review of image analysis techniques

Image analysis within the remote sensing community traditionally refers to image classification, which is described as the systematic grouping of classes or themes extracted from remotely sensed data (McDermid et al., 2005; Xie et al., 2008). Classification is a preferred technique because the methods are well known and widely used within the community. The output is generally simple to understand, and the accuracy of the results can be assessed quantitatively and qualitatively (McDermid et al., 2005). This section will provide an overview of these popular techniques (traditional methods) in addition to a review on improved methods, such as Object Based Image Analysis (OBIA) and Knowledge Based Classifiers.

Traditional classification methods can generally be referred to as either unsupervised or supervised. As stated from the name, unsupervised classification does not require prior knowledge of the area, whereas supervised classification does require *a priori* knowledge for training the classifier. Classes can then be assigned based on predicted variables measured from the training dataset (Černá and Chytrỳ, 2005). Examples of unsupervised algorithms include K-means and ISODATA, and are often used for thematic mapping on a large scale as they do not require spatially detailed ground data initially, and produce useful information by clustering spectrally similar pixels (Tso and Olsen, 2005; Giri et al., 2011). The algorithms are also often widely available in image processing and statistical software packages (Langley et al., 2001). However, the benefits of unsupervised techniques are often outweighed by the difficulty of post classification labelling, which does require ground information (Eve and Merchant, 2007; McDermid et al., 2005). Zak

and Cabido (2002) therefore, state that unsupervised methods are preferred for help in preliminary field campaigns.

The most widely used supervised classification technique is the Maximum Likelihood Classifier (MLC). It has been used to successfully map areas with high classification accuracies (MacAlister and Mahaxay, 2009; Laba et al., 2008; Fuller et al., 2006) but works on the assumption that input data follow a Gaussian distribution. MLC may perform poorly in the presence of non-parametric distributions (Peddle, 1995), as it is heavily reliant on the distribution of the training data.

Another method includes the calculation of spectral indices to characterise specific attributes of plants (DeFries et al., 1995). The most widely used spectral index is the NDVI and is based on the fact that vegetation is highly reflective in the near infrared and has a high absorption rate in the visible red wavelengths. The contrast between these wavelengths can be used as a biophysical parameter that correlates with photosynthetic activity of vegetation, which is an indication of 'greenness' (Wang and Tenhunen, 2004). Therefore, NDVI is a good indicator to reflect dynamic changes of different vegetation groups (Geerken et al., 2005). This area of spectral indices has expanded rapidly and numerous indices are available for different biophysical parameters (e.g, soil moisture, plant senescence). More information on these can be found in Chapter 4.

So far, the methods discussed are per-pixel classifications as opposed to object-based approaches. Environmental objects are parts of the real world for which information can or should become available (e.g, a tree). As soon as the real world part becomes a formal object in a spatial dimension then it can be subject to some kind of classification (Bock et al., 2005b). However, object based analysis is very much dependent on the spatial resolution of available imagery (Figure 6.1). The follow-up map for the UK LCM (Fuller et al., 2002) was one of the principal drivers in the development of OBIA in ecological remote sensing. Lucas et al. (2007) also suggested a similar approach as part of a pilot

study commissioned by the Countryside Council for Wales and the British National Space Centre (BNSC). The study used time-series of Landsat TM/ETM+ data as input to a rule-based segmentation and classification system developed within the eCognition software package (Definiens, 2004). It differs from other traditional OBIA approaches by first segmenting the landscape into objects that varied from pixel size to entire fields (using land parcel boundaries) and then applying a series of numerical rules on the basis of known links between the distribution of habitats in the landscape and their manifestation within EO data.

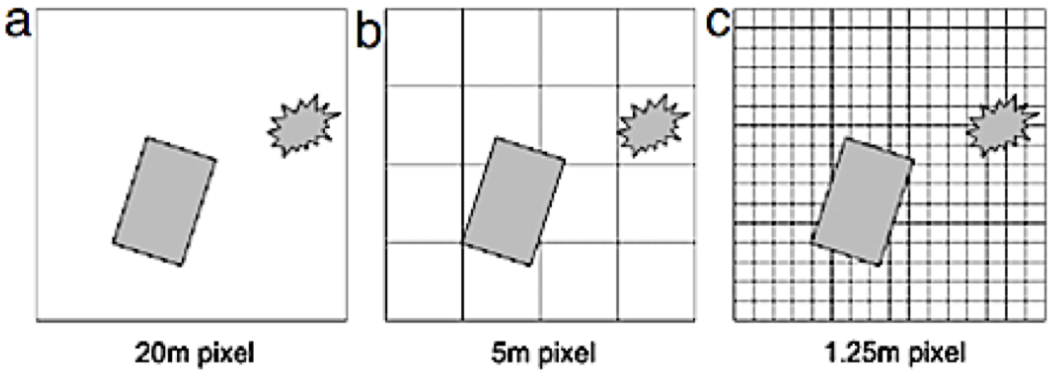

Figure 6.1: Relationship between objects and spatial resolution: (a) low resolution: pixels larger than objects. (b) medium resolution: pixels and objects are of similar size. (c) high resolution: pixels are smaller than objects (Blaschke, 2010).

The advantage of the object-based approach is that it offers new possibilities for image analysis as image objects can be characterised not only by spectral values but by texture, shape, context, relationship and thematic information supplied by ancillary data (Bock et al., 2005b). Additional layers of knowledge can be valuable to a classification system especially when certain habitat types do not have very distinct spectral features. Fuzzy membership functions can also be used which is what classification within eCognition is primarily based (Blaschke, 2010). The main advantages of fuzzy classifiers are to express uncertainty. For example, when an object may belong in more than one class, it is defined by a membership degree where the higher the degree of membership for the most likely

class, the bigger the difference to the second most probable class, therefore creating a more reliable definition for the object (Benz et al., 2004).

Many segmentation algorithms are not adapted to detect the variety of geographical entities comprising a complex scene and while they perform well in delineating some landscape objects, this is rarely true for all objects of interest (Marceau et al., 1994). The issue of scale is problematic for segmentation algorithms as segments in an image will never represent meaningful objects at all scales which is required for many applications, although multi-scale segmentation approaches may be able to combat this (Blaschke et al., 2001). A chessboard segmentation allows users to segment the image based on individual pixels for use in raster attribute tables, but this type of method is still considered as a pixel based approach even after implementing a segmentation algorithm.

Traditional classification methods are able to learn automatically from clustering or training data, while knowledge based classifiers require user-defined thresholds to determine class relationship. While training data is not necessarily required, expert knowledge of the area of interest is needed, which is why knowledge based classifiers require information from ecologists for vegetation characterisation. The use of extensive field knowledge and auxiliary data and the use of empirical rules to extract thematic features has proved successful, and can even improve classification accuracy (Gad and Kusky, 2006; Shrestha and Zinck, 2001). The most common knowledge based classifiers are therefore, rule-based, and are commonly accompanied by image segmentation and OBIA approaches. Lucas et al. (2011) successfully applied a rule-based approach to update the Phase 1 habitat of Wales, by utilising satellite imagery and ancillary data, with classification accuracies in excess of 80%. Approaches like this enable full user control but gathering specific knowledge and obtaining ancillary data is often seen as a time consuming task and can be very costly and to time consuming (Xie et al., 2008). However, in countries such as the UK, much of this data is already acquired by conservation bodies, and better communica-

tion between the remote sensing and ecological communities is encouraged (Lucas et al., 2007).

6.2.4 The EODHaM Method

Most areas in Europe are mapped and monitored using a range of different data sources and methods with varying degrees of success leading to large gaps in the knowledge required to fulfil the EC's habitats directive (Borre et al., 2011). The only project that has attempted to create a systematic approach for mapping habitats from EO data to date is the FP7-funded BIOSOS project, which focused on a multidisciplinary approach to bridge the gap between remote sensing scientists and ecologists so that funding can be used effectively for monitoring and management practices. The project developed the EODHaM system which provided a standardised framework for consistent land cover and habitat mapping and monitoring of Natura 2000 sites. A key component of the system is the inclusion of decision rules within a hierarchical classification structure. This is generated from expert knowledge from both ecologists and remote sensing scientists (Lucas et al., 2015). This section will give a brief overview of the EO components represented as modules within the EODHaM system (Figure 6.2). Although change analysis is a component, this chapter will only be implementing the mapping aspect of the system.

Overall Structure

The system adopts the FAO LCCS (Di Gregorio and Jansen, 2000); Figure 6.3), as it shows the closest correspondence of any common classification scheme (Tomaselli et al., 2013). Bunce et al. (2013) have analysed the appropriateness of implementing the LCCS in the context of habitat and biodiversity monitoring and state that its hierarchical nature provides a useful framework for EO and in situ data integration. Furthermore, the system uses GHCs in combination with information on environmental variables (e.g. bio-

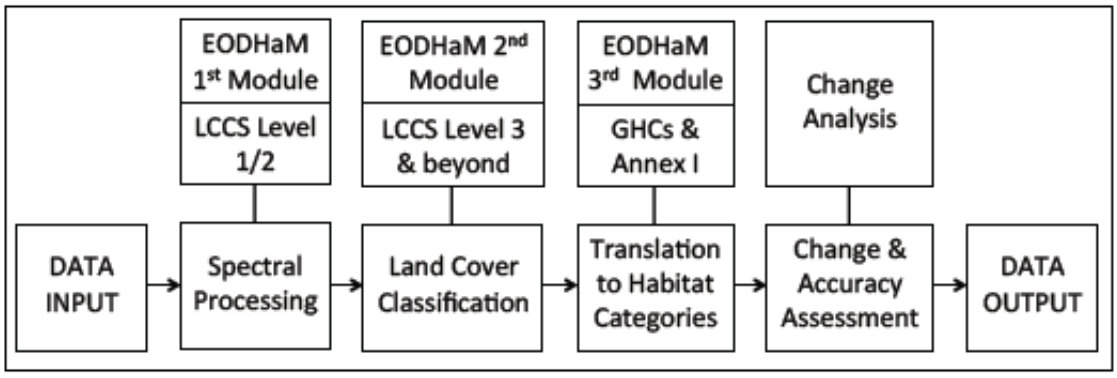

Figure 6.2: Overview of the EO components within the EODHaM system. The system is hierarchical and top down and commences with the classification of Levels 1 and 2, with this based on spectral processing alone, and continues to LCCS Level 3 and beyond. The final LCCS categories are then translated to GHCs and subsequently to Annex I. Change analyses are then performed (Lucas et al., 2015).

geographical regions, surface moisture) and on dominant or indicator species. Annex I habitats can therefore be delineated (Bunce et al., 2012), although end-user interaction is often a requirement at this stage.

The processing of EO data within the EODHaM system is automated, with the exception of threshold value determination, and is undertaken primarily using the RSGISLib software (Bunting et al., 2014), the Geospatial Data Abstraction Library (GDAL), and ORFEO Toolbox (Inglada and Christophe, 2009). All software used within the system is open source, freely available and can be implemented as libraries within the Python scripting language. The classification system also makes use of the KEA image file format (Bunting and Gillingham, 2013), which allows for processing within a raster attribute table (RAT). Within the RAT, which has been developed such that large datasets can be efficiently analysed (Clewley et al., 2014), all pixels/objects have an unique ID. This table is first populated with image data and derived products (e.g. vegetation indices) and class codes from the LCCS are added progressively as the classification proceeds, with the final attribution being Annex I classes.

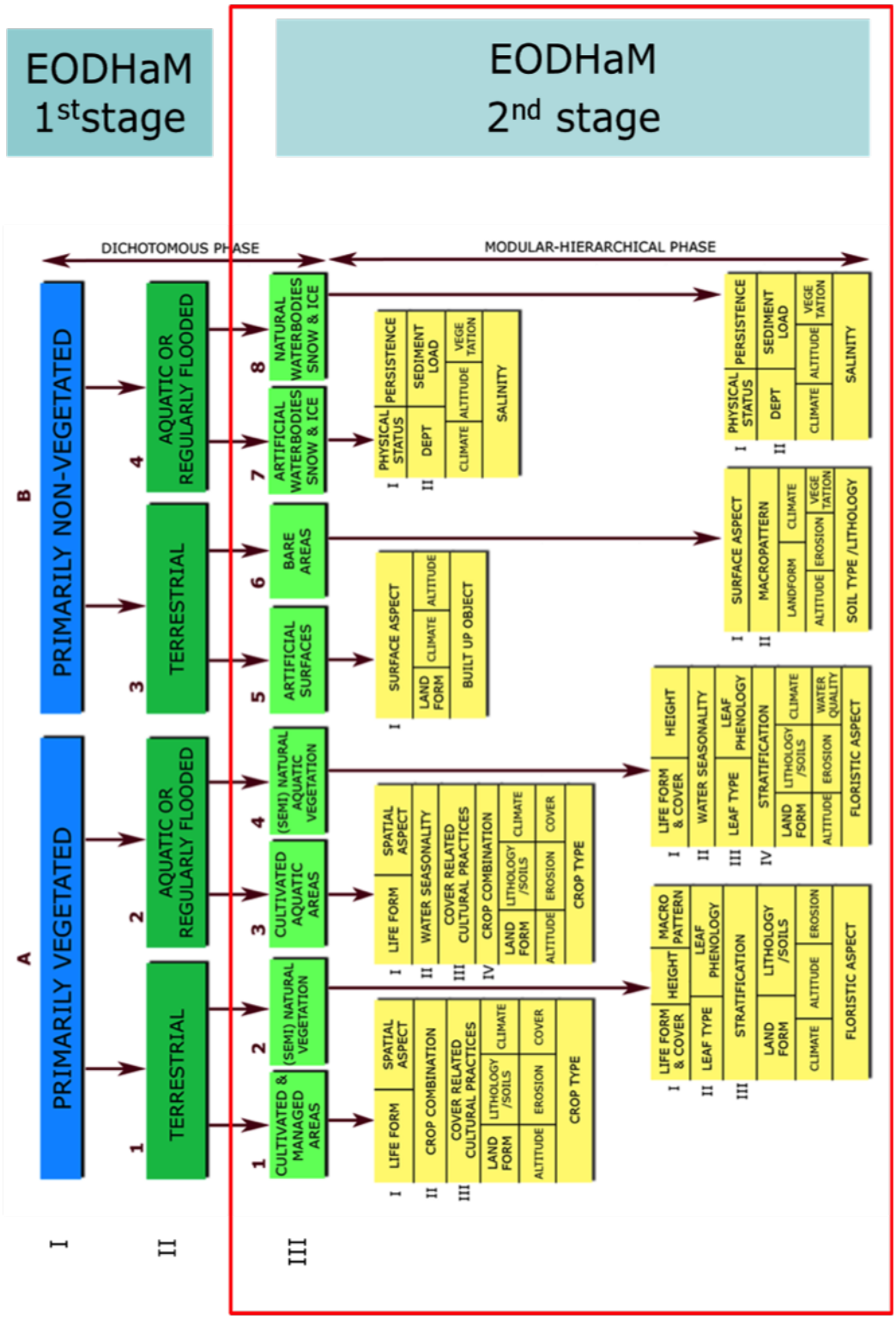

Figure 6.3: The FAO LCCS encompassing Levels 1 to 3 and beyond.

EODHaM 1st Module

The project has mainly focused on using geographic object-based image analysis (GEOBIA)(Hay and Castilla, 2008; Blaschke et al., 2001) but can incorporate pixel-based analysis. The first module therefore includes options for extracting objects, segmenting imagery and classifying the landscape to LCCS Level 2 (Figure 6.3) which are all based on spectral information. However, as previously discussed in the background section, while many studies state that OBIA outperforms traditional pixel based classification methods, the issue of scale and using appropriate segmentation algorithms means that it may not be the best option for all applications.

The object extraction option automatically extracts recognisable features from the image prior to segmentation by utilising specific spectral bands or derived indices within the ORFEO Toolbox (Arias et al., 2013), and is appropriate for delineating features such as individual trees, hedgerows and roads. Following automated extraction of landscape objects, the user has the option of implementing two segmentation algorithms. The first implements a clustering and small object elimination algorithm within RSGISLib while the second applies the Comaniciu and Meer (2002) algorithm within ORFEO Toolbox. However, these options are only appropriate if these features are prominent in the mapping area and can be compromised where boundaries are indistinct or a large number of objects with a high spectral diversity occur within each unit (Lucas et al., 2015), which is common in many small Natura 2000 sites across Europe.

The classification of LCCS Level 1 and 2 utilises a sequence of decision rules based on a narrow range of spectral indices. The recommended indices to use for each module are described at the end of this section. The thresholds applied within the sequence of rules and data layers are subject to change depending on the user's interpretation of the scene although they are generally similar within and often between environments. A binary

mask of the extent of different vegetative states and open water, based on indices such as the NDVI and NDWI (Figure 6.4), is generated for each category. Every pixel/object within the RAT is then progressively attributed with the binary mask information and ultimately the class is assigned (e.g. water, vegetated).

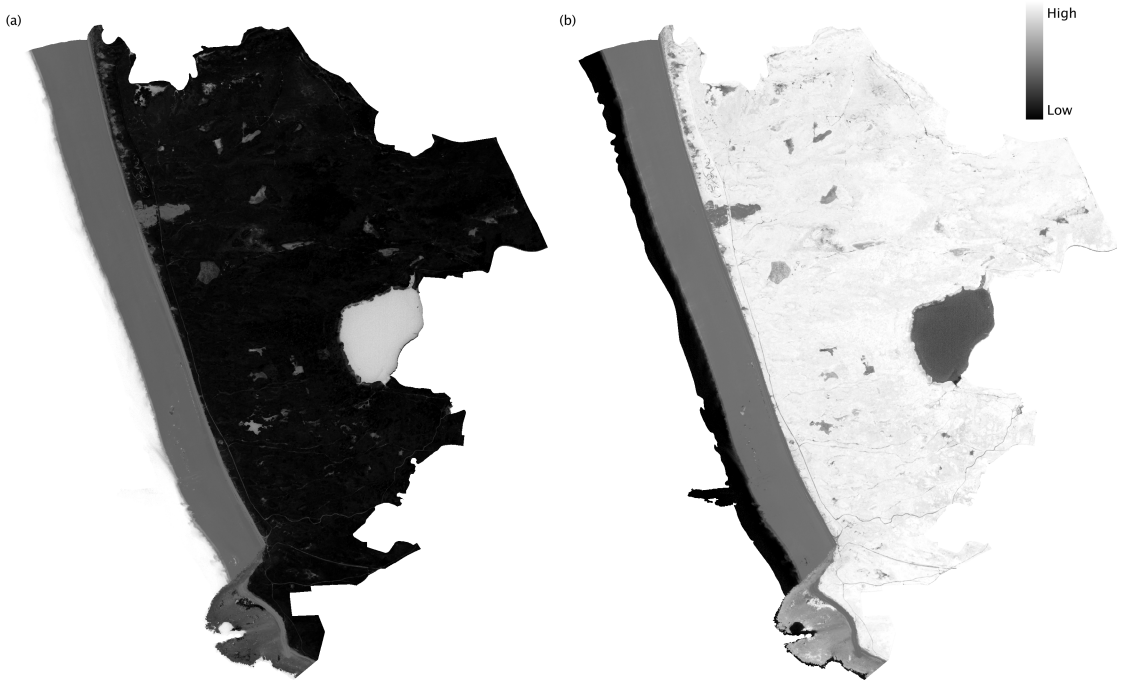

Figure 6.4: (a) the NDWI and (b) the NDVI representing areas of water bodies and green vegetation respectively at Kenfig Burrows SAC.

EODHaM 2nd Module

The second module has two main components focusing on classification of LCCS Level 3 and subsequently, Level 4 (Figure 6.3). The Level 3 classification requires that the landscape be differentiated according to elements that are cultivated, managed, natural or semi-natural which can be extracted from existing thematic layers (e.g. cadastral, infrastructure). For Natura 2000 sites for example, the site boundary can be used as a thematic

layer as most sites mainly include natural or semi-natural elements. Once areas are associated with these labels, they are cross tabulated to generate a classification of Level 3 categories (e.g. natural and semi-natural terrestrial vegetation). These categories are then carried forward to classify beyond Level 3, for example, vegetated areas are delineated into lifeform categories some of which are woody and herbaceous. The production of LCCS codes in this manner is dependent on the information available either from EO data, ancillary data or expert knowledge and some aspects of the LCCS may not be possible, for example height descriptors in the absence of LiDAR data.

EODHaM 3rd Module

The third module includes automated GHCs and Annex I habitat maps being produced based on a translation from the LCCS classes extracted in the previous modules. There are many discrepancies in definitions between the LCCS and GHCs taxonomies with several one-to-many relationships being observed (Kosmidou et al., 2014). Several studies have tried to solve such ambiguities (Adamo et al., 2014; Bunce et al., 2007, 2012; Petrou et al., 2012, 2014b,a) but they all include additional site-specific expert rules such as contextual information. These ambiguities also exist when translating from GHCs to Annex I (Tomaselli et al., 2013). This highlights the difficulties faced when trying to build a systematic approach to mapping specific sites across a vast region encompassing a variety of environments.

Spectral Indices

The EODHaM method utilises a range of spectral indices that are described here. The list below shows which indices provided the most useful information and are therefore recommended for any future mapping exercise within the system (Refer to Chapter 4 for

specific formulas and references). Some of the indices included here are relatively new within the research community, such as the Woody Index, while others such as NDVI and NDWI are popular and widely used within a range of applications (Lu et al., 2009; Lucas et al., 2012). To see equations and references for the indices below refer to Table 4.6 in Chapter 4.

1. Near Infra-red Difference (DiffNIR)
2. Forest Discrimination Index (FDI)
3. Normalised Difference Vegetation Index (NDVI)
4. Normalised Difference Water Index (NDWI)
5. Peak Post Difference (PPD)
6. Plant Senescence Reflectance Index (PSRI)
7. Red Edge Position (REP)
8. Water Band Index (WBI)
9. Woody

6.3 Method

This chapter describes the attempt to use the EODHaM system to generate broad habitat maps which would be appropriate for defining extents of Annex I habitats at two SACs in Wales. As the sites themselves are the only area of interest all data layers have been restricted to the extent of the sites themselves, and the appropriate pre-processing has been performed on all imagery (see Chapter 4). All sites are classed as semi-natural vegetation and boundaries are very diverse and mixed on the ground, therefore all analysis has been

done at a pixel level instead of implementing the object extraction and segmentation options of EODHaM Module 1. Figure 6.5 is a flow chart that explains how the EODHaM method has been adapted to specifically classify each individual site.

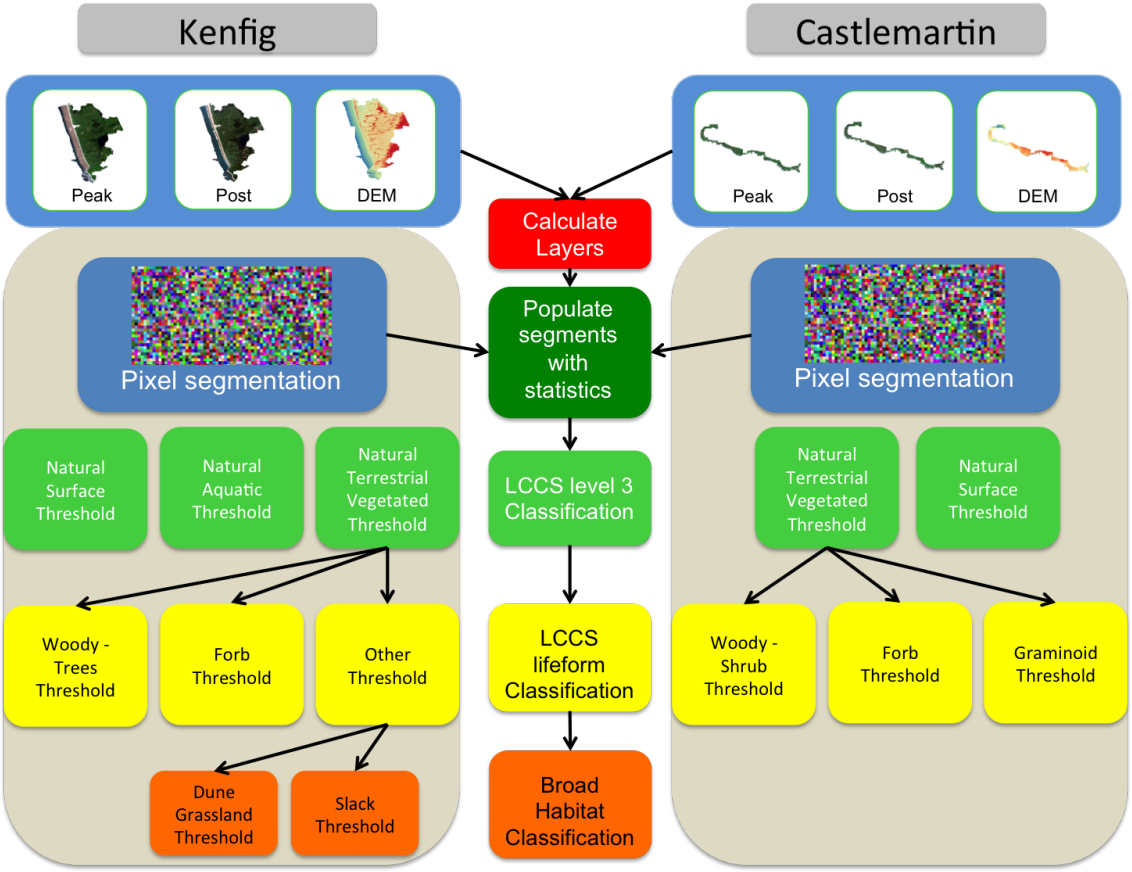

Figure 6.5: Flow chart of adapted EODHaM method applied to the two sites of interest in this study. The pixel segmentation represents a chessboard algorithm implemented for use of images in a raster attribute table (RAT). Other threshold at Kenfig includes multiple types of lifeform including graminoid and woody shrubs.

6.3.1 Mapping to LCCS Level 3

The decision rules chosen for classification of LCCS Level 1 and 2 are the Coastal band from Worldview-2 imagery for delineating terrestrial non-vegetated areas, the NDVI for terrestrial vegetated areas and the NDWI for mapping aquatic non-vegetated areas.

Thresholds were chosen for each layer based on a visual interpretation. As each image and site is different the threshold vary depending on the visual interpretation. Additionally, both images might be used to map a class to determine permanent water bodies for example. The summer image is labelled as Peak while the autumn image is labeled as Post. The hierarchical nature of the method means that once a pixel is assigned a class it cannot be assigned to another. As bare ground and water show the least variety in values they are mapped first. All pixels in the image belong to one of these three land cover types, therefore the vegetation thresholds are low to ensure that all pixels are assigned to a class as vegetation includes areas of low productivity which results in low NDVI values. Once the LCCS Level 1 and 2 are determined, the LCCS Level 3 categories are assigned. As all study areas are classed as natural or semi-natural areas the transition is simple and does not require additional information such as cadastral or urban ancillary data for example. Terrestrial vegetation becomes natural or semi-natural terrestrial vegetation, terrestrial non-vegetated becomes natural surface and aquatic non-vegetated becomes natural water.

6.3.2 Mapping to LCCS Level 4 and Broad Habitats

The first stage of mapping to LCCS Level 4 includes delineating vegetation descriptors for lifeform categories. Therefore, only pixels with the label natural or semi-natural terrestrial vegetation are relevant for lifeform mapping. As the spectral diversity is high within the vegetated areas a more robust method is needed for selecting the data layers that provide the best separability for distinguishing lifeform categories. To maximise the potential of EO data for mapping lifeform categories and beyond, numerous indices available within the literature were calculated from Worldview-2 bands in addition to those already recognised within the EODHaM system. Measures derived from LiDAR data available for all three sites such as slope were also included in this analysis. An

Analysis of Variance (ANOVA) was performed on the data layers using the training data set collected from field data or aerial photography and UAV data (see Chapter 4), to see if a significant difference (at $p<0.05$) existed between the data layers for each lifeform category. The ANOVA coefficient or F-ratio is an extension of Fisher's discriminant and provides a measure of separability between multiple classes. The analysis of variance for between group (Equation 6.1) and within group (Equation 6.2) were calculated and divided (Equation 6.3) to determine the F-ratio (Scheffe, 1959). The magnitude and significance level associated with each ANOVA *F* value were used to determine the most effective data layers in separating the categories where the larger the *F* value , the more likely it is that the null hypothesis of no differences between group means is false, indicating greater separation.

$$Vb = \frac{\sum n(x - \overline{x})^2}{p - 1} \tag{6.1}$$

where:

Vb is sum of squares between categories

p is the total number of categories

n is the total number of samples

$$Vw = \frac{\sum (n - 1)S^2}{N - p} \tag{6.2}$$

where:

Vw is sum of squares within categories

S is the standard deviation for each category

N is the total number of observations

$$F = \frac{Vb}{Vw} \tag{6.3}$$

One of the assumptions of this method is that data are normally distributed but numerous studies have demonstrated that the data's distribution has very little effect on the F-ratio (Tiku, 1971; Box and Watson, 1962). Some of the samples, which have slightly skewed distributions, have therefore been included in the analysis. Once the best layer or layers were selected, boxplots were then used to determine the best threshold values.

Based on expert knowledge it was decided that broad habitat categories can be delineated from lifeform categories eliminating the need to determine GHCs particularly as the discrepancies between the LCCS might decrease classification accuracies significantly.

6.3.3 Accuracy Assessment

An accuracy assessment based on a standard confusion matrix was carried out after each initial stage within the EODHaM system using ground data and point data collected from aerial photography and UAV imagery. An overall accuracy was calculated for all stages, including a producer's accuracy and a user's accuracy. For Kenfig, a total number of 194 points were used, while for Castlemartin, a total number of 87 points were used. Refer to Table 4.7 in Chapter 4 for more details on the number of points used for accuracy split by habitat.The user accuracy refers to the probability of a pixel labelled as a certain class being that class on the ground, and the producers accuracy referring to the probability of the ground point data being classified as such on the image. Additionally, the kappa coefficient (Equation 6.4) was calculated to account for the effect of random distributions and to determine whether the results in the error matrix were significantly better than random classification (Landis and Koch, 1977).

$$\text{Kappa Coefficient} = \frac{N \sum_{c=1}^{r} x_{cc} - \sum_{c=1}^{r} x_{c+} x_{+c}}{N^2 - \sum_{c=1}^{r} x_{c+} x_{+c}} \tag{6.4}$$

where:

r is the number of rows in the error matrix

cc is the number of observations in row c column c

$c+$ is the total number of observations in row c

$+c$ is the total number of observations in column c

N is the total number of observations in the matrix

6.4 Results

6.4.1 Mapping landscape elements - LCCS level 2 and 3

The indices used by the EODHaM system for delineating landscape elements were considered effective for classification of all sites. After visual interpretation the thresholds chosen are stated in Table 6.1. Both Peak and Post images were used to ensure that pixels are classed correctly. Accuracies (Tables 6.2 to 6.4) achieved at this level were high, providing the confidence needed at this stage of the approach to progress to mapping life-form categories. The small confusion that exists on all sites between Natural Surface and Natural Terrestrial Vegetation occur as some vegetation is present in habitats such as dune annuals, shifting dunes and rocky maritime heath which are primarily bare ground.

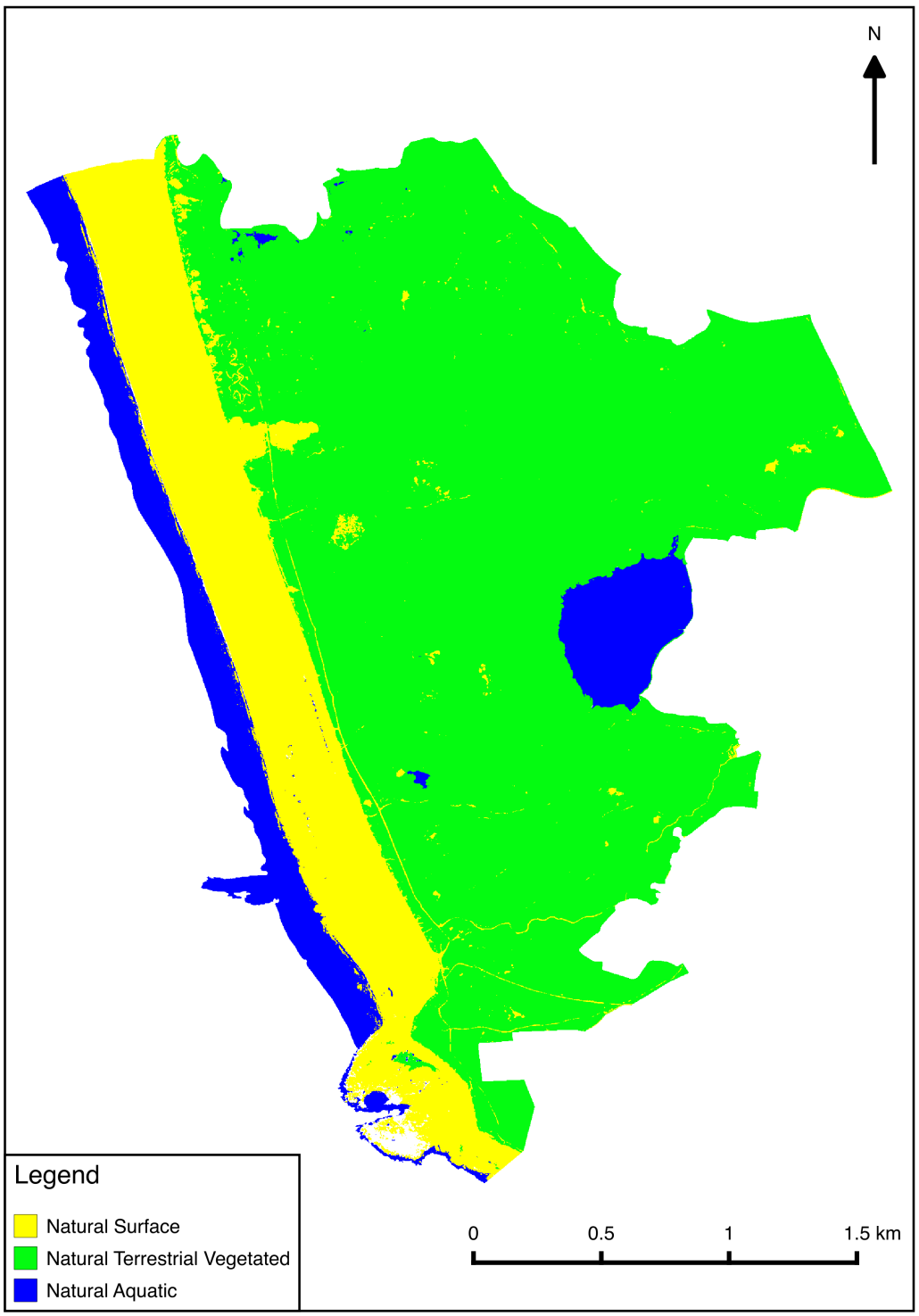

Figure 6.6: LCCS Level 3 classification of Kenfig.

Table 6.1: Thresholds used for determining terrestrial non-vegetated, terrestrial vegetated and aquatic non-vegetated categories for classification of LCCS Level 1 and 2.

Site	Terrestrial Non-Vegetated (WV2 Coastal Band)	Aquatic Non-Vegetated (NDWI)	Terrestrial Vegetated (NDVI)
Kenfig	Peak >30.5	Post >= -0.5	Peak >0
Castlemartin	Peak >33	n/a	Post >0.2

Table 6.2: Accuracy Kenfig Level 3. Overall accuracy = 98 %, Kappa value = 0.95.

	Natural Surface	Natural Terrestrial Vegetation	Natural Aquatic	Sum	Users Accuracy (%)
Natural Surface	36	5	0	41	87.8
Natural Terrestrial Vegetation	0	203	0	203	100
Natural Aquatic	0	0	18	18	100
Sum	36	208	18	262	
Producers Accuracy (%)	100	97.6	100		

6.4.2 Selection of best spectral indices for delineating lifeform LCCS categories and broad habitats.

This section only uses those pixels that were labelled as Natural Terrestrial Vegetation at LCCS level 3. This method utilises the hierarchical approach to minimise errors based on the assumptions that certain categories and habitats have to be labelled as vegetation or bare ground for example.

Kenfig

The lifeform categories mapped at Kenfig Burrows are woody and forb. The woody category consists of only trees as woody shrubs are mostly present on humid dune slacks on

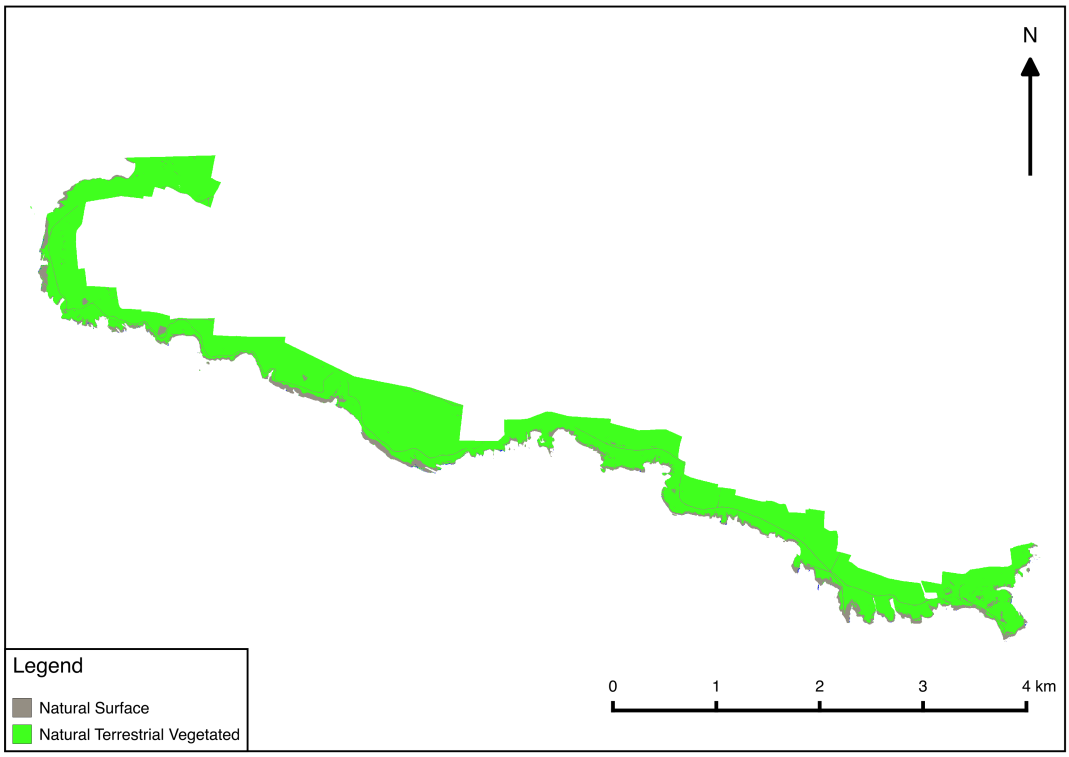

Figure 6.7: LCCS Level 3 classification of Castlemartin.

Table 6.3: Accuracy Castlemartin Level 3. Overall accuracy = 98 %, Kappa value = 0.91.

	Natural Surface	Natural Terrestrial Vegetation	Sum	Users Accuracy (%)
Natural Surface	12	2	14	85.7
Natural Terrestrial Vegetation	0	99	99	100
Sum	12	101	113	
Producers Accuracy (%)	100	98		

this site and are separated at the broad category level further down the classification approach. The other category at Kenfig therefore, includes a mixture of lifeforms including graminoid and woody shrub. *F* scores for determining the woody category (Table 6.4) are high indicating that this category can be separated successfully from the other categories. Further analysis showed that combining the two highest separable indices provides the best chance of separation (Figure 6.8). Thresholds were chosen based on the data which varied within the minimum and maximum range of the boxplots shown in Figure 6.8. The threshold used for index PostSRBY was greater than 0.9 whereas the threshold used for index PeakDatt6 was greater than 0.03.

Table 6.4: Most separable indices for determining the woody category at Kenfig.

Index	Variance Within Class (Vw)	Variance Between Class (Vb)	F Score
peakDatt6	2.51E-05	0.002863297	114.2078871
postSRBY	0.004744669	0.485214932	102.2652795
postSRCY	0.003836479	0.336510977	87.71348392
postSRYB	0.008611035	0.670997317	77.92295926
postDatt6	1.30E-05	0.00098727	76.14802692

Table 6.5: Most separable indices for determining the forb category at Kenfig.

Index	Variance Within Class (Vw)	Variance Between Class (Vb)	F Score
postCVI	0.262128401	10.80309863	41.21300322
peakSRGNIR1	0.146116853	5.121833411	35.05299557
postIPVI	0.00018564	0.005553011	29.91277289
postDatt1	0.001260416	0.036075145	28.62161422
peakSRYB	0.024764245	0.499362973	20.16467546

Table 6.6: Most separable indices for determining slacks thresholds.

Index	Variance Within Class (Vw)	Variance Between Class (Vb)	F Score
Slope	19.50671769	1779.296539	91.21455324
postDatt1	0.001229821	0.042224768	34.3340761
peakDatt1	0.003552732	0.084793576	23.86714763
postCVI	0.282370649	6.734406721	23.84952806
peakSRGNIR1	0.153929226	3.551546402	23.07259307

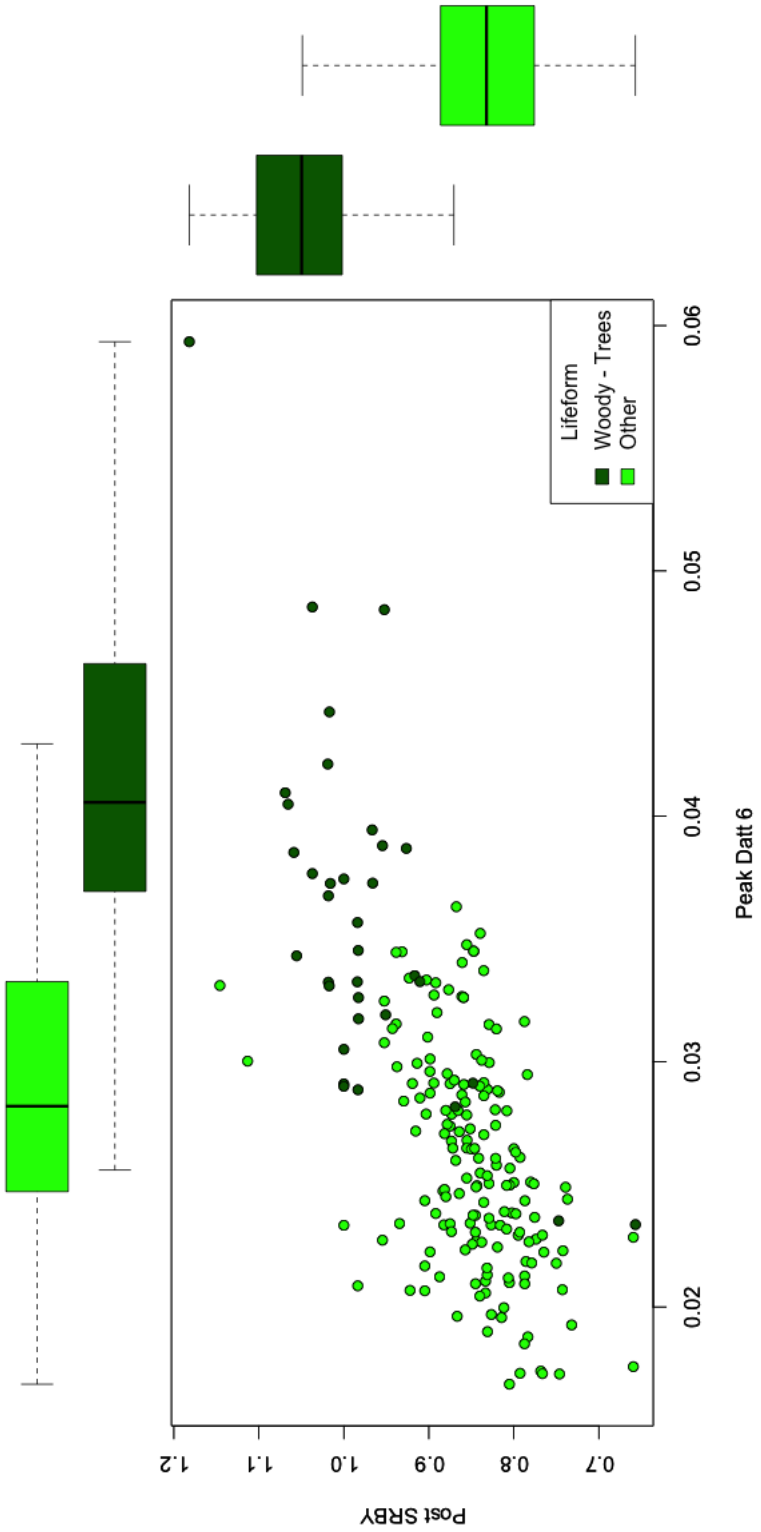

Figure 6.8: Best indices for separation of woody lifeform category with boxplots to determine most suitable threshold for each index.

Once the woody category has been delineated those pixels cannot be classified as another class therefore, the rest of the image can only be classed as a forb or other. *F* scores for this category are relatively low in comparison with the woody separations therefore only the index with the highest *F* score was chosen (Table 6.5). A boxplot of the training data set was used to determine a threshold of greater than 4 (Figure 6.9). Expert knowledge of the site provides information that once these lifeform categories have been separated, the rest of the site can be separated into broad habitat categories, fixed dune grassland and humid dune slacks. Therefore, no more lifeform categories were mapped at this stage of the approach.

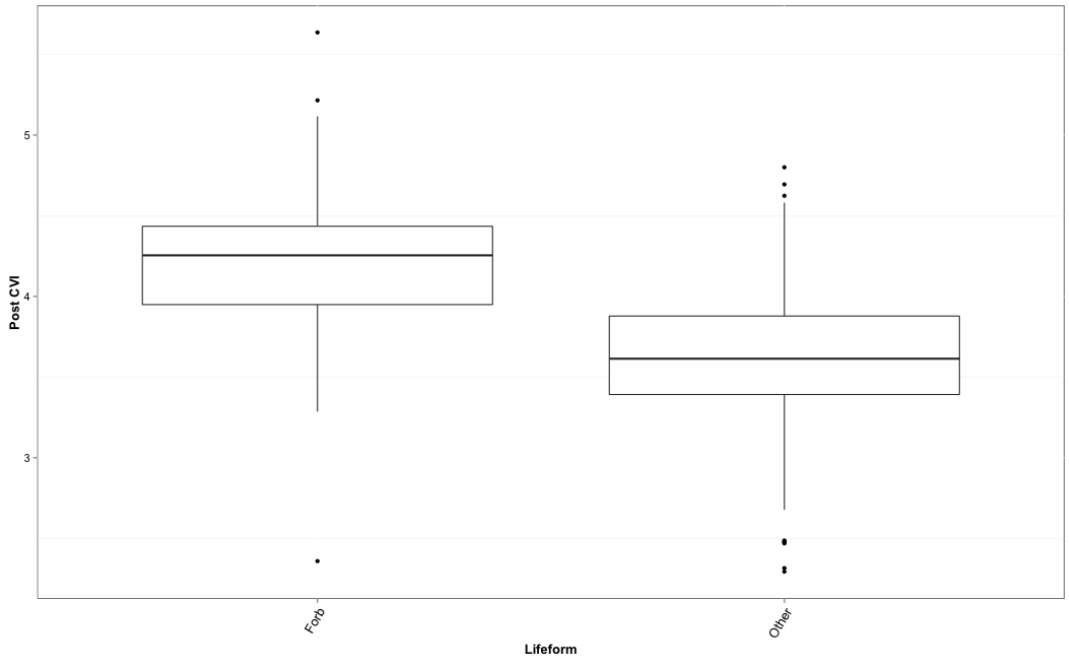

Figure 6.9: A boxplot to determine the most suitable threshold for determining the forb category.

As all humid dune slack habitats are mostly flat in comparison to fixed dune grassland contextual information was used in the form of slope derived from LiDAR data to determine broad habitat categories. Table 6.6 shows that the slope layer has a much higher *F* score than any index or layer derived from the multispectral satellite imagery. A threshold of less than 3 was chosen to separate slack and dune habitats.

Castlemartin

The lifeform categories mapped at Castlemartin are woody, forb and graminoid. The woody class in this instance contains all shrubby vegetation including maritime heath. *F* scores for this site are low therefore, the confidence that the woody category can be separated accurately is low (Table 6.7). Figure 6.10 shows how much confusion there is between both woody and herbaceous classes and although the index PeakCVI had the highest *F* score the ranges within the boxplot overlapped making the second most separable layer (Peak Panchromatic band) the most suitable (Threshold was less than 333).

Table 6.7: Most separable indices for determining the woody category at Castlemartin.

Index	Variance Within Class (Vw)	Variance Between Class (Vb)	F Score
peakCVI	0.601387974	27.70681109	46.07144187
JulyPan	312.5066586	11998.3829	38.39400719
JulyGreen	104.9776641	2802.152837	26.69284806
JulyRedEdge	686.2457531	16765.3751	24.43057028
SepPan	653.0954727	13185.02288	20.18850754

Table 6.8: Most separable indices for determining the forb category at Castlemartin.

Index	Variance Within Class (Vw)	Variance Between Class (Vb)	F Score
postSRRB	0.040698872	3.288351742	80.79712203
postCVI	1.923852374	117.3447943	60.99469787
peakpostDiffNDVI	0.004745475	0.197476377	41.61361414
postSRNIR2NIR1	0.000979002	0.039146497	39.9861154
postDiffNIR	111.0934476	2916.679176	26.25428626

The *F* scores for determining the forb category where higher indicating more confidence in this approach for mapping this category (Table 6.8). Figure 6.11 shows that combining the indices with the highest F scores increases separability where thresholds chosen were greater than 1.8 for index PostSRRB and greater than 8 for index PostCVI. All other pixels with the label Natural Terrestrial Vegetation that has not been classed as woody or

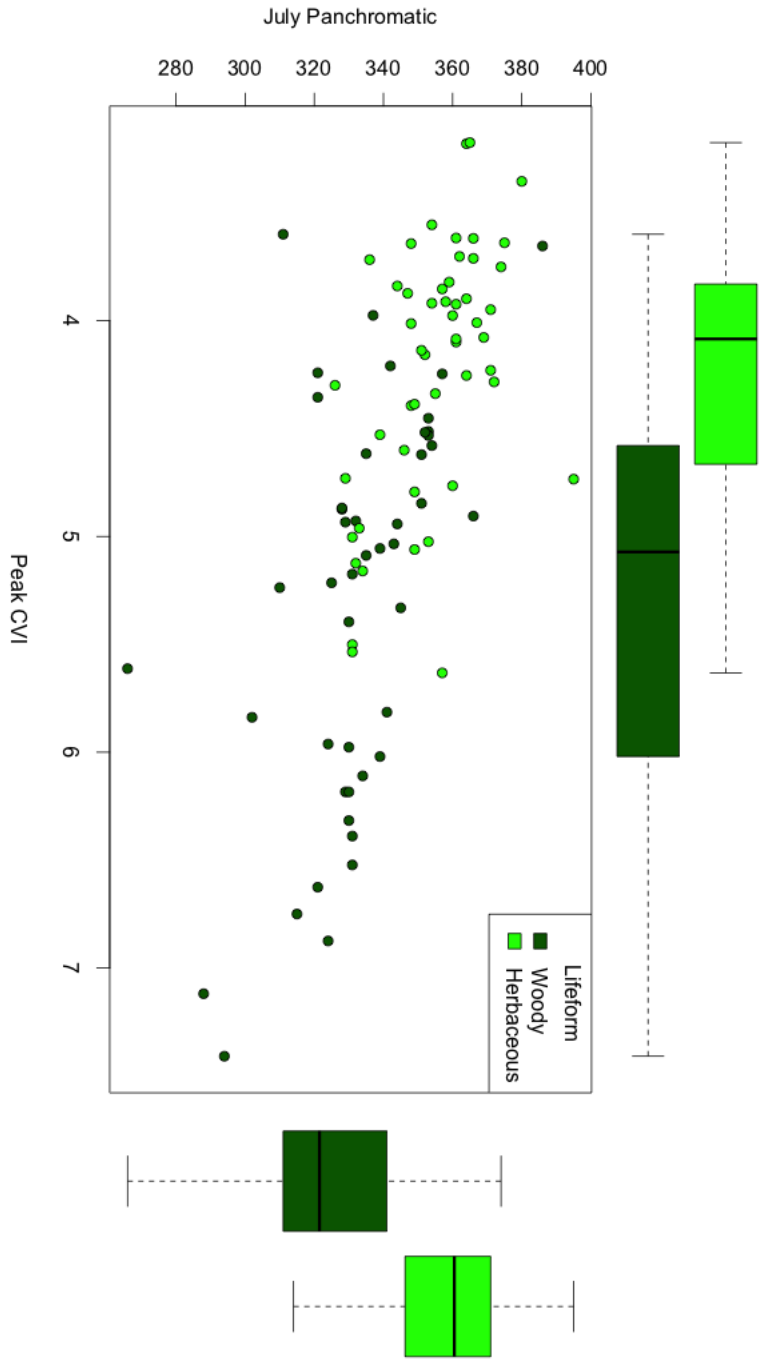

Figure 6.10: Indices show confusion between lifeform categories at Castlemartin.

forb was then given the graminoid label. This approach to try and delineate thresholds for broad habitats at Castlemartin proved unsuccessful as there was a lot of confusion in the features space and no definitive thresholds could be used for separation. Therefore, no broad habitat map is generated in this chapter for Castlemartin.

6.4.3 Lifeform and broad habitat map accuracies.

Once the LCCS level 3 maps were established, the lifeform thresholds were classified. The classification maps and accuracies are shown in this section. A broad habitat map was only initiated for Kenfig using the EODHaM method.

Table 6.9: Accuracy Kenfig Lifeform. Overall accuracy = 85.1 %, Kappa value = 0.77.

	Woody (Trees)	Graminoid	Forb	Other	Sum	Users Accuracy (%)
Woody (Trees)	31	6	0	0	37	83.7
Graminoid	5	115	11	4	135	85.1
Forb	2	7	27	0	36	75
Other	0	3	1	50	54	92.6
Sum	38	131	39	54	262	
Producers Accuracy (%)	81.6	87.8	69.2	92.6		

Table 6.10: Accuracy Castlemartin Lifeform. Overall accuracy = 67.3 %, Kappa value = 0.50.

	Woody	Graminoid	Forb	Other	Sum	Users Accuracy (%)
Woody	17	28	0	0	45	37.8
Graminoid	4	40	0	0	44	90.9
Forb	1	2	7	0	10	70
Other	0	2	0	12	14	85.7
Sum	22	72	7	12	113	
Producers Accuracy (%)	77.3	55.5	100	100		

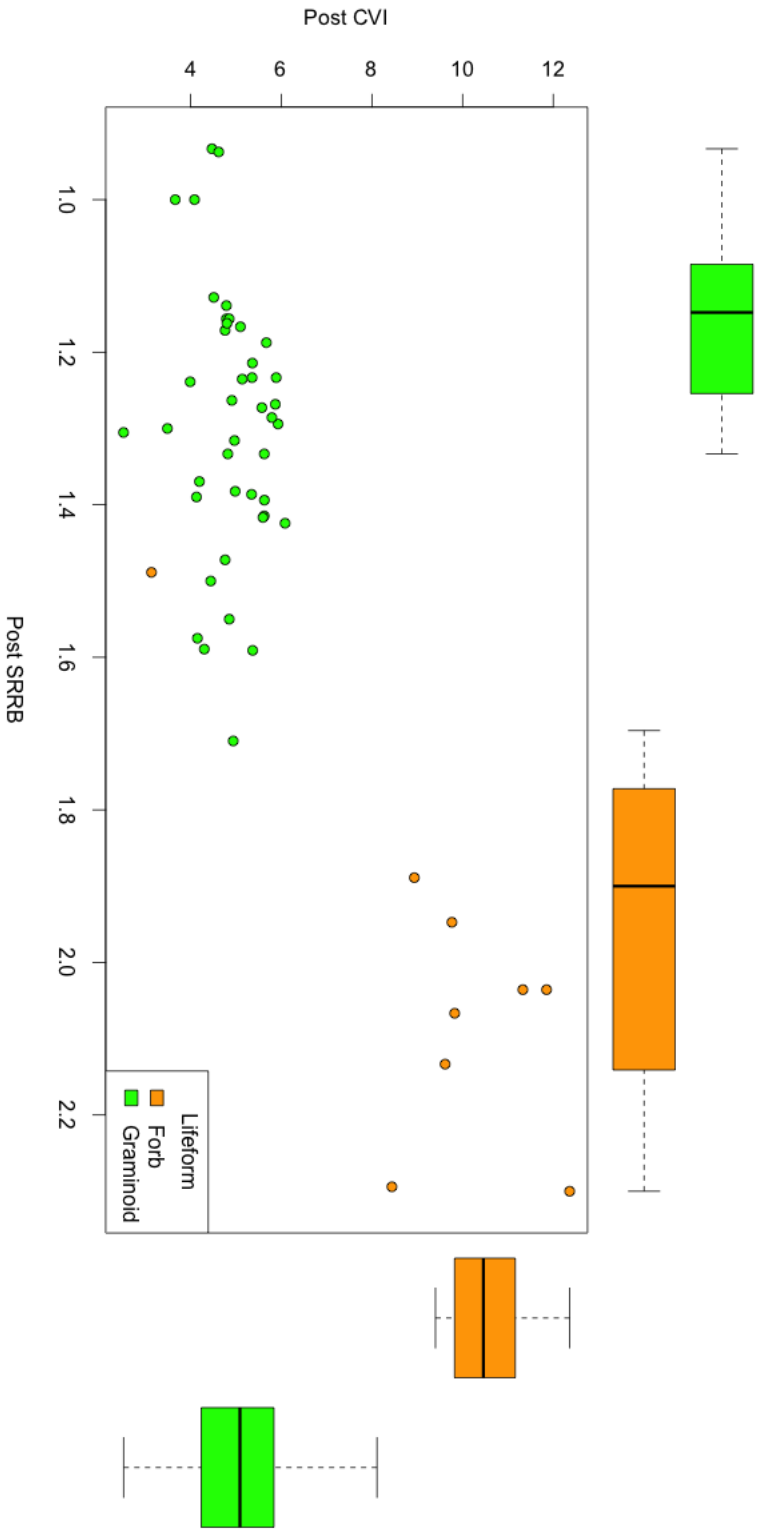

Figure 6.11: Castlemartin Bracken thresholds.

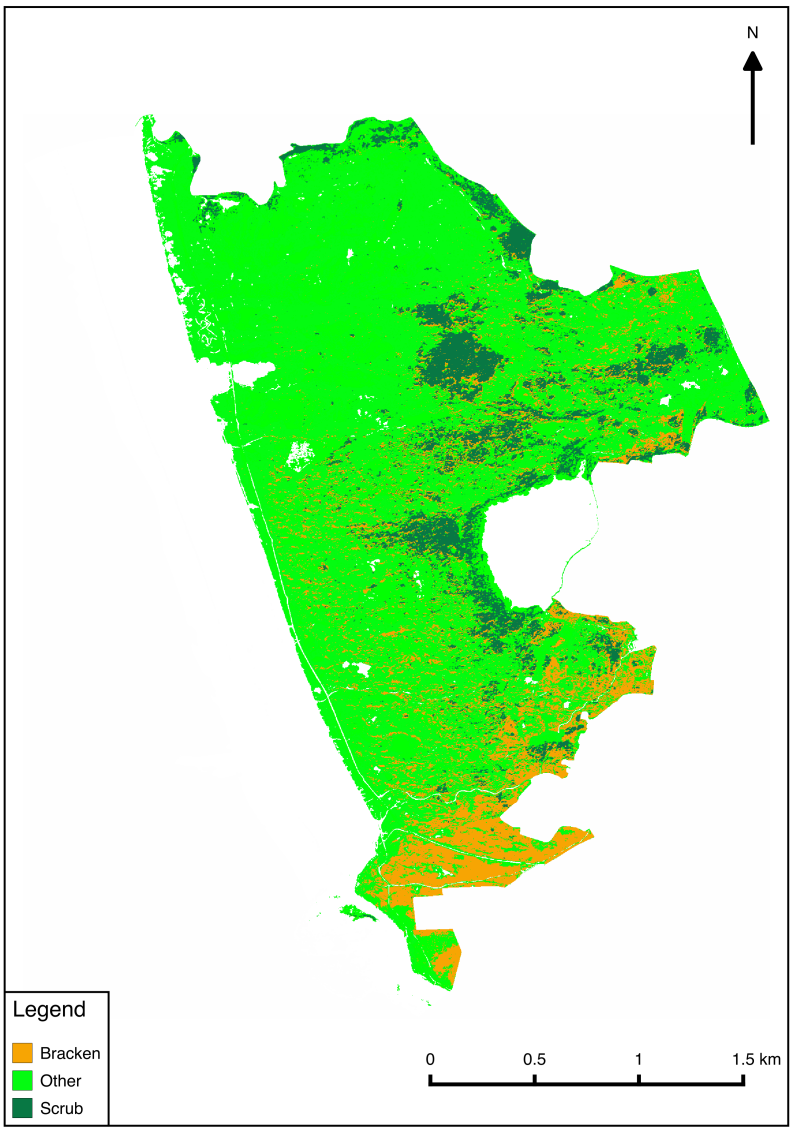

Figure 6.12: Lifeform classification of Kenfig.

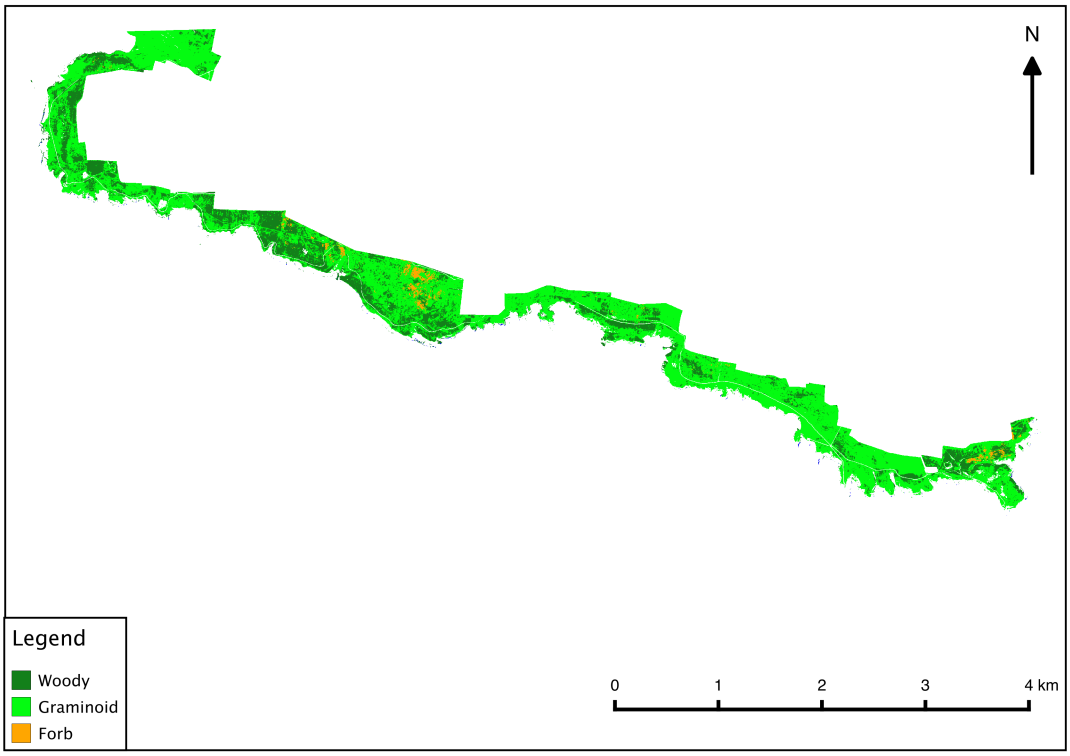

Figure 6.13: Lifeform classification of Castlemartin.

Table 6.11: Accuracy Kenfig Broad Habitat Categories. Overall accuracy = 79.4 %, Kappa value = 0.74.

	Bare Sand	Bracken	Dune Grassland	Dune Slacks	Woody - Trees	Water	Sum	Users Accuracy (%)
Bare Sand	32	1	3	0	0	0	36	88.9
Bracken	0	27	6	1	0	0	36	75
Dune Grassland	4	7	34	7	0	0	52	65.3
Dune Slack	0	4	8	66	5	0	83	79.5
Scrub	0	0	2	4	31	0	37	83.7
Water	0	0	0	0	0	18	18	100
Sum	36	39	53	78	38	18	262	
Producers Accuracy (%)	88.8	69.2	64.2	84.6	81.6	100		

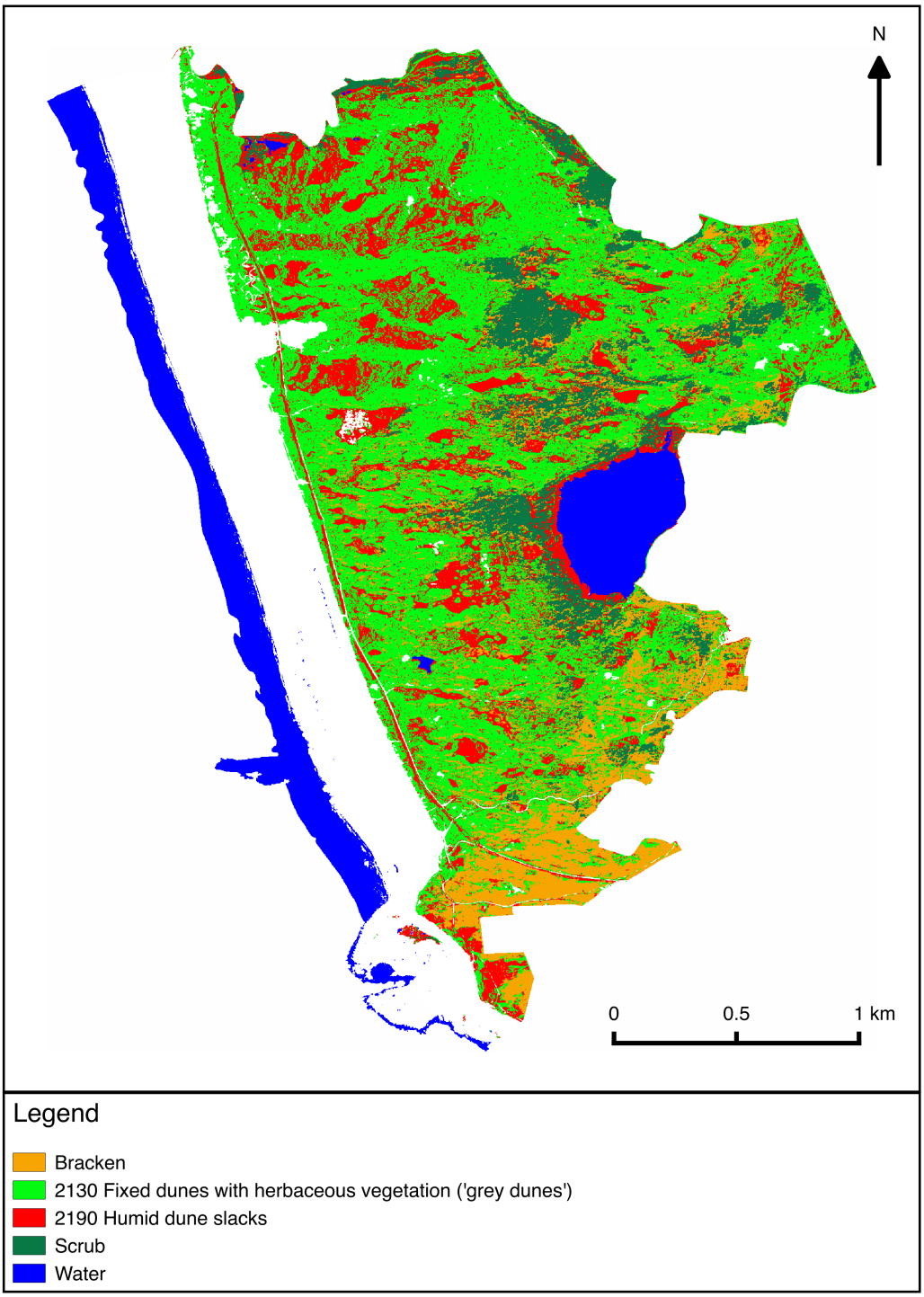

Figure 6.14: Broad habitat classification of Kenfig.

6.5 Discussion

6.5.1 Landscape Mapping

Accuracy assessments for Level 3 classification (overall accuracies of 98% and 97.4% for Kenfig and Castlemartin respectively) proved that this method is highly successful for mapping basic land cover differences. The only discrepancies occur between natural and vegetated surfaces which is to be expected in some areas where vegetation cover is present but very sparse. These instances occur on both sites with semi-fixed dunes, dune annual and successionally young slack communities at Kenfig, which usually have approximately 50% vegetation and 50% sand cover, and pioneer heath and maritime grassland communities at Castlemartin which are also vegetated habitats with plenty of bare ground coverage present. Figure 6.15 shows an example of where these circumstances occur and it is evident from the photographs that it would be difficult to class any of these areas as either bare or vegetated surface. However, these errors can be accounted for when classifying features further along the LCCS hierarchy by applying rules that would apply to both bare and vegetated surfaces for the aforementioned habitats.

Figure 6.15: Photographs of two points that were classified as bare sand with vegetation present. Left: dune annual community; Right: mobile dune (Photographs taken by Clive Hurford).

The rule-based method is successful here as it gives the user complete control over which

index, time of year and threshold that should be applied to generate high accuracy results. Another advantage is the ability to choose the order of classification as once a pixel has been assigned to a class, rules can be applied to prevent that pixel from being assigned to another. This allows the most prominent features in an image, which are also more uniform and homogeneous spectrally than vegetation (i.e. bare ground and water bodies) to be classified first and therefore eliminated from further classification. Everything else can then be assigned as vegetated, which has much larger variability spectrally. This explains the low threshold value applied to the NDVI to determine vegetated surfaces. This method is also easily transferable to other sites as thresholds are likely to be similar at this stage which requires very little modification to the system.

The ability to utilise seasonal information at this stage is also very important. The knowledge allow the user to incorporate knowledge about the management of sites and any climactic abnormalities that was experienced in the year of image acquisition. Kenfig, as a sand dune ecosystem, experiences annual flooding of slack habitat as the water table rises during the winter months. 2012 experienced a very wet June and July with a 157% rainfall of the 1981-2010 average with the record stating the wettest June in England and Wales since 1766 (Met Office, 2013). This means that many of the wetter slacks at Kenfig were still under water in the July image acquired in 2012, therefore the September image was used to determine water bodies instead. This means that only permanent water bodies would be mapped and would provide a much more useful baseline map for use in subsequent years. At Castlemartin, many of the scrub areas get mown as part of the management of the site by the MOD. This is apparent in the September 2012 image, therefore the bare ground threshold was determined by the July image to prevent confusion of non-photosynthetic vegetated areas and actual bare ground cover. The September image was then used to determine vegetated surfaces to ensure that all the non-photosynthetic vegetation was captured (Figure 6.16).

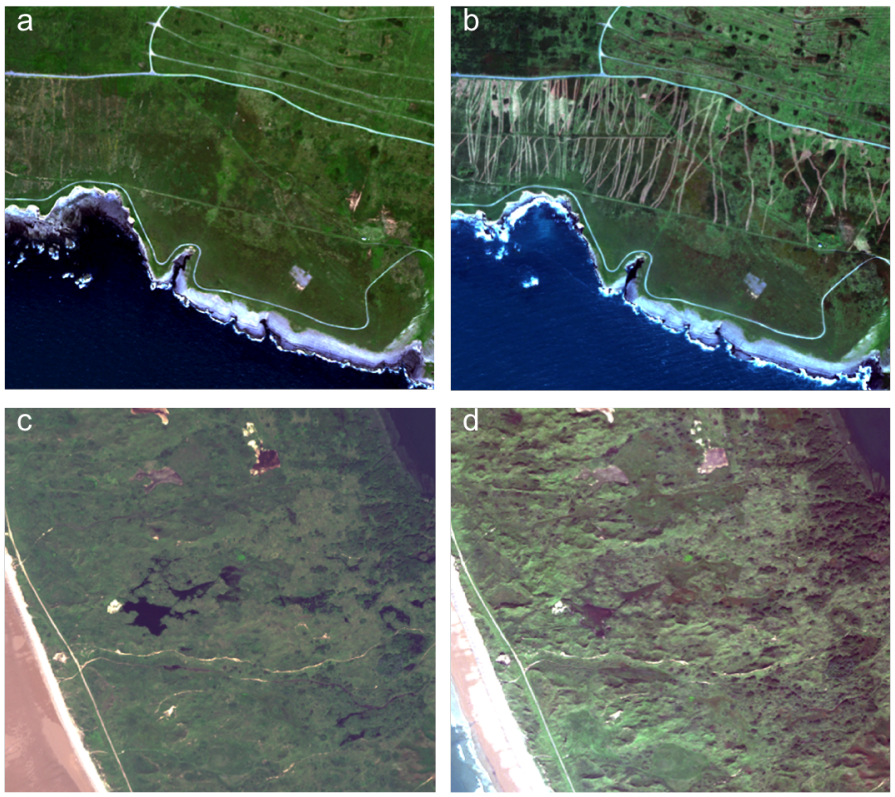

Figure 6.16: Worldview-2 subsets of a) Castlemartin in July; b) Castlemartin in September; c) Kenfig in July; d) Kenfig in September.

6.5.2 Lifeform Mapping

Mapping lifeform categories using the EODHaM method proved to be a bigger challenge, which is why a separability analysis was performed to determine which indices would be more successful at separation of classes, or even if they were separable at all. Lifeform mapping was much more successful at Kenfig (83.3% overall accuracy) in comparison with Castlemartin (64.7% overall accuracy). Problems with the thresholding environment arise as the user is required to draw a straight line in a feature space that is increasingly becoming more complex with the addition of classes.

The woody class, which is separated into trees and shrubs defined by height in the LCCS, was successfully classified at Kenfig as only trees were included within the class. At

Castlemartin, the absence of trees (any woody component higher than 3 metres) meant that the class mostly consisted of shrubs. There are also other differences between the woody categories at both sites, as the trees present at Kenfig are mostly deciduous while the scrub at Castlemartin is largely evergreen. The extent of the deciduous scrub at Castlemartin, mainly Prunus and Rubus are very small in area. The indices with higher *F* scores show that the high chlorophyll content of the deciduous trees in combination with their height and structure provide the biggest separability as seen by the bands used to calculate the spectral indices. The Datt6 index is designed to interact with high chlorophyll content (Datt, 1998) while the simple ratios build on the difference between narrower wavelengths (Coastal and Blue bands) which interact with the structure of vegetation. By combining these indices which interact with different aspects of tree characteristics, an agreeable separation was achieved (Figure 6.8) with user and producer accuracies exceeding 80% after classification. The spectral indices with the higher *F* scores at Castlemartin also interact with chlorophyll (CVI) and structure (Panchromatic band) but evergreen shrubs have lower chlorophyll content which means that the class separability becomes dependent on structure characteristics, which explains the lower *F* scores achieved. Figure 6.10 shows that it would be very hard to distinguish thresholds and introducing more indices to the rule-base added to the confusion and complexity. As soon as a threshold was modified or an index added to the rule-base to change the classification result of a small area, this would have a knock-on effect over the rest of the site, meaning that the accuracy never increases after a certain point.

The bracken class proved to be more successful at Castlemartin than at Kenfig and once again the separability analysis predicted this to be the case as *F* scores were much higher for this class at Castlemartin. The indices that produced the higher F scores at Kenfig interact with chlorophyll (CVI, Datt1) and an adapted version of the productivity ratio (IPVI). This is an unexpected result as bracken is most distinguishable from surrounding vegetation when senescing. This is apparent in the indices used for bracken thresholding

Figure 6.17: Photographs of examples of bracken present in fixed dune grassland habitat. (Photographs taken by Karen Wilkinson).

at Castlemartin, where all are calculated from the post image. The presence of peak-postDiffNDVI in Table 6.8 also shows that the high productivity of bracken during the summer months and its low productivity when senescing is also a useful index. Although, bracken does not cover a large area of Castlemartin and training points are lacking therefore it is reasonable to assume that the accuracy results produced is biased. At Kenfig, most of the confusion arises between bracken and the other category, which means that the class is being overestimated. Part of this can be explained by the presence of bracken in fixed dune grassland communities but not as a dominant feature (Figure 6.17), which evidently confuses the separability of the class. Bracken can also be confused with areas of shadow which occur on steep slopes in imagery acquired at certain times of year due to sun angle.

At this stage, the results suggest that high confidence can only be achieved when mapping trees at the lifeform stage. Overall accuracy at Kenfig is still over 80% and it was decided that this was high enough to continue using this method to delineate broad habitats at the site. Overall accuracy at Castlemartin (64.7%) was deemed too low to continue with further analysis in the rule-based environment, as accuracy will logically only decrease at this point. The repeatability of the method at this stage is also questioned as the in-

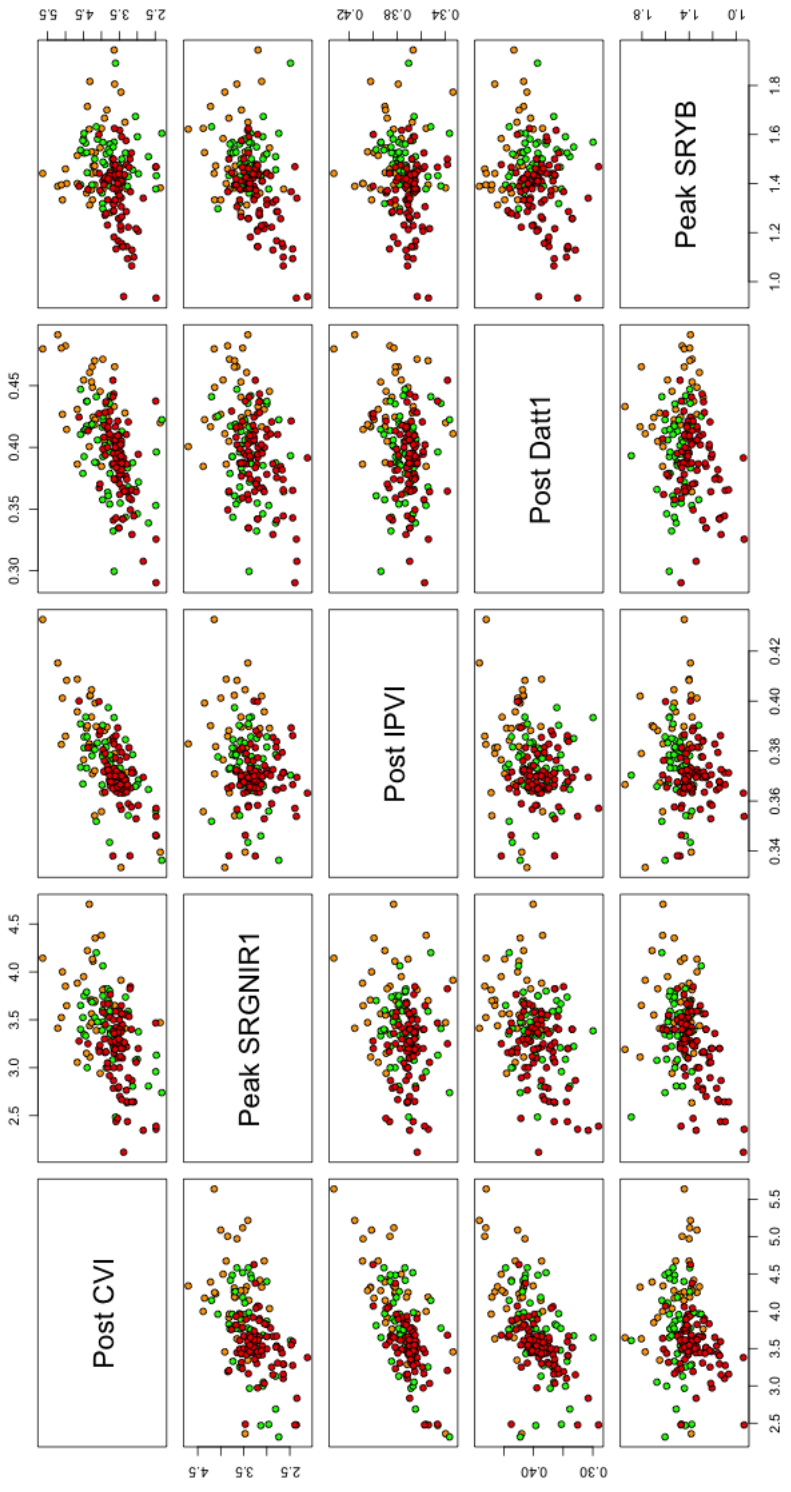

Figure 6.18: Confusion within the feature space between bracken (orange), slacks (red) and dune grassland (green) at Kenfig.

formation and knowledge gained from contextual information and ecological expertise might not be enough to separate classes in a feature space. It is noted that other methods are available for classification, which could combat the thresholding nature of rule-based techniques, and these are explored in the next Chapter.

6.5.3 Broad Habitat Mapping

As the difference between humid dune slacks and fixed dune grassland can essentially be explained by a difference in slope (slacks are almost always flat), it was decided that further exploration of this knowledge was acceptable at Kenfig. Table 6.6 shows a high score using slope for thresholding in comparison with the relatively low separation scores derived from spectral indices alone. The accuracy produced was still high (79.9%) in terms of remote sensing mapping products but most of the confusion lies between the bracken (previously classed in the lifeform stage), slack and dune grassland classes. Using slope alone did not prove efficient enough as there are some areas at Kenfig which are flat and vegetated but are not a humid dune slack, for example the haul road running through the site (Figure 6.19). Figure 6.18 shows that it is difficult to draw thresholds between these three classes and there is no clear separation. However, the accuracy of the result shows promise and if other classification methods that restrain from using straight lines in feature spaces are used (e.g. machine learning algorithms) then higher accuracies can be achieved.

6.6 Conclusions

This chapter explored the use of the EODHaM system for mapping habitats from VHR EO data. The results prove that mapping landscape elements was highly successful and that visual interpretation alone was sufficient to determine thresholds. The rule-based

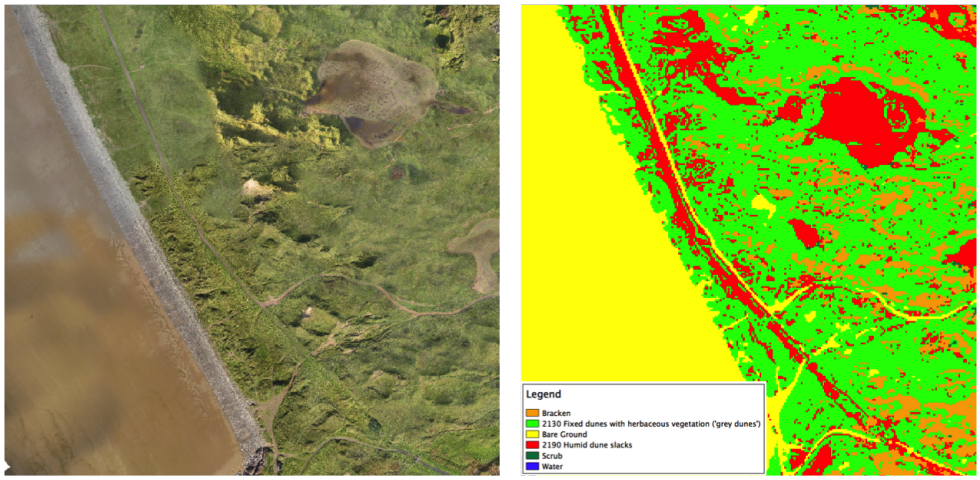

Figure 6.19: Example of where flat areas next to the haul road are classified incorrectly as slack.

method also proved to be appropriate at this level as it allows complete control to the user and once the software has been set in place it is a simple and repeatable process to apply for other sites. Mapping lifeform categories proved more difficult in terms of the choice of index for class discrimination and the separability of those classes with the available data. Some classes were more successful than others and this varied between sites e.g, trees were classed accurately at Kenfig whereas the woody category at Castlemartin was not as successful. The ability to incorporate seasonal imagery added valuable information that further increased the capability of the system to discriminate between classes.

The constraints of trying to draw straight lines in a feature space where none exist limits the systematic rule-based approach recommended by the EODHaM system and although some high overall accuracies were achieved some ambiguities within the classified maps were still present. Future recommendations include further development of the EODHaM method to incorporate more efficient classification algorithms within its approach that allows the expert knowledge of ecologists to be incorporated without some of the constraints mentioned in this chapter.

Chapter 7

Classification of Annex I Habitats

7.1 Introduction

The heterogeneous nature of habitats, particularly beyond broad habitat level presents difficulties when utilising remotely sensed imagery as they are difficult to separate spectrally due to low inter-class separability and high intra-class variability. Many classification methods are available within the remote sensing literature that addresses the complexity of habitat mapping. For monitoring purposes algorithms need to be automated and readily interpreted with simple user defined parameters that can be adjusted easily. In addition, the choice of algorithm depends on its ability to handle noisy observations, complex measurement spaces and a small number of training data relative to the size of study area (DeFries and Chan, 2000; Rogan et al., 2008). In recent years, machine learning algorithms have emerged as alternatives to more traditional classification techniques within remote sensing when faced with large dimensional and complex data spaces (Rodriguez-Galiano et al., 2012a). This chapter will explore the suitability of machine learning algorithms for delineating Annex I habitats from EO data at 2 study locations.

7.2 Background

Algorithms used within remote sensing typically involve statistical pattern recognition, the theory of which was mostly developed in the 1960s and 1970s. Some major developments include the Bayes decision theory problem (Chow, 1957), nearest neighbour decision rules (Cover and Hart, 1967) and, supervised and unsupervised learning (Fukunaga, 2013). During the latter part of the 1980s use of artificial neural networks and support vector machines were developed as statistical classifiers having a significant impact on the remote sensing community (Bishop, 2006; Jain et al., 2000; Webb, 2003). The early assumption that each pixel in a multispectral image band has a histogram that has an approximate Gaussian distribution was made by Fu (1982) and became most popular in classifying multispectral data with use of the maximum likelihood algorithm for example. Even with the use of new sensors and the expanded applications of remote sensing, the Gaussian assumption remains to be a good approximation (Chen and Ho, 2008), which explains the popularity of such algorithms. However, most parametric classifiers are heavily reliant on this assumption and data used within the remote sensing community may not always represent normally distributed curves. This section will therefore, focus on non-parametric algorithms.

7.2.1 Non-parametric Classification Algorithms

A variety of non-parametric machine learning algorithms exist within the remote sensing literature such as k-Nearest Neighbour (Grabowski et al., 2003), Bagging (Breiman, 1996), Adaboost (Freund et al., 1996), Decision Trees (Breiman et al., 1984), Ensemble of classifiers (Breiman, 2001), Artificial Neural Networks (Mas and Flores, 2008), and Support Vector Machines (Mountrakis et al., 2011). A brief summary of each will be provided here with their advantages and limitations outlined.

k-NN

The kNN algorithm classifies unknown pixel values to the nearest number of k training class values where the user defines the value of k. The nearest neighbours are defined in terms of the standard Euclidean distance (Mitchell, 1997; Franco-Lopez et al., 2001). kNN is the simplest of machine learning algorithms but becomes less effective as the value of k increases because the distances between training class values is calculated based on all input features. A high number of input features create many dimensions in a complex feature space that can lead to a large number of irrelevant features dominating the distance between neighbours which can be misleading. This difficulty is referred to as the curse of dimensionality (or the Hughes phenomenon (Hughes, 1968)) and nearest neighbour approaches are particularly sensitive to this problem (Mitchell, 1997), which leads to over fitting of the data. However, the algorithm is robust to noisy training data providing a sufficiently large set of training data is used. The approach has been applied successfully, particularly in forest inventory estimation problems using low k values (Collins et al., 2004, LeMay and Temesgen, 2005, McRoberts et al., 2002, Reese et al., 2002 and Tomppo, 2006). The key advantages of the algorithm lies with its simplicity and the fact that it produces unbiased results as proven by Franco-Lopez et al. (2001) and McRoberts et al (2002), but a sufficient training data set is needed which may not always be available when using EO data.

Decision Trees

A decision tree classifier works by breaking down an often complex classification problem into multiple stages of simpler decision-making processes. It is composed of nodes at different levels; a root node, a set of internal nodes (splits) and a set of terminal nodes (leaves) (Figure 7.1). The training samples form the root node and a statistical measure

is applied to split the nodes to form a tree-structured decision space with the terminal nodes representing the assignment of classes (Chan and Paelinckx, 2008). The most popular statistical measures used for the split include the gini index (Breiman et al., 1984), the chi-square measure (Mingers, 1989b) and the information gain ratio (Quinlan, 2014). The split can be based on one input feature (univariate) or several (multivariate). Univariate decision trees have been successfully used to develop global land cover products (De Fries et al., 1998; Hansen et al., 2000; Friedl et al., 1999) as the rules utilised are easy to interpret within the classification structure (DeFries and Chan, 2000). Multivariate decision trees are often more compact and can be more accurate although they involve more complex algorithms (Friedl and Brodley, 1997).

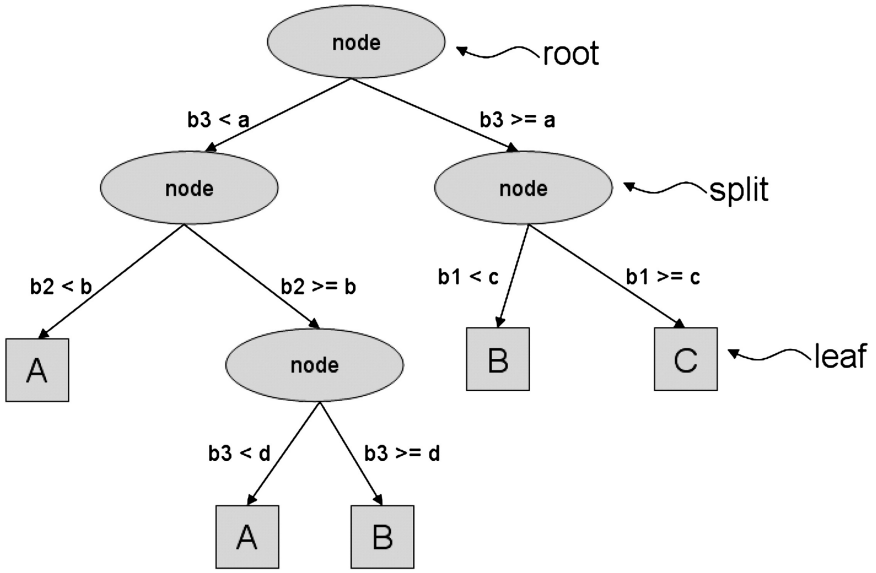

Figure 7.1: A hypothetical decision tree classifier with three class labels (A, B and C). Figure adapted from Friedl and Brodley (1997).

There are many advantages to applying decision tree classifiers. The algorithm is computed effectively reducing the computing burden significantly. The structure of the tree provides information about input features that are used for classification, which is particularly important for deriving a physical understanding of the classification process (DeFries and Chan, 2000) evaluating the features' effectiveness for given applications. Al-

though the method is robust to any errors in classifications and training samples (Mitchell, 1997), decision trees are considered 'weak' learners as the learning algorithm performs just slightly better than random guessing (Freund et al., 1996). However, over fitting the training data is an important issue as the tree is grown in such a way that all training data are classified correctly. Pruning measures exist which only allow the split if the contribution to accuracy improvement has reached a predefined threshold (Chan and Paelinckx, 2008). Some common pruning methods are discussed in Quinlan (1987) and Mingers (1989a).

Ensemble Classifiers

An emerging type of technique utilises an ensemble of classifiers such as random forests, bagging and boosting (Friedl et al., 1999; Ghimire et al., 2010; Gislason et al., 2004; Hansen and Salamon, 1990; Krogh et al., 1995; Sesnie et al., 2008; Steele, 2000). Ensemble algorithms can either use the same base classifier to produce repeated multiple classifications of the same data (Breiman, 2001; Friedl et al., 1999) or use a combination of different base classifiers (Mountrakis et al., 2009). When using a combination of base classifiers and a single training dataset, their decisions are combined by simple voting, or more sophisticated methods like consensus theory (Benediktsson and Swain, 1992) and stacking (Džeroski and Ženko, 2004). However, the complexity of processing increases significantly when handling different learning algorithms and its effectiveness relies very much on the combining technique which does not always give a more accurate classification (Foody et al., 2007).

When the same base classifier is used the ensemble is created by changing the training set. Bootstrap aggregating or bagging (Breiman, 1996), and boosting or AdaBoost (Freund et al., 1996) are two popular methods to generate new training sets. In theory they can be applied to any learning algorithm they were originally designed to boost the accuracy

of 'weak' learners such as decision trees (Breiman, 2001). The AdaBoost algorithm has been shown to produce accuracies comparable with those produced using a support vector machine (Chan et al., 2001) and a neural network (Pal and Mather, 2003) as it tends to exhibit virtually no over-fitting when the data is noiseless (Benediktsson et al., 2007). However, Adaboost is susceptible to noise (Briem et al., 2002) whereas the advantages of bagging methods are its stability and the fact that it is not very sensitive to noise (Chan et al., 2001; DeFries and Chan, 2000).

Random Forest is a tree-based ensemble classifier that uses the bagging technique to create new training sets. The algorithm can be seen as an improved version of bagging (Benediktsson et al., 2007) as its use of the random feature space allows a much faster construction of trees (Chan and Paelinckx, 2008). As a random subset of the training data is run at each iteration of the base classifier, the algorithm limits the number of variables used for a split in the tree (Figure 7.1) therefore, decreasing the correlation between trees and computational complexity. This allows the algorithm to handle high dimensional data and use a large number of trees in an ensemble. The computational efficiency of this algorithm has been key to its increased popularity in recent remote sensing applications such as land cover classifications using optical data (Chan and Paelinckx, 2008; Ghimire et al., 2010; Lawrence et al., 2006; Pal and Mather, 2005; Sesnie et al., 2008), and LiDAR and radar data (Guo et al., 2011; Latifi et al., 2010; Martinuzzi et al., 2009; Waske and Braun, 2009). Random Forest also utilises the out-of-bag estimates method that allows the user to evaluate the relative importance of each input feature (Breiman, 2001).

Artificial Neural Network

Artificial Neural Networks (ANNs) attempt to mimic the neurons in our brain to solve problems (Paul and Magaly, 2011). ANNs are particularly suitable in remote sensing applications as they are effective with less reliable training samples, which is common when

it comes to land cover classification for example, and are less subject to the 'Hughes phenomenon' (Mas and Flores, 2008; Chen and Ho, 2008). Many authors have reported considerable advantages of ANNs over conventional methods including the ability to learn complex patterns (Lek and Guégan, 1999) and to generalise in noisy environments (Hewitson and Crane, 1994). Comparative studies have shown higher accuracies from ANNs than maximum likelihood (Kavzoglu and Mather, 1999; Seto and Liu, 2003; Joshi et al., 2006). A few studies however, have reported higher accuracies from other methods such as Support Vector Machines (Michelson et al., 2000; Combal et al., 2003; Pu and Gong, 2004; Shupe and Marsh, 2004). One of the most important drawbacks of ANNs is the difficulty in designing the network and the parameters that control the training process are difficult to set (Paul and Magaly, 2011; Mas and Flores, 2008).

Support Vector Machines

Support Vector Machines (SVMs) aim to determine the location of decision boundaries that produce the optimal separation of classes (Vapnik and Vapnik, 1998). In its simplest form, SVMs are linear binary classifiers and the decision boundary that minimises the generalisation error is chosen among the infinite number of linear decision boundaries. The selected decision boundary is therefore defined as the sum of the distances to the hyperplane from the closest points of the two classes. The data points that are closest to the hyperplane are used to the measure the margin and these are called 'support vectors' (Figure7.2). SVMs can also be extended to handle non-linear decision surfaces by projecting the data onto a high-dimensional feature space using kernel functions and formulating a linear classification problem in that feature space (Boser et al., 1992; Vapnik and Vapnik, 1998). As SVMs were originally designed for binary problems, two multiclass methods were developed. The first approach is described as 'one against the rest' where one class is compared to all the others combined. The second approach is to com-

bine several classifiers where a pairwise comparison between all classes is performed. Each classifier is applied to the test data vectors and a vote is given to the winning class. The data is then assigned to the class with the most votes. This approach is called 'one against one' (Knerr et al., 1990).

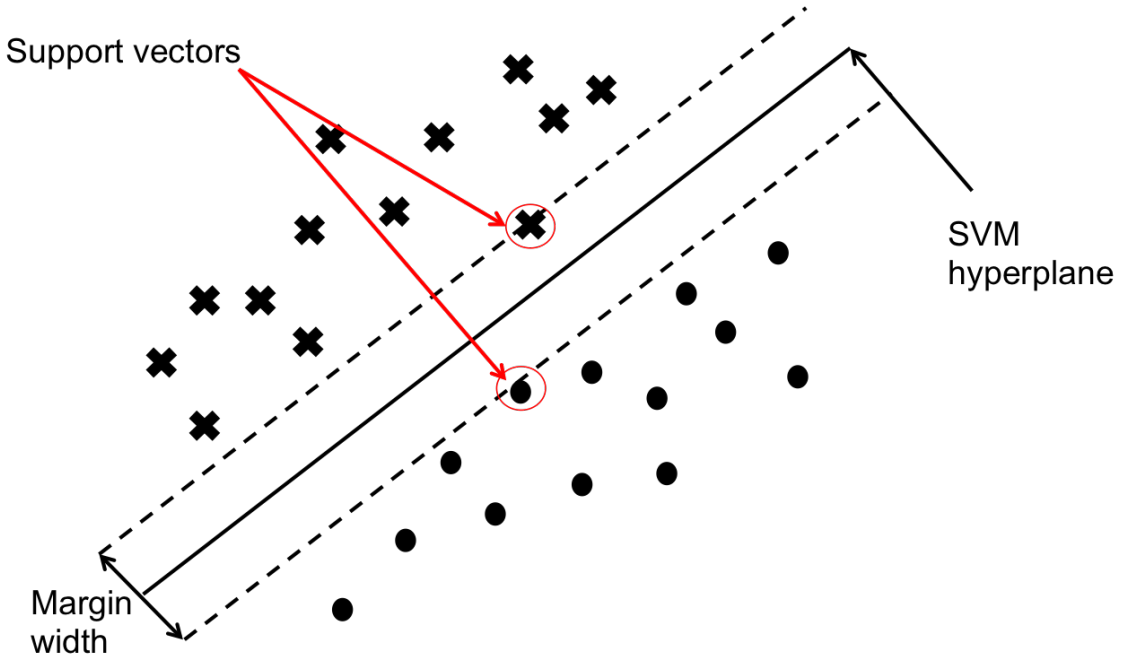

Figure 7.2: A linear support vector machine example for separable samples. Figure adapted from Burges (1998).

Similar to ANNs, SVMs can successfully handle small training data sets, often producing higher classification accuracy than traditional methods, making the method particularly appealing in remote sensing applications (Mantero et al., 2005). Numerous studies have compared SVMs with decision trees (Boyd et al., 2006), Maximum likelihood (Huang et al., 2002; Dixon and Candade, 2008; Keuchel et al., 2003), k-NN (Dalponte et al., 2008; Melgani and Bruzzone, 2004), and ANNs (Camps-Valls and Gómez-Chova, 2004; Pal, 2005), stating that SVMs outperformed these methods in terms of accuracy, simplicity and robustness. The most important characteristic is SVMs ability to generalise well from limited amount or quality of training data and can perform well with a much

smaller training dataset than ANNs (Camps-Valls and Gómez-Chova, 2004). However, the major drawback to SVMs is the difficulty in selecting key parameters such as the kernel functions, for example, choosing a small value for the kernel width parameter (i.e. the kernel footprint in that multi-dimensional space) may lead to over fitting, while large kernel width values may lead to over smoothing (Mountrakis et al., 2011).

7.3 Methods

7.3.1 Classification Algorithms

To ensure that all algorithms can be run in an automated way a python library called scikit-learn was used to perform all classifications. This allowed the process to be re-run on different input features, masks, and when new field data became available without having to start from the beginning each time. As Kohavi (1996) and Chan and Paelinckx (2008) stated, no one algorithm has demonstrated to be superior for all problems so as many techniques as possible was investigated. Table 7.1 describes the algorithms under scrutiny and which ones were eventually chosen for analysis.

Scikit-learn has a wealth of algorithms at hand therefore, some parametric algorithms were also investigated. Nearest neighbours are good as a baseline for small datasets and easy to explain, whilst linear and quadratic models are always appropriate as a first algorithm to try as they are good for very large datasets and very high dimensional data. Decision trees are very fast, do not need scaling of the data and are easily explained visually, while Naive Bayes is for classification only and hold many of the characteristics of linear models although they often produce less accurate outputs. None of these algorithms were chosen however as they are prone to over-fitting and/or under-fitting which means they either focus too much on the training data or are unable to capture the vari-

Table 7.1: Algorithms that were investigated and subsequently chosen for further classification analysis.

Algorithm	Description	Chosen
AdaBoost	Meta-estimator that begins by fitting a classifier on the original dataset and then fits additional copies of the classifier on the same dataset but where the weights of incorrectly classified instances are adjusted such that subsequent classifiers focus more on difficult cases.	✓
Decision Tree	A decision tree classifier.	
Extremely Random Forest (ERF)	Meta-estimator that fits a number of randomised decision trees on various sub-samples of the dataset and use averaging to improve the predictive accuracy and control over-fitting.	✓
Linear Discriminant Analysis	A classifier with a linear decision boundary, generated by fitting class conditional densities to the data and using Bayes' rule. The model fits a Gaussian density to each class, assuming that all classes share the same covariance matrix.	
Gaussian Naive Bayes	Implements the Gaussian Naive Bayes algorithm for classification where the likelihood of the features is assumed to be Gaussian.	
Nearest Neighbour	Classifier implementing the k-nearest neighbours vote.	
Quadratic Discriminant Analysis	A classifier with a quadratic decision boundary, generated by fitting class conditional densities to the data and using Bayes' rule. The model fits a Gaussian density to each class.	
Random Forest (RF)	Meta-estimator that fits a number of decision tree classifiers on various sub-samples of the dataset and use averaging to improve the predictive accuracy and control over-fitting. The sub-sample size is always the same as the original input sample size but the samples are drawn with replacement if bootstrap is used.	✓
Support Vector Machine (SVM)	Support vector classification where the multi-class support is handled according to one against one scheme.	✓

ations present in the training data. This leads to overestimation of some classes leading to other classes not being classified at all, which is the result of the Gaussian distribution assumption and the bias that is known in the training data. This bias is a result of the presence of sparse or rare habitats and emulates the situation on the ground, and indeed in nature therefore, the chosen algorithms had to be able to overcome statistical problems like this.

It is no surprise that ensemble learning techniques have been chosen as they are known to produce higher accuracies and are particularly more robust than the decision tree al-

gorithm for example, as a group of classifiers performs more accurately than any single classifier (Ghimire et al., 2010; Kotsiantis and Pintelas, 2004). The ensemble classifiers are also known to overcome over-fitting issues and are able to generalise by not focussing too much on the training dataset (Breiman, 2001), which is the phenomenon seen by the parametric algorithms. Random forests are very robust and powerful and do not need scaling of the data, however they are not good for very high dimensional sparse data. They are included for analysis as a comparison to the extremely random forest algorithm which addresses the dimensionality issue by removing the boosting aspect of random forest. AdaBoost perform similarly to random forests but are slower to train and more sensitive to parameter tuning.

For the ensemble algorithms chosen, the main parameter that needs consideration is the number of estimators or trees needed to train as they all use the decision tree as their base estimator. Due to time constraints on the project and the need to produce outputs before the fieldwork season begins to be able to utilise the expertise of the ecologists, assumptions were made on parameter tuning based on similar projects in scale. For example it was decided that the number of trees to be used each time was a 100. Figure 7.3 and 7.4 show that this was the optimum number of trees for their subsequent projects which were of similar scale and complexity, as this project focus.

The SVM also proved robust, as they are powerful for medium-sized datasets with similar meaning. They do require scaling of the data however and are sensitive to parameters. As SVMs are traditionally a binary algorithm, the kernels are necessary to combat multivariate problems. For this project the radial basis function (rbf) and linear kernels were chosen for the experiment as they are the ones best understood and most utilised in the literature (Mountrakis et al., 2011). They were run with the minimum amount of parameters needed as it is recognised that the SVM is particularly sensitive to parameter estimation. Scikit-learn also allows the user to use the ‘one against the rest’ and the ‘one against one’

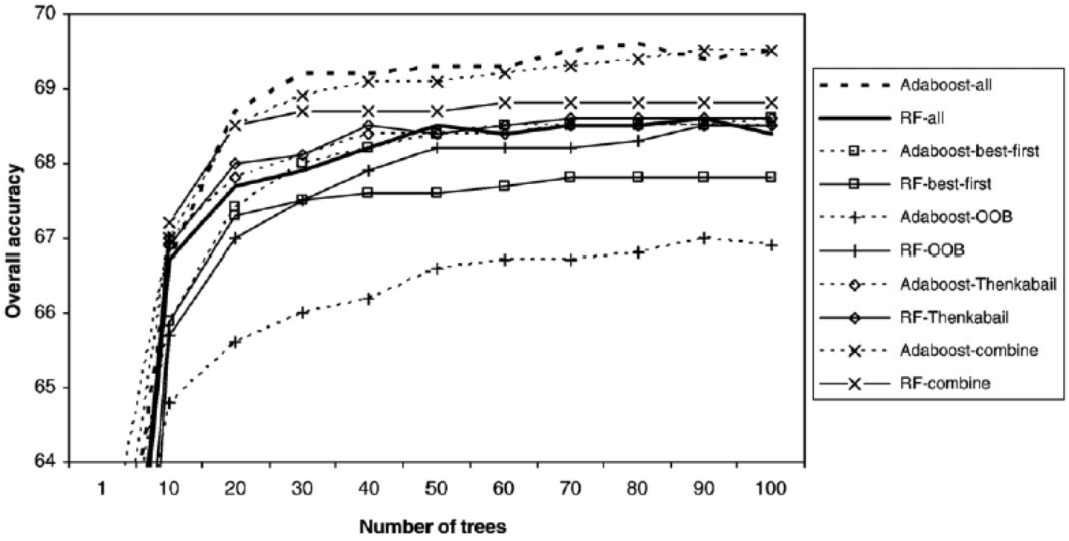

Figure 7.3: Snapshots of overall accuracies at 10 trees interval for AdaBoost and Random Forest using different input features (Chan and Paelinckx, 2008).

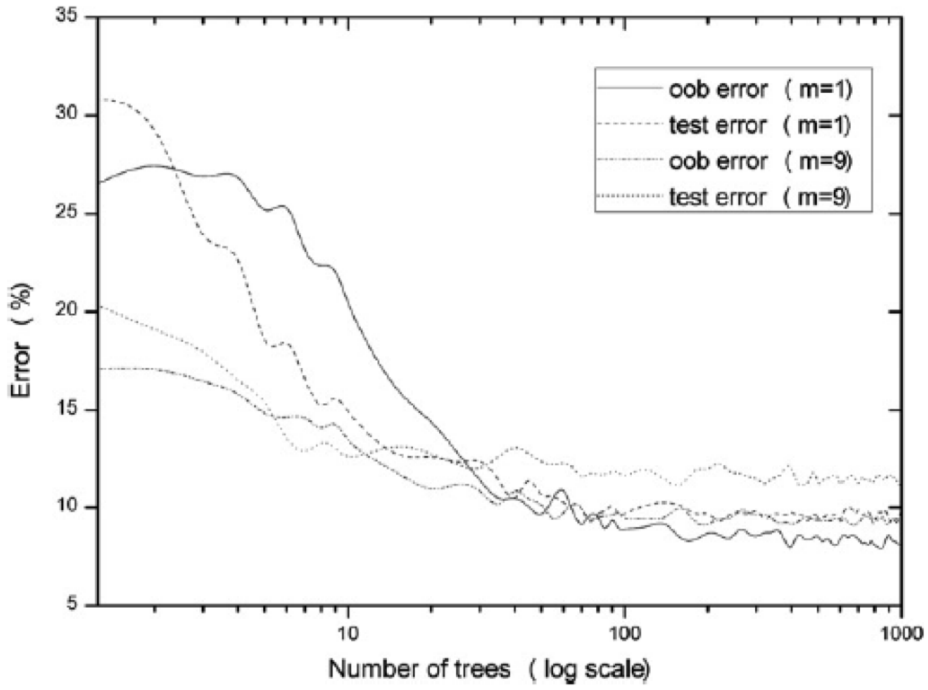

Figure 7.4: Effect of number of trees (k) and random split variables (m) on out of bag estimates (oob) and test errors (Rodriguez-Galiano et al., 2012b).

method for dealing with the multivariate problem, where the latter of those was chosen (Pal, 2005). The lack of parameter tuning for all algorithms used in this project is recognised as a limitation and will therefore be considered when analysing the results.

7.3.2 Independent Variable Selection

Independent variable selection to provide inputs for predicting classification algorithms is a key aspect that could affect the efficacy and accuracy of results. Another reason to select independent variables is the curse of high dimensionality, or the Hughes phenomenon, where classification performance will reach a peak without proportional increase in the training sample size, beyond which the performance degrades. As the number of training samples in this study are fixed the high dimensions of the data needs to be reduced to ensure predictive power of the algorithm (Landgrebe, 2005). It is therefore, important that many different scenarios are tested so that a recommendation can be made on the most effective method of delineating independent variables. Techniques such as Principal Components Analysis (PCA) or Independent Component Analysis (ICA) are often employed to reduce data dimensionality where only the first few components are used as variable vector input to the classifiers. However, in this process, some useful information may be lost (Chen and Ho, 2008), and are therefore not considered here. There will be 5 different scenarios that are described below. A maximum of 20 independent variables is chosen each time, if available, for consistency of method and repeatability. A plateau of lower importance is reached at this point in many of the scenarios presented, and the variance needed for separation is believed to be present.

1. Image bands and DEM layers such as slope etc. To test the variation included in the raw data without calculating vegetation indices and incorporating any additional expertise considered as added value to any classification process. Known as ‘Im-

ages' for the rest of the thesis;

2. Indices chosen on their recommendation from the EODHaM method in Chapter 6. A direct comparison with the above where the vegetation indices are chosen based on the extensive literature proving their success for representing particular characteristics of the landscape e.g. NDVI = productivity. Known as 'EODHaM';

3. Indices with the highest separation for each class using ANOVA, results taken from Chapter 6 analysis. To test the significance of each possible input variable by analysing their variance based on the training dataset and combining the outputs, Known as 'ANOVA';

4. Indices that have a low correlation value for each class. Also to test the significance of each possible input variable by removing variables that are highly correlated and assume that the variance needed is captured by those remaining. The absolute values of pair-wise correlations are considered. If two variables have a high correlation, the mean absolute correlation of each variable is calculated and the variable with the largest mean absolute correlation is removed. Known as 'Uncorrelated';

5. Indices with the highest importance values as delineated from the Random Forest (RF) algorithm using out of bag estimates. To test the variable importance aspect implemented by the random forests algorithms. Only suitable for these specific algorithms but used as an input variable group for all algorithms for consistency. Known as 'RF'.

Training data is required for numbers 3 to 5 whereas number one and two are based on the baseline image bands and information from the literature. Training data used is explained in Chapter 4. The correlation analysis was carried out using R software and Spearman's rank correlation coefficient. It is defined as:

$$\rho = 1 - \frac{6 \sum d^2}{n(n^2 - 1)} \tag{7.1}$$

where:

$\sum d^2$ is sum of the difference between ranks of each observation

n is the number of observations

Every observation that has a ρ of 0.75 or above is discarded from any further analysis.

7.3.3 Classifying Process

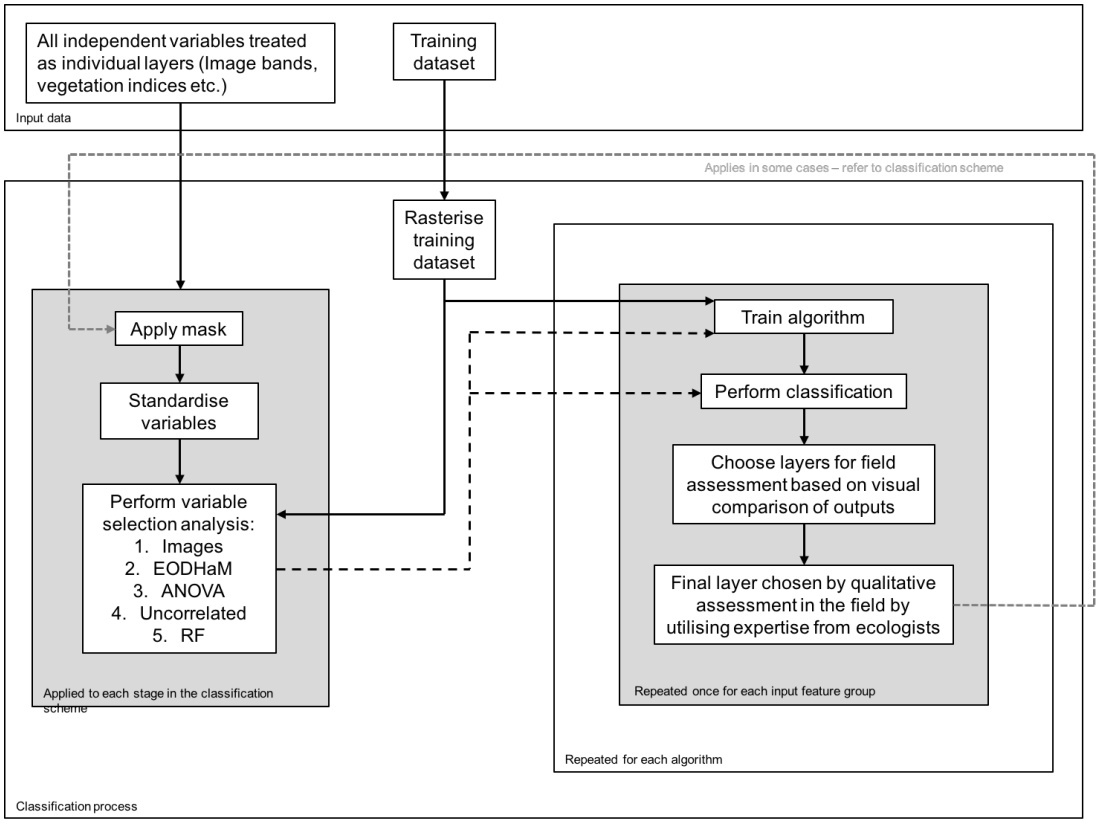

Figure 7.5: Schematic of the classifying process.

Figure 7.5 shows a schematic of the classifying process. The independent variables are chosen using the different statistical techniques outlined in the previous section. The four classification algorithms will be run on each independent variable selection for each category. For SVM, they are run twice with the linear and rbf kernel.

Figure 7.6 shows the classification scheme for Kenfig, while Figure 7.7 shows the scheme for Castlemartin. The land cover layers are generated using the EODHaM system from Chapter 6 and are the starting point for each scheme. They have been tailored to each specific site and the schemes represent the habitats and dominant species present.

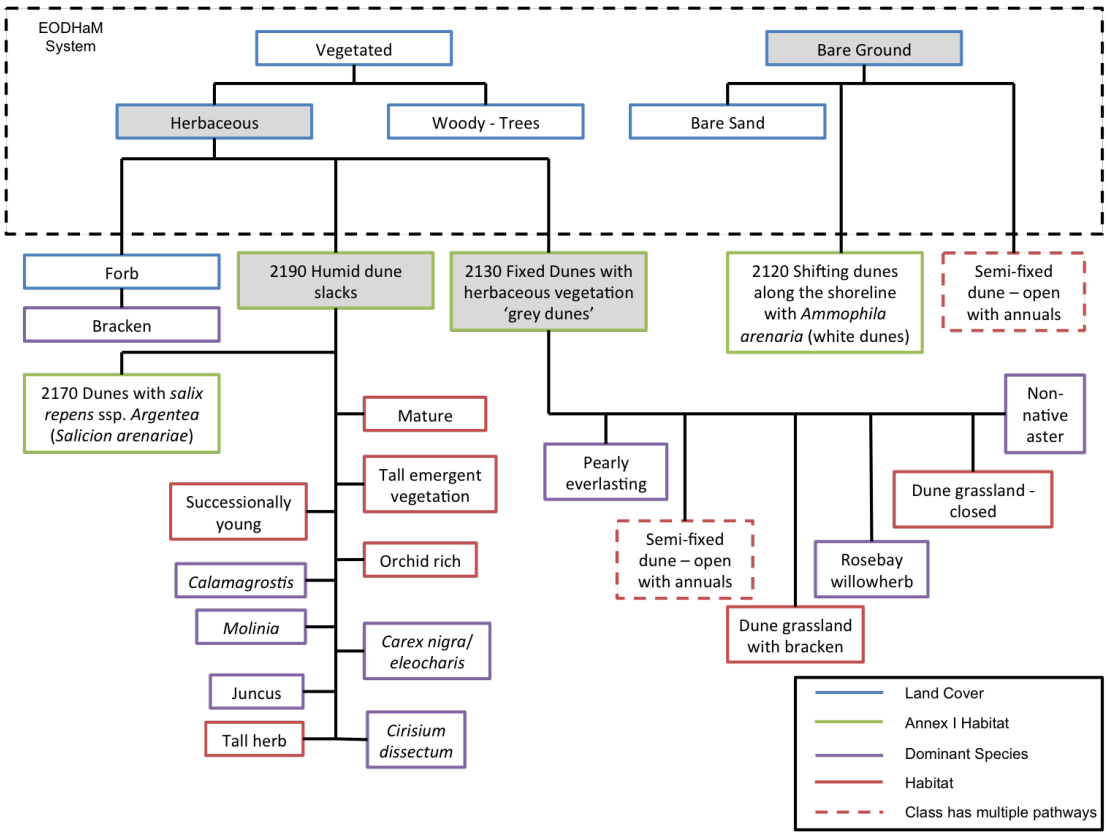

Figure 7.6: Classification structure for Kenfig. Each box that splits into nodes is used as a mask each time the algorithms are run (highlighted in grey).

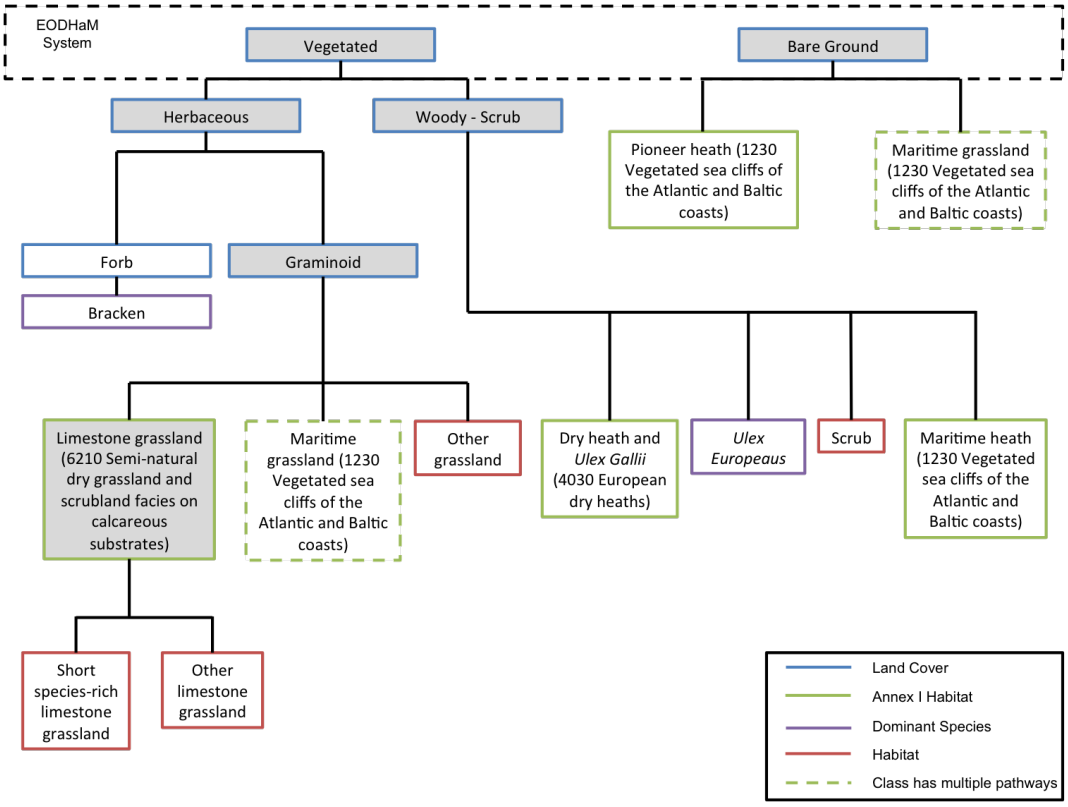

Figure 7.7: Classification structure for Castlemartin. Each box that splits into nodes is used as a mask each time the algorithms are run (highlighted in grey).

7.3.4 Accuracy Assessment

The accuracy assessment is carried out as outlined in Chapter 6, which is a confusion matrix, users and producers accuracy, overall accuracy and a kappa coefficient. For more information on the number of samples used for accuracy see Table 4.7 in Chapter 4. There are known issues with quantitative techniques of measuring uncertainty of remotely sensed products such as maps produced with classification methods. Foody (2002), states several main issues with accuracy assessments carried out in the EO community:

1. The accuracy measure and reporting itself lacks standardisation. In reality, it is noted that a single, all-purpose measure of classification accuracy does not exist and it may be preferable to derive more than one measure to provide a fuller description

of accuracy (Arbia et al., 1998; Muller et al., 1998). The provision of a confusion matrix and two more measures of accuracy seem feasible, as provided for each map in this study, but interpretation may be lacking or often ignored (Fisher, 1994) as measures such as the overall accuracy dominate.

2. Sampling issues are a common problem. A simple random sampling can be appropriate if the sample size is large enough but on the ground this method of data collection is constrained as physical access to some sites, or areas within sites are inaccessible. Sample sizes per class are also a problem as it depends on presence of class on site i.e. rare habitats or species can be missed in random sampling schemes and these are more often the areas of interest for ecologists and conservation managers.

3. Different types of errors are not captured in a confusion matrix which typically addresses thematic accuracy. Non-thematic errors such as misregistration of image data with ground data, which can often be larger sources of error than thematic accuracy itself are not captured in traditional quantitative methods (Canters, 1997; Muller et al., 1998). This problem was known before field data was acquired for this study and measures were put in place to minimise this issue (explained in Chapter 4). However, this was not always possible in mosaic areas.

4. Accuracy of ground or reference data can also present a problem especially when using reference data that was not acquired specifically for a study and required significant cleaning before use. Ground data labels typically vary in confidence depending on objectives of data collection and the term 'truth' should be avoided when referring to reference datasets as these can contain errors too. Accuracy assessments are therefore, only measuring the degree of agreement or correspondence between image and reference datasets (Congalton and Green, 1993). Field data was collected specifically tailored for this study so the confidence is very high in the

reference datasets, limiting this issue.

5. Spatial distribution of error are not captured in confusion matrices which generally work on point datasets. This is particularly problematic as much of the error occurs at boundaries of different classes and are associated with misregistration and mixed pixels.

With these issues in mind, measures of qualitative techniques are also explored in this study. As the main aim is to generate a useful baseline map of habitats at the two study locations, visual comparisons of classifications are deemed extremely valuable, especially when this qualitative assessment is carried out by site specialists with years of accumulated knowledge of the sites. As a large number of maps are generated initially, these will be narrowed down before the most promising are taken into the field on a GPS for final analysis. This method not only address the spatial distribution of error which is missing in quantitative accuracy assessments, but includes the ecologists expert knowledge in the mapping process increasing understanding and confidence in final products. Although the final maps are chosen from a qualitative assessment, the quantitative measure will also be calculated for comparison. To make sure the qualitative assessment is unbiased, no quantitative assessments are revealed before the final field analysis.

7.4 Results

This section will show results of the independent variable selection analysis that includes the ANOVA results from Chapter 6, the random forest variable importance results and the results from the correlation analysis. A qualitative assessment of all layers will be included stating which layers were chosen for field assessment. A confusion matrix will be included for each field assessment layer in addition to a map of the final layer chosen, as selected in the field.

7.4.1 Kenfig

Herbaceous Category

Table 7.2: Variables selected from different methods as inputs for running machine learning algorithms for the Herbaceous category at Kenfig (listed in order of variable importance for ANOVA and RF; Uncorrelated only had 19 features). For more information on layer naming convention, see Table 4.6 in Chapter 4.

ANOVA	Random Forest	Uncorrelated
Slope	Slope	Slope
July Green Band	July Yellow Band	peakCCCI
post Datt6	post CVI	peakDatt1
peakSRGB	July Panchromatic Band	peakDatt6
peakI	July Green Band	peakDiffNIR
peak Woody	peak SRGB	peakIPVI
July Red Edge Band	peak I	peakpostDiffNDVI
July Yellow Band	July Blue Band	peakSRCB
July Panchromatic Band	July Coastal Band	peakSRGNIR1
peakSRGB	peakSRYC	postBRI
July Blue Band	peakSRREB	postCVI
September Green Band	peakSRYB	postDatt1
July NIR2 Band	peakSRPanB	postDiffNIR
July NIR1 Band	postIPVI	postmSR
peakSRREC	postCIrededge	postSRCB
peakGDVI	July NIR2 Band	postSRNIR1NIR2
peakD800-550	post I	postSRPanG
peakSRNIR1C	peakSRBY	July Coastal Band
peakDDn	July Red Band	September Panchromatic Band
peakSRYB	September Yellow Band	

Table 7.2 shows the results from the independent variable selection analysis. Chosen indices for analysis include more peak index selection and image bands that, according to the training data, suggests that the classes are more separable in the summer months than in autumn. As expected, slope was identified as the most important variable selected by all three methods.

Table 7.3 shows the initial visual comparison of layers and states the chosen layers for field assessment. In this case only layers that are deemed to have the correct representation for every class is chosen for the field. ERF is the most popular algorithm while there is a layer chosen from each input feature except the correlation analysis. Figure 7.8 shows the chosen layer for the final map of this category as depicted by the accuracy analysis. This category is a three-class problem, and is split into Forb, 2190 Humid dune slacks

Input Features	Classifier	Distribution of habitats[a]			Comment
		FDG	Slack	Bracken	
ANOVA	AdaBoost	↑	↓	↑	Slack features are missing; bracken is over-represented
	RF	↑	↓	□	Slack features are missing
	ERF	↓	↑	□	Mixing of FDG and Slack features
	SVM rbf	↓	↑	↑	Mixing of FDG and Slack features; bracken is over-represented
	SVM linear	□	□	□	Chosen for field assessment
EODHaM	AdaBoost	↑	↓	□	Slack features are missing
	RF	□	□	□	Chosen for field assessment
	ERF	□	□	□	Chosen for field assessment
	SVM rbf	↓	↑	□	Slack features are over-represented
	SVM linear	↓	□	↑	Mixing of FDG and bracken
Images	AdaBoost	↑	↓	↓	FDG is over-represented and bracken nearly absent
	RF	↓	↑	□	Slight mixing of FDG and Slack features
	ERF	□	□	□	Chosen for field assessment
	SVM rbf	↓	↑	□	Mixing of FDG and Slack features
	SVM linear	↓	↑	↑	Mixing of FDG and Slack features; bracken is over-represented
Uncorrelated	AdaBoost	↑	↓	□	Slack features are missing
	RF	↓	□	↑	Bracken over-represented
	ERF	↓	↑	↑	Slack features and bracken are dominant
	SVM rbf	↓	↑	↑	Slack features and bracken are dominant
	SVM linear	↓	↑	↑	Mixing of FDG and Slack features; bracken is over-represented
Random Forest	AdaBoost	↑	↓	□	Slack features are missing
	RF	↑	↓	□	Slack features are missing
	ERF	□	□	□	Chosen for field assessment
	SVM rbf	↓	↑	↑	Slack features and bracken are dominant
	SVM linear	↓	↑	↑	Mixing of FDG and Slack features; bracken is over-represented

Interpretation Keys: ↑ Over-representation; ↓ Under-representation; □ Correct representation; ○ Absent; ✖ Difficult to comment

[a] Habitat Keys: FDG = Fixed Dune Grassland

Table 7.3: Visual comparison of all output classifiers. Chosen layers for field assessment highlighted in grey.

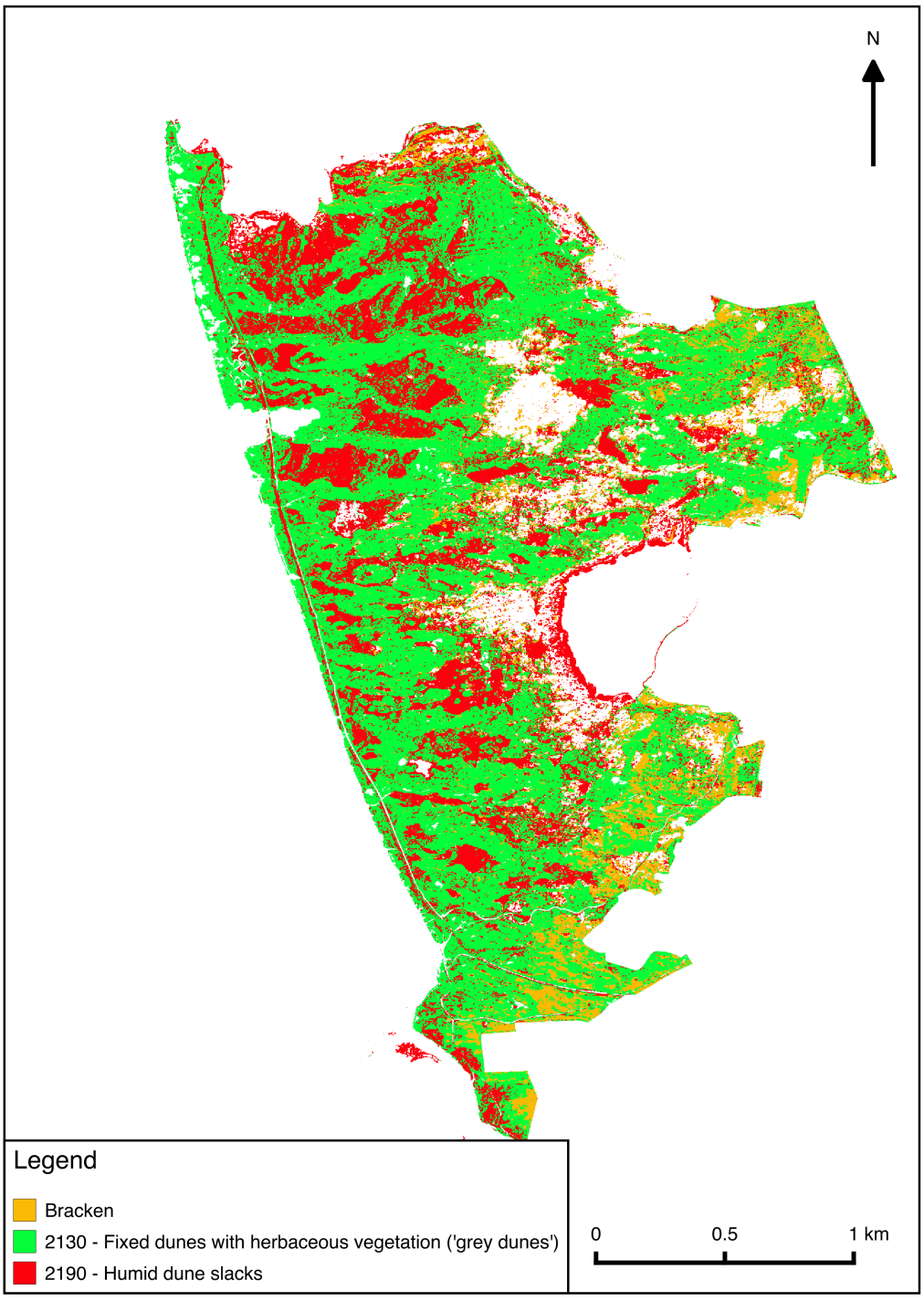

Figure 7.8: Broad habitat map of Kenfig. The layer was created using the EODHaM independent variables and the ERF algorithm.

A: Input Features = EODHaM; Algorithm = ERF; Overall Accuracy = 81.7%; Kappa Coefficient = 0.75

	Bracken	2190 Slacks	2130 FDG	Other	Sum	Users Accuracy (%)
Bracken	**28**	0	6	2	36	77.7
2190 Slacks	0	**70**	8	5	83	84.3
2130 FDG	8	5	**35**	4	52	67.3
Other	0	5	5	**81**	91	89
Sum	36	80	54	92	262	
Producers Accuracy (%)	77.7	87.5	64.8	88		

B: Input Features = ANOVA; Algorithm = SVC linear; Overall Accuracy = 81.3%; Kappa Coefficient = 0.74

	Bracken	2190 Slacks	2130 FDG	Other	Sum	Users Accuracy (%)
Bracken	**31**	0	3	2	36	86.1
2190 Slacks	2	**64**	12	5	83	77.1
2130 FDG	8	3	**37**	4	52	71.2
Other	4	3	3	**81**	91	89
Sum	45	70	55	92	262	
Producers Accuracy (%)	68.9	91.4	67.2	88		

D: Input Features = Images; Algorithm = ERF; Overall Accuracy = 82.4%; Kappa Coefficient = 0.76

	Bracken	2190 Slacks	2130 FDG	Other	Sum	Users Accuracy (%)
Bracken	**31**	1	2	2	36	86.1
2190 Slacks	0	**68**	10	5	83	81.9
2130 FDG	7	5	**36**	4	52	69.2
Other	1	5	4	**81**	91	89
Sum	39	79	52	92	262	
Producers Accuracy (%)	79.5	86.1	69.2	88		

C: Input Features = EODHaM; Algorithm = RF; Overall Accuracy = 80.2%; Kappa Coefficient = 0.73

	Bracken	2190 Slacks	2130 FDG	Other	Sum	Users Accuracy (%)
Bracken	**28**	1	5	2	36	77.7
2190 Slacks	2	**64**	12	5	83	77.1
2130 FDG	6	5	**37**	4	52	71.2
Other	1	5	4	**81**	91	89
Sum	37	75	58	92	262	
Producers Accuracy (%)	75.6	85.3	63.8	88		

E: Input Features = RF; Algorithm = ERF; Overall Accuracy = 82.4%; Kappa Coefficient = 0.76

	Bracken	2190 Slacks	2130 FDG	Other	Sum	Users Accuracy (%)
Bracken	**32**	0	2	2	36	88.9
2190 Slacks	1	**64**	13	5	83	77.1
2130 FDG	6	3	**39**	4	52	75
Other	1	4	5	**81**	91	89
Sum	40	71	59	92	262	
Producers Accuracy (%)	80	90.1	66.1	88		

Table 7.4: Error matrices of all layers chosen for field analysis. A is the error matrix for Figure 7.8.

and 2130 Fixed Dunes with herbaceous vegetation 'grey dunes'. Overall accuracy is high at 81.7%, while the kappa coefficient is also high.

Table 7.4 shows the error matrices for the five layers chosen for field analysis. The top table is the chosen layer from the field assessment but the analysis of the error matrices show that two of the layers are quantitatively more accurate in each of the measures. However, going back to the spatial aspect of the quantitative measures and the lack of information on boundaries, a map that has better spatial representation of classes will be of more use to an end user of the final product, especially as knowing habitat extent is a policy requirement. The overall accuracy and kappa coefficient are marginal in the difference between the chosen layer and others which have slightly higher numbers but the users and producers accuracy are more significant. Both are higher for the slack class in the chosen layer than any of the others which is in line with the importance of that class for this site.

2190 Humid Dune Slacks Category

Table 7.5: Independent variables selected from different methods as inputs for running machine learning algorithms for the Slacks mask at Kenfig (listed in order of variable importance for ANOVA and Random Forest). For more information on layer naming convention, see Table 4.6 in Chapter 4.

ANOVA	Random Forest	Uncorrelated
peak SRNIR1RE	peak SRRC	Slope
peak SRGRE	peak NDchl	peak CCCI
peak SRNIR2B	peak CI	peak Datt6
peak SRRG	peak NGRDI	peakpost DiffNDVI
peak NGRDI	peak NPCI	peak SRBC
post NGRDI	peak SRRENIR2	peak SRNIR2Pan
peak RI	peak SRYB	peak SRPanNIR1
peak SRREY	peak PPR	post CVI
peak SRNIR2RE	post DDn	post Datt1
peak SRPanB	peak SRRG	post DDn
peak SRNIR1G	peak SRNIR1NIR2	post DiffNIR
peak SRRNIR1	peak Chlrededge	post IPVI
peak ARI	peak SRCNIR2	post mSR
peak SRNIR1NIR2	peak SRNIR2RE	post SRBC
peak mSR	peakpost DiffNDVI	post SRGPan
peak SRNIR2G	Slope	post SRNIR1NIR2
peak SRPanRE	peak SRRB	post SRYC
peak reNDVI	September Green Band	post SRYR
peak SRNIR2NIR1	peak IPVI	July Coastal Band
peak CIgreen	peak RI	September Coastal Band

Table 7.5 shows the results from the independent variable selection analysis. Once again, peak indices are selected over post indices, suggesting that summer images include better separation for the classes mapped here, according to the training data. However, for the Uncorrelated variables it is a mixture of both peak and post indices. Individual image bands are not so significant for this category but of the three that were included, it's interesting that the coastal band from Worldview-2 is chosen for this specific category. As a band, it is specifically included for coastal regions and wetlands as there is less absorption of light from wet areas and water-bodies in this part of the spectrum.

Input Features	Classifier	Distribution of habitats[a]											Comment
		C	SY	TH	CN	CD	DwS	J	MS	M	OS	OR	
ANOVA	AdaBoost	✖	↑	↑	O	O	O	O	O	O	O	O	Classified as mostly SY and TH. Other classes absent.
	RF	□	□	□	□	✖	↑	□	↓	✖	□	↓	Chosen for field assessment.
	ERF	□	↓	□	↓	✖	□	□	□	✖	↑	↓	Key classes such as SY, CN and OR under-represented.
	SVM rbf	↓	O	□	↑	↑	↓	↑	O	↑	O	O	Key classes such as SY and MS missing.
	SVM linear	□	↓	□	↓	✖	□	□	□	✖	↑	□	Chosen for field assessment.
EODHaM	AdaBoost	O	↑	↑	↑	↑	↑	O	O	O	O	O	Only five classes present.
	RF	□	□	↓	□	✖	↑	□	↓	✖	□	□	Chosen for field assessment.
	ERF	□	□	↓	↓	✖	↑	□	↓	✖	↑	□	Mixing of TH, CN an OS classes.
	SVM rbf	↓	O	O	□	↑	↓	↓	O	↑	O	O	Key classes such as SY, MS and OR missing.
	SVM linear	□	↓	↓	↓	✖	↑	□	↓	✖	↑	□	Mixing of TH, CN and OS classes.
Images	AdaBoost	O	↑	↑	↑	O	↓	O	O	O	O	O	Only four classes present.
	RF	↑	□	□	□	✖	□	↓	□	✖	□	□	Chosen for field assessment.
	ERF	↑	□	□	□	✖	□	↓	□	✖	□	□	Chosen for field assessment.
	SVM rbf	□	O	□	□	↑	↓	↑	O	↑	O	O	Key classes such as SY, MS and OR missing.
	SVM linear	↑	O	□	□	↑	↑	↓	↓	✖	□	↓	Key class SY missing.
Uncorrelated	AdaBoost	↓	↑	↑	↓	O	O	O	O	O	O	O	Only four classes present.
	RF	↑	↓	↓	↑	✖	□	↓	□	✖	□	□	Mixing of SY and CN classes.
	ERF	↑	□	□	□	✖	□	↓	□	✖	□	□	Chosen for field assessment.
	SVM rbf	↓	O	↓	□	↑	↓	↑	O	↑	O	O	Key classes such as SY, MS and OR missing.
	SVM linear	↑	↓	O	↓	✖	□	↓	□	✖	↑	↓	Key classes such as SY, CN and OR under-represented.
Random Forest	AdaBoost	↓	↓	↑	↓	O	↑	O	O	O	O	O	Key classes such as MS and OR missing.
	RF	□	↓	↓	□	✖	↓	↓	↑	✖	↓	↓	Key classes such as SY, DwS and OR under-represented.
	ERF	□	□	↓	□	✖	□	↓	□	✖	↓	↓	Mixing of TH, J and OS classes.
	SVM rbf	□	O	↓	□	↑	↓	↑	O	↑	O	O	Key classes such as SY, MS and OR missing.
	SVM linear	□	O	O	↓	✖	□	↓	□	✖	↑	□	Key class SY missing.

Interpretation Keys: ↑ Over-representation; ↓ Under-representation; □ Correct representation; O Absent; ✖ Difficult to comment

[a] Habitat Keys: C = *Calamagrostis*; SY = Successionally Young; TH = Tall Herb; CN = *Carex Nigra*; CD = *Cirisium Dissectum*; DwS = Dunes with *Salix*; J = *Juncus*; MS = Mature Slack; M = *Molinia*; OS = Open Water Slack; OR = Orchid Rich

Table 7.6: Visual comparison of all output classifiers. Chosen layers for field assessment highlighted in grey.

Table 7.6 shows the initial visual comparison of layers and states the chosen layers for field assessment. RF and ERF dominate the chosen layers with a single SVM layer cho-

sen, however not a single layer from the random forest input feature analysis showed promise. Another observation here is that the AdaBoost algorithm failed to classify many of the classes regardless of input variables. Figure 7.9 shows the chosen layer for the final map for this category. This category is a many class problem featuring habitat classes such as Dunes with *Salix repens* and classes that map dominant species within humid dune slacks. Overall Accuracy is 41.5 % and the kappa coefficient is 0.34.

A: Input Features = Images; Algorithm = ERF; Overall Accuracy = 42.4%; Kappa Coefficient = 0.34

	C	SY	TH	CN	CD	DS	J	MS	M	OS	OR	Sum	Users Accuracy (%)
C	**1**	0	0	0	0	1	1	1	0	0	0	4	25
SY	1	**4**	0	0	0	0	3	0	0	0	0	8	50
TH	0	0	**0**	0	0	0	0	1	0	1	0	2	0
CN	1	0	1	**6**	0	0	1	1	0	0	0	10	60
CD	0	0	0	0	**1**	0	0	0	0	0	1	2	50
DS	0	0	0	0	0	**3**	0	4	0	0	0	7	43
J	1	0	0	0	0	2	**3**	0	0	0	0	6	50
MS	1	2	1	0	0	4	1	**5**	0	0	0	14	36
M	0	1	0	0	0	0	0	0	**0**	0	0	1	0
OS	0	0	0	1	0	0	1	0	0	**0**	0	2	0
OR	2	1	0	0	0	1	0	1	0	0	**5**	10	50
Sum	7	8	2	7	0	11	10	13	0	1	6	66	
Producers Accuracy (%)	14	50	0	85.7	100	27.3	30	38.5	0	0	83.3		

D: Input Features = Images; Algorithm = RF; Overall Accuracy = 43.3%; Kappa Coefficient = 0.35

	C	SY	TH	CN	CD	DS	J	MS	M	OS	OR	Sum	Users Accuracy (%)
C	**1**	0	0	1	0	1	1	0	0	0	0	4	25
SY	1	**4**	0	0	0	0	3	0	0	0	0	8	50
TH	0	0	**0**	1	0	0	0	1	0	0	0	2	0
CN	1	0	1	**6**	0	0	1	1	0	0	0	10	60
CD	0	0	0	0	**1**	0	0	1	0	0	0	2	50
DS	0	0	0	0	0	**5**	0	2	0	0	0	7	71.4
J	1	0	0	0	0	2	**3**	0	0	0	0	6	50
MS	1	2	0	1	0	5	1	**4**	0	0	1	14	26.7
M	0	1	0	0	0	0	0	0	**0**	0	0	1	0
OS	0	0	0	1	0	0	1	0	0	**0**	0	2	0
OR	2	1	0	0	0	1	0	1	0	0	**5**	10	50
Sum	7	8	1	10	1	14	10	10	0	0	6	66	
Producers Accuracy (%)	14.3	50	0	60	100	35.7	30	40	0	0	83.3		

B: Input Features = ANOVA; Algorithm = RF; Overall Accuracy = 40.9%; Kappa Coefficient = 0.31

	C	SY	TH	CN	CD	DS	J	MS	M	OS	OR	Sum	Users Accuracy (%)
C	**0**	0	0	0	0	0	1	2	0	0	1	4	0
SY	0	**4**	0	0	0	0	2	0	0	1	1	8	50
TH	0	0	**2**	0	0	0	0	0	0	0	0	2	100
CN	0	1	0	**3**	0	0	1	1	0	2	2	10	30
CD	0	0	0	0	**0**	0	0	2	0	0	0	2	0
DS	0	0	0	0	0	**3**	0	4	0	0	0	7	42.9
J	0	1	0	0	0	1	**2**	1	0	0	1	6	33.3
MS	0	1	1	0	0	3	0	**8**	0	0	1	14	57.1
M	0	0	0	0	0	0	0	1	**0**	0	0	1	0
OS	0	0	1	1	0	0	0	0	0	**0**	0	2	0
OR	0	2	0	0	0	1	1	1	0	0	**5**	10	50
Sum	0	9	4	4	0	8	7	20	0	3	11	66	
Producers Accuracy (%)	0	44.4	50	75	0	37.5	28.6	40	0	0	45.5		

E: Input Features = EODHaM; Algorithm = RF; Overall Accuracy = 39.4%; Kappa Coefficient = 0.30

	C	SY	TH	CN	CD	DS	J	MS	M	OS	OR	Sum	Users Accuracy (%)
C	**1**	0	0	0	0	1	1	1	0	0	0	4	25
SY	0	**3**	0	0	0	0	3	0	0	1	1	8	37.5
TH	0	0	**0**	1	0	0	0	1	0	0	0	2	0
CN	0	0	0	**4**	0	0	3	1	0	1	1	10	40
CD	0	0	0	0	**0**	0	0	2	0	0	0	2	0
DS	0	0	0	0	0	**2**	0	4	0	0	1	7	28.6
J	1	0	0	0	0	2	**3**	0	0	0	0	6	50
MS	1	1	0	1	0	4	0	**6**	0	0	1	14	42.9
M	0	0	0	0	0	0	0	1	**0**	0	0	1	0
OS	0	1	0	1	0	0	0	0	0	**0**	0	2	0
OR	0	0	0	0	0	1	1	1	0	0	**7**	10	70
Sum	3	5	0	7	0	10	11	17	0	2	11	66	
Producers Accuracy (%)	33.3	60	0	57.1	0	20	27.3	35.3	0	0	63.6		

C: Input Features = ANOVA; Algorithm = SVC linear; Overall Accuracy = 42.4%; Kappa Coefficient = 0.33

	C	SY	TH	CN	CD	DS	J	MS	M	OS	OR	Sum	Users Accuracy (%)
C	**0**	0	0	0	0	0	0	2	0	0	2	4	0
SY	1	**3**	0	0	0	0	0	0	0	1	3	8	37.5
TH	0	0	**2**	0	0	0	0	0	0	0	0	2	100
CN	1	0	0	**2**	0	0	2	1	0	4	0	10	20
CD	0	0	0	0	**0**	0	0	2	0	0	0	2	0
DS	0	0	0	0	0	**4**	0	3	0	0	0	7	57.1
J	1	0	0	0	0	1	**1**	1	0	0	2	6	16.7
MS	1	0	0	1	0	3	0	**9**	0	0	0	14	64.3
M	0	0	0	0	0	0	0	1	**0**	0	0	1	0
OS	0	0	0	1	0	0	0	0	0	**1**	0	2	50
OR	0	1	0	0	0	2	0	1	0	0	**6**	10	60
Sum	4	4	2	4	0	10	3	20	0	6	13	66	
Producers Accuracy (%)	0	75	100	50	0	40	33.3	45	0	16.7	46.2		

F: Input Features = Uncorrelated; Algorithm = ERF; Overall Accuracy = 45.5%; Kappa Coefficient = 0.38

	C	SY	TH	CN	CD	DS	J	MS	M	OS	OR	Sum	Users Accuracy (%)
C	**0**	0	0	0	0	2	1	1	0	0	0	4	0
SY	1	**5**	0	0	0	0	2	0	0	0	0	8	62.5
TH	0	0	**0**	0	0	0	1	1	0	0	0	2	0
CN	1	0	1	**5**	0	0	2	1	0	0	0	10	50
CD	0	0	0	0	**0**	1	0	1	0	0	0	2	0
DS	0	0	0	0	0	**5**	1	1	0	0	0	7	71.4
J	1	0	0	0	0	0	**4**	0	0	0	1	6	66.7
MS	1	0	0	0	0	6	1	**5**	0	0	1	14	35.7
M	0	0	0	0	0	0	0	1	**0**	0	0	1	0
OS	0	1	1	0	0	0	0	0	0	**0**	0	2	0
OR	1	2	0	0	0	1	0	0	0	0	**6**	10	60
Sum	5	8	2	5	0	15	12	11	0	0	8	66	
Producers Accuracy (%)	0	62.5	0	100	0	33.3	33.3	45.5	0	0	75		

Table 7.7: Error matrices of all layers chosen for field analysis. A is the error matrix for Figure 7.9. C = *Calamagrostis*; SY = Successionally Young; TH = Tall Herb; CD = *Cirisium dissectum*; DS = Dunes with *Salix*; J = *Juncus*; MS = Mature Slack; M = *Molinia*; OS = Tall Emergent Vegetation; OR = Orchid Rich.

Table 7.7 shows the error matrices for the six layers chosen for field analysis. This is

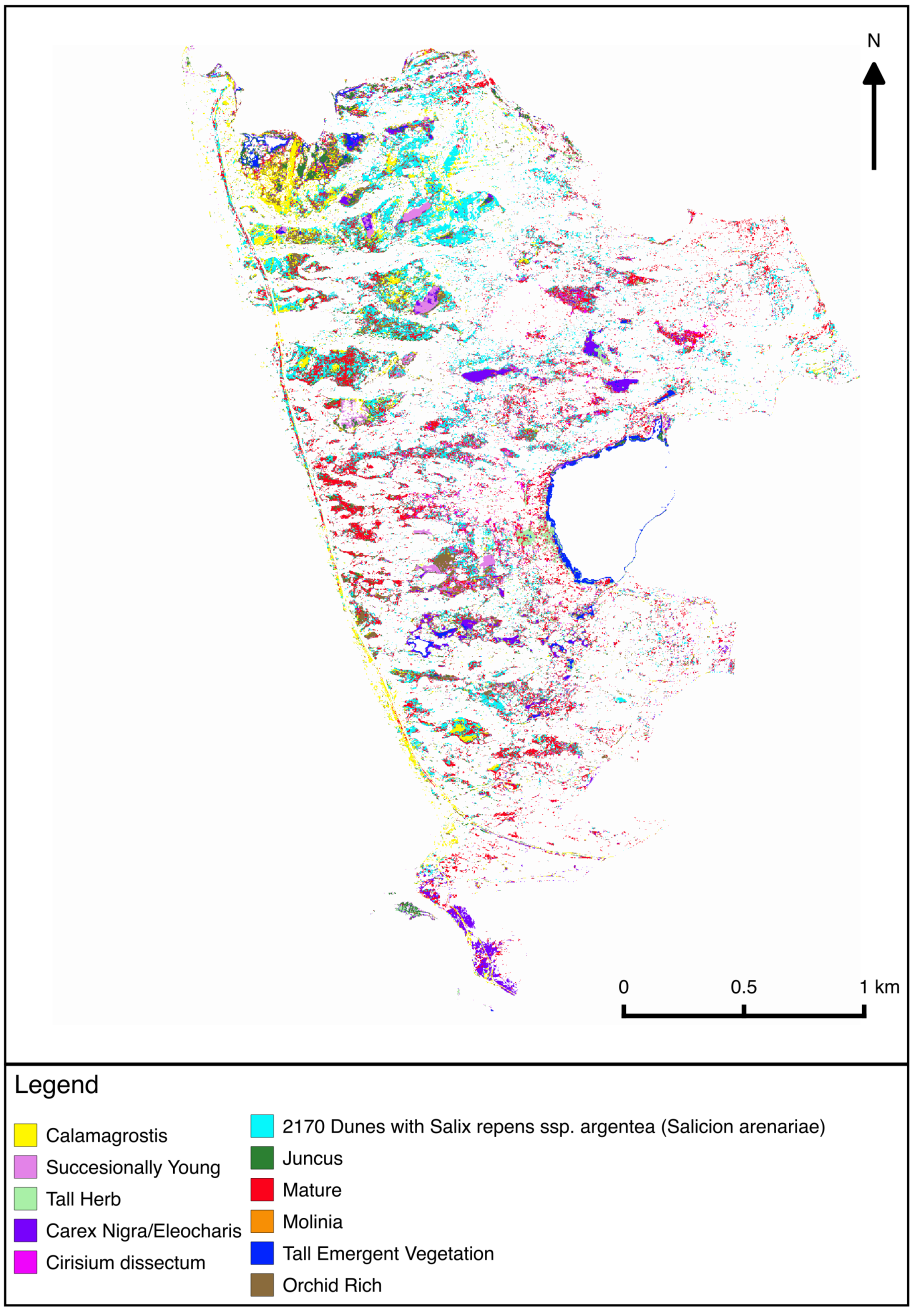

Figure 7.9: Slacks habitat map of Kenfig. The layer was created using the Images independent variables and the ERF algorithm.

an example where the traditional measures of quantifying accuracy are not appropriate as there are not enough sampling points to adequately represent each class. However, they still provide valuable information that can be used for interpretation. Once again, the most accurate layer from the quantitative accuracy measures are not chosen which makes the qualitative accuracy assessment used in this study even more important. The numbers here do not represent how useful the final map is as a slack habitat map due to lack of representation in the sample. Although there are still errors present, many of the important slack types such as successionally young were correctly represented to a degree.

2130 Fixed Dune Grassland Category

Table 7.8: Independent variables selected from different methods as inputs for running machine learning algorithms for the Fixed Dune Grassland mask at Kenfig (listed in order of variable importance for ANOVA and Random Forest; Uncorrelated only had 17 features). For more information on layer naming convention, see Table 4.6 in Chapter 4.

ANOVA	Random Forest	Uncorrelated
peak SRYG	post SRBPan	Slope
peak SRNIR1B	post SRPanB	peak CVI
peak SRCG	post SRNIR1NIR2	peak Datt1
peak PPR	post SRRY	peak DDn
peak SRRB	peak SRPanG	peak DiffNIR
peak SRGNIR1	peak BRI	peak SRCY
peak SRYPan	post SRYC	peak SRREB
peak SRPanG	post SRYR	peak SRYB
peak SRGB	post Maccioni	post Datt1
peak SRPanC	post SRYB	post IPVI
peak Woody	peak SRNIR2NIR1	post mSR
peak SRRG	post Datt1	post SRCB
peak SRBG	post SRPanC	post SRNIR2NIR1
peak SRPanB	post SRBC	post SRPanG
peak ARI	post Datt6	July Green Band
peak SRNIR2G	peak SRRC	July Panchromatic Band
peak SRREG	peak SRBG	September Panchromatic Band
peak BRI	peak PSRI	
peak SRPanRE	peak SRBR	
peak SRNIR2B	peak SRPanB	

Table 7.8 shows the results from the independent variable selection analysis. Peak indices are marginally more popular than post indices overall. However, while the Uncorrelated is fairly even, as it has been for the previous results, ANOVA are all peak indices while

Random Forest tends to favour post indices. This suggests that seasonal imagery has a significance for separation of classes for this category, according to the training data. Once again, individual image bands are not so significant for this category. Slope seems to be included in most Uncorrelated as expected as it is calculated from terrain data and not the image data and a high correlation is very unlikely.

Input Features	Classifier	Distribution of habitats[a]						Comment
		DG	DB	SF	A	PE	RW	
ANOVA	AdaBoost	↑	↓	□	O	O	O	Invasive species absent.
	RF	↑	↓	↓	□	□	O	DB and SF under-represented.
	ERF	↑	↓	↓	□	□	□	DB and SF under-represented.
	SVM rbf	↑	↓	O	O	↓	O	DB and PE under-represented. Other classes absent.
	SVM linear	↑	↓	↓	□	□	O	DB and SF under-represented.
EODHaM	AdaBoost	↑	↓	↓	O	↓	O	DB and SF under-represented. Some Invasive species absent.
	RF	↑	□	↓	□	□	O	Chosen for field assessment.
	ERF	↑	□	↓	□	□	O	Chosen for field assessment.
	SVM rbf	↑	□	↓	O	O	O	SF under-represented. Invasive species absent.
	SVM linear	↑	□	↓	□	□	□	Chosen for field assessment.
Images	AdaBoost	↑	↓	□	O	O	O	Invasive species absent.
	RF	↑	↓	↓	□	□	□	DB and SF under-represented.
	ERF	↑	↓	↓	□	□	□	DB and SF under-represented.
	SVM rbf	↑	↓	O	O	O	O	Only two classes present.
	SVM linear	□	□	□	□	□	□	Chosen for field assessment.
Uncorrelated	AdaBoost	↑	↓	□	↓	↓	↓	DB and Invasive species under-represented.
	RF	↑	↓	□	↓	↓	↓	DB and Invasive species under-represented.
	ERF	↑	↓	□	↓	↓	↓	DB and Invasive species under-represented.
	SVM rbf	↑	↓	↓	O	O	O	DB and SF under-represented. Invasive species absent.
	SVM linear	↓	□	□	↑	↑	↑	Invasive species over-represented.
Random Forest	AdaBoost	↑	↑	↓	O	O	O	DB over-represented. Invasive species absent.
	RF	↓	↑	□	O	□	O	DB over-represented.
	ERF	↑	↑	↓	O	□	O	DB over-represented.
	SVM rbf	↑	□	↓	O	O	O	Invasive species absent.
	SVM linear	↓	↑	↑	O	↑	↑	DG under-represented.

Interpretation Keys: ↑ Over-representation; ↓ Under-representation; □ Correct representation; O Absent; ✖ Difficult to comment

[a] Habitat Keys: DG = Dune Grassland; DB = Dune grassland with Bracken; SF = Semi-fixed Dunes; A = Non-native Aster; PE = Pearly Everlasting; RW = Rosebay Willowherb

Table 7.9: Visual comparison of all output classifiers. Chosen layers for field assessment highlighted in grey.

Table 7.9 shows the initial visual comparison of layers and states the chosen layers for field assessment. There are less layers with correct representation of all classes than for previous categories and none of the statistical analyses proved sufficient at delineating input variables. The indices chosen for the EODHaM system are most dominant as are the

RF, ERF and SVC linear algorithms. Figure 7.10 shows the chosen layer for the final map for this category. This category is also a many class problem mostly featuring invasive species that are particularly dominant such as rosebay willowherb and mixed grassland classes. Overall accuracy of the layer is 64.8% which is again lower as the problem becomes more complicated spectrally and there are less training data per class.

A: Input Features = Images; Algorithm = SVC linear; Overall Accuracy = 64.8%; Kappa Coefficient = 0.20

	DG	DB	SF	A	PE	RW	Sum	Users Accuracy (%)
DG	**22**	0	0	1	0	0	23	95.7
DB	1	**0**	0	0	0	0	1	0
SF	7	0	**0**	0	0	0	7	0
A	1	0	0	**1**	0	0	2	50
PE	2	0	0	0	**0**	0	2	0
RW	0	0	0	0	1	**1**	2	50
Sum	33	0	0	2	1	2	37	
Producers Accuracy (%)	66.7	0	0	50	0	100		

C: Input Features = EODHaM; Algorithm = ERF; Overall Accuracy = 62.2%; Kappa Coefficient = 0.07

	DG	DB	SF	A	PE	RW	Sum	Users Accuracy (%)
DG	**23**	0	0	0	0	0	23	100
DB	1	**0**	0	0	0	0	1	0
SF	6	1	**0**	0	0	0	7	0
A	2	0	0	**0**	0	0	2	0
PE	2	0	0	0	**0**	0	2	0
RW	1	0	0	0	1	**0**	2	0
Sum	35	1	0	0	1	0	37	
Producers Accuracy (%)	65.7	0	0	0	0	0		

B: Input Features = EODHaM; Algorithm = RF; Overall Accuracy = 62.2%; Kappa Coefficient = 0

	DG	DB	SF	A	PE	RW	Sum	Users Accuracy (%)
DG	**23**	0	0	0	0	0	23	100
DB	1	**0**	0	0	0	0	1	0
SF	7	0	**0**	0	0	0	7	0
A	2	0	0	**0**	0	0	2	0
PE	2	0	0	0	**0**	0	2	0
RW	2	0	0	0	0	**0**	2	0
Sum	37	0	0	0	0	0	37	
Producers Accuracy (%)	62.2	0	0	0	0	0		

D: Input Features = EODHaM; Algorithm = SVC linear; Overall Accuracy = 67.6%; Kappa Coefficient = 0.23

	DG	DB	SF	A	PE	RW	Sum	Users Accuracy (%)
DG	**23**	0	0	0	0	0	23	100
DB	1	**0**	0	0	0	0	1	0
SF	6	0	**1**	0	0	0	7	14.3
A	2	0	0	**0**	0	0	2	0
PE	2	0	0	0	**1**	0	2	50
RW	1	0	0	0	1	**0**	2	0
Sum	34	0	1	0	2	0	37	
Producers Accuracy (%)	67.6	0	100	0	50	0		

Table 7.10: Error matrices of all layers chosen for field analysis. A is the error matrix for Figure 7.10. DG= Dune grassland (closed); DB= Dune grassland with bracken; SF= Semi-fixed dune; A= Non-native Aster; PE= Pearly Everlasting; RW= Rosebay Willowherb..

Table 7.10 shows the error matrices for the four layers chosen for field analysis. Again, this is another example where the traditional measures of quantifying accuracy are not appropriate as there are not enough sampling points to adequately represent each class, and the most accurate according the accuracy measures were not chosen.

Bare Sand Category

Table 7.11 shows the results from the independent variable selection analysis. Peak indices are very dominant in all of the statistical methods for independent variable analysis, suggesting that summer images include better separation for the classes mapped in this

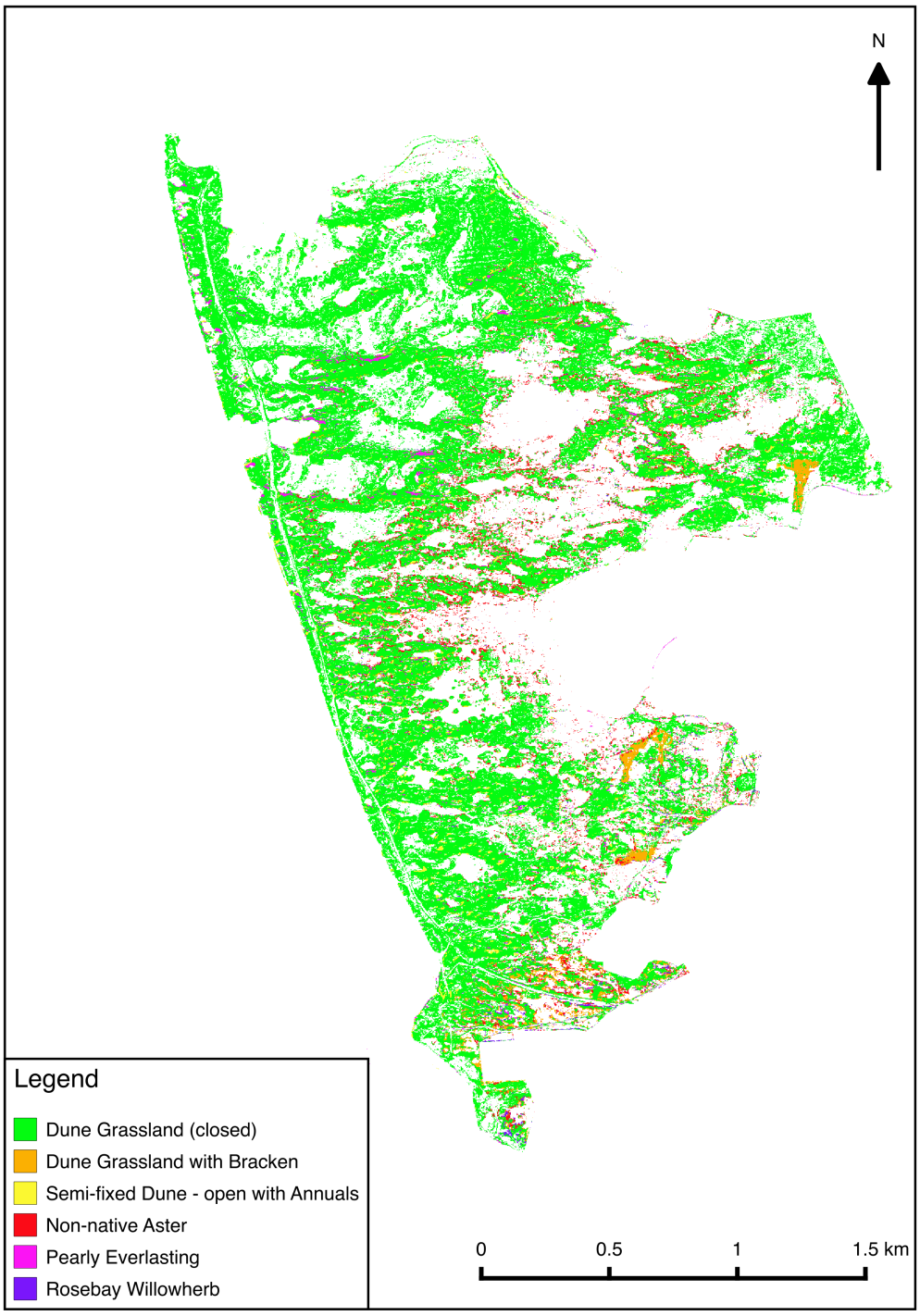

Figure 7.10: Fixed Dune Grassland habitat map of Kenfig. The layer was created using the Images independent variables and the linear SVM algorithm.

Table 7.11: Independent variables selected from different methods as inputs for running machine learning algorithms for the Bare sand mask at Kenfig (listed in order of variable importance for ANOVA and Random Forest; Uncorrelated only had 12 features). For more information on layer naming convention, see Table 4.6 in Chapter 4.

ANOVA	Random Forest	Uncorrelated
peak CCCI	peak SRRY	Slope
peak Datt4	peak SRRG	peak CCCI
July Green Band	July Red Band	peak Datt1
peak I	peak SRRB	peak Datt4
July Blue Band	peak SRGR	peakpost DiffNDVI
July Panchromatic Band	peak SRRNIR1	peak SRNIR1Pan
July Red Band	Slope	peak SRYC
July Red Edge Band	peak RI	post Datt4
July Yellow Band	post SRRG	post DiffNIR
July Coastal Band	peak SRYR	post IPVI
peak DDn	peak D678/500	post mSR
peak SRRPan	July Red Edge Band	post SRREPan
peak D678/500	peak I	
peak SRGR	peak NPCI	
peak SRRNIR2	post SRYC	
peak ND550/531	peak SRRPan	
peak PRI	post SRYG	
peak ND750-680	peak SRRC	
peak mNDVI	peak SRBR	
post mNDVI	July Green Band	

category, according to the training data. There are many individual image bands selected here too which means that the variance and separability are substantial enough within the imagery itself.

Table 7.12 shows the initial visual comparison of layers and states the chosen layers for field assessment. Only three layers were deemed to have the correct representation for all classes. The EODHaM independent variables are once again proving to be better performing. It is also becoming apparent that the best performing algorithms are RF, ERF and a SVM with the linear kernel. Figure 7.11 shows the chosen layer for the final map of this category. This category is also a many class problem with habitats such as semi fixed dunes and shifting dunes. Overall accuracy is 79.3%.

Table 7.13 shows the error matrices for the three layers chosen for field analysis. Again, this is another example where the traditional measures of quantifying accuracy are not appropriate as there are not enough sampling points to adequately represent each class. However, the three chosen layers have very similar results and what's interesting is the

Input Features	Classifier	Distribution of habitats[a]				Comment
		BS	SD	SF	SL	
ANOVA	AdaBoost	↓	↑	↑	O	SD and SF dominant.
	RF	↓	↑	↑	↓	SD and SF dominant.
	ERF	□	□	↑	↓	SF over-represented.
	SVM rbf	□	↑	↑	↓	SD and SF dominant.
	SVM linear	□	□	↑	↓	SF over-represented.
EODHaM	AdaBoost	↓	↑	↑	↑	BS under-represented.
	RF	□	□	□	□	Chosen for field assessment.
	ERF	□	□	□	□	Chosen for field assessment.
	SVM rbf	□	↑	O	O	Only two classes present.
	SVM linear	↓	□	□	↑	BS under-represented.
Images	AdaBoost	↓	↓	↑	↓	SF dominant.
	RF	↓	↓	↑	↓	SF dominant.
	ERF	↓	↑	↑	↑	BS under-represented.
	SVM rbf	↑	□	□	↓	BS dominant.
	SVM linear	↓	↑	↑	↓	SD and SF dominant.
Uncorrelated	AdaBoost	↓	↑	↑	O	SD dominant.
	RF	↓	□	□	↑	SL dominant.
	ERF	↓	□	□	↑	SL dominant.
	SVM rbf	↑	↓	↓	O	BS dominant.
	SVM linear	□	□	□	□	Chosen for field assessment.
Random Forest	AdaBoost	□	↑	O	O	SD dominant.
	RF	↓	↑	↑	□	SD and SF dominant.
	ERF	↓	↑	↓	↑	BS and SF under-represented.
	SVM rbf	↑	□	↑	O	BS and SF over-represented.
	SVM linear	↓	↑	□	↓	SD dominant.

Interpretation Keys: ↑ Over-representation; ↓ Under-representation; □ Correct representation; O Absent; ✖ Difficult to comment

[a] Habitat Keys: BS = Bare Sand; SD = Shifting Dunes; SF = Semi-fixed dunes; SL = Strand Line

Table 7.12: Visual comparison of all output classifiers. Chosen layers for field assessment highlighted in grey.

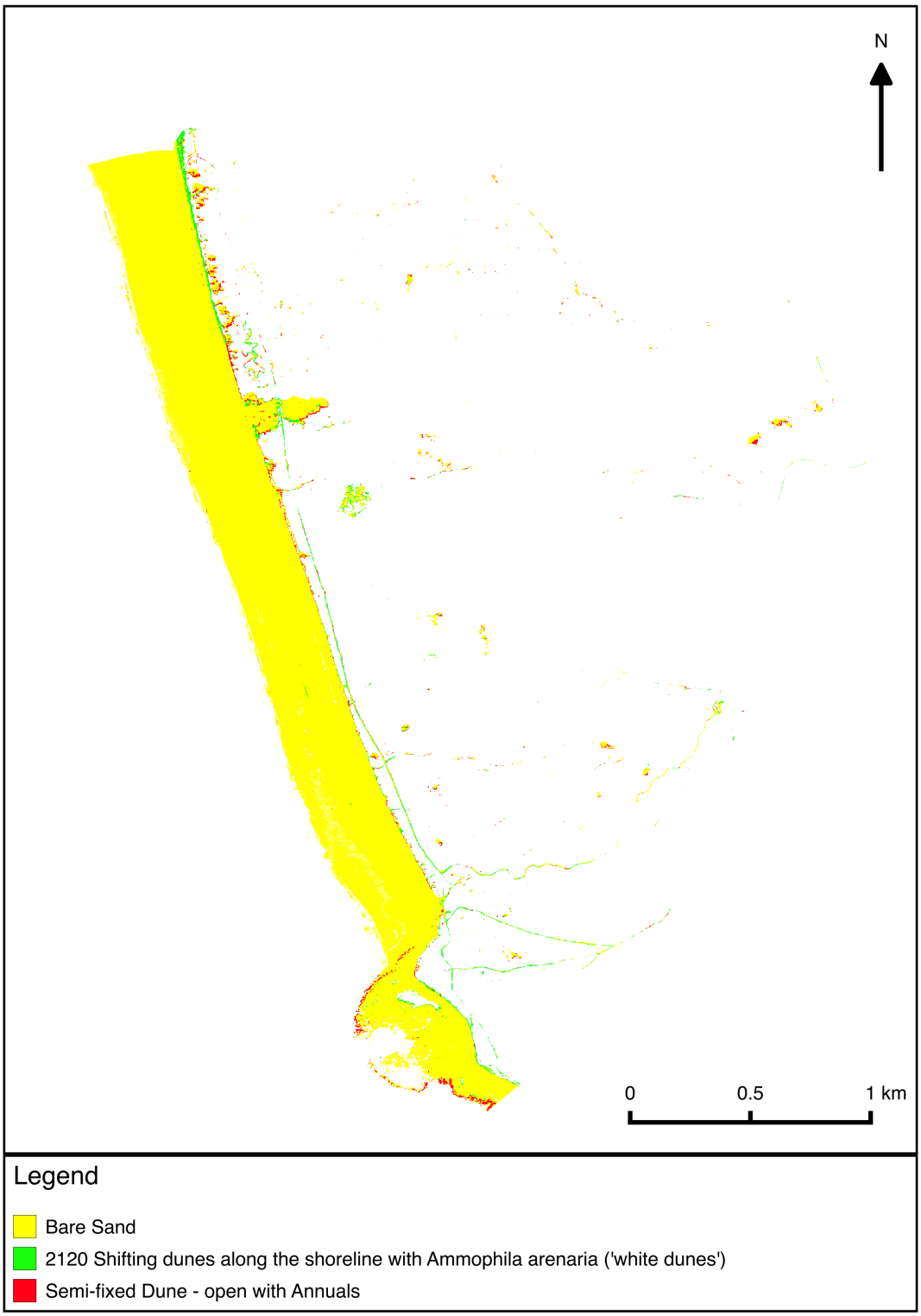

Figure 7.11: Bare sand habitat map of Kenfig. The layer was created using the Uncorrelated independent variables and the linear SVM algorithm.

A: Input Features = Uncorrelated; Algorithm = SVC linear; Overall Accuracy = 79.3%; Kappa Coefficient = 0.33

	Sand	Shifting Dunes	Semi-fixed Dunes	Sum	Users Accuracy (%)
Sand	**21**	0	1	22	95.5
Shifting Dunes	4	**1**	0	5	20
Semi-fixed Dunes	1	0	**1**	2	50
Sum	26	1	2	29	
Producers Accuracy (%)	80.7	100	50		

B: Input Features = EODHaM; Algorithm = RF; Overall Accuracy = 79.3%; Kappa Coefficient = 0.47

	Sand	Shifting Dunes	Semi-fixed Dunes	Sum	Users Accuracy (%)
Sand	**20**	0	2	22	90.9
Shifting Dunes	1	**3**	1	5	60
Semi-fixed Dunes	1	1	**0**	2	0
Sum	22	4	3	29	
Producers Accuracy (%)	90.9	75	0		

C: Input Features = EODHaM; Algorithm = ERF; Overall Accuracy = 75.9%; Kappa Coefficient = 0.43

	Sand	Shifting Dunes	Semi-fixed Dunes	Sum	Users Accuracy (%)
Sand	**19**	0	3	22	86.4
Shifting Dunes	1	**2**	2	5	40
Semi-fixed Dunes	1	0	**1**	2	50
Sum	21	2	6	29	
Producers Accuracy (%)	90.4	100	16.7		

Table 7.13: Error matrices of all layers chosen for field analysis. A is the error matrix for Figure 7.11.

chosen layer has the lowest kappa coefficient. The kappa values are much lower number than their overall accuracy counterparts which suggest that the results of these maps are only slightly better than random guessing.

7.4.2 Castlemartin

Lifeform Category

Table 7.14: Independent variables selected from different methods as inputs for running machine learning algorithms to determine woody and herbaceous areas within the vegetation mask at Castlemartin (listed in order of variable importance for ANOVA and Random Forest; Uncorrelated only had 17 features). For more information on layer naming convention, see Table 4.6 in Chapter 4.

ANOVA	Random Forest	Uncorrelated
peak CVI	September Red Band	Slope
July Panchromatic Band	September Panchromatic Band	peakCVI
July Green Band	September NIR1 Band	peak Datt1
peak IPVI	September Coastal Band	peak DDn
July Red Edge Band	September NIR2 Band	peak DiffNIR
peak CCCI	September Green Band	peakpostDiffNDVI
September Panchromatic Band	September Blue Band	peakSRBR
peak SRRC	September Yellow Band	peak SRBY
peak SRBR	September Red Edge Band	peak SRREB
post DDn	peak CVI	post DiffNIR
peak Datt4	post SRGY	post SRBC
July NIR1 Band	post mSR	post SRGB
September Green Band	July Green Band	post SRNIR2NIR1
peak SRNIR1B	peak RI	post SRRB
peak SRGRE	post Datt 4	July Green Band
July NIR2 Band	post SRYG	July Panchromatic Band
peak SRNIR1Pan	post CVI	September Panchromatic Band
peak SRNIR2Pan	Slope	
peak CI	peak ND550/531	
peak SRCR	peak Datt 6	

As the method utilised in Chapter 6 produced low accuracies for determining the lifeform categories several machine learning algorithms were run on the vegetation mask at Castlemartin to see if they performed better than the rule-based classification method utilised by the EODHaM method. It was found that higher accuracies were achieved by separating this category into two sections where one separates woody and herbaceous categories and the other separates forbs and graminoids within the herbaceous category. Table 7.14 and Table 7.15 shows the results of the independent variable selection analysis performed using the training data split into firstly woody and herbaceous categories, secondly, within the herbaceous mask created by this layer, graminoid and forb. The algorithms were also

run on the image bands and slope feature and the indices utilised in Chapter 6. Post features are dominant in the independent variable selection with the index CVI appearing in all categories.

Table 7.15: Independent variables selected from different methods as inputs for running machine learning algorithms for the Herbaceous mask at Castlemartin (listed in order of variable importance for ANOVA and Random Forest; Uncorrelated only had 13 features). For more information on layer naming convention, see Table 4.6 in Chapter 4.

ANOVA	Random Forest	Uncorrelated
post SRRB	peak SRNIR2B	Slope
peak SRREG	post CVI	peakCVI
post CVI	post SRNIR2NIR1	peakDatt1
peak SRGNIR1	post CCCI	peakDiffNIR
peak SRNIR1G	peak NPCI	peakSRBR
peak SRNIR2G	peak SRREB	peakSRREB
peak SRGB	post RI	postDDn
peak SRPanG	peak SRREC	postSRBR
post PSRI	post Datt6	postSRGB
post SRRY	post Datt4	postSRRC
peak SRYC	post SRYB	July Panchromatic Band
peakpostDiffNDVI	peak PSNDc1	July Red Edge Band
post SRNIR2NIR1	post SRRB	September Red Edge Band
post SRRG	post SRNIR2RE	
peak SRREC	post SRYG	
post SRBR	peak BWDRVI	
peak SRBC	post ARI	
post SRNIR1NIR2	peak CI	
peak Woody	post CI	
post Datt4	July Red Edge Band	

Table 7.16 shows the initial visual comparison of layers and states the chosen layers for field assessment. In this case only layers that are deemed to have the correct representation for every class is chosen for the field. As for Kenfig, the layers RF, ERF and SVM with the linear kernel appear to outperform the others. No layers were chosen from the ANOVA or Random Forest independent variable analysis. Figure 7.12 shows the chosen layer for the final map of this category as depicted by the accuracy analysis. Overall accuracy is high at 81.4%, while the kappa coefficient is also high. Table 7.18 shows the error matrices for the layers chosen for field analysis. The top tables (A and F) are the chosen layers from the field assessment and they are also the most accurate according to the quantitative measures.

A

Input Features	Classifier	Distribution of habitats	
		Woody	Herbaceous
ANOVA	AdaBoost	↑	↓
	RF	↑	↓
	ERF	↑	↓
	SVM rbf	↑	↓
	SVM linear	↑	↓
EODHaM	AdaBoost	↓	↑
	RF	□	□
	ERF	↓	↑
	SVM rbf	↓	↑
	SVM linear	□	□
Images	AdaBoost	↑	↓
	RF	□	□
	ERF	↑	↓
	SVM rbf	↓	↑
	SVM linear	↑	↓
Uncorrelated	AdaBoost	↑	↓
	RF	□	□
	ERF	↓	↑
	SVM rbf	↑	↓
	SVM linear	□	□
Random Forest	AdaBoost	↑	↓
	RF	↓	↑
	ERF	↑	↓
	SVM rbf	↑	↓
	SVM linear	↑	↓

Interpretation Keys: ↑ Over-representation; ↓ Under-representation; □ Correct representation; O Absent; ✖ Difficult to comment

B

Input Features	Classifier	Distribution of habitats	
		Graminoid	Forb
ANOVA	AdaBoost	↓	↑
	RF	↓	↑
	ERF	↓	↑
	SVM rbf	↓	↑
	SVM linear	↓	↑
EODHaM	AdaBoost	↓	↑
	RF	□	□
	ERF	↓	↑
	SVM rbf	↑	↓
	SVM linear	↓	↑
Images	AdaBoost	↑	↓
	RF	↑	↓
	ERF	↑	↓
	SVM rbf	↑	↓
	SVM linear	□	□
Uncorrelated	AdaBoost	↑	↓
	RF	↑	↓
	ERF	□	□
	SVM rbf	↑	↓
	SVM linear	↓	↑
Random Forest	AdaBoost	↓	↑
	RF	↓	↑
	ERF	↓	↑
	SVM rbf	↑	↓
	SVM linear	↓	↑

Interpretation Keys: ↑ Over-representation; ↓ Under-representation; □ Correct representation; O Absent; ✖ Difficult to comment

Table 7.16: Visual comparison of all output classifiers. Chosen layers for field assessment highlighted in grey. A = Layers representing the Woody and Herbaceous categories; B = Layers representing the Graminoid and Forb categories.

Overall Accuracy = 81.4%; Kappa Coefficient = 0.71						
	Woody	Graminoid	Forb	Bare Ground	Sum	Users Accuracy (%)
Woody	**38**	7	0	0	45	84.4
Graminoid	12	**32**	0	0	44	72.7
Forb	0	0	**10**	0	10	100
Bare Ground	1	1	0	**12**	14	85.7
Sum	22	72	7	12	113	
Producers Accuracy (%)	74.5	80	100	100		

Table 7.17: The error matrix for Figure 7.12. A combination of two layers form the final lifeform map.

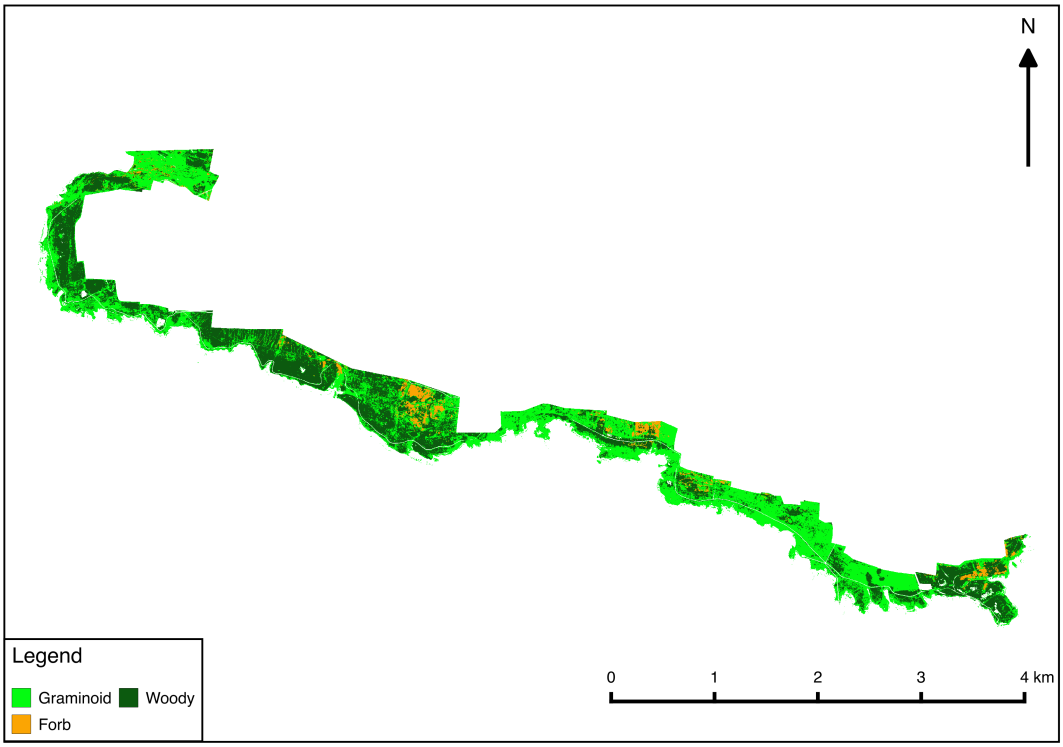

Figure 7.12: Lifeform map of Castlemartin. The woody layer was created by separating the vegetation mask into woody and herbaceous using the EODHaM independent variables and a SVM using a linear kernel. The graminoid and forb layers were created by separating the herbaceous mask using the uncorrelated independent variable and the Extremely Random Forest algorithm.

A: Input Features: EODHaM; Algorithm: SVC linear; Overall Accuracy = 81.4%; Kappa Coefficient = 0.69

	Woody	Herbaceous	Other	Sum	Users Accuracy (%)
Woody	**38**	7	0	45	84.4
Herbaceous	12	**42**	0	54	77.8
Other	1	1	**12**	14	85.7
Sum	50	49	12	113	
Producers Accuracy (%)	76	85.7	100		

B: Input Features: EODHaM; Algorithm: RF; Overall Accuracy = 69.9%; Kappa Coefficient = 0.50

	Woody	Herbaceous	Other	Sum	Users Accuracy (%)
Woody	**26**	18	1	45	57.8
Herbaceous	8	**43**	3	54	79.6
Other	1	3	**10**	14	71.4
Sum	34	61	14	113	
Producers Accuracy (%)	76.5	70.5	71.4		

C: Input Features: Images; Algorithm: RF; Overall Accuracy = 73.5%; Kappa Coefficient = 0.57

	Woody	Herbaceous	Other	Sum	Users Accuracy (%)
Woody	**31**	13	1	45	68.9
Herbaceous	9	**42**	3	54	77.8
Other	1	3	**10**	14	71.4
Sum	40	55	14	113	
Producers Accuracy (%)	77.5	76.4	71.4		

D: Input Features: Uncorrelated; Algorithm: RF; Overall Accuracy = 73.5%; Kappa Coefficient = 0.57

	Woody	Herbaceous	Other	Sum	Users Accuracy (%)
Woody	**31**	13	1	45	68.8
Herbaceous	9	**42**	3	54	77.8
Other	1	3	**10**	14	71.4
Sum	40	55	14	113	
Producers Accuracy (%)	77.5	76.4	71.4		

E: Input Features: Uncorrelated; Algorithm: SVC linear; Overall Accuracy = 76%; Kappa Coefficient = 0.61

	Woody	Herbaceous	Other	Sum	Users Accuracy (%)
Woody	**36**	8	1	45	80
Herbaceous	11	**40**	3	54	74.1
Other	1	3	**10**	14	71.4
Sum	47	48	14	113	
Producers Accuracy (%)	76.6	83.3	71.4		

F: Input Features: Uncorrelated; Algorithm: ERF; Overall Accuracy = 82.3%; Kappa Coefficient = 0.69

	Forb	Graminoid	Other	Sum	Users Accuracy (%)
Forb	**10**	0	0	10	100
Graminoid	0	**32**	12	44	72.7
Other	1	7	**51**	59	86.4
Sum	11	39	63	113	
Producers Accuracy (%)	90.9	82.1	81		

G: Input Features: EODHaM; Algorithm: RF; Overall Accuracy = 75.2%; Kappa Coefficient = 0.55

	Forb	Graminoid	Other	Sum	Users Accuracy (%)
Forb	**7**	1	2	10	70
Graminoid	1	**29**	14	44	65.9
Other	0	10	**49**	59	83.1
Sum	8	40	65	113	
Producers Accuracy (%)	87.5	72.5	75.4		

H: Input Features: Images; Algorithm: ERF; Overall Accuracy = 76.1%; Kappa Coefficient = 0.57

	Forb	Graminoid	Other	Sum	Users Accuracy (%)
Forb	**8**	0	2	10	80
Graminoid	1	**29**	14	44	65.9
Other	1	9	**49**	59	83.1
Sum	10	38	65	113	
Producers Accuracy (%)	80	76.3	75.4		

Table 7.18: Error matrices of all layers chosen for field analysis.

Woody Category

Table 7.19 shows the results from the independent variable analysis. Peak and post features are fairly evenly distributed in variable selection that suggests that both summer and autumn images are needed to generate a high accuracy map of woody classes.

Table 7.19: Independent variables selected from different methods as inputs for running machine learning algorithms for the Woody classes within the woody mask at Castlemartin (listed in order of variable importance for ANOVA and Random Forest; Uncorrelated only had 19 features). For more information on layer naming convention, see Table 4.6 in Chapter 4.

ANOVA	Random Forest	Uncorrelated
post SRYB	post SRBPan	Slope
post SRBY	peak NDRE	peak CVI
peak SRNIR2G	peak SRNIR2B	peak Datt1
peak Datt6	September Blue Band	peak DDn
peak SRNIR1G	post SRRENIR1	peak DiffNIR
peak SRREG	post LCI	peakpost DiffNDVI
peak SRPanG	post SRNIR2NIR1	peak SRBY
post SRRB	post SRGC	peak SRREB
peak SRGNIR1	peak Maccioni	peak SRRER
peak SRYC	peak GBNDVI	post CVI
peak CIgreen	peak SRBNIR1	post DDn
peak SRNIR2NIR1	post PRI	post DiffNIR
peak SRBC	July Red Edge Band	post SRBC
post SRBR	post NormG	post SRBR
peak SRNIR1NIR2	post SRNIR1RE	post SRGB
peak SRREB	post NDWI	post SRNIR2NIR1
post SRNIR1B	peak SRGNIR2	post SRPanG
peak SRCY	peak SRNIR2C	post SRYR
peak NormG	post SRBG	July Green Band
peak NPCI	peak SRYNIR1	

Table 7.13 shows the initial visual comparison of layers and states the chosen layers for field assessment. In this case only layers that are deemed to have the correct representation for every class is chosen for the field. As for Kenfig, the layers RF, ERF and SVM with the linear kernel appear to outperform the others. Figure 6.10 shows the chosen layer for the final map for this category. It is a many class problem with habitats and dominant species listed as classes. Overall accuracy is very high at 84.2%. Table 7.20 shows the error matrices for the four layers chosen for field analysis. Table A is the chosen layers from the field assessment and they are also the most accurate according to the quantitative measures.

Input Features	Classifier	Distribution of habitats[a]				Comment
		DH	UE	Scrub	MH	
ANOVA	AdaBoost	O	↓	↑	↑	MH dominant.
	RF	↓	↓	O	↑	DH and UE under-represented.
	ERF	□	↓	O	↑	UE under-represented.
	SVM rbf	□	O	O	↑	Only two classes present.
	SVM linear	□	□	↑	□	Chosen for field assessment.
EODHaM	AdaBoost	↑	↓	O	↓	DH over-represented.
	RF	↑	□	↓	↓	DH over-represented.
	ERF	□	□	↓	□	Chosen for field analysis.
	SVM rbf	□	O	O	↑	Only two classes present.
	SVM linear	↑	↑	□	↓	DH and UE dominant.
Images	AdaBoost	↑	↑	□	↓	DH and UE dominant.
	RF	□	□	↓	□	Chosen for field assessment.
	ERF	□	□	□	□	Chosen for field assessment.
	SVM rbf	□	O	O	↑	Only two classes present.
	SVM linear	↑	↑	O	↓	DH and UE dominant.
Uncorrelated	AdaBoost	↓	↓	O	↑	Mixing of DH and UE. MH dominant.
	RF	↓	□	↓	↑	MH dominant.
	ERF	↓	□	↓	↑	MH dominant.
	SVM rbf	□	↓	O	↑	MH dominant.
	SVM linear	↑	↑	□	↓	DH and UE dominant.
Random Forest	AdaBoost	↓	↑	O	↓	Mixing of DH and UE. UE dominant.
	RF	↑	↓	O	↓	Mixing of DH and UE. DH dominant.
	ERF	↑	↓	O	↓	DH dominant.
	SVM rbf	↑	↓	O	↓	DH dominant.
	SVM linear	↑	↓	O	↓	DH dominant.

Interpretation Keys: ↑ Over-representation; ↓ Under-representation; □ Correct representation; O Absent; ✖ Difficult to comment

[a] Habitat Keys: DH = Dry Heath; UE =*Ulex Europeaus*; MH = Maritime Heath

Figure 7.13: Visual comparison of all output classifiers. Chosen layers for field assessment highlighted in grey.

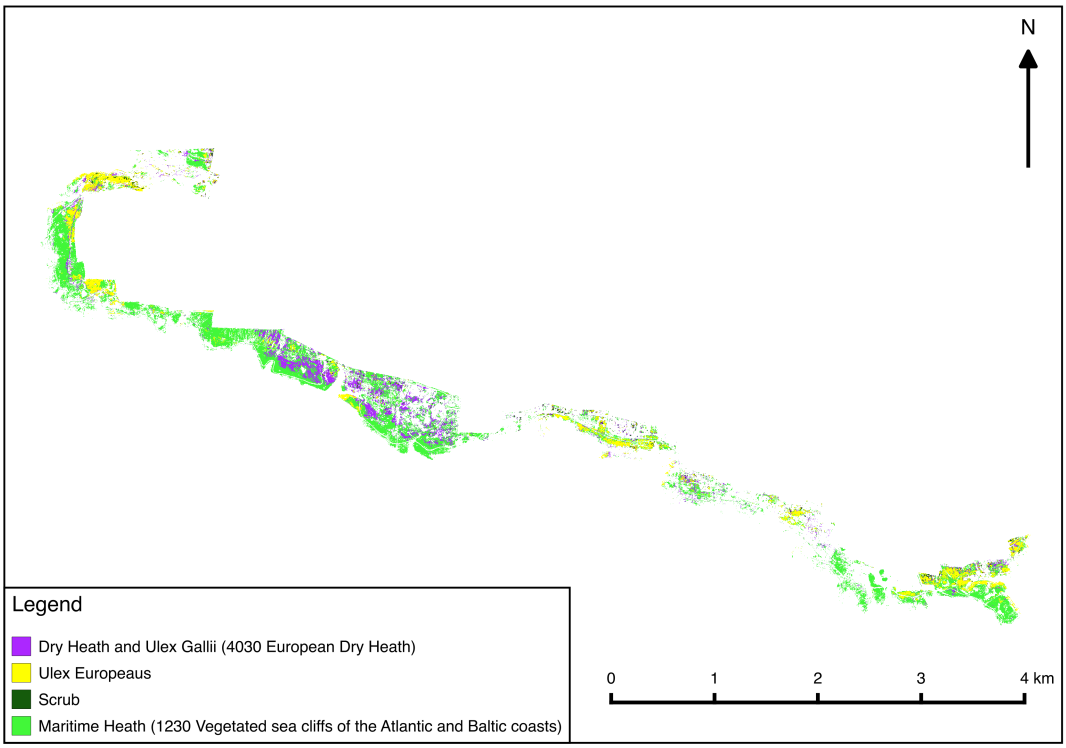

Figure 7.14: Woody map of Castlemartin. The woody layer was created using the Images and slope as independent variables and the ERF algorithm.

A: Input Features = Images; Algorithm = ERF; Overall Accuracy = 84.2%; Kappa Coefficient = 0.70

	Dry Heath	*Ulex Europeaus*	Scrub	Maritime Heath	Sum	Users Accuracy (%)
Dry Heath	**5**	1	0	0	6	83.3
Ulex Europeaus	1	**3**	0	2	6	50
Scrub	0	1	**1**	0	2	50
Maritime Heath	1	0	0	**23**	24	95.8
Sum	7	5	1	25	38	
Producers Accuracy (%)	71.4	60	100	92		

C: Input Features = EODHaM; Algorithm = ERF; Overall Accuracy = 68.4%; Kappa Coefficient = 0.39

	Dry Heath	*Ulex Europeaus*	Scrub	Maritime Heath	Sum	Users Accuracy (%)
Dry Heath	**3**	0	0	3	6	50
Ulex Europeaus	2	**2**	0	2	6	33.3
Scrub	1	1	**0**	0	3	0
Maritime Heath	1	2	0	**21**	24	87.5
Sum	7	5	0	26	38	
Producers Accuracy (%)	42.9	40	0	80.8		

B: Input Features = ANOVA; Algorithm = SVC linear; Overall Accuracy = 65.8%; Kappa Coefficient = 0.37

	Dry Heath	*Ulex Europeaus*	Scrub	Maritime Heath	Sum	Users Accuracy (%)
Dry Heath	**3**	0	0	3	6	50
Ulex Europeaus	0	**2**	2	2	6	33.3
Scrub	1	1	**0**	0	2	0
Maritime Heath	1	2	1	**20**	24	83.3
Sum	5	5	3	25	38	
Producers Accuracy (%)	60	40	0	80		

D: Input Features = Images; Algorithm = RF; Overall Accuracy = 65.8%; Kappa Coefficient = 0.36

	Dry Heath	*Ulex Europeaus*	Scrub	Maritime Heath	Sum	Users Accuracy (%)
Dry Heath	**3**	0	0	3	6	50
Ulex Europeaus	2	**2**	0	2	6	33.3
Scrub	1	1	**0**	0	3	0
Maritime Heath	1	3	0	**20**	24	83.3
Sum	7	6	0	25	38	
Producers Accuracy (%)	42.9	33.3	0	80		

Table 7.20: Error matrices of all layers chosen for field analysis. A is the error matrix for Figure 7.14.

Grassland Category

Table 7.21 shows the results from the independent variable selection analysis. Peak variables are slightly dominant in this category but not by much, which again points towards needing seasonal imagery to have a good chance at class separation.

Table 7.21: Independent variables selected from different methods as inputs for running machine learning algorithms for the grassland classes within the grass mask at Castlemartin (listed in order of variable importance for ANOVA and Random Forest; Uncorrelated only had 18 features). For more information on layer naming convention, see Table 4.6 in Chapter 4.

ANOVA	Random Forest	Uncorrelated
peak CVI	peak DiffNIR	Slope
July Panchromatic Band	peak SRYC	peak CVI
July Green Band	peak CVI	peak Datt1
peak IPVI	post SRGB	peakpost DiffNDVI
July Red Edge Band	peak SRREB	peak SRBR
peak CCCI	peak PSNDb2	peak SRCR
September Panchromatic Band	post SRREPan	peak SRYB
peak SRRC	peak CIrededge	post CVI
peak SRBR	peak FDI	post DDn
post DDn	peak SRREPan	post IPVI
peak Datt4	peak SRNIR1NIR2	post SRNIR1NIR2
July NIR1 Band	peak SRCY	post SRRC
September Green Band	post SRNIR2NIR1	post SRYB
peak SRNIR1B	peak SRNIR1Pan	July Panchromatic Band
peak SRGRE	September NIR2 Band	July Red Edge Band
July NIR2 Band	September Panchromatic Band	September Panchromatic Band
peak SRNIR1Pan	peak SRRC	September Red Edge Band
peak SRNIR2Pan	peak PPR	
peak CI	peak D800-680	
peak SRCR	post NDchl	

Figure 7.16 shows the chosen layer for the final map. This category is a many class problem with habitats and dominant species listed as classes. Overall accuracy in this category is low at 50%. Table 7.22 shows the error matrices for the four layers chosen for field anaylsis. Table A is the chosen layers from the field assessment and they are also the most accurate according to the quantitative measures.

Input Features	Classifier	Distribution of habitats[a]			Comment
		LG	MG	Other	
ANOVA	AdaBoost	↑	↓	↓	LG dominant.
	RF	↓	↑	↓	MG dominant.
	ERF	↓	↑	↓	MG dominant.
	SVM rbf	↑	↓	O	Only two classes present. LG dominant.
	SVM linear	↓	↑	↓	MG dominant.
EODHaM	AdaBoost	↓	↑	↓	MG dominant.
	RF	□	↑	↓	Mixing of MG and Other.
	ERF	□	↑	↓	Mixing of MG and Other.
	SVM rbf	↓	↑	O	Only two classes present. MG dominant.
	SVM linear	□	□	□	Chosen for field assessment.
Images	AdaBoost	↑	↓	↓	LG very dominant.
	RF	↓	↑	↓	MG dominant.
	ERF	↓	↑	↓	MG dominant.
	SVM rbf	↑	O	↑	Only two classes present.
	SVM linear	↓	↓	↑	Other dominant.
Uncorrelated	AdaBoost	↑	↓	↓	LG dominant.
	RF	□	↑	↓	Mixing of MG and Other.
	ERF	↓	↑	↓	MG dominant.
	SVM rbf	↑	↓	O	Only two classes present.
	SVM linear	↓	↑	↑	Mixing of MG and Other.
Random Forest	AdaBoost	↑	↑	↓	Other under-represented.
	RF	□	↑	↓	Mixing of MG and Other.
	ERF	↓	↑	↓	MG dominant.
	SVM rbf	↓	↑	O	Only two classes present.
	SVM linear	↓	↑	↓	MG dominant.

Interpretation Keys: ↑ Over-representation; ↓ Under-representation; □ Correct representation; O Absent; ✖ Difficult to comment

[a] Habitat Keys: LG = Limestone Grassland; MG = Maritime Grassland

Figure 7.15: Visual comparison of all output classifiers. Chosen layers for field assessment highlighted in grey.

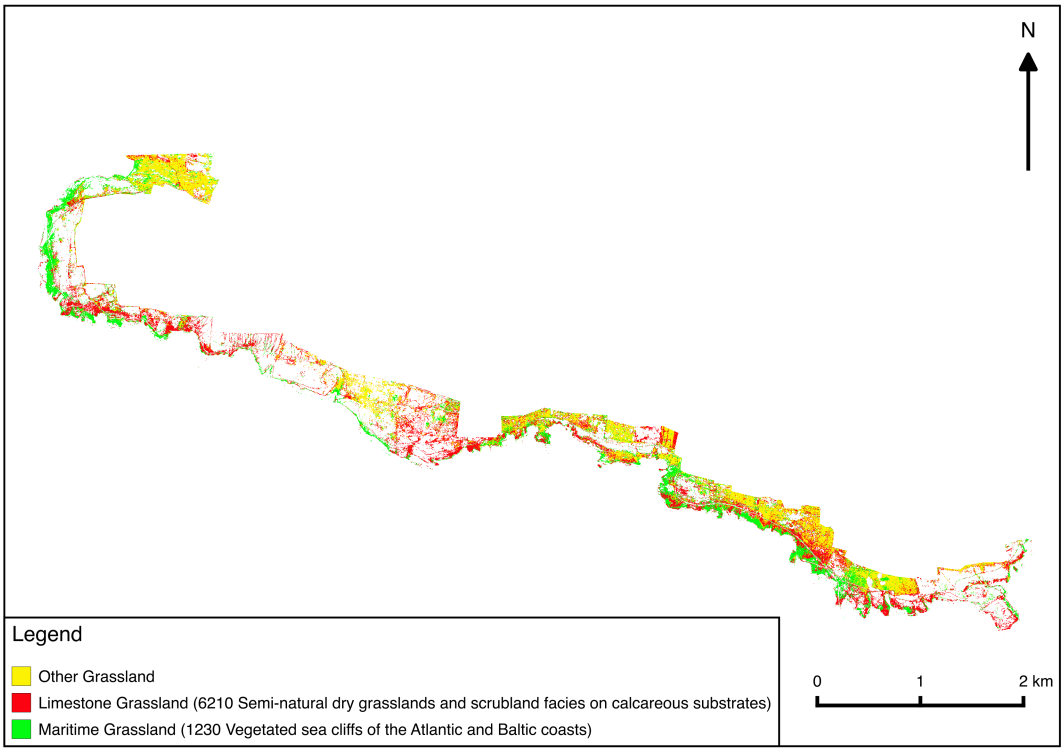

Figure 7.16: Grassland map of Castlemartin. The grassland layer was created using the EODHaM independent variables and a SVM using the linear kernel.

A: Input Features = EODHaM; Algorithm = SVC linear; Overall Accuracy = 50%; Kappa Coefficient = 0.18

	Other Grassland	Limestone Grassland	Maritime Grassland	Sum	Users Accuracy (%)
Other Grassland	**1**	2	1	4	25
Limestone Grassland	2	**6**	5	13	46.2
Maritime Grassland	2	4	**9**	15	60
Sum	5	12	15	32	
Producers Accuracy (%)	20	50	60		

B: Input Features = EODHaM; Algorithm = RF; Overall Accuracy = 40.1%; Kappa Coefficient = -0.01

	Other Grassland	Limestone Grassland	Maritime Grassland	Sum	Users Accuracy (%)
Other Grassland	**1**	2	1	4	25
Limestone Grassland	1	**4**	8	13	30.8
Maritime Grassland	1	6	**8**	15	53.3
Sum	3	12	17	32	
Producers Accuracy (%)	33.3	33.3	47.1		

D: Input Features = Uncorrelated; Algorithm = RF; Overall Accuracy = 56.3%; Kappa Coefficient = 0.24

	Other Grassland	Limestone Grassland	Maritime Grassland	Sum	Users Accuracy (%)
Other Grassland	**0**	3	1	4	0
Limestone Grassland	1	**9**	3	13	69.2
Maritime Grassland	0	6	**9**	15	60
Sum	1	18	13	32	
Producers Accuracy (%)	0	50	69.2		

C: Input Features = EODHaM; Algorithm = ERF; Overall Accuracy = 46.9%; Kappa Coefficient = 0.08

	Other Grassland	Limestone Grassland	Maritime Grassland	Sum	Users Accuracy (%)
Other Grassland	**1**	2	1	4	25
Limestone Grassland	1	**5**	7	13	38.5
Maritime Grassland	0	6	**9**	15	60
Sum	3	16	20	32	
Producers Accuracy (%)	50	38.5	52.9		

E: Input Features = RF; Algorithm = RF; Overall Accuracy = 50%; Kappa Coefficient = 0.13

	Other Grassland	Limestone Grassland	Maritime Grassland	Sum	Users Accuracy (%)
Other Grassland	**1**	2	1	4	25
Limestone Grassland	1	**5**	7	13	38.5
Maritime Grassland	0	5	**10**	15	66.7
Sum	2	12	18	32	
Producers Accuracy (%)	50	41.7	55.6		

Table 7.22: Error matrices of all layers chosen for field analysis. A is the error matrix for Figure 7.16.

Bare Ground Category

Table 7.23 shows the results from the independent variable selection analysis. There is an even selection between peak and post variables which means that the seasonal aspects is once again important for separation.

Table 7.23: Independent variables selected from different methods as inputs for running machine learning algorithms for the bare ground classes within the bare ground mask at Castlemartin (listed in order of variables importance for ANOVA and Random Forest; Uncorrelated only had 7 features). For more information on layer naming convention, see Table 4.6 in Chapter 4.

ANOVA	Random Forest	Uncorrelated
peak PSRI	peak NGRDI	Slope
peak SRRNIR1	post SRNIR2NIR1	peak Datt1
peak SRNIR1B	post SRGR	peakpost DiffNDVI
peak NGRDI	post NGRDI	peak SRNIR2Pan
peak SRGR	peak BRI	post D678/500
peak RI	peak SRYB	post SRRY
peak SRYG	peak SRGR	September Panchromatic Band
peak SRBR	post PPR	
peak D678/500	peak SRCY	
peak SRRC	post SRYC	
peak SRGRE	Slope	
post SRRG	peak SRREPan	
post NGRDI	peak RI	
post SRGRE	peak SRNIR2C	
post RI	post SRRB	
post SRGR	peak SRRG	
post SRYG	peak SRNIR2NIR1	
post BRI	post SRGY	
post SRGY	post SRBY	
post ARI	peak NDVI	

Figure 7.18 shows the chosen layer for the final map. This category is a many class problem with habitats and dominant species listed as classes. Overall accuracy is excellent at a 100%. Table 7.24 shows the error matrices for the layers chosen for field analysis. Table A is the chosen layers from the field assessment and they are also the most accurate according to the quantitative measures.

Input Features	Classifier	Distribution of habitats[a]			Comment
		PH	MG	BG	
ANOVA	AdaBoost	↑	↑	↓	MG dominant.
	RF	□	↑	↓	BS under-represented.
	ERF	↑	↑	↓	BS under-represented.
	SVM rbf	□	↑	O	BS absent.
	SVM linear	↑	↑	↓	BS under-represented.
EODHaM	AdaBoost	↓	↑	↓	MG dominant.
	RF	□	↑	O	BS absent.
	ERF	□	□	□	Chosen for field assessment.
	SVM rbf	↓	↑	O	BS absent.
	SVM linear	↓	↑	↓	MG dominant.
Images	AdaBoost	↑	↓	↑	Mixing of PH and BG.
	RF	□	↑	O	BS absent.
	ERF	□	□	□	Chosen for field assessment.
	SVM rbf	↓	↑	O	BS absent.
	SVM linear	↓	↑	O	BS absent.
Uncorrelated	AdaBoost	↑	↓	O	PH dominant.
	RF	□	↑	O	BS absent.
	ERF	□	□	□	Chosen for field assessment.
	SVM rbf	↑	↑	O	BS absent.
	SVM linear	□	↑	↓	MG dominant.
Random Forest	AdaBoost	□	↑	O	BS absent.
	RF	□	↑	O	BS absent.
	ERF	□	↑	O	BS absent.
	SVM rbf	□	↑	O	BS absent.
	SVM linear	□	↑	O	BS absent.

Interpretation Keys: ↑ Over-representation; ↓ Under-representation; □ Correct representation; O Absent; ✖ Difficult to comment

[a] Habitat Keys: PH = Pioneer Heath; MG = Maritime Grassland; BG = Bare Ground

Figure 7.17: Visual comparison of all output classifiers. Chosen layers for field assessment highlighted in grey.

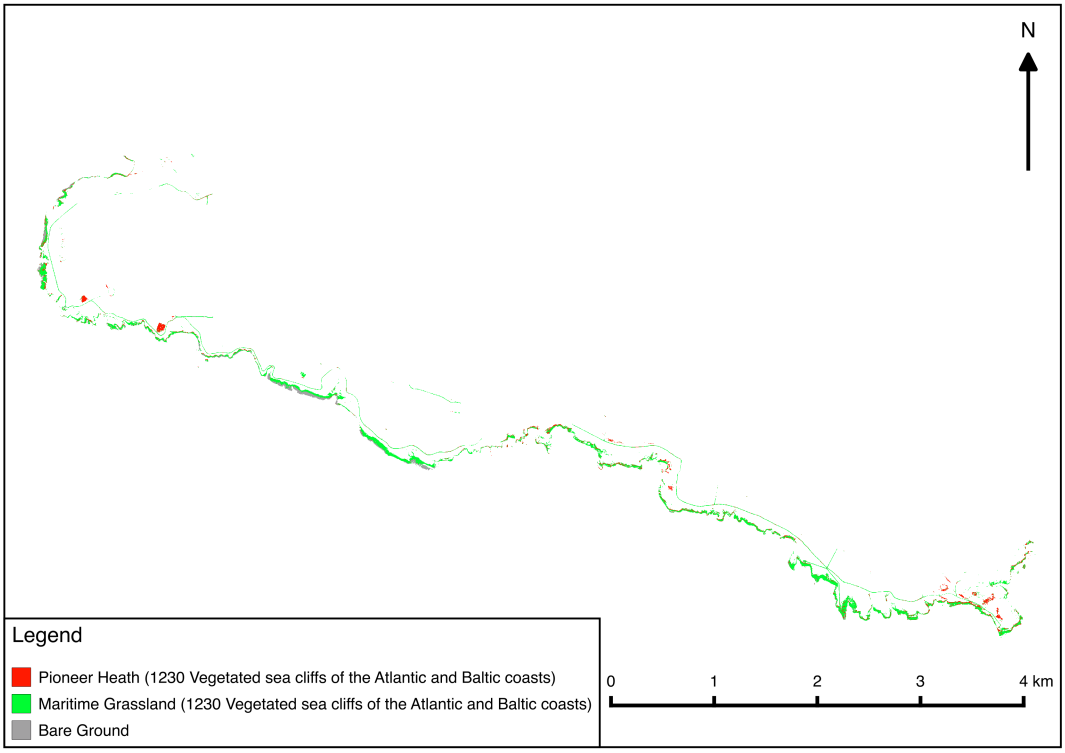

Figure 7.18: Bare ground map of Castlemartin. The bare ground layer was created using the Images and slope as independent variables and the ERF algorithm.

A: Input Features = Images; Algorithm = ERF; Overall Accuracy = 100%; Kappa Coefficient = 1					
	Pioneer Heath	Maritime Grassland	Bare Ground	Sum	Users Accuracy (%)
Pioneer Heath	**5**	0	0	5	100
Maritime Grassland	0	**7**	0	7	100
Bare Ground	0	0	**2**	2	100
Sum	5	7	2	14	
Producers Accuracy (%)	100	100	100		

B: Input Features = EODHaM; Algorithm = ERF; Overall Accuracy = 21.4%; Kappa Coefficient = -0.27					
	Pioneer Heath	Maritime Grassland	Bare Ground	Sum	Users Accuracy (%)
Pioneer Heath	**1**	4	0	5	20
Maritime Grassland	2	**2**	3	7	28.6
Bare Ground	1	1	**0**	2	0
Sum	4	7	3	14	
Producers Accuracy (%)	25	28.6	0		

C: Input Features = Uncorrelated; Algorithm = ERF; Overall Accuracy = 35.7%; Kappa Coefficient = 0.15					
	Pioneer Heath	Maritime Grassland	Bare Ground	Sum	Users Accuracy (%)
Pioneer Heath	**1**	4	0	7	20
Maritime Grassland	0	**4**	3	5	57.1
Bare Ground	1	1	**0**	2	0
Sum	2	9	3	14	
Producers Accuracy (%)	50	44.4	0		

Table 7.24: Error matrices of all layers chosen for field analysis. A is the error matrix for Figure .

Short Species Rich Limestone Grassland Category

Table 7.25: Independent variables selected from different methods as inputs for running machine learning algorithms for the Limestone grassland species rich within the limestone grassland mask at Castlemartin in order to determine condition (listed in order of variable importance for ANOVA and Random Forest; Uncorrelated only had 13 features). For more information on layer naming convention, see Table 4.6 in Chapter 4.

ANOVA	Random Forest	Uncorrelated
July Panchromatic Band	peak SRGB	Slope
peak Datt1	peak SRRENIR2	peak CVI
peak Maccioni	peak SRRB	peak DiffNIR
peak SRYB	post mNDVI	peakpost DiffNDVI
post SRYG	July Panchromatic Band	peak SRBY
post SRGY	post SRCRE	peak SRCR
peak SRBY	peak NPCI	peak SRGB
post SRPanY	post SRRENIR2	peak SRRER
post Datt6	post SRCY	post DDn
peak DDn	post SRNIR1NIR2	post SRNIR2NIR1
September Yellow Band	peak ND900/680	post SRRC
July Red Edge Band	post SRGNIR2	July Panchromatic Band
post SRPanG	peak SRYC	September Panchromatic Band
post SRNIR2Y	post SRRG	
September Green Band	Slope	
post SRREY	peak NormG	
post SRYPan	peak DiffNIR	
post SRNIR1Y	post IPVI	
post SRPanB	post NGRDI	
post NPCI	post SRCPan	

Table 7.25 shows the results from the independent variable selection analysis. There is an even selection between peak and post variables which means that the seasonal aspects is once again important for separation. It is evident that capturing seasonality is important for many, if not all categories for class separation, as predicted.

Figure 7.20 shows the chosen layer for the final map for this category. This category is a many class problem with habitats and dominant species listed as classes. Overall accuracy is at 66.7%, however the kappa coefficient is very low suggesting that the result of this classification is no better than random guessing. Table 7.26 shows the error matrices for the layers chosen for field analysis. Table A is the chosen layers from the field assessment and they are also the most accurate according to the quantitative measures.

Input Features	Classifier	Distribution of habitats[a]	
		SSR	LG
ANOVA	AdaBoost	↑	↓
	RF	↓	↑
	ERF	↓	↑
	SVM rbf	↓	↑
	SVM linear	↑	↓
EODHaM	AdaBoost	↑	↓
	RF	↓	↑
	ERF	□	□
	SVM rbf	↓	↑
	SVM linear	□	□
Images	AdaBoost	↓	↑
	RF	↓	↑
	ERF	↓	↑
	SVM rbf	↓	↑
	SVM linear	□	□
Uncorrelated	AdaBoost	↓	↑
	RF	↓	↑
	ERF	□	□
	SVM rbf	O	↑
	SVM linear	□	□
Random Forest	AdaBoost	↓	↑
	RF	↓	↑
	ERF	↓	↑
	SVM rbf	↓	↑
	SVM linear	↑	↓

Interpretation Keys: ↑ Over-representation; ↓ Under-representation; □ Correct representation; O Absent; ✖ Difficult to comment

[a] Habitat Keys: SSR = Short Species-rich Grassland; LG = Limestone Grassland

Figure 7.19: Visual comparison of all output classifiers. Chosen layers for field assessment highlighted in grey.

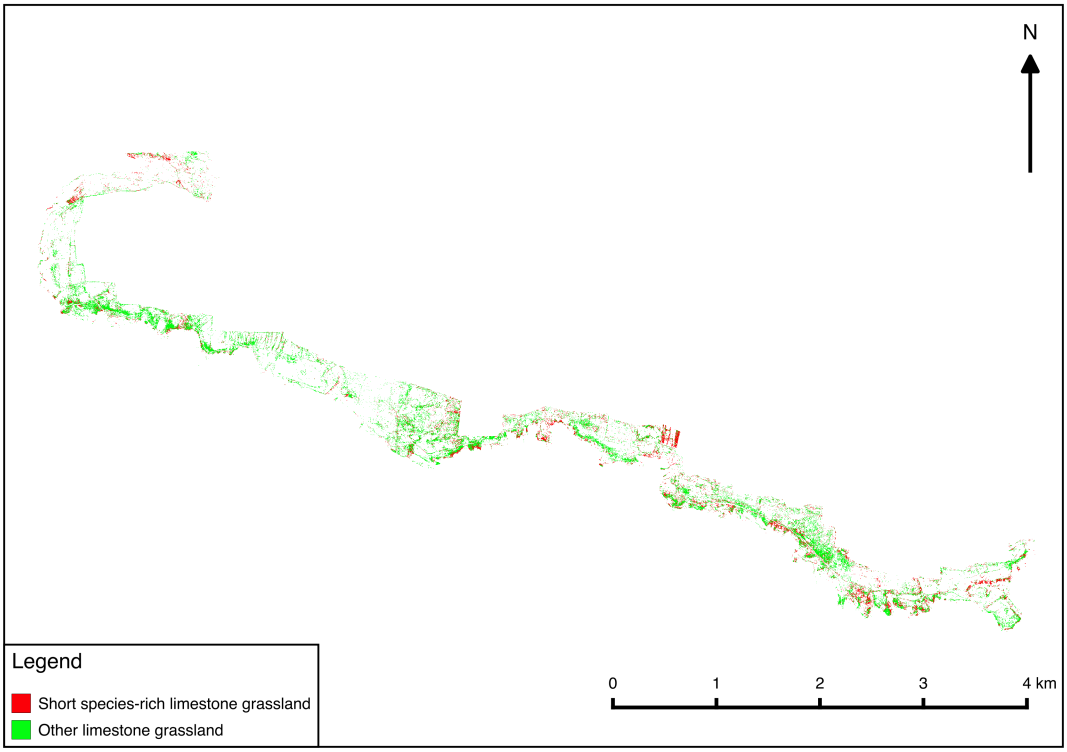

Figure 7.20: Short species rich limestone grassland map of Castlemartin. This layer was created using the Uncorrelated as independent variables and the ERF algorithm.

A: Input Features = Uncorrelated; Algorithm = ERF; Overall Accuracy = 66.7%; Kappa Coefficient = 0.25

	SSR	Limestone Grassland	Sum	Users Accuracy (%)
SSR	**1**	1	2	50
Limestone Grassland	1	**3**	4	75
Sum	2	4	6	
Producers Accuracy (%)	50	75		

B: Input Features = EODHaM; Algorithm = ERF; Overall Accuracy = 50%; Kappa Coefficient = -0.29

	SSR	Limestone Grassland	Sum	Users Accuracy (%)
SSR	**0**	2	2	0
Limestone Grassland	1	**3**	4	75
Sum	1	5	6	
Producers Accuracy (%)	0	60		

D: Input Features = Images; Algorithm = SVC linear; Overall Accuracy = 50%; Kappa Coefficient = 0

	SSR	Limestone Grassland	Sum	Users Accuracy (%)
SSR	**1**	1	2	50
Limestone Grassland	2	**2**	4	50
Sum	3	3	6	
Producers Accuracy (%)	33.3	66.7		

C: Input Features = EODHaM; Algorithm = SVC linear; Overall Accuracy = 66.7%; Kappa Coefficient = 0.25

	SSR	Limestone Grassland	Sum	Users Accuracy (%)
SSR	**1**	1	2	50
Limestone Grassland	1	**3**	4	75
Sum	2	4	6	
Producers Accuracy (%)	50	75		

E: Input Features = Uncorrelated; Algorithm = SVC linear; Overall Accuracy = 66.7%; Kappa Coefficient = 0.25

	SSR	Limestone Grassland	Sum	Users Accuracy (%)
SSR	**1**	1	2	50
Limestone Grassland	1	**3**	4	75
Sum	2	4	6	
Producers Accuracy (%)	50	75		

Table 7.26: Error matrices of all layers chosen for field analysis. A is the error matrix for Figure 7.20.

7.4.3 Final Annex I Habitat Maps

Overall Accuracy = 83.8%; Kappa Coefficient = 0.69						
	2170	2120	2130	2190	Sum	Users Accuracy (%)
2170	**3**	0	4	4	11	27.3
2120	0	**1**	0	0	1	100
2130	0	0	**35**	5	40	87.5
2190	0	0	8	**70**	78	89.7
Sum	3	1	47	79	130	
Producers Accuracy (%)	100	100	74.5	88.6		

Table 7.27: Accuracy Final Annex I habitat map for Kenfig.

Overall Accuracy = 84.8%; Kappa Coefficient = 0.62					
	1230	6210	4030	Sum	Users Accuracy (%)
1230	**45**	4	1	50	90
6210	5	**6**	0	11	54.5
4030	0	0	**5**	5	100
Sum	50	10	6	66	
Producers Accuracy (%)	90	60	83.3		

Table 7.28: Accuracy Final Annex I habitat map for Kenfig.

7.5 Discussion

There are several aspects to this method that requires discussion. Two of the main components, which were explored in this chapter are the choice of independent variables and algorithm for classification. The accuracy of the final maps and the chosen methods of validation will also be discussed.

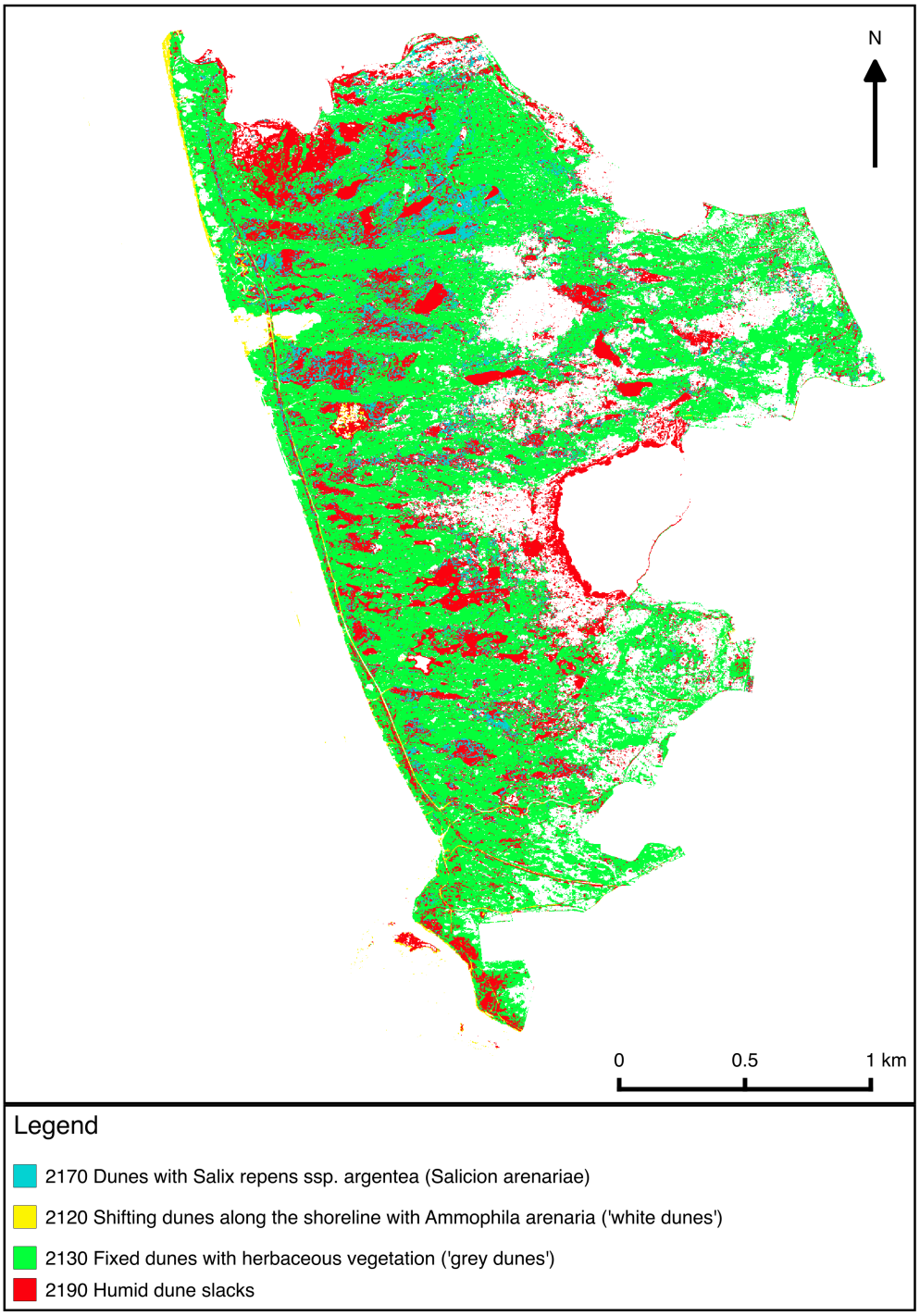

Figure 7.21: Final Annex I habitat map for Kenfig.

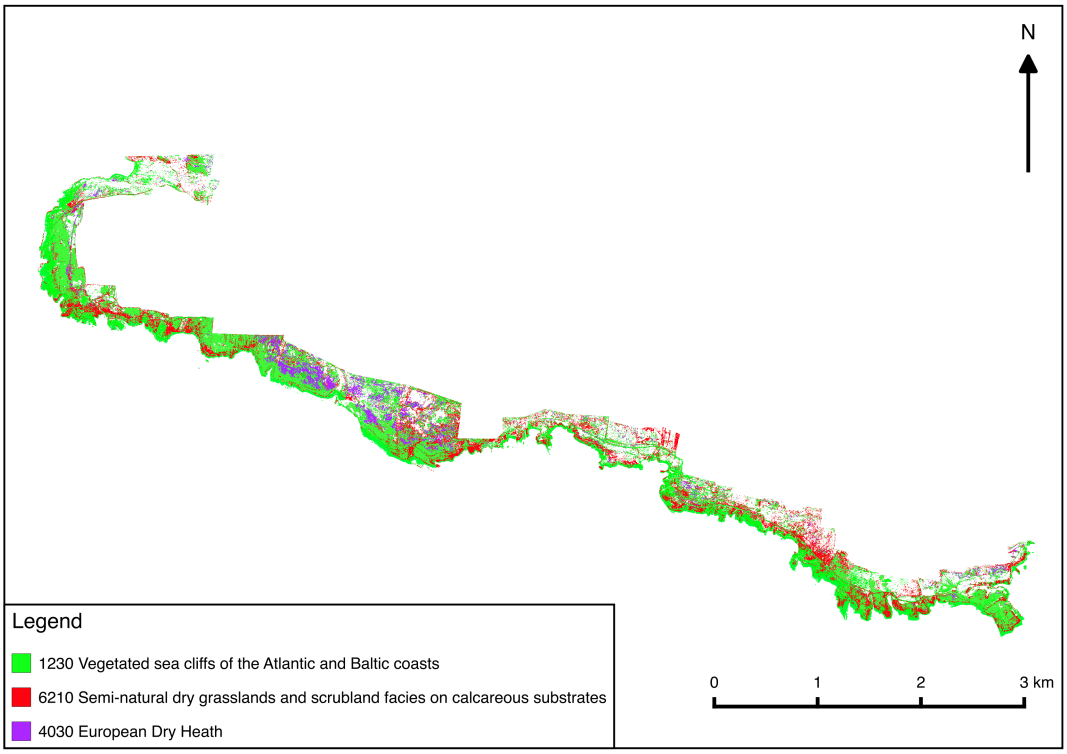

Figure 7.22: Final Annex I habitat map for Castlemartin.

7.5.1 Independent Variables

The choice of independent variables for predicting the classification algorithms is particularly important as they can affect the efficacy of algorithms to perform accurately. Although there were 5 scenarios chosen, only 3 were based on statistical methodologies and will be discussed in this section. The other 2 scenarios had fixed independent variables and did not vary in choice of variable. The variables for the statistical scenarios were chosen based on the training data and the focus on this section is the choice of feature not the choice of statistical method. That will be discussed in the next section.

Table 7.29 shows the most popular variables chosen by all three scenarios for all classes and the number of times they were selected. An interesting observation is the selection of image bands as stand alone variables with the Panchromatic, Green and Red Edge bands featuring high in selection. The Coastal band also features high for Kenfig that is encouraging as that band is an additional feature in comparison with many other optical sensors, and represents the benefit of increased spectral resolution (Digital Globe, 2009). The inclusion of the Panchromatic band as a variable is particularly interesting as its wide spectral width refers to textural information within vegetation communities and therefore explains its inclusion as a popular independent variable (Agera et al., 2008; Pacificia et al., 2009). Simple ratios are also selected often, particularly for Castlemartin which suggests that there is enough variance in the image bands to provide high separability between classes. Contextual information such as slope are also popular which was expected, particularly at Kenfig, where the difference in slope is the key difference between two of the main Annex I habitats.

As for vegetation indices, there are not many that feature in Table 7.29, and some of the most influential indices in the literature like NDVI are not selected at all. The problems with NDVI are well documented (Price, 1993), such as the saturation problem in dense

Table 7.29: Most popular variables chosen by all 3 statistical methods for individual sites and both.

Both Sites	Total	Kenfig Only	Total	Castlemartin Only	Total
Panchromatic	24	Slope	8	Panchromatic	16
CVI	21	Green	7	CVI	14
Slope	17	Datt1	7	SRNIR2NIR1	10
Green	16	Panchromatic	6	Red Edge	10
DDn	14	IPVI	6	SRBR	10
Red Edge	13	SRYB	6	Slope	9
Datt1	13	SRRG	5	DDn	9
DiffNIR	13	SRYC	5	Green	9
SRNIR2NIR1	13	I	5	DiffNIR	8
SRYB	12	DDn	5	SRGB	7
SRBR	12	mSR	5	SRRC	7
SRGB	10	DiffNIR	5	SRBY	6
SRYC	10	Coastal	5	SRYB	6
IPVI	10	SRPanB	5	Datt1	6
DiffNDVI	10	SRNIR1NIR2	5	DiffNDVI	6
SRNIR1NIR2	10	CCCI	4	SRRB	6
SRRC	10	DiffNDVI	4	SRREB	6
SRRG	9	SRPanG	4	NGRDI	5
SRRB	9	CVI	4	SRYG	5
Datt6	8	Datt6	4	SRYC	5

vegetation (Huete et al., 1997), and it should not be a surprise that there are better vegetation indices available. For example CVI, which interacts with chlorophyll content of vegetation, features highly and does not have the same issues as NDVI (Hunt Jr. et al., 2013). Difference indices are also popular (DiffNIR and DiffNDVI), which shows that the breadth of information collected in the NIR part of the spectrum is key for separability of vegetation communities which is expected. The seasonal information captured in DiffNDVI is also important as it captures some of the different seasonal cycles experienced by different habitats and uses that for separability.

To find out which image bands were the most significant either as an individual variable or within an index calculation, Table 7.30 shows the total number of times each band was selected for each site. Although the Green, Panchromatic and Red Edge bands are

popular as stand alone features, their popularity in index calculations that were chosen is more varied. It is interesting that the Red band is in fact the most popular image band to be chosen within index calculation. The Panchromatic does not perform so well when combined with other sources of information in an index.

Table 7.30: Most popular image bands chosen by all 3 statistical methods for individual sites.

Image Band	Kenfig	Castlemartin
Red	88	117
Green	83	105
NIR2	55	73
Red Edge	47	71
NIR1	46	68
Blue	45	61
Coastal	43	46
Panchromatic	41	46
Yellow	26	41

One other consideration here is the choice of index in terms of seasonality. The ratio of peak versus post is 330/195 and although indices that represent peak flush in the summer were chosen more often, the fact that most approaches choose a mix of both seasons as independent variables cannot be overlooked. It is expected that the summer image, where vegetation is in flush, is necessary to distinguish between habitats, particularly grassland communities at Castlemartin, but classes such as bracken would have been particularly difficult to separate if the autumn image was not present. The time of year of image acquisition is important too, and ecological knowledge as to when certain habitats are most distinguishable from its surroundings should be utilised to ensure maximum efficacy.

7.5.2 Algorithm

Table 7.31 shows which algorithm and independent variables scenario were chosen for each mask in the approach for both sites. Algorithms that were not chosen include AdaBoost, Random Forest and the SVM using the rbf kernel. The same is true for independent variables derived from ANOVA separability analysis and random forest variable importance. All other independent variables and algorithms proved effective. In terms of independent variables, one of the assumptions of ANOVA is that all data are normally distributed, and so far, all statistical methods that require the Gaussian distribution assumption have not worked well due to the know bias in the training data. It is therefore expected that the separability analysis from this approach does not adequately represent the variance on sites. What is interesting is the absence of the random forest algorithm in selected layers, although, by including the extremely random forest algorithm in analysis, it is not wholly unexpected that it outperformed it's less random counterpart (Geurts et al., 2006).

	Algorithms																			
	AdaBoost					Random Forest					Extremely Random Forest					Support Vector Machine (linear kernel)					Support Vector Machine (rbf kernel)				
Input Features	A	B	I	R	U	A	B	I	R	U	A	B	I	R	U	A	B	I	R	U	A	B	I	R	U
Kenfig																									
Herb Mask											✓														
Slacks Mask													✓												
Sand Mask																				✓					
FDG Mask																			✓						
Castlemartin																									
Vegetation Mask																			✓						
Herb Mask															✓										
Woody Mask													✓												
Grassland Mask																			✓						
Bare Mask													✓												
Limestone Grassland Mask															✓										

Table 7.31: The algorithm and independent variables scenario chosen as the final layer for mapping outputs. A = ANOVA; B = EODHaM; I = Images and Slope; R = Random Forest; U = Uncorrelated.

The importance of the image bands proves that the variance displayed in the raw band alone is sufficient for separation of habitats. This corresponds with the influence of image bands, in particular the Green, Panchromatic and Red Edge bands, in variable selection. The success of the correlation analysis is also not a surprise as it removes highly correlated features and is in line with the assumption that the variance needed to separate classes exists in a small number of independent variables. This method often chose difference indices that emulates the importance of obtaining seasonal information to maximise separability and success of mapping approach. If only one image was available, the efficacy of these approaches would almost certainly of declined. The popularity of the suite of indices preferred by the EODHaM system, which utilised the most influential vegetation indices in the literature can also be explained by ensuring that each index is calculated for each seasonal image.

As mentioned in Section 7.3.1, parameter selection for algorithms was not investigated thoroughly before generating results as it was a time sensitive experiment with respect to the availability of the field support expertise. This limitation is addressed here where a grid search is applied to the algorithms and input features of the chosen layers. Table 7.32 shows the results of the grid search applied to the tree based ensemble algorithm where the number of trees and features where investigated, and the SVM parameters, where the kernel, C and gamma where explored. C is common to all SVM kernels and focuses on the misclassification of training samples against simplicity of the decision surface so a low C value makes a decision surface smooth, while a high C value aims at classifying all training samples correctly. The gamma parameter defines how much influence a single training point has so the larger the gamma value, the closer other examples must be to be affected (scikit learn.org, 2016).

The assumption that a 100 trees was appropriate for running algorithms was close to optimal in most cases as the grid search results returned the same number for most of the

A	Trees	Features
Kenfig		
Herb Mask	100	4
Slacks Mask	100	5
Castlemartin		
Herb Mask	10	2
Woody Mask	100	2
Bare Mask	100	2
SSR Mask	500	4

B	Kernel	C	Gamma
Kenfig			
FDG Mask	sigmoid	100	0.005
Sand Mask	rbf	100	0.01
Castlemartin			
Veg Mask	rbf	10	0.005
Grass Mask	linear	1	0.1

Table 7.32: A: Results of the grid search on tree based algorithms. Parameters are set to Trees = 100 and Features = 2 without grid search function; B: Results of grid search on SVM algorithms. Parameters are run on linear and rbf kernels with C = 1 and gamma = auto without grid search function.

categories. The number of features varies from the set number so a visual comparison of the outputs was carried out. Figure 7.23 shows the final chosen layer with the algorithm run with the grid search outputs in comparison with the final result. The differences visually are hard to find, however a comparison of the error matrix and overall accuracy tells a different story. The overall accuracy for the final result was 81.7% while the overall accuracy for the output from the grid search result is 83.4%. The differences are marginal however, the fact that they are similar visually and produce a better quantitative accuracy means that a grid search should be added to the overall processing workflow. The visual comparison of all outputs produce the same result even for the SVM outputs as the parameters returned from the grid search vary a lot. It is interesting that the rbf kernel is deemed as the best parameter for two of the categories as these layers did not perform well without parameter tuning. This shows, as stated in the literature that the SVM is indeed sensitive to parameter estimation and that the rbf kernel is capable of performing much better when this is taken into consideration. Figure 7.24 shows an updated processing workflow which is recommended.

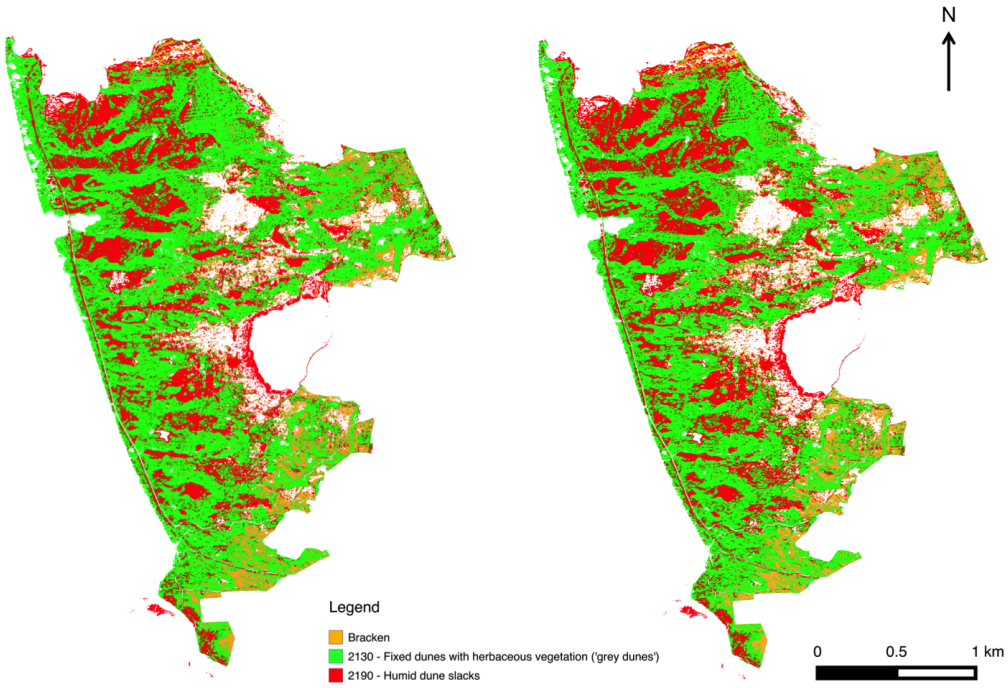

A: Input Features = EODHaM; Algorithm = ERF; Overall Accuracy = 81.7%; Kappa Coefficient = 0.75

	Bracken	2190 Slacks	2130 FDG	Other	Sum	Users Accuracy (%)
Bracken	**28**	0	6	2	36	77.7
2190 Slacks	0	**70**	8	5	83	84.3
2130 FDG	8	5	**35**	4	52	67.3
Other	0	5	5	**81**	91	89
Sum	36	80	54	92	262	
Producers Accuracy (%)	77.7	87.5	64.8	88		

B: Input Features = EODHaM; Algorithm = ERF; Overall Accuracy = 83.4%; Kappa Coefficient = 0.77

	Bracken	2190 Slacks	2130 FDG	Other	Sum	Users Accuracy (%)
Bracken	**31**	2	3	0	36	86.1
2190 Slacks	1	**72**	8	2	83	86.8
2130 FDG	8	6	**35**	3	52	67.3
Other	0	5	5	**81**	91	89
Sum	36	80	54	92	262	
Producers Accuracy (%)	77.5	84.7	68.6	94.2		

Figure 7.23: A comparison between (A) the herbaceous result from Kenfig without the grid search applied to algorithm and (B) with the grid search.

7.5.3 Accuracy

When validating maps created from remotely sensed methods, the traditional method of generating an error matrix, usually with point data, only captures measures of class accuracy and does not capture the spatial distribution of error (Foody, 2002). The purpose of this research was to generate habitat extent maps, and even though it is important to classify each point collected on the ground correctly, the ability of a method to map the spatial extent of the habitat is vital. The chosen approach to combat this validation issue

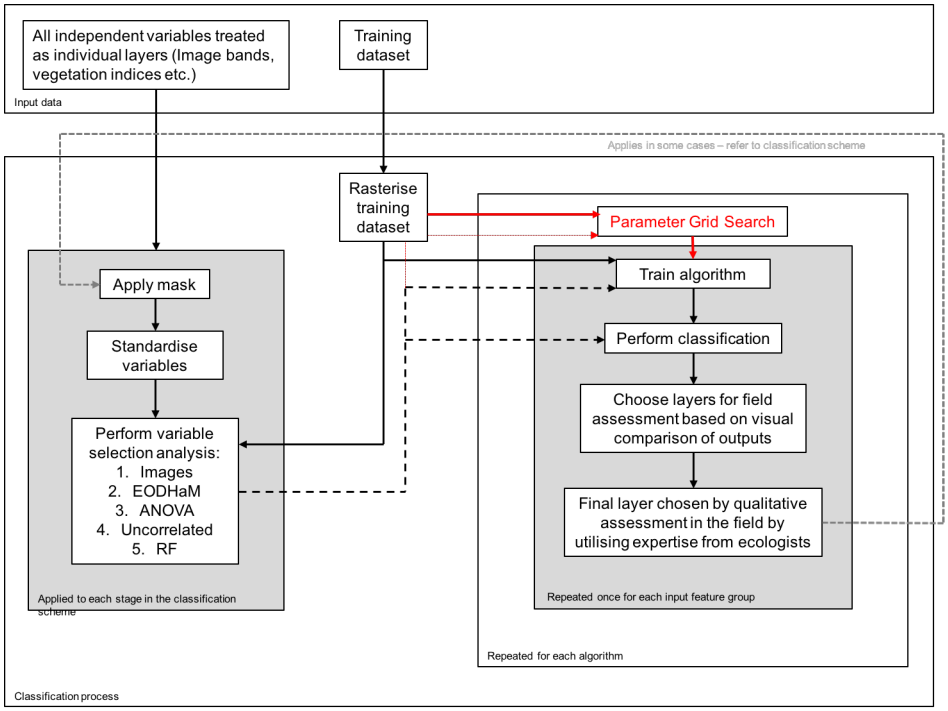

Figure 7.24: Updated processing workflow with the grid search feature included.

was to generate multiple layers for the same classes using different independent variables and algorithms, and ask the ecologists to choose layers based on spatial extent in the field. They do not know which one was the most accurate, and one of the most interesting observations from this exercise was that the chosen representative layer was not always the one with the highest overall accuracies. Figure 7.25 show overall accuracies as defined by the traditional error matrix method and, although the difference between accuracies are minimal, usually down to 2-3 points being misclassified, it is clear that the chosen layer is not the most accurate. However, the small differences from one classification approach to another may not be statistically significant. This exercise proved that there are problems with the way products from remotely sensed data are validated and that a subjective, visual validation method can also provide useful information.

As an example of this exercise, Figure 7.26 shows slack boundaries collected using a hand-held GPS device on the ground. Figure 7.27 shows the results of zonal statistics

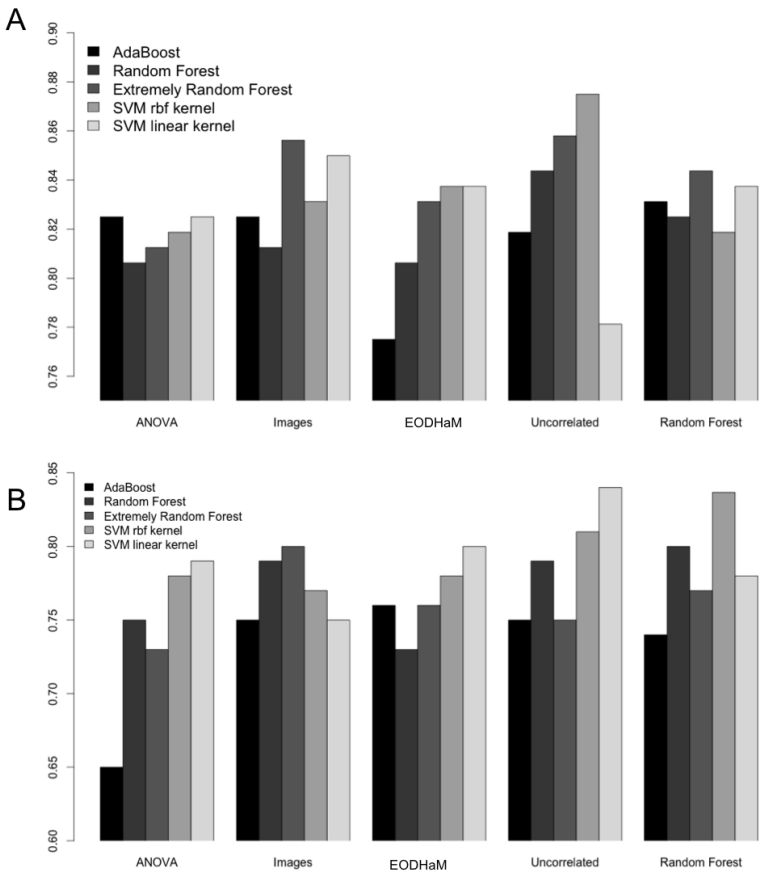

Figure 7.25: Bar charts of accuracy for all output layers for A: the herb category at Kenfig where the chosen layer was EODHaM independent variables with the ERF algorithm; and B: the woody category for Castlemartin where the chosen layer was Images independent variables with the ERF algorithm.

performed on the layers chosen for field analysis for the herb category at Kenfig. As can be seen, this graph represent the main reason behind the chosen layer as it classified more pixels as slack than any other layer even though quantitative analyses showed more accurate layers. This is also true of the EODHaM system result which was the poorest layer at classifying these areas of slack correctly. Figure 7.28 shows the difference between the chosen algorithm in comparison with the algorithm performed with a grid search and shows very little difference in this exercise. Again, it is very likely that the small differences seen in overall accuracies between layers are not statistically significant. This proves that there is merit in a visual, qualitative analysis and the benefits of multiple iterations in a mapping approach, that involves the ecologist and site specialists in the validation process. This guarantees a better understanding of the approach from the end user (the ecologists) and allows better confidence in the final map ensuring its use operationally in future monitoring.

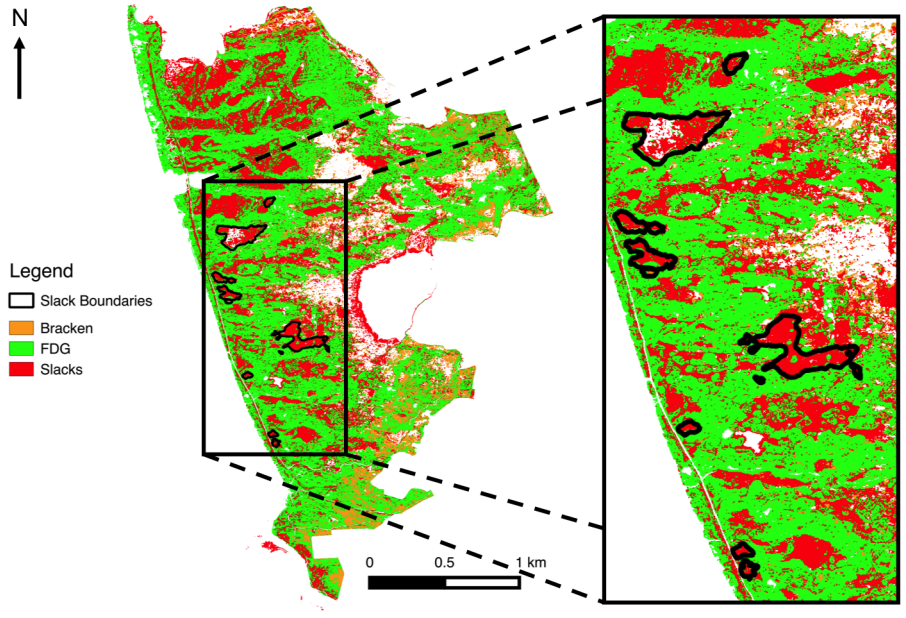

Figure 7.26: Location of the slack boundaries collected using a hand-held GPS device.

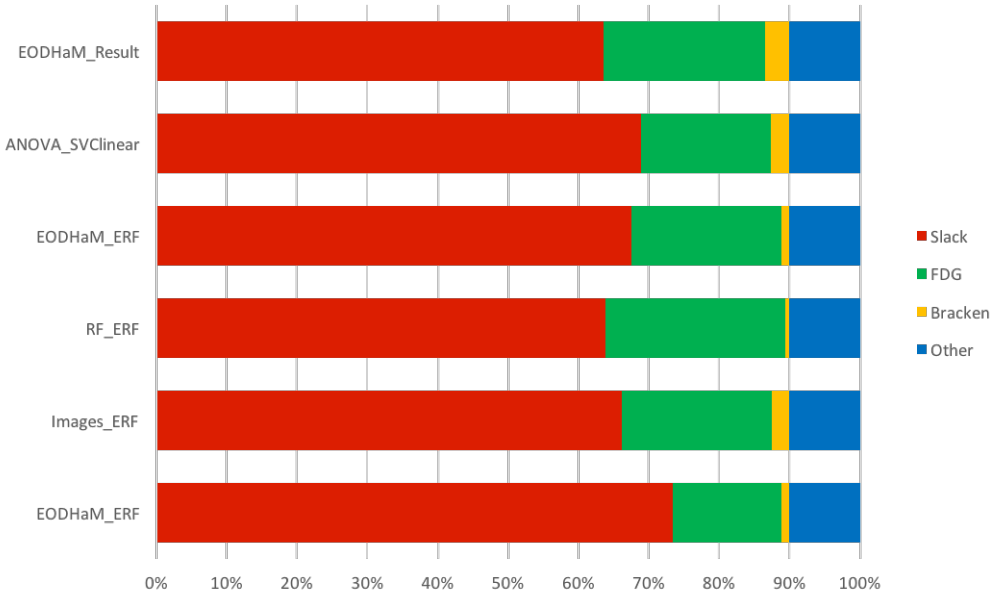

Figure 7.27: Class percentage of pixels present within the slack boundaries as seen in Figure 7.26.

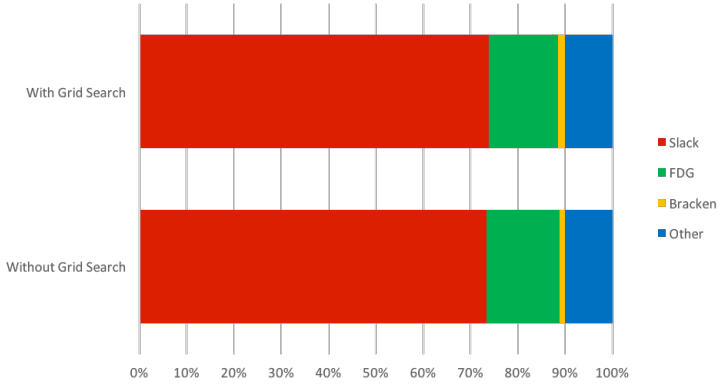

Figure 7.28: Percentage of pixels classified correctly within the slack boundaries as seen in Figure 7.26 for grid search experiment.

7.5.4 Habitat Condition

The ability to map dominant species as a proxy to determine condition was also explored, even though training data for some of the classes were not sufficient due to the small distribution of the classes on sites. Figure 7.29 shows notes taken on the chosen slacks mask at Kenfig and it is evident that the algorithm was successful in separating several classes including succesionally young slack, *carex nigra* and *eleocharis* dominant and the distinction between dunes with *salix repens* and mature slack where the difference is due to wetness of the extent. Other classes such as *Juncus* were under-represented and were most often confused with *calamagrostis* dominant vegetation, which can be explained by the absence of training points for a certain species of *Juncus (subnodulosus)*. The accuracy was stated as low, but there are very few points to validate the class. This is another example where the error matrix is not sufficient when validating maps that represent sparse or rare habitats on sites.

Another example of where maps of certain types of habitats or dominant species can be used as a proxy for condition is the short species rich limestone grassland map at Castlemartin. Figure 7.30 shows the classification or chosen layer and the distribution of point data for this class across the site. The class is rare and is seen in areas near the coastline. Again, overall accuracies are low from the point data, but the general distribution of the class on site matches the map. This result can not only provide site managers with an indication of spatial extent of a class that is not mapped to this detail, but also direct them to areas for monitoring a certain habitat's condition that is not known.

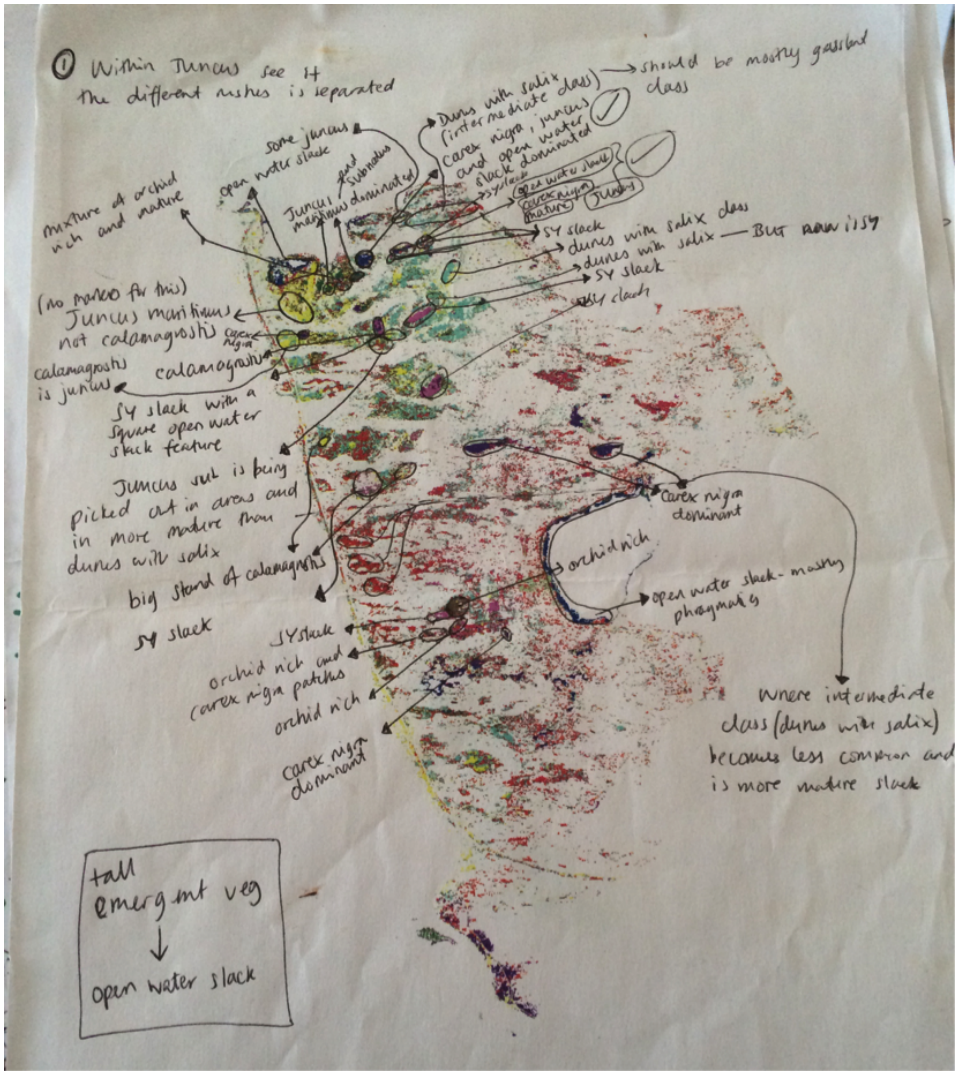

Figure 7.29: Notes taken in the field on the accuracy of the chosen layer for distribution of dominant species within the humid dune slack habitat mask at Kenfig.

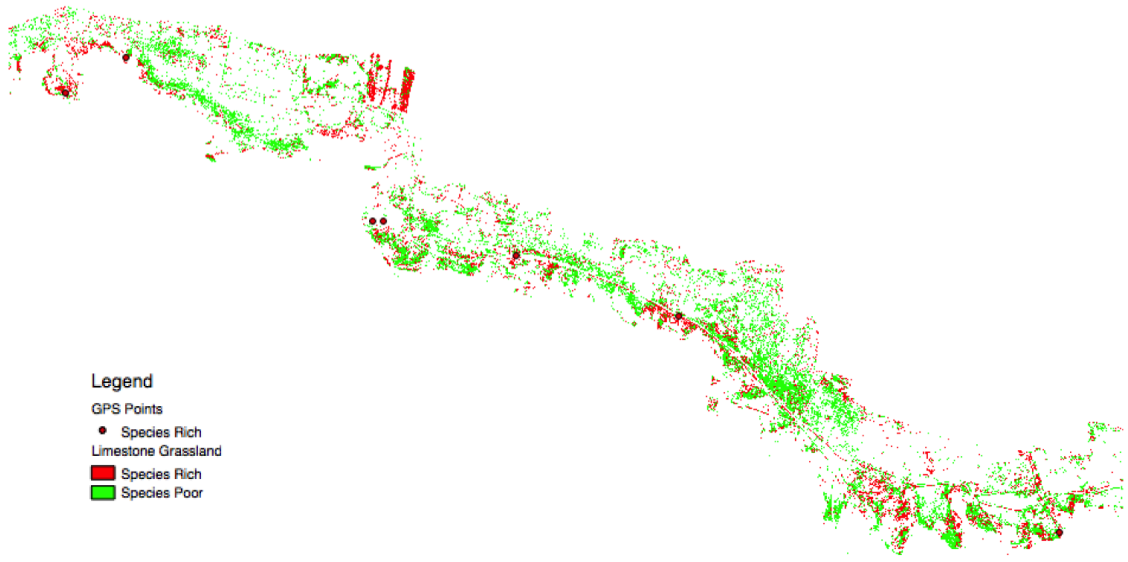

Figure 7.30: A section of the short species rich limestone grassland mask with GPS points for that class that show correlation with actual habitat location and map distributions.

7.6 Conclusions

Machine learning algorithms are more effective than thresholding even if training data is biased, and scarce for certain classes. They are also less time consuming during processing allowing more iterations of the approach.

There is enough variance and information in the image bands to successfully separate habitats and the calculation of multiple indices does not add significant value to independent variable selection.

Seasonal information is necessary, where a peak flush image is absolutely key with at least one additional image, either in the spring or autumn.

Multiple iterations is key to determine which layer best emulates the distribution of habitats on site in base mapping exercises.

Not one algorithm fits all and it is key that several ones are tested, which is quick with the scripts written to implement the approach in this chapter (Kohavi, 1996; Chan and Paelinckx, 2008).

Accuracy assessments that are traditionally done for remotely sensed products are not adequate for validation (i.e. overall accuracy and *kappa* values).

Including ecologists in the validation and feedback process enhances understanding of approach and ensures uptake of products for future monitoring activities by the end user.

Mapping of dominant species is possible and the resulting maps can be used as a proxy for habitat condition. These maps are designed to focus condition fieldwork locations in addition to providing approximate extents.

Chapter 8

Change Detection

8.1 Introduction

Previous chapters have explored mapping techniques for developing baseline maps that adequately provide boundaries, extent and in some cases, proxies for condition of Annex I habitats. The next stage is to explore change detection approaches to see if remote sensing can be used for monitoring, which is another important aspect of Article 17 reporting. Evidence is required to prove that habitats continue to exist in favourable condition and have not changed status or decreased in extent. This chapter will provide a brief background on change detection approaches utilising remote sensing, providing examples which were deemed successful and those that are currently used operationally within the environmental monitoring sector. The chosen method for implementation will then be explained and carried out before the results are explored. Unfortunately, only Kenfig had very high resolution data acquired in consequent years after the initial acquisition.

8.2 Background

Mapping approaches provide information of one time period, but policy and decision makers need information on selected Annex I habitats through time. Remote sensing provides consistent, repeatable and frequent data over large areas within a much shorter time-frame than it would take to collect the data with a similar frequency in the field. The scale at which remote sensing data is acquired will not be suitable for mapping and monitoring all habitats, this will depend on the patch-size of the habitat, however, the focus should be on identifying areas where fieldwork is necessary and eliminating areas that do not require field visits as frequently.

8.2.1 Change Detection Methods

Generally, change detection methods can be divided into two broad categories called map-to-map and image-to-image approaches (Singh, 1989). The first approach is the comparison of independently produced classifications and is dependent on the generation of products from remotely sensed data, from different time periods, ideally using the same methods. The second approach simultaneously analyses values of pixels/objects from multi-temporal remote sensing data and utilises several different image processing algorithms and techniques. Advances have been made in recent years in change detection methods utilising objects, however, object based image analysis has not been considered in this research and those methods will not be synthesised here. It is worth noting however, that many studies have stated that pixel based change detection approaches utilising VHR imagery is unsuitable as no textural changes can be identified which is seen as the major advantage of higher resolution imagery in comparison with medium to coarse resolution remote sensing data (Chen et al., 2012).

Map-to-Map Approach

The map-to-map change detection approach, or post-classification change, is the comparison of independently produced thematic maps. The advantages of this technique is that the baseline classification and the change transitions are explicitly known and radiometric normalisation is not necessary as the maps are produced separately (Coppin et al., 2004; Warner et al., 2009). This method is one of the most established and has been applied to maps created from Landsat imagery (El-Kawy et al., 2011; Dingle Robertson and King, 2011) and VHR imagery (Boldt et al., 2012; Demir et al., 2013; Hester et al., 2010). However, map-to-map change detection is limited as the accuracy of the change is compounded in the errors of map production making it a costly and difficult method to adopt (Tewkesbury et al., 2015). Furthermore, input maps may be produced using different algorithms and types of input data resulting in complications identifying real change on the ground from classification inconsistencies (Comber et al., 2004). Obtaining meaningful change results is often difficult and expensive (Lu et al., 2004; Serra et al., 2003), especially as a continuous monitoring approach, and is therefore unsuitable for use in this study.

Image-to-Image Approach

There are several reviews that present exhaustive lists of image-to-image change detection techniques containing many comparison methods (Coppin et al., 2004; Hussain et al., 2013; Lu et al., 2004). Table 8.1 is an overview of the most commonly used of these techniques including any advantages and limitations.

The unit of change detection (pixel or objects) is pivotal and Tewkesbury et al. (2015) states that more research is required to identify optimum approaches for change detection. A direct classification of a complicated data stack is probably the most effective method of identifying semantic changes, but the required training data is extremely difficult to obtain

Table 8.1: Image-to-image change detection techniques.

	Description	Advantages	Limitations	Example Studies
Layer arithmetic	Image radiance or derivative features are numerically compared to identify change	Can be simple to implement	Usually gives little insight into the type of change	Coulter et al. (2011); Dams et al. (2013) Im and Jensen (2005)
Direct classification	A multi-temporal data stack is classified directly identifying both static and dynamic land covers.	Only one classification stage is required. Provides an effective framework to mine a complicated time series. Produces a labelled change map.	Classification training datasets can be difficult to construct, especially for a time series of images.	Chehata et al. (2011); Gao et al. (2012) Schneider (2012)
Transformation	A mathematical transformation to highlight variance between images.	Provides an elegant way to handle high dimensional data.	There is no defined thematic meaning to the results. Change may be difficult to locate and interpret.	Deng et al. (2008); Doxani et al. (2012) Listner and Niemeyer (2011)
Change Vector Analysis	The computation of difference vectors between analysis units giving both the magnitude and direction of change.	Gives insight into the type of change occurring.	In its raw form the change direction and magnitude may be ambiguous.	Bovolo et al. (2012)
Hybrid change detection	The use of multiple comparison methods within a workflow. The most commonly used strategy is a combination of layer arithmetic to identify change and direct classification to label it.	Training data does not have to be collected over radiometrically stable areas.		Bruzzone and Bovolo (2013) Doxani et al. (2012) Xian and Homer (2010)

since the location of change before analysis is unknown (Lu et al., 2004). Advancements in CVA also provide a powerful framework to compare multi-dimensional data but remain largely untested in the literature (Tewkesbury et al., 2015). These comparison methods vary in complexity and the main aim of this chapter is to identify location of change, in the most automated way possible, meaning that most of these approaches are too complex in this instance.

8.3 Methods

The approaches mentioned above, particularly the image-to-image methods focus on change detection with results indicating two classes; change and no change. The dynamics of specific classes are often lost with these methods as no spatial information or description of classes and possible changes are assumed. The policy (EC Habitat's Directive) that this research is focused on is about to proceed into a fourth round of reporting (every 6 years), and instead of producing a new extent map each time and comparing outputs to previous classifications, which is a common change detection method (map-to-map), it would be more cost effective to first detect whether any change has occurred. This section presents a novel change detection method, first described in Thomas (2016), which is an example of a map-to-image approach. Figure 8.1 is a schematic of the method used in this chapter.

8.3.1 Map-to-Image Change Detection

The concept assumes that the spatial extents of the classes of interest are known, and change features can be differentiated from the class using the distribution of pixel/object values that are contained within the class extent. Classes are expected to show normal

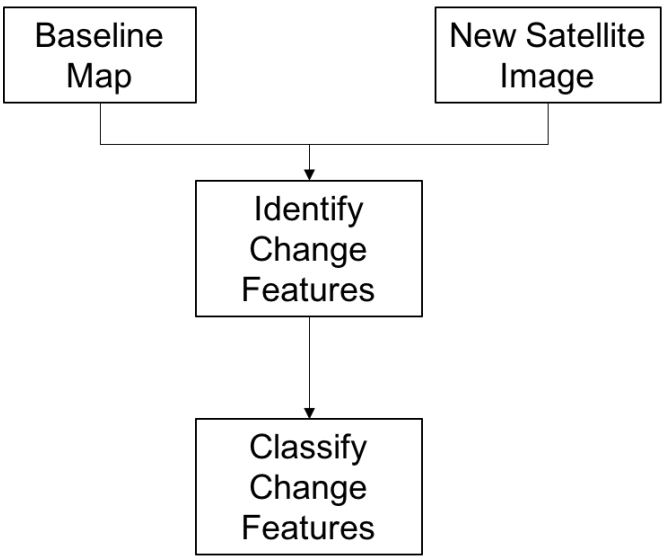

Figure 8.1: Schematic of the method.

distributions and any deviations are identified as change features. There are three assumptions that are fundamental for correctly identifying change:

1. Class values are normally distributed.

2. Object values of the class are separable i.e. majority of values that represent the class are close to the median while values that represent change will not.

3. Change features make up a proportionately smaller component of the class so that change values are found within the normal distribution of a class.

Figure 8.2 shows an example of the assumptions above and in order to separate change features a threshold needs to be established. The method proposes an iterative approach where the normality of the distribution is calculated based upon skewness and kurtosis and is also demonstrated in Figure 8.2. The combination of the lowest skewness and kurtosis values are used to identify the iteration at which the class distribution is most normal (Thomas, 2016).

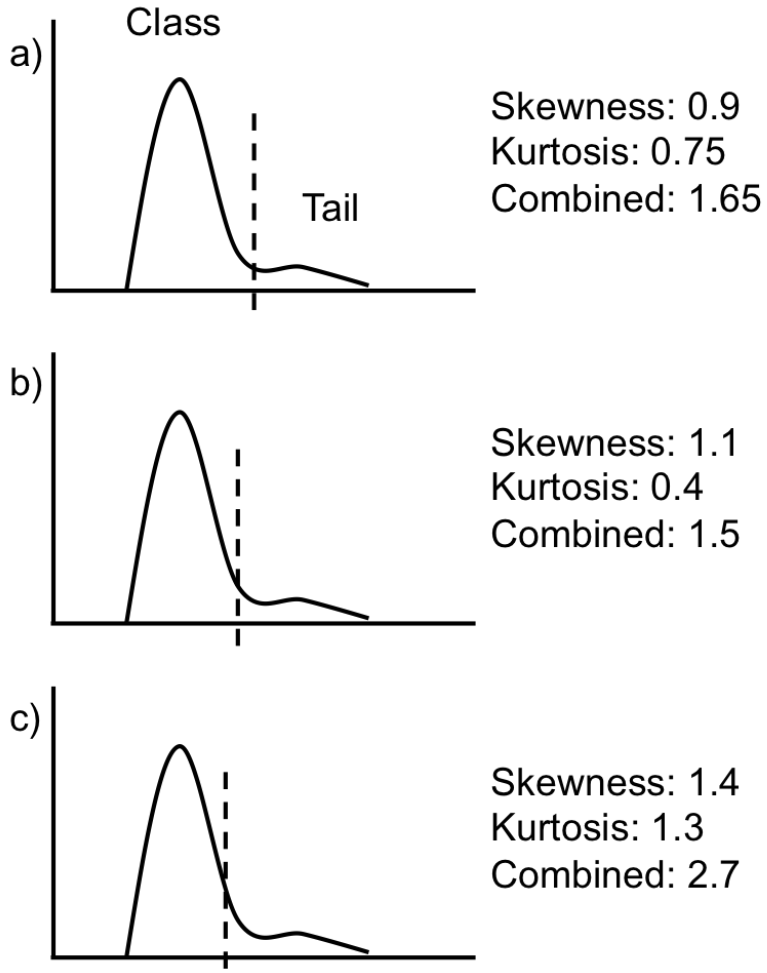

Figure 8.2: The variation in combined skewness and kurtosis with the sub-sampling of the distribution at varying points in the tail. b) demonstrates the lowest combined skewness and kurtosis value over a) or c) and is used to select the threshold to separate change features. Modified from Thomas (2016).

8.3.2 Input Data and Class Selection

The site of interest is Kenfig Burrows SAC. The original map was created from Worldview-2 data collected in 2012 (see Chapter 6 and 7). Another Worldview-2 image was acquired in June 2014 and was pre-processed to the same standards as outlined in Chapter 4. The change class will be vegetated, as sand dune systems should be dynamic in its nature with the movement of bare sand key to several functions within the ecosystem. Kenfig is also a site where several drastic management steps were taken to try and facilitate more movement of sand on the site, so change features should be recognised.

As VHR imagery such as Worldview-2 is relatively expensive, this could affect the cost effectiveness of the monitoring system suggested in this study. The newly launched Sentinel-2 satellites, which are free at the point of use and have the luxury of a huge swath width and a high frequency, are also used to test the approach. Currently, with only Sentinel-2 A launched, the globe is captured every 10 days, but when Sentinel-2 B is launched in early 2017 that frequency will increase to 5 days. In actual fact, as the swath width of the sensor is so large, the whole UK coverage is captured every 2-3 days, depending on cloud cover, which could increase the amount of available optical data over land at much higher resolutions than before. This sensor acquires data in the visible to the near infrared at 10m resolution with 4 red-edge bands and 2 shortwave infrared bands at 20m resolution.

The image used for this chapter was acquired on the 19th of July, 2016 and is downloaded as an orthorectified, top-of-atmosphere product from the ESA Science Hub (ESA, 2016). ESA also provide open source software to process the data, however, the software did not produce optimal results for surface reflectance, and other software for atmospheric correction did not have Sentinel-2 capability at the time of writing. Therefore, a Dark Object Subtraction (DOS) was used using open source software RSGISLib (Bunting et al.,

2014) to normalise the image and emulate a surface reflectance product. To ensure that images overlay properly with the classification the Sentinel-2 image was also warped using GCPs generated from the Worldview-2 image. To implement this the process, the Worldview-2 image was resampled to 10 m, the spatial resolution of the Sentinel-2 image, using a nearest neighbour resampling algorithm.This exercise ensures that images are co-registered to each other, limiting the issues of mis-registration on the output change detection analysis. However, the images are typically mis-registered by a pixel in some areas.

For both images, measures such as vegetation indices were used to try and distinguish change features. The main index was the NDVI, as differences in vegetation cover are the focus of the approach. For Worldview-2, another vegetation index will also be tested, the CVI, as results from Chapter 7 and the literature (Hunt Jr. et al., 2013) suggest that this index is better at separating vegetation from other classes and is less susceptible to saturation. As the change features are evident in the imagery (bare sand vs vegetation), the results will be classified in a post classification stage and error matrices produced based on land cover. Stratified random points are generated for each change layer and are visually inspected for measures of accuracy. There are three types of change which are likely to be classified, which are:

1. Seasonal change.

2. Actual land cover change.

3. Change resulting from error in image corrections.

The type of change that are of interest is actual land cover change although seasonal changes, particularly within slacks are expected due to the fact that they are inundated throughout the winter months and dry out at different rates throughout the summer.

8.3.3 Post Classification

The method so far has only identified potential change and further analysis is required to determine actual change in class. This will be done by implementing the first stage of the EODHaM system but with the thresholds applied to the new imagery. The classification procedure will only be employed on the areas identified as potential change in each of the resulting layers. Seasonal changes are to be expected, particularly in the 2014 image as the slacks are unlikely to have completely dried out at this stage of the year, and is evident in the Worldview-2 image. These are seen as land cover change but are unlikely to be interpreted as habitat change. For accuracy assessment this is dealt with by analysing the results through the error matrices. When validating change detection methods, most studies apply a post classification on outputs to determine whether those areas identified as change are features that have changed on the ground or not, as is proposed in this method. What is missing from the literature is statistical methods of quantifying omission errors when implementing change detection algorithms. It is recognised that the method proposed in this chapter does not tackle the problem of omission error, however, the changes expected at Kenfig (vegetation to bare sand) are visible enough in the imagery for visual inspection.

8.4 Results

8.4.1 Change Detection

This section describes the results from the change detection analysis. Figure 8.3 shows Kenfig from the Worldview-2 image in June 2014 next to the July 2016 image acquired from Sentinel-2. The difference in resolution is clearly visible, especially when focusing

on infrastructure present in the images. A progression of management on site is evident with an extension of the bare sand area in the north west of the site and several of the slacks. Although the resolution of the Sentinel-2 image is lower at 10m the features on site are evident and shows potential for future monitoring applications of broad habitat extent.

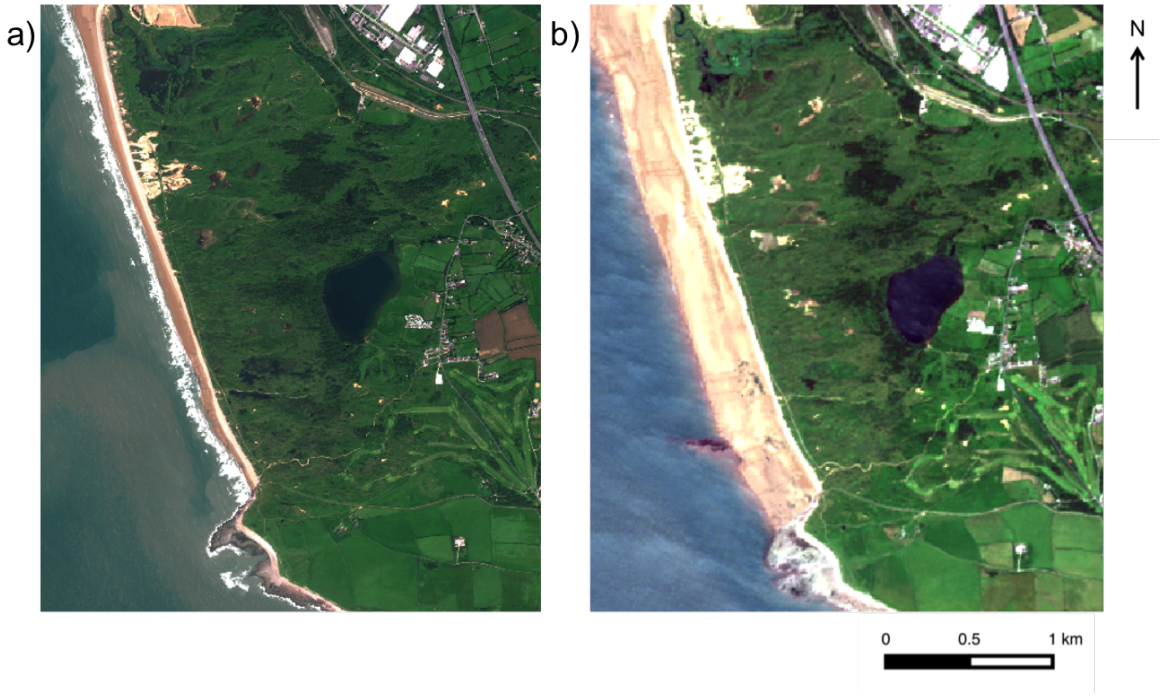

Figure 8.3: The two images used for change detection analysis in this chapter where a) is the June 2014 Worldview-2 image and b) is the July 2016 Sentinel-2 image.

Figure 8.4 shows the results of the method using the NDVI in comparison with the 2012 reference baseline map. The results from the Worldview-2 image appears very noisy especially to the south of the image where a lot of vegetated areas have been classified as change. However, all of the expected bare sand areas and still partially inundated slacks have also been classified as change. There is clearly an overestimation of change areas making it difficult to separate seasonal and actual change on the ground from this result. The Sentinel-2 NDVI result is much more promising with areas of actual change evident. Some changes seen are most likely down to pixel size, for example, some of the

track area are identified as change when in reality, these are a results of artefacts from adjacency effects of lower resolution imagery.

Figure 8.4 also shows the results from using the CVI as opposed to NDVI from the Worldview-2 image. The classified result is a lot less noisy than the NDVI results but there are still many pixels being classified as change distributed across the site giving the appearance of "salt and pepper" effect. However, the boundaries for actual change are much sharper in comparison and it is a lot easier to distinguish between seasonal and actual change.

8.4.2 Thresholding

Figure 8.5 shows the thresholds used for detecting change from each input variable. The threshold difference between the two NDVI results is interesting as the chosen thresholds vary a lot, 0.78 for Worldview-2 and 0.44 for Sentinel-2. The tail of the distribution is much more gradual for Worldview-2 NDVI than it is for Sentinel-2, i.e. there are many more pixels below the respective thresholds for Worldview-2 than there is present for Sentinel-2. This means that nearly 6000 pixels are classified as change from Worldview-2 in comparison to the 3000 pixels for Sentinel-2. This could be due to the resolution of the Sentinel-2 imagery, which also needs to be taken into account. The distribution shown for CVI from Worldview-2 is also interesting as there is a lot more activity in the tail in comparison with NDVI, which shows a higher sensitivity to those pixels that represent change. The threshold value is 3.8 and about 4000 pixels have been classified as change.

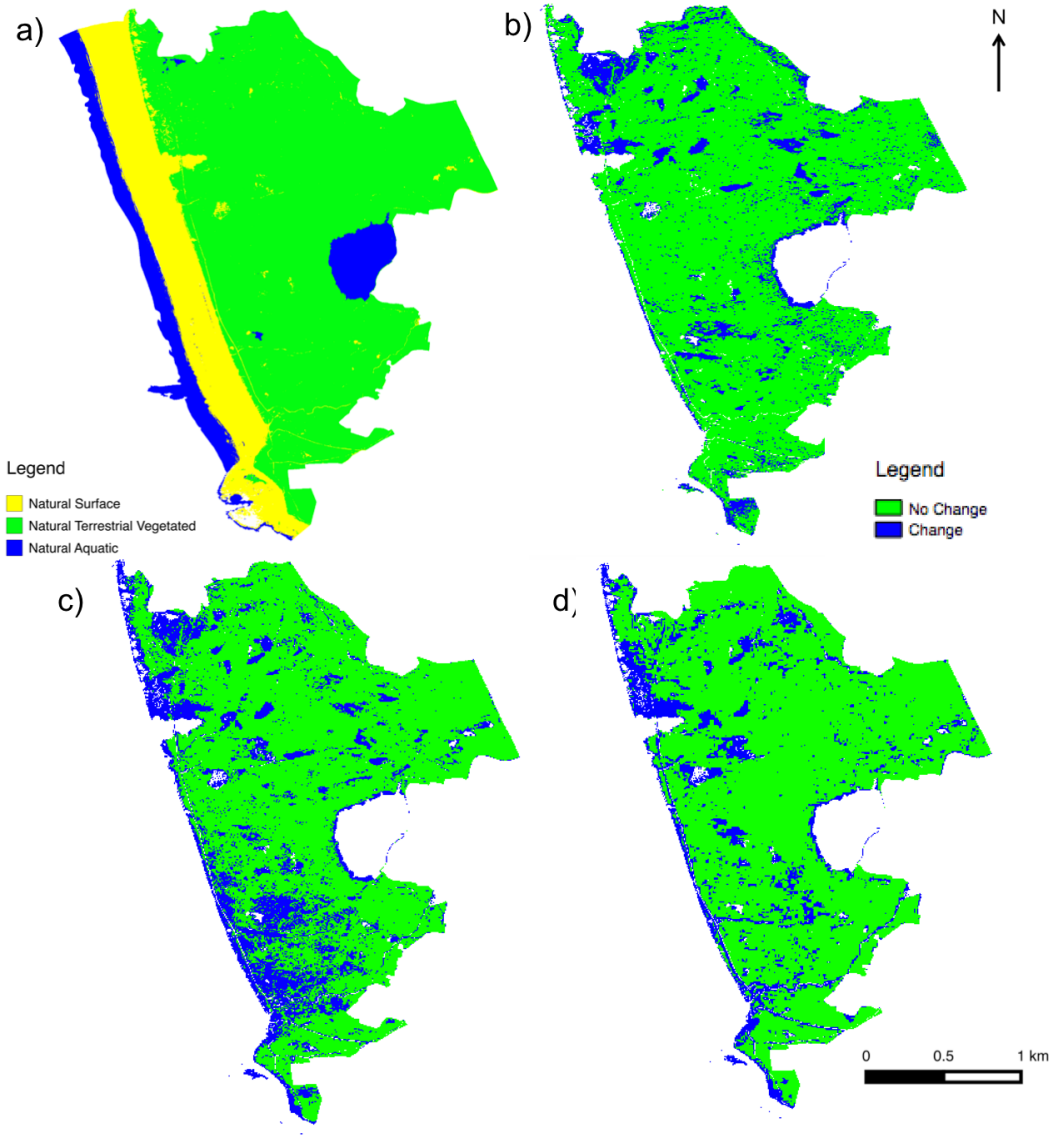

Figure 8.4: Results from the change detection analysis where a) is reference map from 2012 (results from Chapter 6) b) is using CVI from the June 2014 Worldview-2 image; c) is using NDVI from the June 2014 Worldview-2 image and d) is using NDVI from the July 2016 Sentinel-2 image.

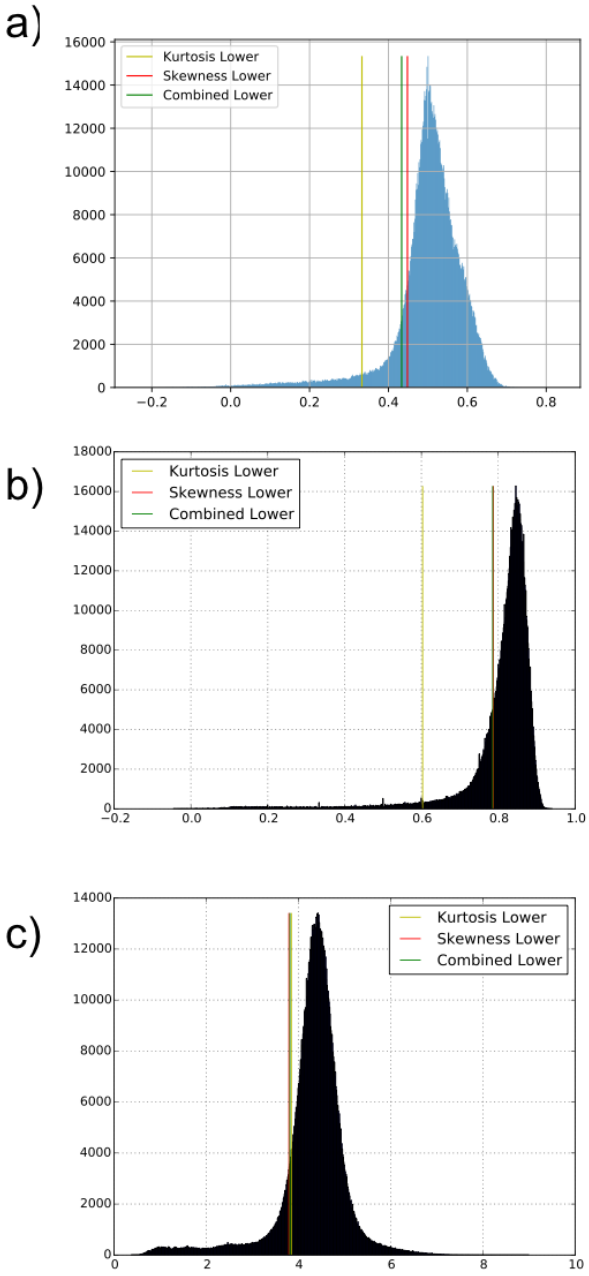

Figure 8.5: Results from the threshold determination for each classification of change detection where a) is NDVI from Sentinel-2, b) is NDVI from Worldview-2, and c) is CVI from Worldview-2.

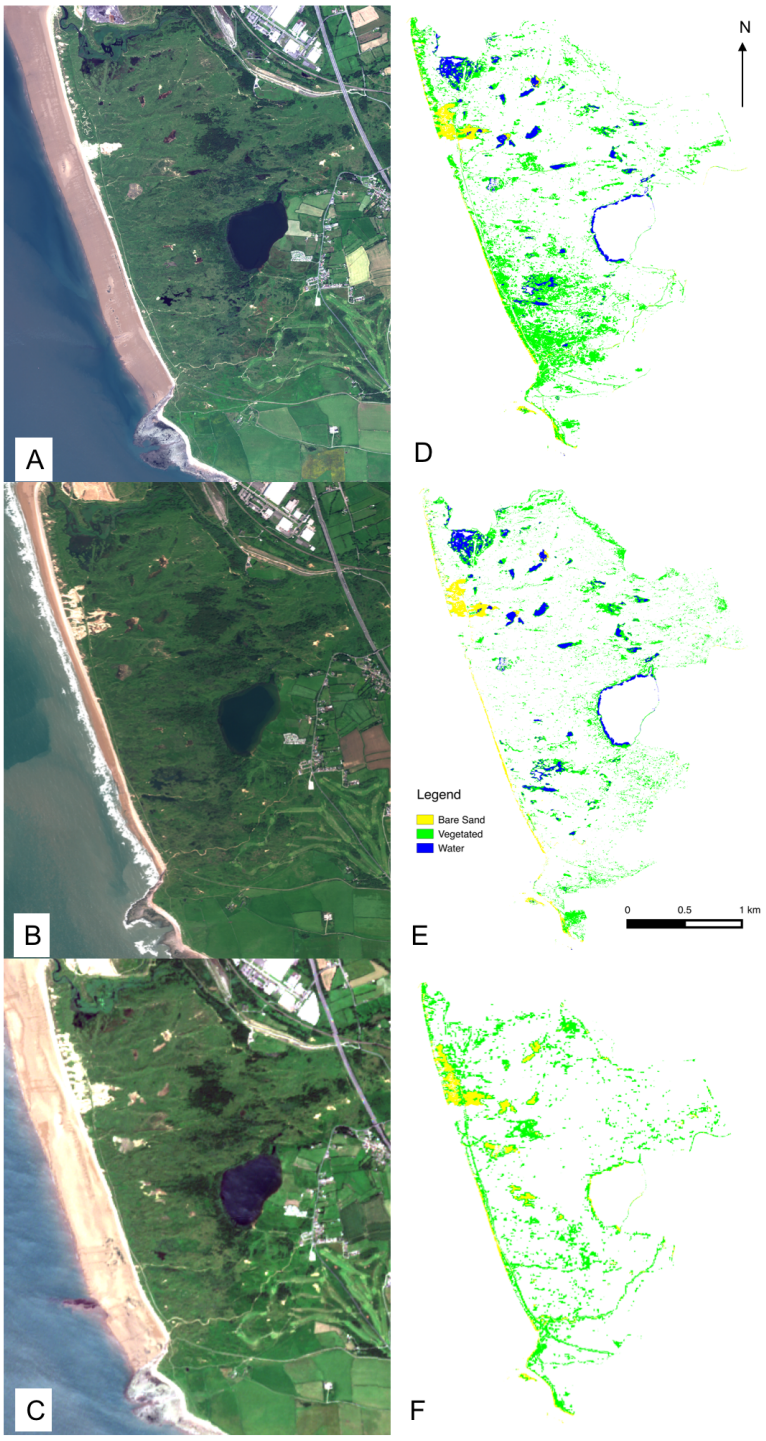

Figure 8.6: Results from the post classification where A is Worldview-2 image from 2012, B is Worldview-2 image from 2014, C is Sentinel-2 image from 2016, D is change map from Worldview-2 NDVI 2014, E is change map from CVI from Worldview-2 2014, and F is change map from NDVI from Sentinel-2 2016.

8.4.3 Post Classification

The exact same thresholds from Chapter 6 are used to classify the Worldview-2 images and an initial visual inspection show that these are effective (Figure 8.6). For Sentinel-2, thresholds needed to be changed as there is no coastal band to delineate bare sand areas. NDVI and NDWI only are used. As expected, no new water areas are classified in the Sentinel-2 change layer.

A) 2014 NDVI Change: Overall Accuracy = 80.7%; Kappa Coefficient = 0.71					
	Sand	Vegetated	Water	Sum	Users Accuracy (%)
Sand	**39**	11	o	50	78
Vegetated	4	**39**	7	50	78
Water	3	4	**43**	50	86
Sum	46	54	50	150	
Producers Accuracy (%)	84.8	72.2	86		

B) 2014 CVI Change: Overall Accuracy = 90%; Kappa Coefficient = 0.85					
	Sand	Vegetated	Water	Sum	Users Accuracy (%)
Sand	**45**	5	o	50	90
Vegetated	0	**44**	6	50	88
Water	4	0	**46**	50	92
Sum	49	49	52	150	
Producers Accuracy (%)	91.8	89.9	88.5		

C) 2016 NDVI Change: Overall Accuracy = 94%; Kappa Coefficient = 0.88				
	Sand	Vegetated	Sum	Users Accuracy (%)
Sand	**46**	4	50	92
Vegetated	2	**48**	50	96
Sum	48	52	100	
Producers Accuracy (%)	95.8	92.3		

Table 8.2: Error matrices where A is change map from Worldview-2 NDVI 2014, B is change map from CVI from Worldview-2 2014, and C is change map from NDVI from Sentinel-2 2016.

For measures of accuracy an error matrix is produced for each layer (Table 8.2). The stratified random sampling points are only generated within the change layers. As the NDVI layer identified more areas of change than the CVI layer, more errors are identified as the layer overestimation change. Many of the slack scrapes are still under water so confusion between all three of these classes are expected. However, these are unlikely to result in change of habitat as most are areas of shallow water. The difference between an area of inundated vegetation and sand are therefore, evident in the visual interpretation of the imagery. For the Sentinel-2 layer, changes are classified at a high accuracy rate.

As mentioned in the methods section, a weakness of this approach, and indeed in many change detection algorithms available in the literature, is identifying areas of possible change that the algorithm has failed to outline. A visual inspection of the imagery, as seen in Figure 8.6, shows that the algorithms have not missed any areas of the type of change being investigated, which is vegetation to bare sand. However, if this method was used in other, more complex scenarios, then omission error will need to be considered.

8.5 Discussion

A change detection method was successfully implemented with the application of a novel map-to-image approach, which demonstrated that the method can work using different sensors with different resolutions. The automation of the method also exemplifies its potential for future monitoring methods. The successful detection of change from the exciting Sentinel-2 sensor is very promising for future monitoring approaches as imagery is acquired much more frequently over global coverage and is free at the point of use, which is essential for cost effectiveness and long term prospects.

8.5.1 Image characteristics and pre-processing

Although the method was successful, there are some key considerations that are important to acknowledge, and one that applies to all types of change detection is differences between the imagery used (Singh, 1989). For the novel map-to-image approach here, it was not a requirement for images to be similar in any traditional way in terms of type of sensor, calibration or pixel resolution. However, image registration is very important as are the errors produced in atmospheric correction, while the choice of pixel resolution should be considered when interpreting results. The use of vegetation indices somewhat reduces the effect of atmospheric correction errors as issues related to specific indices, such as the well-known saturation problems with NDVI, are much more prevalent in the results. The use of the CVI index was proved once again to perform slightly better than NDVI in the Worldview-2 image.

The Worldview-2 and Sentinel-2 images were processed differently in terms of orthorectification, therefore differences in registration are to be expected unless further steps are taken to compensate for these differences. All of the Worldview-2 images were processed in exactly the same way and were available as digital number with very little processing therefore, issues of registration between the resulting map from the mapping approach and the change analysis are minimal. The Sentinel-2 images are provided as an orthorectified, top-of-atmosphere reflectance product in its raw format making it harder to compensate for registration problems without further processing and warping of the images. The image registration issues are a result of the global 30 m DEM used for orthorectifying Sentinel-2 imagery and the datum transformation when re-projecting from WGS 84 to British National Grid. These errors were minimised by applying a procedure to register the Sentinel-2 image to the Worldview-2 image, however, errors are likely to still exist due to resampling method and pixel size. Change features were still successfully mapped

meaning that the ability of the method to detect abnormalities in the class associated with change features definitely showed potential. This has implications for monitoring systems as additional pre-processing steps to ensure the data is registered with greater accuracy and precision are needed if Sentinel-2 is to be used after the initial baseline mapping exercise. Registration errors were not evident between the map and Worldview-2 image, as pixel sizes were the same.

The resolution of imagery used for change analysis provided similar results, which is particularly encouraging for the future use of Sentinel-2 in similar applications. The results from the Worldview-2 imagery were especially noisy as the analysis was pixel-based. Chen et al. (2012) stated that the value of VHR imagery in many applications is the ability to create objects at small enough scales to be meaningful while eliminating the "salt and pepper" effect associated with pixel-based approaches. This phenomenon is evident here making it difficult to separate change resulting from method limitation and real change on the ground, whether that is seasonal or landscape based. This is not seen in the Sentinel-2 imagery, meaning that providing a larger minimum mapping unit eliminates some of the less desired effects of pixel based analysis. However, by sacrificing the finer detail, this limits the chance of identifying change in fine-grained habitats and the condition element of the habitat in particular, meaning that the output can also be less useful to a degree. This is an interesting concept as most remote sensing scientist have regarded the salt and pepper effect in a negative manner when the effect can still represent useful information.

8.5.2 Landscape and seasonal change

This method is designed to identify change within a class, seasonal change is expected to be visible within the analysis in addition to changes in the landscape. For sand dune

ecosystems like Kenfig, the seasonal changes in the landscape are drastic with the slacks often inundated throughout the winter months (particularly in wet winters). The rate that the slacks dry out varies year on year and depends on various characteristics such as climate. The June 2014 image acquired from Worldview-2 (Figure 8.3) shows that some of the slacks are still inundated and the map-to-image method successfully recognised change in land cover. However, this does not represent a change in habitat type as this is the natural behaviour of humid dune slacks. In the July 2016 image, acquired a full month after the 2014 image, the slacks have dried up and management work involving the scraping of the top layer of vegetation is evident. Here, there is once again a change in land cover but there is also a change in habitat condition. The habitat type is expected to be the same at Annex I level but the state of the slack is reversed from its mature label to a young successional label. In the managed areas closer to the coastline, the scraping involves the removal of vegetation from dunes in addition to slack areas, where the successful detection of change in land cover also represents a change in habitat type, from fixed dune grassland to shifting dune habitat. Although this method is utilised to detect all types of change, care needs to be taken when interpreting the results. The time of year of image acquisition is also very important as it can affect the way an expert interprets the analysis results. Figure 8.7 shows how this method can be implemented in a continuous monitoring system where land cover and even some broad habitats changes can be recognised with all of the above considerations in place. As errors are identified, or seasonal change is identified, they can be addressed in the red area.

8.5.3 Advantages and limitations

The novel map-to-image approach introduces several advantages over more traditional methods described in Section 8.2. This approach does not require a new extent map for the site using images and data acquired at a later date, so that two independent results

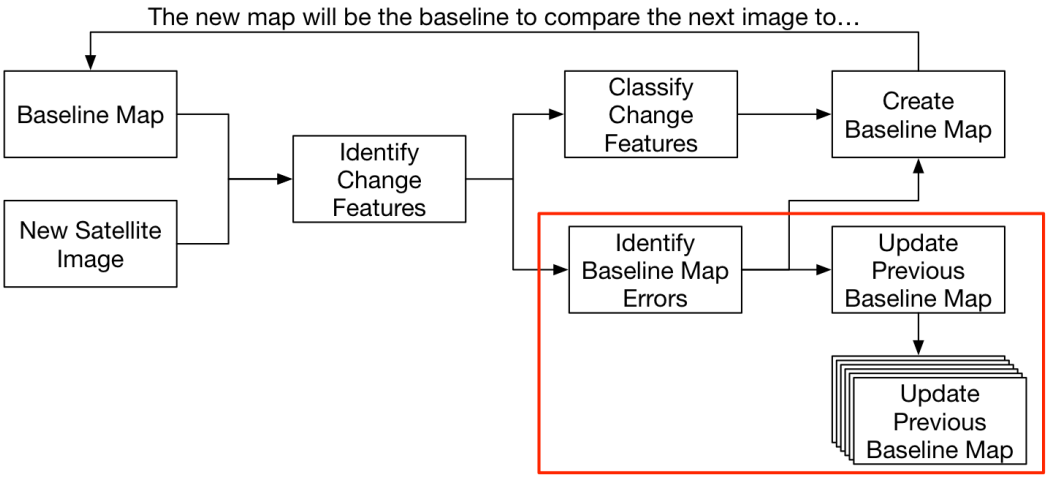

Figure 8.7: Example of how this change detection method can be integrating into a continuous monitoring system.

can be analysed. This is an advantage as the fundamental limitation for map-to-map techniques are their dependencies on accuracies of input maps (Tewkesbury et al., 2015). The successful application of a map-to-image approach does not rely on errors of comparison input data and required a lot less time and effort for repeated detection of change through time. However, the benefit of a map-to-map technique include a full matrix of available change in all classes in addition to identifying the class of change areas (Singh, 1989; Coppin et al., 2004).

Advantages over image-to-image techniques include the ability to use data from different sensors, and the ability to focus the analysis based on class. For example, image-to-image techniques traditionally detect change in all classes which would not have been suitable for this study due to the very high scale of analysis (Chen et al., 2012). Some image-to-image techniques acquire accurate results, such as CVA (Im and Jensen, 2005), but are much more complex to operate in an automated, consistent way with very little input from the user, in comparison to the approach used in this chapter. Image rationing also has some advantages but are limited by threshold detection as the distribution of values are

typically bi-modal (Coppin et al., 2004), which the map-to-image approach overcomes by focusing on the typical univariate nature of class distribution.

A limitation to the map-to-image approach is that it can only be applied to one class at a time. However, the automated nature of the method means that it can be applied regularly and repeatedly at high temporal resolution, without the requirement of independent classifications, and can be scripted to apply to several classes sequentially (Thomas, 2016). Other limitations, as previously stated, are the error associated with input data, whether that's map accuracy or issues with image registration, and class variation not represented as a normal distribution and therefore seasonal change incorrectly found. However, these can be addressed at the post-classification stage. Another limitation is the lack of validation for detection of omission errors.

8.6 Conclusions

This study was able to successfully detect change from an automated, novel map-to-image technique that is capable of using imagery from any sensor. The unique approach of using class statistics allows change to be detected in expected areas, taking advantage of methods that are similar to the hierarchical approach used in mapping approaches used in previous chapters, making it easier to integrate expert ecologist knowledge.

The method was capable of detecting change from imagery at 2 m and 10 m resolution over two-year periods but does not provide information on type of change, making it difficult to separate seasonal and landscape change features. The method also does not take into account errors of omission.

Pixel size was an issue with Sentinel-2 and would require further pre-processing steps to correct for misalignment between the baseline map and future imagery used for analy-

sis.

The successful application of Sentinel-2 has potential for broad scale monitoring as the sensor has a very high temporal frequency of image acquisition at a high enough resolution for defining ecologically meaningful products in some broad habitat types.

An interesting concept of the salt and pepper effect as a bad thing is challenged when the effect can still represent useful information.

Chapter 9

Conclusions

This final chapter concludes the thesis by presenting major outcomes of this research and their contribution to current systems of monitoring Annex I habitats. The concluding discussion focuses on the aspects where improvements can be made, their implications and future recommendations. This discussion also outlines how these methods can be applied to other sites and upscaled to incorporate national scale mapping initiatives. Finally, application of these methods to implement policy requirements at national, European and global scales are discussed.

9.1 Major findings and conclusions

The aim of this study as stated in Chapter 1 was to explore remote sensing techniques for monitoring coastal Annex I habitats in Wales and to develop a method that will form a basis of an operational habitat monitoring system. The study focuses on the use of VHR optical imagery for retrieving parameters to identify associations that can separate habitat boundaries for extent mapping down to species level for indicators of condition.

The aims could be achieved by successfully achieving the following objectives:

1. Reviewed current land cover and habitat classification systems and asses their suitability for determining Annex I habitat definitions, focusing on their retrieval from EO data and associated parameters.

2. Implemented and evaluated the EODHaM system for mapping Annex I habitats utilising Worldview-2 data from two periods (July and September), in situ data and local ecological knowledge from ecologists, conservation and site managers.

3. Developed and adapted the EODHaM system by integrating more advanced remote sensing techniques such as machine learning to aid automation, and generate a baseline map of Annex I habitats, including mapping down to species level for proxies of condition.

4. Explored the use of automated change detection techniques, specifically map-to-image methods to identify any changes in habitat extent and generate an updated Annex I habitat map.

The following provides a summary of the main conclusions derived from the above objectives before actions to improve the findings are suggested.

9.1.1 Classification schemes and their suitability for monitoring.

- Standardisation and harmonisation is recognised as an issue at all scales especially when integrating such schemes into monitoring systems where change detection is key. New global schemes such as LCCS have tackled this issue with some success, while translation concepts such as EAGLE are designed to harmonise transferability between existing schemes at varying scales.

- Translation between land cover products and habitat information is not straight for-

ward and need special consideration when developing monitoring systems, depending on application.

- Developing new schemes for new policies does not guarantee uptake in conservation communities as existing schemes are usually tailored to national, regional or even local flora and fauna. This is particularly a problem when monitoring large geographic areas (e.g., Europe). This is an issue for integration of EO into operational monitoring systems as not all classes of interest are possible to separate using EO techniques. The Crick framework can help by giving an indication of EO capabilities.

9.1.2 Evaluation of EODHaM system for mapping Annex I habitats.

- The rule-based application of the EODHaM method proved successful at landscape scales as the thresholds derived from expert knowledge and visual interpretation are relatively simple and effective.

- As more detail is required, the rules are increasingly hard to define from EO data alone, even when using statistics and training data to determine highest separation from available data. However, knowledge on the most useful datasets coupled with ecological expertise have been demonstrated to be essential for successful mapping exercises.

- Iterations of the mapping procedure are important for accuracy but not feasible using this method as the thresholds are constrained by drawing straight lines in a feature space where, in reality none exist, resulting in little improvements with each iteration.

9.1.3 Machine learning, automation, and habitat condition.

- Machine learning algorithms are more effective at separating classes in complex feature spaces where the appropriate training data are available. They are also quick to reproduce once an automated processing workflow is generated meaning that several iterations can be run with different types of algorithms when focusing on detailed habitat extent mapping.

- In terms of data, seasonal information is key where a summer image with at least a spring or autumn image are required for separation of classes within the environments studied. The spatial resolution of the VHR imagery proved effective at separating many detailed habitats including providing information on dominant species where these areas were homogeneous enough.

- Well established vegetation indices within the remote sensing community were effective at separation increasing the value of ecological knowledge in not only the training and validating stage, but at choosing the appropriate EO parameters for separation.

- Traditional accuracy assessments for maps generated from EO data are not adequate for validating detailed habitat maps where some classes are small in extent or rare. The qualitative assessments used in this research not only proved effective at choosing the most accurate spatial representation of detailed habitat maps, but included the ecologists and site specialist in the process from the beginning, enhancing the understanding between the two communities. This also increased confidence in the outputs making the target users more likely to use the final maps and implement these methods in the future.

- Some dominant species were mapped successfully resulting in valuable information

that can be used as a proxy for habitat condition. This only gives an indication of condition extent however and is not a solution for long term monitoring.

9.1.4 Change detection and contribution to monitoring system.

- A novel map-to-image change detection was implemented successfully on natural and anthropogenic land cover changes at Kenfig.
- The method can incorporate different types of data which was demonstrated by applying the change detection method on Sentinel-2 data as opposed to Worldview-2 data.

9.2 Role within operational monitoring system

First of all, it is worth noting that translating the methods used here for ecologists to use as an operational approach for monitoring habitats is unlikely as expertise from the EO community will be required to implement further baseline mapping across other sites. Although methods researched and implemented have tried to incorporate operational use and standardisation for users in land management and conservation, the generation of accurate baseline maps at the detail required proved to be complex. However, users from both communities can benefit from introducing more standardisation into processes regardless.

For generation of baseline maps where the focus is habitat extent it became evident that standardisation of methods was very unlikely with specific schemes designed for each site to increase accuracy. Similar conclusions were provided in Herold et al. (2006). The Annex I habitat definitions are derived from a mixture of land cover and habitat schemes. Land cover information is more straight forward to delineate from EO as the concept

of classification uses the assumption of homogeneous areas based on similar spectral characteristics which is in line with land cover definitions (Di Gregorio and Jansen, 2000). Habitats meanwhile, are likely to include more than one land cover type. The hierarchical nature of the LCCS provided high quality products with EO data as once certain land cover types have been separated, it decreases the chances of confusion from more detailed classes. When transferring some of the land cover classes to habitat, the implementation of the hierarchy also proved useful.

Once baseline maps have been established, it is recommended that the exercise is not repeated but instead updated after detecting areas of change when new information becomes available. As each site is unique, this means that any classification scheme can be implemented using the methods explored in this research as it depends on the design of the initial monitoring system. It is unlikely that detailed habitat discrimination can be scaled up to regional or national scale as the variations seen within habitat types across different biogeographical regions are too large (Bunce et al., 2012). However, the methods can be upscaled if enough local training data is provided.

Evaluation of the EODHaM system showed that transferability between sites for detailed Annex I extent of different habitat are likely to be need adaption per site decreasing its value as a standard, harmonised, system. This is also time consuming and the benefits of using EO in comparison to field assessments only are less significant. However, the flexibility of the system to incorporate multiple types of data from a variety of sources and its use of the LCCS has shown more potential for standardisation and harmonisation than many other projects in this area of research (Lucas et al., 2015). The system also draws attention to the importance of incorporating ecological knowledge into such monitoring systems as this increases the probability of correctly identifying and classifying habitats from EO data. Including the field experts and conservation managers in the process is also likely to increase understanding of both areas between the ecologists and remote sensing

scientist which is crucial for a successful monitoring system utilising EO.

By exploring more advanced classification techniques, detailed habitat maps were produced by a process of creating hierarchical classes and iterations which would have been difficult to implement through a rule-based method alone. As the machine learning algorithms are dependent on the training data and input features, the classification process can be automated. However, training datasets that is free of bias and that encompasses enough information to be representative of the classes being mapped are required (Chan and Paelinckx, 2008). This can be very difficult to create and a significant training dataset per site will be needed for accurate detailed habitat delineation. Baseline maps are therefore, always likely to be labour intensive and site specific.

The within class variance seen in some of the Annex I habitats across both sites in this study shows how much of a challenge generating habitat maps as opposed to land cover maps can be. When considering upscaling these methods, the complicated nature of habitats need to be considered as these variances will be even more significant when working across different biogeographical regions. Seasonality is a key factor here too as it is recognised that the differences can be used to our advantage for separation of habitats. It is possible for the seasonality to be a limiting factor in upscaling the method however, which means that the incorporation of ecological knowledge is even more important.

In terms of habitat condition, this research has investigated the mapping of condition through presence of dominant species. In many cases, this information alone will not supply a full picture of habitat condition, but instead, can focus areas in the field that need to be visited and monitored. For example, this study provided detailed information on sparse, but important features, such as the short species rich limestone grassland at Castlemartin. Previously, this level of detail does not exist for this site. It is therefore, difficult to fully understand the true accuracy of these classes, but areas with potential presence of that habitat provide an excellent starting point for field surveys, and is there-

fore valuable information.

Measures of accuracy/validation within the EO community is still an issue (Foody, 2002), but by doing qualitative assessments where ecologists' knowledge are crucial, more individuals are included in the conversation. This increases awareness of issues (Nagendra et al., 2013), tackling the confidence questions with map products made with EO while still making sure the quantitative error models are included. The quantitative accuracies can be misleading but the error matrices should always be included and interpreted as they explain the differences between classes that can be mapped precisely, as opposed to those that cannot from EO. By including all parties in the processing workflow, this increases the chances of final products being more accurate and used for operational activity.

To investigate monitoring techniques it was crucial that change detection methods were explored. The concept is that baseline maps should be updated, reducing the effort needed for mapping exercises. Generating a new map each time is not sustainable or effective for monitoring systems as mapping methods are unlikely to be consistent and transferable (Borre et al., in press). The main advantage of the change detection method used is that any kind of sensor data can be provided. These include data from different modalities (e.g., SAR and Optical) for the change products will find different change features. However, it is noted that changes in pixel resolutions are likely to produce areas of change that are artefacts from the image characteristics instead of actual change on the ground. By using VHR imagery with increased spectral information like Worldview-2, the level of detail from the original baseline map can be retained in any change mapping.

As this method requires a baseline map as input, it has the potential to be much more scalable than the mapping methods themselves. However, processing of data before analysis is extremely important to ensure that changes on the ground only are identified. Any errors resulting from lack of consistency in the pre-processing of the data should be minimised before analysis (Eklundh et al., 2011). The EO community would benefit by setting stan-

dards for pre-processing techniques that would tackle some of the inconsistencies that are of concern for change detection analyses.

9.3 Application to policy

The policy relevance for this research is the ECs Habitat's directive relating to the list of habitats defined in Annex I. The mapping aims of this study have been met and detailed information on habitat extent have been provided for the two study sites. The transferability of the methods used have been tested, and although the baseline mapping methods are labour intensive, there is scope for a monitoring system but this study only carried it out once. This means that updated habitat extent information is available for those sites with known error estimates, which is what current and traditional methods of extent mapping is missing. The type of information that mapping techniques can provide on habitat condition has also been explored. Although it is recognised that these techniques alone will not provide all the information needed to fulfil the requirements for the Habitat's directive.

Recent and upcoming political decisions will have an impact on the UK's policies in relation to the Habitat's directive. However, the methods are transferable and could be applied to any site across Europe or adapted to what ever new legislation the UK adopts following the withdrawal from the EU. On the global scale, other policies related to biodiversity monitoring are likely to be more important for UK conservation in the future such as the CBD Aichi Biodiversity Targets. CBD Target 1 requires knowledge in the trends of extent, condition and vulnerability of ecosystems, biomes and habitats (Balmford et al., 2005), which means that this research still has a lot of relevance to other existing policy areas. The methods employed can also be applied to fulfil CBD Target 2 by monitoring change and providing a potential platform for assessing trends in abundance and distri-

bution from habitat presence. This information can feed into habitat suitability models which provide indicators for biodiversity assessments. Although this method looked at baseline mapping and updating baseline maps, the EODHaM system has potential to ingest temporal data in a consistent way to reflect changes or trends in habitat condition (Lucas et al., 2015). These methods will also provide valuable information that can feed into the Wildlife and Countryside Act 1981, which is the national law for implementing the Bern Convention.

9.4 Future Work

This research had an operational focus which is why so much emphasis was put into automation and producing an accurate product. In exploring how these methods could be developed further and incorporated into other application areas the following should be considered:

1. Test the transferability of the method across a wider range of habitats. When discussing transferability, there are several aspects to consider such as the pre-processing methods of EO data - can standardisation of these methods across different sensors help eliminate errors related to image artefacts in products? Work related to producing the Landsat archive for Wales are challenging the concept with a similar project currently running for generation of Analysis Ready Data (ARD) for Sentinel-2 with the JNCC and Space Applications Catapult. Formats of ARD from Sentinel-1 data is also currently being explored, and the addition of radar products into any monitoring system would be seen as beneficial, particularly as the sensor is not affected by cloud.

2. Can the methods be upscaled to regional or national scale mapping initiatives? Current work within the Living Maps project carried out by Natural England are using

these methods to test their effectiveness on different scales. This mainly includes exploring the methods developed in Chapter 7, particularly the independent variable selection, and the use of machine learning algorithms for classification. The classification schema used is much broader than the scale this research was focused on, which is tailored to Natural England and Defra policy requirements. The Living Map approach so far has utilised radar data in addition to spectral bands and indices. The use of other products derived from EO, such as the Rural Payments Agency's (RPA) crop map derived wholly from Sentinel-1 data, is also included in the independent variable selection. As a large proportion of England is managed by crop, and the annual production of the crop map by RPA, it adds potential to the scalability of the living map project up to national scale. So far, maps of North Devon and Cumbria have been successfully completed.

3. Can the relationships between EO products such as vegetation indices like NDVI, and fauna and flora be explored even further to provide better information on biodiversity indicators? This research explored a large number of vegetation indices to try an identify those with close relationships to the features on the ground for separation during classification. The use of CVI was particularly successful in this project for specific habitats. If vegetation indices, or modelled outputs can be generated from EO data that represent a biophysical relationship on the ground, then these biophysical layers can be used for monitoring particular aspects of biodiversity properties, which goes beyond the classification stage and can aid change detection techniques. Will the change detection technique explored in this research be more successful at identifying the types of change needed for monitoring habitats if these types of relationships are better understood? The Living Wales concept is currently exploring the use of biophysical variables as inputs into a monitoring system of this kind. The concept in this project is based on research carried out

in the European H2020 funded Ecopotential project, which adapted the EODHaM system for use in land cover classification.

4. Can data from the ESA Sentinel missions be incorporated into the monitoring system to identify change and update baseline maps? As the Sentinel sensors provide regular high frequency data over the globe at 10 m spatial resolutions and above, as a complete open dataset for everyone, it is an EO resource that cannot be overlooked when trying to establish a continuous, regularly updated monitoring system. Using Sentinel-2 for change detection was initially explored in Chapter 8, with some success, but it is anticipated that these datasets would work better at regional, national, or indeed, global scales. The use of radar data for monitoring land masses can also be explored for operational use as Sentinel-1 is the first radar sensor to provide data as an open, free at the point of use, dataset. Major barriers for the use of radar data in the past was the initial cost of acquisition and the expertise needed to interpret the data, both expensive resources. Now that the cost of acquisition has been eliminated, it opens up opportunities for use of the data beyond research.

Bibliography

Adam, E., Mutanga, O., Rugege, D., Dec. 2009. Multispectral and hyperspectral remote sensing for identification and mapping of wetland vegetation: a review. Wetlands Ecology and Management 18 (3), 281–296.

Adamo, M., Tarantino, C., Tomaselli, V., Kosmidou, V., Petrou, Z., Manakos, I., Lucas, R. M., Mücher, C. A., Veronico, G., Marangi, C., 2014. Expert knowledge for translating land cover/use maps to General Habitat Categories (GHC). Landscape Ecology 29 (6), 1045–1067.

Aguilar, M. A., Agüera, F., Aguilar, F. J., Carvajal, F., Dec. 2008. Geometric accuracy assessment of the orthorectification process from very high resolution satellite imagery for Common Agricultural Policy purposes. International Journal of Remote Sensing 29 (24), 7181–7197.

Agera, F., Aguilar, F. J., Aguilar, M. A., Nov. 2008. Using texture analysis to improve per-pixel classification of very high resolution images for mapping plastic greenhouses. ISPRS Journal of Photogrammetry and Remote Sensing 63, 635–646.

Ahamed, T., Tian, L., Zhang, Y., Ting, K., 2011. A review of remote sensing methods for biomass feedstock production. Biomass and Bioenergy 35 (7), 2455–2469.

Alcaraz-Segura, D., Cabello, J., Paruelo, J. M., Delibes, M., 2009. Use of descriptors of ecosystem functioning for monitoring a national park network: a remote sensing approach. Environmental Management 43 (1), 38–48.

Alexandridis, T. K., Lazaridou, E., Tsirika, A., Zalidis, G. C., 2009. Using earth observation to update a natura 2000 habitat map for a wetland in greece. Journal of Environmental Management 90 (7), 2243–2251.

Ali, I., Schuster, C., Zebisch, M., Förster, M., Kleinschmit, B., Notarnicola, C., 2013. First results of monitoring nature conservation sites in alpine region by using very high

resolution (vhr) x-band sar data. IEEE Journal of Selected Topics in Applied Earth Observations and Remote Sensing 6 (5), 2265–2274.

Amarnath, G., Murthy, M., Britto, S., Rajashekar, G., Dutt, C., 2003. Diagnostic analysis of conservation zones using remote sensing and gis techniques in wet evergreen forests of the western ghats–an ecological hotspot, tamil nadu, india. Biodiversity & Conservation 12 (12), 2331–2359.

Amazon Cloud Platform, 2016. Sentinel-2 Public Dataset. URL: https://aws.amazon.com/public-datasets/sentinel-2/.

Anderson, M., Neale, C., Li, F., Norman, J., Kustas, W., Jayanthi, H., Chavez, J., 2004. Upscaling ground observations of vegetation water content, canopy height, and leaf area index during smex02 using aircraft and landsat imagery. Remote Sensing of Environment 92 (4), 447–464.

Apan, A., Held, A., Phinn, S., Markley, J., 2003. Formulation and assessment of narrowband vegetation indices from eo-1 hyperion imagery for discriminating sugarcane disease. Spatial Sciences, 1–13.

Aparicio, N., Villegas, D., Royo, C., Casadesus, J., Araus, J., 2004. Effect of sensor view angle on the assessment of agronomic traits by ground level hyper-spectral reflectance measurements in durum wheat under contrasting mediterranean conditions. International Journal of Remote Sensing 25 (6), 1131–1152.

Arbia, G., Griffith, D., Haining, R., 1998. Error propagation modelling in raster gis: overlay operations. International Journal of Geographical Information Science 12 (2), 145–167.

Arias, M., Inglada, J., Lucas, R., Blonda, P., 2013. Hedgerow segmentation on vhr optical satellite images for habitat monitoring. In: Geoscience and Remote Sensing Symposium (IGARSS), 2013 IEEE International. IEEE, pp. 3301–3304.

Arino, O., 2010. GlobCover 2009.

Arnold, S., Kosztra, B., Banko, G., Smith, G., Hazeu, G., 2013. The EAGLE concept—A vision of a future European Land Monitoring Framework.

Asner, G. P., 1998. Biophysical and biochemical sources of variability in canopy reflectance. Remote sensing of Environment 64 (3), 234–253.

Asner, G. P., Braswell, B., Schimel, D. S., Wessman, C. A., 1998. Ecological research

needs from multiangle remote sensing data. Remote Sensing of Environment 63 (2), 155–165.

Asner, G. P., Hughes, R. F., Vitousek, P. M., Knapp, D. E., Kennedy-Bowdoin, T., Boardman, J., Martin, R. E., Eastwood, M., Green, R. O., 2008. Invasive plants transform the three-dimensional structure of rain forests. Proceedings of the National Academy of Sciences 105 (11), 4519–4523.

Asner, G. P., Keller, M., Pereira Jr, R., Zweede, J. C., Silva, J. N., 2004. Canopy damage and recovery after selective logging in amazonia: field and satellite studies. Ecological Applications 14 (sp4), 280–298.

Asner, G. P., Palace, M., Keller, M., Pereira Jr, R., Silva, J. N., Zweede, J. C., 2002. Estimating canopy structure in an amazon forest from laser range finder and ikonos satellite observations 1. Biotropica 34 (4), 483–492.

Atzberger, C., Guérif, M., Baret, F., Werner, W., 2010. Comparative analysis of three chemometric techniques for the spectroradiometric assessment of canopy chlorophyll content in winter wheat. Computers and Electronics in Agriculture 73 (2), 165–173.

Baker, C., Lawrence, R., Montagne, C., Patten, D., Jun. 2006. Mapping wetlands and riparian areas using Landsat ETM+ imagery and decision-tree-based models. Wetlands 26 (2), 465–474.

Balmford, A., Bennun, L., Ten Brink, B., Cooper, D., Côté, I. M., Jun. 2005. The Convention on Biological Diversitys 2010 Target. Science 3 (5), 43–45.

Baret, F., Guyot, G., Major, D., 1989. Crop biomass evaluation using radiometric measurements. Photogrammetria 43 (5), 241–256.

Bargiel, D., 2013. Capabilities of high resolution satellite radar for the detection of semi-natural habitat structures and grasslands in agricultural landscapes. Ecological Informatics 13, 9–16.

Barnes, E., Clarke, T., Richards, S., Colaizzi, P., Haberland, J., Kostrzewski, M., Waller, P., Choi, C., Riley, E., Thompson, T., et al., 2000. Coincident detection of crop water stress, nitrogen status and canopy density using ground based multispectral data. In: Proceedings of the 5th International Conference on Precision Agriculture, Bloomington, MN. pp. 16–19.

Bartholomé, E., Belward, A. S., May 2005. GLC2000: a new approach to global land

cover mapping from Earth observation data. International Journal of Remote Sensing 26 (9), 1959–1977.

Belluco, E., Camuffo, M., Ferrari, S., Modenese, L., Silvestri, S., Marani, A., Marani, M., 2006. Mapping salt-marsh vegetation by multispectral and hyperspectral remote sensing. Remote sensing of environment 105 (1), 54–67.

Belward, A., ROBERT, B., Cohen, W., Gao, F., Goward, S. N., Helder, D., Helmer, E., Nemani, R., Oreopoulos, L., Schott, J., et al., 2008. Free access to landsat imagery. Science 320, 1011–1011.

Benediktsson, J. A., Chanussot, J., Fauvel, M., 2007. Multiple classifier systems in remote sensing: from basics to recent developments. In: International Workshop on Multiple Classifier Systems. Springer, pp. 501–512.

Benediktsson, J. A., Swain, P. H., 1992. Consensus theoretic classification methods. IEEE transactions on Systems, Man, and Cybernetics 22 (4), 688–704.

Benz, U. C., Hofmann, P., Willhauck, G., Lingenfelder, I., Heynen, M., Jan. 2004. Multi-resolution, object-oriented fuzzy analysis of remote sensing data for GIS-ready information. ISPRS Journal of Photogrammetry and Remote Sensing 58 (3-4), 239–258.

Berger, M., Moreno, J., Johannessen, J. A., Levelt, P. F., Hanssen, R. F., 2012. Esa's sentinel missions in support of earth system science. Remote Sensing of Environment 120, 84–90.

Bishop, C. M., 2006. Pattern recognition and machine learning. Springer.

Blackburn, G. A., 1998. Spectral indices for estimating photosynthetic pigment concentrations: a test using senescent tree leaves. International Journal of Remote Sensing 19 (4), 657–675.

Blackburn, G. A., Steele, C. M., 1999. Towards the remote sensing of matorral vegetation physiology: Relationships between spectral reflectance, pigment, and biophysical characteristics of semiarid bushland canopies. Remote sensing of Environment 70 (3), 278–292.

Blanco, L. J., Ferrando, C. A., Biurrun, F. N., 2009. Remote sensing of spatial and temporal vegetation patterns in two grazing systems. Rangeland ecology & management 62 (5), 445–451.

Blaschke, T., Jan. 2010. Object based image analysis for remote sensing. ISPRS Journal of Photogrammetry and Remote Sensing 65 (1), 2–16.

Blaschke, T., Strobl, J., et al., 2001. Whats wrong with pixels? some recent developments interfacing remote sensing and gis. GeoBIT/GIS 6 (1), 12–17.

Bock, M., Rossner, G., Wissen, M., Remm, K., Langanke, T., Lang, S., Klug, H., Blaschke, T., Vrščaj, B., 2005a. Spatial indicators for nature conservation from european to local scale. Ecological Indicators 5 (4), 322–338.

Bock, M., Xofis, P., Mitchley, J., Rossner, G., Wissen, M., 2005b. Object-oriented methods for habitat mapping at multiple scales–case studies from northern germany and wye downs, uk. Journal for Nature Conservation 13 (2), 75–89.

Boldt, M., Thiele, A., Schulz, K., 2012. Object-based urban change detection analyzing high resolution optical satellite images. In: SPIE Remote Sensing. International Society for Optics and Photonics, pp. 85380E–85380E.

Bolstad, P. V., Lillesand, T., 1992. Improved classification of forest vegetation in northern wisconsin through a rule-based combination of soils, terrain, and landsat thematic mapper data. Forest Science 38 (1), 5–20.

Borre, J., Spanhove, T., Haest, B., in press. Towards a mature age of remote sensing for natura 2000 habitat conservation: poor method transferability as a prime obstacle. In: The Roles of Remote Sensing in Nature Conservation: A practical guide and case studies. Springer Nature.

Borre, J. V., Paelinckx, D., Mücher, C. A., Kooistra, L., 2011. Integrating remote sensing in Natura 2000 habitat monitoring: Prospects on the way forward. Journal for Nature Conservation 19 (1), 116–125.

Boser, B. E., Guyon, I. M., Vapnik, V. N., 1992. A training algorithm for optimal margin classifiers. In: Proceedings of the fifth annual workshop on Computational learning theory. ACM, pp. 144–152.

Bossard, M., Feranec, J., Otahel, J., et al., 2000. Corine land cover technical guide: Addendum 2000.

Bovolo, F., Marchesi, S., Bruzzone, L., 2012. A framework for automatic and unsupervised detection of multiple changes in multitemporal images. IEEE Transactions on Geoscience and Remote Sensing 50 (6), 2196–2212.

Box, G. E., Watson, G. S., 1962. Robustness to non-normality of regression tests. Biometrika 49 (1-2), 93–106.

Boyd, D., Phipps, P., Foody, G., Walsh, R., 2002. Exploring the utility of noaa avhrr middle infrared reflectance to monitor the impacts of enso-induced drought stress on sabah rainforests. International Journal of Remote Sensing 23 (23), 5141–5147.

Boyd, D. S., Sanchez-Hernandez, C., Foody, G. M., 2006. Mapping a specific class for priority habitats monitoring from satellite sensor data. International Journal of Remote Sensing 27 (13), 2631–2644.

Brazier, P., Birch, K., Brunstrom, A., Bunker, A., Jones, M., Lough, N., Salmon, L., Wyn, G., 2007. When the tide goes out: The biodiversity and conservation of the shores of wales–results from a 10 year intertidal survey of wales.

Breiman, L., 1996. Bagging predictors. Machine learning 24 (2), 123–140.

Breiman, L., 2001. Random forests. Machine learning 45 (1), 5–32.

Breiman, L., Friedman, J., Stone, C. J., Olshen, R. A., 1984. Classification and regression trees. CRC press.

Breyer, J., 2009. Habitat classification using airborne and spaceborne remote sensing for biodiversity assessment in Wales (PhD). Aberystwyth University.

Briem, G. J., Benediktsson, J. A., Sveinsson, J. R., 2002. Multiple classifiers applied to multisource remote sensing data. IEEE transactions on geoscience and remote sensing 40 (10), 2291–2299.

Bruzzone, L., Bovolo, F., 2013. A novel framework for the design of change-detection systems for very-high-resolution remote sensing images. Proceedings of the IEEE 101 (3), 609–630.

Buchanan, G. M., Nelson, A., Mayaux, P., Hartley, A., Donald, P. F., 2009. Delivering a global, terrestrial, biodiversity observation system through remote sensing. Conservation Biology 23 (2), 499–502.

Buchanan-Wollaston, V., 1997. The molecular biology of leaf senescence. Journal of Experimental Botany 48 (2), 181–199.

Bunce, R., Bogers, M., Evans, D., Halada, L., Jongman, R., Mucher, C., Bauch, B.,

de Blust, G., Parr, T., Olsvig-Whittaker, L., 2013. The significance of habitats as indicators of biodiversity and their links to species. Ecological Indicators 33, 19–25.

Bunce, R., Bogers, M., Evans, D., Jongman, R., 2012. Field identification of habitats directive Annex I habitats as a major European biodiversity indicator. Ecological Indicators 33, 105–110.

Bunce, R., Groom, G., Jongman, R., Padoa-Schippa, E., Metzger, M., 2005. Handbook for surveillance and monitoring of european habitats. Tech. rep., Alterra.

Bunce, R., Pérez-Soba, M., Gómez-Sanz, V., del Barrio, J. G., Elena-Rosselló, R., 2006. European framework for surveillance and monitoring of habitats: a methodological approach for spain. Forest Systems 15 (3), 249–261.

Bunce, R. G. H., Bogers, M., Roche, P., Walczak, M., Geijzendorffer, I., Jongman, R., 2011. Manual for habitat and vegetation surveillance and monitoring: temperate, mediterranean and desert biomes. Tech. rep., Alterra.

Bunce, R. G. H., Metzger, M. J., Jongman, R. H. G., Brandt, J., Blust, G., Elena-Rossello, R., Groom, G. B., Halada, L., Hofer, G., Howard, D. C., Kovář, P., Mücher, C. A., Padoa-Schioppa, E., Paelinx, D., Palo, A., Perez-Soba, M., Ramos, I. L., Roche, P., Skånes, H., Wrbka, T., Nov. 2008. A standardized procedure for surveillance and monitoring European habitats and provision of spatial data. Landscape Ecology 23 (1), 11–25.

Bunce, R. G. H., Metzger, M. J., Jongman, R. H. G., Brandt, J., Blust, G., Elena-Rossello, R., Groom, G. B., Halada, L., Hofer, G., Howard, D. C., Kovář, P., Mücher, C. A., Padoa-Schioppa, E., Paelinx, D., Palo, A., Perez-Soba, M., Ramos, I. L., Roche, P., Skånes, H., Wrbka, T., Nov. 2007. A standardized procedure for surveillance and monitoring European habitats and provision of spatial data. Landscape Ecology 23 (1), 11–25.

Bunting, P., Clewley, D., Lucas, R. M., Gillingham, S., Jan. 2014. The Remote Sensing and GIS Software Library (RSGISLib). Computers & Geosciences 62, 216–226.

Bunting, P., Gillingham, S., 2013. The KEA image file format. Computers & Geosciences 57, 54–58.

Burges, C. J., 1998. A tutorial on support vector machines for pattern recognition. Data Mining and Knowledge Discovery 2 (2), 121–167.

Büttner, G., Feranec, J., Jaffrain, G., Mari, L., Maucha, G., Soukup, T., 2004. The corine land cover 2000 project. EARSeL eProceedings 3 (3), 331–346.

Calaciura, B., Spinelli, O., 2008. Management of Natura 2000 Habitats Semi-Natural Dry Grasslands (Festuco-Brometalia) 6210. European Commission.

Camps-Valls, G., Gómez-Chova, L., 2004. Robust support vector method for hyperspectral data classification and knowledge discovery. IEEE on Geoscience and Remote Sensing 42, 1530–542.

Canters, F., 1997. Evaluating the uncertainty of area estimates derived from fuzzy land-cover classification. Photogrammetric Engineering & Remote Sensing 63 (4), 403–414.

Carrão, H., Gonçalves, P., Caetano, M., 2008. Contribution of multispectral and multitemporal information from modis images to land cover classification. Remote Sensing of Environment 112 (3), 986–997.

CCW, 2013. CCW Website. URL: http://www.ccw.gov.uk.

CCW, 2013a. Kenfig/cynffig sac.

CCW, 2013b. Limestone coast of south wales/ arfordir calchfaen de orllewin cymru sac.

Černá, L., Chytrỳ, M., 2005. Supervised classification of plant communities with artificial neural networks. Journal of Vegetation Science 16 (4), 407–414.

Chan, J. C.-W., Huang, C., DeFries, R., 2001. Enhanced algorithm performance for land cover classification from remotely sensed data using bagging and boosting. IEEE Transactions on Geoscience and Remote Sensing 39 (3), 693–695.

Chan, J. C.-W., Paelinckx, D., 2008. Evaluation of random forest and adaboost tree-based ensemble classification and spectral band selection for ecotope mapping using airborne hyperspectral imagery. Remote Sensing of Environment 112 (6), 2999–3011.

Charnock, R. B., 2016. Assessment of remote sensing attributes as biodiversity indicators on a European protected raised bog (PhD). Aberystwyth University.

Chehata, N., Orny, C., Boukir, S., Guyon, D., 2011. Object-based forest change detection using high resolution satellite images. Remote sensing and spatial information sciences 38.

Chen, C. H., Ho, P.-G. P., 2008. Statistical pattern recognition in remote sensing. Pattern Recognition 41 (9), 2731–2741.

Chen, J., Chen, J., Liao, A., Cao, X., Chen, L., Chen, X., He, C., Han, G., Peng, S., Lu, M., et al., 2015. Global land cover mapping at 30m resolution: A pok-based operational approach. ISPRS Journal of Photogrammetry and Remote Sensing 103, 7–27.

Chen, X., Chen, J., Shi, Y., Yamaguchi, Y., 2012. An automated approach for updating land cover maps based on integrated change detection and classification methods. ISPRS Journal of Photogrammetry and Remote Sensing 71, 86–95.

Cherrill, A., McClean, C., 1999. The reliability of phase 1habitat mapping in the uk: the extent and types of observer bias. Landscape and Urban Planning 45 (2), 131–143.

Chichester, C., Nakayama, T., 1965. Pigment changes in senescent and stored tissue. Chemistry and biochemistry of plant pigments 439, 458.

Chow, C. K., 1957. An optimum character recognition system using decision functions. IRE Transactions on Electronic Computers 4, 247–254.

Civco, D., 1989. Knowledge-based land use and land cover mapping. In: 1989 ASPRS/ACSM Annual Convention, Baltimore, MD. pp. 276–291.

Clewley, D., Bunting, P., Shepherd, J., Gillingham, S., Flood, N., Dymond, J., Lucas, R., Armston, J., Moghaddam, M., 2014. A python-based open source system for geographic object-based image analysis (GEOBIA) utilizing raster attribute tables. Remote Sensing 6 (7), 6111–6135.

Cohen, W. B., Goward, S. N., 2004. Landsat's Role in Ecological Applications of Remote Sensing. BioScience 54 (6), 535.

Coleman, A., 1961. The second land use survey: progress and prospect. The Geographical Journal 127 (2), 168–180.

Comaniciu, D., Meer, P., 2002. Mean shift: A robust approach toward feature space analysis. IEEE Transactions on pattern analysis and machine intelligence 24 (5), 603–619.

Combal, B., Baret, F., Weiss, M., Trubuil, A., Mace, D., Pragnere, A., Myneni, R., Knyazikhin, Y., Wang, L., 2003. Retrieval of canopy biophysical variables from bidirectional reflectance: Using prior information to solve the ill-posed inverse problem. Remote sensing of environment 84 (1), 1–15.

Comber, A., Fisher, P., Wadsworth, R., 2004. Assessment of a semantic statistical approach to detecting land cover change using inconsistent data sets. Photogrammetric Engineering & Remote Sensing 70 (8), 931–938.

Comber, A., Fisher, P., Wadsworth, R., 2005. What is land cover? Environment and Planning B: Planning and Design 32 (2), 199–209.

Comber, A., Medcalf, K., Lucas, R., Bunting, P., Brown, A., Clewley, D., Breyer, J., Keyworth, S., 2010. Managing uncertainty when aggregating from pixels to objects: habitats, context-sensitive mapping and possibility theory. International Journal of Remote Sensing 31 (4), 1061–1068.

Congalton, R., Green, K., 1993. A practical look at the sources of confusion in error matrix generation. Photogrammetric engineering and remote sensing 59 (5), 641–644.

Convention on the Conservation of European Wildlife and Natural Habitats, 1979. Texts Adopted. By the Standing Committee of the Bern Convention on the Conservation of European Wildlife and Natural Habitats (19 September 1979), 1982-96. Council of Europe.

Coppin, P., Jonckheere, I., Nackaerts, K., Muys, B., Lambin, E., 2004. Review articledigital change detection methods in ecosystem monitoring: a review. International Journal of Remote Sensing 25 (9), 1565–1596.

Corbane, C., Lang, S., Pipkins, K., Alleaume, S., Deshayes, M., Millán, V. E. G., Strasser, T., Borre, J. V., Toon, S., Michael, F., 2015. Remote sensing for mapping natural habitats and their conservation status–new opportunities and challenges. International Journal of Applied Earth Observation and Geoinformation 37, 7–16.

Costanza, J. K., Moody, A., Peet, R. K., 2011. Multi-scale environmental heterogeneity as a predictor of plant species richness. Landscape Ecology 26 (6), 851–864.

Coulter, L. L., Hope, A. S., Stow, D. A., Lippitt, C. D., Lathrop, S. J., 2011. Time–space radiometric normalization of tm/etm+ images for land cover change detection. International Journal of Remote Sensing 32 (22), 7539–7556.

Cover, T., Hart, P., 1967. Nearest neighbor pattern classification. IEEE transactions on information theory 13 (1), 21–27.

Cracknell, A., 1998. Review article synergy in remote sensing-what's in a pixel? International Journal of Remote Sensing 19 (11), 2025–2047.

Dalmayne, J., Möckel, T., Prentice, H. C., Schmid, B. C., Hall, K., 2013. Assessment of fine-scale plant species beta diversity using worldview-2 satellite spectral dissimilarity. Ecological Informatics 18, 1–9.

Dalponte, M., Bruzzone, L., Gianelle, D., 2008. Fusion of hyperspectral and lidar remote sensing data for classification of complex forest areas. IEEE Transactions on Geoscience and Remote Sensing 46 (5), 1416–1427.

Dams, J., Dujardin, J., Reggers, R., Bashir, I., Canters, F., Batelaan, O., 2013. Mapping impervious surface change from remote sensing for hydrological modeling. Journal of Hydrology 485, 84–95.

Dash, J., Curran, P. J., 2004. The meris terrestrial chlorophyll index.

Datt, B., 1998. Remote sensing of chlorophyll a, chlorophyll b, chlorophyll a+b, and total carotenoid content in eucalyptus leaves. Remote Sensing of Environment 66 (2), 111–121.

Datt, B., 1999. Remote sensing of water content in eucalyptus leaves. Australian Journal of Botany 47 (6), 909–923.

Davies, C. E., Moss, D., Hill, M. O., 2004. Eunis habitat classification revised 2004. Report to: European Environment Agency-European Topic Centre on Nature Protection and Biodiversity, 127–143.

de Colstoun, E. C. B., Story, M. H., Thompson, C., Commisso, K., Smith, T. G., Irons, J. R., 2003. National park vegetation mapping using multitemporal landsat 7 data and a decision tree classifier. Remote Sensing of Environment 85 (3), 316–327.

De Fries, R., Hansen, M., Townshend, J., Sohlberg, R., 1998. Global land cover classifications at 8 km spatial resolution: the use of training data derived from landsat imagery in decision tree classifiers. International Journal of Remote Sensing 19 (16), 3141–3168.

Definiens, 2004. eCognition user guide. URL: http://www. definiens-imaging. com.

DeFries, R., Chan, J. C.-W., 2000. Multiple criteria for evaluating machine learning algorithms for land cover classification from satellite data. Remote Sensing of Environment 74 (3), 503–515.

DeFries, R., Hansen, A., Newton, A. C., Hansen, M. C., 2005. Increasing isolation of protected areas in tropical forests over the past twenty years. Ecological Applications 15 (1), 19–26.

DeFries, R., Hansen, M., Townshend, J., 1995. Global discrimination of land cover types from metrics derived from avhrr pathfinder data. Remote Sensing of Environment 54 (3), 209–222.

DeFries, R., Townshend, J., 1994. Ndvi-derived land cover classifications at a global scale. International Journal of Remote Sensing 15 (17), 3567–3586.

Demir, B., Bovolo, F., Bruzzone, L., 2013. Updating land-cover maps by classification of image time series: A novel change-detection-driven transfer learning approach. IEEE Transactions on Geoscience and Remote Sensing 51 (1), 300–312.

Deng, J., Wang, K., Deng, Y., Qi, G., 2008. Pca-based land-use change detection and analysis using multitemporal and multisensor satellite data. International Journal of Remote Sensing 29 (16), 4823–4838.

Devillers, P., Devillers-Terschuren, J., Ledant, J., 1991. Corine biotopes manual. Habitats of the European Community. Office for Official Publications of the European Communities, Luxembourg 685.

Di Gregorio, A., Jansen, L. J., 2000. Land cover classification system (LCCS): classification concepts and user manual for software version 1.0. FAO.

Digital Globe, 2009. Digital Globe Website. URL: https://www.digitalglobe.com/about/our-constellation.

Dingle Robertson, L., King, D. J., 2011. Comparison of pixel-and object-based classification in land cover change mapping. International Journal of Remote Sensing 32 (6), 1505–1529.

Dixon, B., Candade, N., 2008. Multispectral landuse classification using neural networks and support vector machines: one or the other, or both? International Journal of Remote Sensing 29 (4), 1185–1206.

Dobson, M. C., Ulaby, F. T., LeToan, T., Beaudoin, A., Kasischke, E. S., Christensen, N., 1992. Dependence of radar backscatter on coniferous forest biomass. IEEE Transactions on Geoscience and remote Sensing 30 (2), 412–415.

Doxani, G., Karantzalos, K., Tsakiri-Strati, M., 2012. Monitoring urban changes based on scale-space filtering and object-oriented classification. International Journal of Applied Earth Observation and Geoinformation 15, 38–48.

Drusch, M., Del Bello, U., Carlier, S., Colin, O., Fernandez, V., Gascon, F., Hoersch, B., Isola, C., Laberinti, P., Martimort, P., et al., 2012. Sentinel-2: Esa's optical high-resolution mission for gmes operational services. Remote Sensing of Environment 120, 25–36.

Džeroski, S., Ženko, B., 2004. Is combining classifiers with stacking better than selecting the best one? Machine learning 54 (3), 255–273.

EC Birds Directive, 1979. Council Directive 79/409/EEC of 2 April 1979 on the conservation of wild birds. Official Journal L.

EC Habitats Directive, 1992. Council Directive 92/43/EEC of 21 May 1992 on the conservation of natural habitats and of wild fauna and flora. Brussels.

Eckert, S., 2012. Improved forest biomass and carbon estimations using texture measures from worldview-2 satellite data. Remote sensing 4 (4), 810–829.

Ehammer, A., Fritsch, S., Conrad, C., Lamers, J., Dech, S., 2010. Statistical derivation of fpar and lai for irrigated cotton and rice in arid uzbekistan by combining multi-temporal rapideye data and ground measurements. In: Remote Sensing. pp. 782409–782409.

Eklundh, L., Jin, H., Schubert, P., Guzinski, R., Heliasz, M., 2011. An optical sensor network for vegetation phenology monitoring and satellite data calibration. Sensors 11 (8), 7678–7709.

El-Kawy, O. A., Rød, J., Ismail, H., Suliman, A., 2011. Land use and land cover change detection in the western nile delta of egypt using remote sensing data. Applied Geography 31 (2), 483–494.

Elachi, C., Van Zyl, J. J., 2006. Introduction to the physics and techniques of remote sensing. Vol. 28. John Wiley & Sons.

Elvidge, C. D., Lyon, R. J., 1985. Influence of rock-soil spectral variation on the assessment of green biomass. Remote Sensing of Environment 17 (3), 265–279.

Environment Agency Geomatics Group, 2013. Geomatics Website. URL: https://www.geomatics-group.co.uk/geocms/.

ESA, 2016. ESA Sentinels Scientific Data Hub. URL: https://scihub.copernicus.eu/.

Escadafal, R., 1993. Soil optical properties and environmental applications of remote sensing. International Archives of Photogrammetry and Remote Sensing 29, 709–709.

Escadafal, R., Belghith, A., Ben Moussa, H., 1994. Indices spectraux pour la degradation des milieux naturels en tunisie aride. 6éme symp. Int. Mesures Physiques et Signatures en Télédétection., Val d'lsère, France, ISPRS-CNES.

Ettrich, G., 2013. Mapping the coastal zone using earth observation: Application of linear spectral unmixing to coastal dune systems in wales.

European Environment Agency, 2010. The European Environment - State and Outlook 2010: Synthesis. URL: http://www.eea.europa.eu/soer/synthesis/.

Evans, D., 2006. The habitats of the european union habitats directive. In: Biology and Environment: Proceedings of the Royal Irish Academy. pp. 167–173.

Evans, D., 2010. Interpreting the habitats of annex i: past, present and future. Acta Botanica Gallica 157 (4), 677–686.

Eve, M., Merchant, J., 2007. A national survey of land cover mapping protocols used in the gap analysis program. final report.

Everitt, J. H., Yang, C., Deloach, C., 2005. Remote sensing of giant reed with quickbird satellite imagery. Journal of Aquatic Plant Management 43, 81–85.

Fassnacht, K. S., Cohen, W. B., Spies, T. A., 2006. Key issues in making and using satellite-based maps in ecology: A primer. Forest Ecology and Management 222 (1), 167–181.

Feeley, K. J., Gillespie, T. W., Terborgh, J. W., 2005. The utility of spectral indices from landsat etm+ for measuring the structure and composition of tropical dry forests. Biotropica 37 (4), 508–519.

Fisher, P., 1994. Visualization of the reliability in classified remotely sensed images. Photogrammetric Engineering and Remote Sensing 60 (7), 905–910.

Foley, J. A., Jul. 2005. Global Consequences of Land Use. Science 309 (5734), 570–574.

Foody, G., Boyd, D., Sanchez-Hernandez, C., 2007. Mapping a specific class with an ensemble of classifiers. International Journal of Remote Sensing 28 (8), 1733–1746.

Foody, G., Hill, R., 1996. Classification of tropical forest classes from landsat tm data. International Journal of Remote Sensing 17 (12), 2353–2367.

Foody, G. M., 2002. Status of land cover classification accuracy assessment. Remote sensing of environment 80 (1), 185–201.

Forrnan, R., 1995. Land mosaics: the ecology of landscapes and regions.

Förster, M., Kleinschmit, B., 2008. Object-based classification of quickbird data using

ancillary information for the detection of forest types and natura 2000 habitats. In: Object-based image analysis. Springer, pp. 275–290.

Franco-Lopez, H., Ek, A. R., Bauer, M. E., 2001. Estimation and mapping of forest stand density, volume, and cover type using the k-nearest neighbors method. Remote sensing of environment 77 (3), 251–274.

Fraser, C. S., Dial, G., Grodecki, J., May 2006. Sensor orientation via RPCs. ISPRS Journal of Photogrammetry and Remote Sensing 60 (3), 182–194.

Fraser, C. S., Yamakawa, T., Jul. 2004. Insights into the affine model for high-resolution satellite sensor orientation. Journal of Photogrammetry and Remote Sensing 58 (5–6), 275–288.

Freund, Y., Schapire, R. E., et al., 1996. Experiments with a new boosting algorithm. In: icml. Vol. 96. pp. 148–156.

Friedl, M. A., Brodley, C. E., 1997. Decision tree classification of land cover from remotely sensed data. Remote sensing of environment 61 (3), 399–409.

Friedl, M. A., Brodley, C. E., Strahler, A. H., 1999. Maximizing land cover classification accuracies produced by decision trees at continental to global scales. IEEE Transactions on Geoscience and Remote Sensing 37 (2), 969–977.

Friedl, M. A., McIver, D. K., Hodges, J. C., Zhang, X., Muchoney, D., Strahler, A. H., Woodcock, C. E., Gopal, S., Schneider, A., Cooper, A., et al., 2002. Global land cover mapping from modis: algorithms and early results. Remote Sensing of Environment 83 (1), 287–302.

Friedl, M. A., Sulla-Menashe, D., Tan, B., Schneider, A., Ramankutty, N., Sibley, A., Huang, X., 2010. Modis collection 5 global land cover: Algorithm refinements and characterization of new datasets. Remote Sensing of Environment 114 (1), 168–182.

Fu, K. S., 1982. Applications of pattern recognition. CRC.

Fuentes, D., Gamon, J., Qiu, H.-l., Sims, D., Roberts, D., 2001. Mapping canadian boreal forest vegetation using pigment and water absorption features derived from the aviris sensor. Journal of Geophysical Research. D. Atmospheres 106, 33.

Fukunaga, K., 2013. Introduction to statistical pattern recognition. Academic press.

Fuller, D., 2005. Remote detection of invasive melaleuca trees (melaleuca quinquenervia)

in south florida with multispectral ikonos imagery. International Journal of Remote Sensing 26 (5), 1057–1063.

Fuller, D. O., 2006. Tropical forest monitoring and remote sensing: A new era of transparency in forest governance? Singapore Journal of Tropical Geography 27 (1), 15–29.

Fuller, L. M., Morgan, T. R., Aichele, S. S., 2006. Wetland delineation with ikonos high-resolution satellite imagery, fort custer training center, battle creek, michigan, 2005. Tech. rep., US Geological Survey.

Fuller, R., Groom, G., Jones, A., 1994. Land cover map of great britain. an automated classification of landsat thematic mapper data. Photogrammetric Engineering and Remote Sensing 60 (5).

Fuller, R. M., Smith, G. M., Sanderson, J. M., Hill, R. A., Thomson, A. G., 2002. The UK Land Cover Map 2000: Construction of a Parcel-Based Vector Map from Satellite Images. The Cartographic Journal 39 (1), 15–25.

Gad, S., Kusky, T., 2006. Lithological mapping in the eastern desert of egypt, the barramiya area, using landsat thematic mapper (tm). Journal of African Earth Sciences 44 (2), 196–202.

Gao, B.-C., 1996. Ndwia normalized difference water index for remote sensing of vegetation liquid water from space. Remote Sensing of Environment 58 (3), 257–266.

Gao, B.-C., Goetz, A. F., 1994. Extraction of dry leaf spectral features from reflectance spectra of green vegetation. Remote Sensing of Environment 47 (3), 369–374.

Gao, F., de Colstoun, E. B., Ma, R., Weng, Q., Masek, J. G., Chen, J., Pan, Y., Song, C., 2012. Mapping impervious surface expansion using medium-resolution satellite image time series: a case study in the yangtze river delta, china. International Journal of Remote Sensing 33 (24), 7609–7628.

Gao, J., 1999. A comparative study on spatial and spectral resolutions of satellite data in mapping mangrove forests. International Journal of Remote Sensing 20 (14), 2823–2833.

Garbulsky, M. F., Paruelo, J. M., Woods, K., 2004. Remote sensing of protected areas to derive baseline vegetation functioning characteristics. Journal of Vegetation Science 15 (5), 711–720.

Geerken, R., Zaitchik, B., Evans, J., 2005. Classifying rangeland vegetation type and coverage from ndvi time series using fourier filtered cycle similarity. International Journal of Remote Sensing 26 (24), 5535–5554.

Geurts, P., Ernst, D., Wehenkel, L., Apr. 2006. Extremely randomized trees. Machine Learning 31, 3–42.

Ghimire, B., Rogan, J., Miller, J., 2010. Contextual land-cover classification: incorporating spatial dependence in land-cover classification models using random forests and the getis statistic. Remote Sensing Letters 1 (1), 45–54.

Ghiyamat, A., Shafri, H. Z., 2010. A review on hyperspectral remote sensing for homogeneous and heterogeneous forest biodiversity assessment. International Journal of Remote Sensing 31 (7), 1837–1856.

Gillespie, T. W., 2005. Predicting woody-plant species richness in tropical dry forests: A case study from south florida, usa. Ecological Applications 15 (1), 27–37.

Giri, C., Ochieng, E., Tieszen, L. L., Zhu, Z., Singh, A., Loveland, T., Masek, J., Duke, N., 2011. Status and distribution of mangrove forests of the world using earth observation satellite data. Global Ecology and Biogeography 20 (1), 154–159.

Giri, C., Pengra, B., Long, J., Loveland, T. R., 2013. Next generation of global land cover characterization, mapping, and monitoring. International Journal of Applied Earth Observation and Geoinformation 25, 30–37.

Gislason, P. O., Benediktsson, J. A., Sveinsson, J. R., 2004. Random forest classification of multisource remote sensing and geographic data. In: Geoscience and Remote Sensing Symposium, 2004. IGARSS'04. Proceedings. 2004 IEEE International. Vol. 2. IEEE, pp. 1049–1052.

Gitelson, A. A., Kaufman, Y. J., Merzlyak, M. N., 1996. Use of a green channel in remote sensing of global vegetation from eos-modis. Remote Sensing of Environment 58 (3), 289–298.

Gitelson, A. A., Kaufman, Y. J., Stark, R., Rundquist, D., 2002. Novel algorithms for remote estimation of vegetation fraction. Remote sensing of Environment 80 (1), 76–87.

Gitelson, A. A., Keydan, G. P., Merzlyak, M. N., 2006. Three-band model for noninvasive

estimation of chlorophyll, carotenoids, and anthocyanin contents in higher plant leaves. Geophysical research letters 33 (11).

Gitelson, A. A., Merzlyak, M., Zur, Y., Stark, R., Gritz, U., 2001. Non-destructive and remote sensing techniques for estimation of vegetation status.

Gobron, N., Pinty, B., Verstraete, M. M., Widlowski, J.-L., 2000. Advanced vegetation indices optimized for up-coming sensors: Design, performance, and applications. IEEE Transactions on Geoscience and Remote Sensing 38 (6), 2489–2505.

Gong, P., Wang, J., Yu, L., Zhao, Y., Zhao, Y., Liang, L., Niu, Z., Huang, X., Fu, H., Liu, S., et al., 2013. Finer resolution observation and monitoring of global land cover: First mapping results with landsat tm and etm+ data. International Journal of Remote Sensing 34 (7), 2607–2654.

Google Cloud Platform, 2016. Sentinel-2 Public Dataset. URL: https://cloud.google.com/storage/docs/public-datasets/sentinel-2.

Grabowski, S., Jóźwik, A., Chen, C., 2003. Nearest neighbor decision rule for pixel classification in remote sensing. In: Frontiers Of Remote Sensing Information Processing. World Scientific, pp. 315–327.

Graf, R. F., Mathys, L., Bollmann, K., 2009. Habitat assessment for forest dwelling species using lidar remote sensing: Capercaillie in the alps. Forest Ecology and Management 257 (1), 160–167.

Griffiths, H. I., Thomas, D. H., et al., 1997. The conservation and management of the European badger (Meles meles):(revised results of an enquiry into the species, originally presented as a report to the Standing Committee of the Convention on the Conservation of European Wildlife and Natural Habitats, on the population and management status and conservation needs of the species in the Western Palaearctic). Vol. 90. Council of Europe.

Grime, J. P., Hodgson, J. G., Hunt, R., 2014. Comparative plant ecology: a functional approach to common British species. Springer.

Guo, L., Chehata, N., Mallet, C., Boukir, S., 2011. Relevance of airborne lidar and multispectral image data for urban scene classification using random forests. ISPRS Journal of Photogrammetry and Remote Sensing 66 (1), 56–66.

Guyot, G., et al., 1990. Optical properties of vegetation canopies. Optical properties of vegetation canopies., 19–43.

Hall, K., Reitalu, T., Sykes, M. T., Prentice, H. C., 2012. Spectral heterogeneity of quickbird satellite data is related to fine-scale plant species spatial turnover in semi-natural grasslands. Applied Vegetation Science 15 (1), 145–157.

Hallegatte, S., 2009. Strategies to adapt to an uncertain climate change. Global environmental change 19 (2), 240–247.

Hancock, D. W., 2006. Spectral reflectance of canopies of rainfed and subsurface irrigated alfalfa.

Hansen, L. K., Salamon, P., 1990. Neural network ensembles. IEEE transactions on pattern analysis and machine intelligence 12 (10), 993–1001.

Hansen, M., DeFries, R., Townshend, J., Sohlberg, R., Dimiceli, C., Carroll, M., 2002. Towards an operational modis continuous field of percent tree cover algorithm: examples using avhrr and modis data. Remote Sensing of Environment 83 (1), 303–319.

Hansen, M., DeFries, R., Townshend, J. R., Sohlberg, R., 2000. Global land cover classification at 1 km spatial resolution using a classification tree approach. International journal of remote sensing 21 (6-7), 1331–1364.

Harris, A., Bryant, R. G., 2009. A multi-scale remote sensing approach for monitoring northern peatland hydrology: Present possibilities and future challenges. Journal of Environmental Management 90 (7), 2178–2188.

Harvey, K. R., Hill, G. J. E., Nov. 2001. Vegetation mapping of a tropical freshwater swamp in the Northern Territory, Australia: A comparison of aerial photography, Landsat TM and SPOT satellite imagery. International Journal of Remote Sensing 22 (15), 2911–2925.

Hatunen, S., Härmä, P., Kallio, M., Törmä, M., 2008. Classification of natural areas in northern finland using remote sensing images and ancillary data. In: SPIE Remote Sensing. International Society for Optics and Photonics, pp. 71100W–71100W.

Hay, G. J., Castilla, G., 2008. Geographic object-based image analysis (geobia): A new name for a new discipline. In: Object-based image analysis. Springer, pp. 75–89.

He, K. S., Rocchini, D., Neteler, M., Nagendra, H., 2011. Benefits of hyperspectral remote sensing for tracking plant invasions. Diversity and Distributions 17 (3), 381–392.

Heiden, U., Segl, K., Roessner, S., Kaufmann, H., Dec. 2007. Determination of robust spectral features for identification of urban surface materials in hyperspectral remote sensing data. Remote Sensing of Environment 111 (4), 537–552.

Herold, M., Mayaux, P., Woodcock, C., Baccini, A., Schmullius, C., 2008. Some challenges in global land cover mapping: An assessment of agreement and accuracy in existing 1 km datasets. Remote Sensing of Environment 112 (5), 2538–2556.

Herold, M., Woodcock, C. E., Di Gregorio, A., Mayaux, P., Belward, A. S., Latham, J., Schmullius, C. C., 2006. A joint initiative for harmonization and validation of land cover datasets. IEEE Transactions on Geoscience and Remote Sensing 44 (7), 1719–1727.

Herrmann, I., Karnieli, A., Bonfil, D., Cohen, Y., Alchanatis, V., 2010. Swir-based spectral indices for assessing nitrogen content in potato fields. International Journal of Remote Sensing 31 (19), 5127–5143.

Hester, D., Nelson, S., Cakir, H., Khorram, S., Cheshire, H., 2010. High-resolution land cover change detection based on fuzzy uncertainty analysis and change reasoning. International Journal of Remote Sensing 31 (2), 455–475.

Hestir, E. L., Khanna, S., Andrew, M. E., Santos, M. J., Viers, J. H., Greenberg, J. A., Rajapakse, S. S., Ustin, S. L., 2008. Identification of invasive vegetation using hyperspectral remote sensing in the california delta ecosystem. Remote Sensing of Environment 112 (11), 4034–4047.

Hewitson, B. C., Crane, R. G., 1994. Looks and uses. In: Neural Nets: Applications in Geography. Springer, pp. 1–9.

Hewitt, M. J., 1990. Synoptic inventory of riparian ecosystems: the utility of landsat thematic mapper data. Forest ecology and management 33, 605–620.

Higinbotham, C. B., Alber, M., Chalmers, A. G., 2004. Analysis of tidal marsh vegetation patterns in two georgia estuaries using aerial photography and gis. Estuaries and Coasts 27 (4), 670–683.

Horler, D., Dockray, M., Barber, J., 1983. The red edge of plant leaf reflectance. International Journal of Remote Sensing 4 (2), 273–288.

Houston, J. A., 2008. Management of Natura 2000 habitats. 2190 Humid dune slacks. European Commission.

Howard, D., Watkins, J., Clarke, R., Barnett, C., Stark, G., 2003. Estimating the extent and change in broad habitats in great britain. Journal of Environmental Management 67 (3), 219–227.

Howard, J. A., et al., 1970. Aerial photo-ecology. Aerial photo-ecology.

Howe, L., Blackstock, T., Burrows, C., Stevens, J., 2005. The habitat survey of wales. British Wildlife 16 (3), 153–162.

Howland, W. G., et al., 1980. Multispectral aerial photography for wetland vegetation mapping. Photogrammetric Engineering and Remote Sensing 46 (1), 87–99.

Huang, C., Davis, L., Townshend, J., 2002. An assessment of support vector machines for land cover classification. International Journal of Remote Sensing 23 (4), 725–749.

Huete, A., Liu, H., Batchily, K. v., Van Leeuwen, W., 1997. A comparison of vegetation indices over a global set of tm images for eos-modis. Remote sensing of environment 59 (3), 440–451.

Hughes, G., 1968. On the mean accuracy of statistical pattern recognizers. IEEE transactions on information theory 14 (1), 55–63.

Hulbert, I. A., French, J., 2001. The accuracy of gps for wildlife telemetry and habitat mapping. Journal of Applied Ecology 38 (4), 869–878.

Hunt Jr., E. R., Doraiswamya, P. C., McMurtreya, J. E., Daughtrya, C. S. T., Perryb, E. M., Akhmedova, B., Apr. 2013. A visible band index for remote sensing leaf chlorophyll content at the canopy scale. International Journal of Applied Earth Observation and Geoinformation 21, 103–112.

Hunting Surveys and Consultants, 1986. Monitoring Landscape Change. Hunting Technical Surveys.

Hurford, C., 2006. Remote sensing of dune habitats at kenfig nnr. In: Monitoring Nature Conservation in Cultural Habitats. Springer, pp. 341–352.

Hussain, M., Chen, D., Cheng, A., Wei, H., Stanley, D., 2013. Change detection from remotely sensed images: From pixel-based to object-based approaches. ISPRS Journal of Photogrammetry and Remote Sensing 80, 91–106.

Hyde, P., Dubayah, R., Walker, W., Blair, J. B., Hofton, M., Hunsaker, C., 2006. Mapping

forest structure for wildlife habitat analysis using multi-sensor (lidar, sar/insar, etm+, quickbird) synergy. Remote Sensing of Environment 102 (1), 63–73.

Im, J., Jensen, J. R., 2005. A change detection model based on neighborhood correlation image analysis and decision tree classification. Remote Sensing of Environment 99 (3), 326–340.

Inglada, J., Christophe, E., 2009. The orfeo toolbox remote sensing image processing software. In: Geoscience and Remote Sensing Symposium, 2009 IEEE International, IGARSS 2009. Vol. 4. IEEE, pp. IV–733.

Ingram, J. C., Dawson, T. P., Whittaker, R. J., 2005. Mapping tropical forest structure in southeastern madagascar using remote sensing and artificial neural networks. Remote Sensing of Environment 94 (4), 491–507.

Ishii, J., Lu, S., Funakoshi, S., Shimizu, Y., Omasa, K., Washitani, I., 2009. Mapping potential habitats of threatened plant species in a moist tall grassland using hyperspectral imagery. Biodiversity and Conservation 18 (9), 2521–2535.

Jacobsen, K., 2005. High Resolution Satellite Imaging Systems-an Overview. Photogrammetrie Fernerkundung Geoinformation 2005 (6), 487.

Jain, A. K., Duin, R. P. W., Mao, J., 2000. Statistical pattern recognition: A review. IEEE Transactions on pattern analysis and machine intelligence 22 (1), 4–37.

JNCC, Jan. 2006. Common Standards Monitoring for Designated Sites.

JNCC, 2007a. Second Report by the United Kingdom under Article 17 on the implementation of the Directive from January 2001 to December 2006. H1230: Vegetated sea cliffs of the Atlantic and Baltic coasts . JNCC Peterborough.

JNCC, 2007b. Second Report by the United Kingdom under Article 17 on the implementation of the Directive from January 2001 to December 2006. H2130: Fixed dunes with herbaceous vegetation (‘grey dunes‘). JNCC Peterborough.

JNCC, 2007c. Second Report by the United Kingdom under Article 17 on the implementation of the Directive from January 2001 to December 2006. H2170: Dunes with Salix repens ssp. argentea (Salicion arenariae). JNCC Peterborough.

JNCC, 2007d. Second Report by the United Kingdom under Article 17 on the implementation of the Directive from January 2001 to December 2006. H2190: Humid dune slacks. JNCC Peterborough.

Jones, D. A., Hansen, A. J., Bly, K., Doherty, K., Verschuyl, J. P., Paugh, J. I., Carle, R., Story, S. J., 2009. Monitoring land use and cover around parks: A conceptual approach. Remote Sensing of Environment 113 (7), 1346–1356.

Jordan, C. F., 1969. Derivation of leaf-area index from quality of light on the forest floor. Ecology 50 (4), 663–666.

Joseph, S., Murthy, M., Thomas, A., 2011. The progress on remote sensing technology in identifying tropical forest degradation: a synthesis of the present knowledge and future perspectives. Environmental Earth Sciences 64 (3), 731–741.

Joshi, C., De Leeuw, J., Skidmore, A. K., Van Duren, I. C., Van Oosten, H., 2006. Remotely sensed estimation of forest canopy density: A comparison of the performance of four methods. International Journal of Applied Earth Observation and Geoinformation 8 (2), 84–95.

Jung, M., Henkel, K., Herold, M., Churkina, G., 2006. Exploiting synergies of global land cover products for carbon cycle modeling. Remote Sensing of Environment 101 (4), 534–553.

Karjalainen, M., Pyysalo, U., Karila, K., Hyyppa, J., 2008. Forest biomass estimation using alos palsar images in challenging natural forest area in finland.

Kasischke, E. S., Melack, J. M., Dobson, M. C., 1997. The use of imaging radars for ecological applicationsa review. Remote Sensing of Environment 59 (2), 141–156.

Kavzoglu, T., Mather, P. M., 1999. Pruning artificial neural networks: an example using land cover classification of multi-sensor images. International Journal of Remote Sensing 20 (14), 2787–2803.

Kenfig Website, 2013. Management at kenfig burrows nnr.

Kerr, J. T., Ostrovsky, M., 2003. From space to species: ecological applications for remote sensing. Trends in Ecology & Evolution 18 (6), 299–305.

Keshava, N., Mustard, J. F., 2002. Spectral unmixing. IEEE signal processing magazine 19 (1), 44–57.

Keuchel, J., Naumann, S., Heiler, M., Siegmund, A., 2003. Automatic land cover analysis for tenerife by supervised classification using remotely sensed data. Remote sensing of environment 86 (4), 530–541.

Klemas, V., 2011. Remote sensing of wetlands: case studies comparing practical techniques. Journal of Coastal Research 27 (3), 418–427.

Knee, M., 1988. Carotenol esters in developing apple fruits. Phytochemistry 27 (4), 1005–1009.

Knerr, S., Personnaz, L., Dreyfus, G., 1990. Single-layer learning revisited: a stepwise procedure for building and training a neural network. In: Neurocomputing. Springer, pp. 41–50.

Koch, B., 2010. Status and future of laser scanning, synthetic aperture radar and hyperspectral remote sensing data for forest biomass assessment. ISPRS Journal of Photogrammetry and Remote Sensing 65 (6), 581–590.

Kohavi, R., 1996. Scaling up the accuracy of naive-bayes classifiers: A decision-tree hybrid. In: KDD. Vol. 96. Citeseer, pp. 202–207.

Kooistra, L., Leuven, R., Wehrens, R., Nienhuis, P., Buydens, L., 2003. A comparison of methods to relate grass reflectance to soil metal contamination. International Journal of Remote Sensing 24 (24), 4995–5010.

Kosmidou, V., Petrou, Z., Bunce, R. G., Mücher, C. A., Jongman, R. H., Bogers, M. M., Lucas, R. M., Tomaselli, V., Blonda, P., Padoa-Schioppa, E., 2014. Harmonization of the Land Cover Classification System (LCCS) with the General Habitat Categories (GHC) classification system. Ecological Indicators 36, 290–300.

Kotliar, N. B., Wiens, J. A., 1990. Multiple scales of patchiness and patch structure: a hierarchical framework for the study of heterogeneity. Oikos, 253–260.

Kotsiantis, S., Pintelas, P., 2004. Combining bagging and boosting. International Journal of Computational Intelligence 1 (4), 324–333.

Krogh, A., Vedelsby, J., et al., 1995. Neural network ensembles, cross validation, and active learning. Advances in neural information processing systems 7, 231–238.

Kumar, S., Simonson, S. E., Stohlgren, T. J., 2009. Effects of spatial heterogeneity on butterfly species richness in rocky mountain national park, co, usa. Biodiversity and Conservation 18 (3), 739–763.

Kuplich, T. M., 2006. Classifying regenerating forest stages in amazonia using remotely sensed images and a neural network. Forest Ecology and Management 234 (1), 1–9.

Laba, M., Downs, R., Smith, S., Welsh, S., Neider, C., White, S., Richmond, M., Philpot, W., Baveye, P., 2008. Mapping invasive wetland plants in the hudson river national estuarine research reserve using quickbird satellite imagery. Remote Sensing of Environment 112 (1), 286–300.

Landgrebe, D. A., 2005. Signal theory methods in multispectral remote sensing. Vol. 29. John Wiley & Sons.

Landis, J. R., Koch, G. G., 1977. An application of hierarchical kappa-type statistics in the assessment of majority agreement among multiple observers. Biometrics, 363–374.

Langley, S. K., Cheshire, H. M., Humes, K. S., 2001. A comparison of single date and multitemporal satellite image classifications in a semi-arid grassland. Journal of Arid Environments 49 (2), 401–411.

Latifi, H., Nothdurft, A., Koch, B., 2010. Non-parametric prediction and mapping of standing timber volume and biomass in a temperate forest: application of multiple optical/lidar-derived predictors. Forestry 83 (4), 395–407.

Lawrence, R. L., Wood, S. D., Sheley, R. L., 2006. Mapping invasive plants using hyperspectral imagery and breiman cutler classifications (randomforest). Remote Sensing of Environment 100 (3), 356–362.

Le Maire, G., Francois, C., Dufrene, E., 2004. Towards universal broad leaf chlorophyll indices using prospect simulated database and hyperspectral reflectance measurements. Remote sensing of environment 89 (1), 1–28.

Le Maire, G., François, C., Soudani, K., Berveiller, D., Pontailler, J.-Y., Bréda, N., Genet, H., Davi, H., Dufrêne, E., 2008. Calibration and validation of hyperspectral indices for the estimation of broadleaved forest leaf chlorophyll content, leaf mass per area, leaf area index and leaf canopy biomass. Remote Sensing of Environment 112 (10), 3846–3864.

Lee, M., Park, G., Park, M., Park, J., Lee, J., Kim, S., 2010. Evaluation of non-point source pollution reduction by applying best management practices using a swat model and quickbird high resolution satellite imagery. Journal of Environmental Sciences 22 (6), 826–833.

Legleiter, C. J., Marcus, W., Lawrence, R., 2002. Effects of sensor resolution on mapping instream habitats. Photogrammetric Engineering and Remote Sensing 68 (8), 801–807.

Lehmann, A., Lachavanne, J.-B., 1997. Geographic information systems and remote sensing in aquatic botany. Aquatic Botany 58 (3-4), 195–207.

Leidner, A., Turner, W., Pettorelli, N., Leimgruber, P., Wegmann, M., 2012. Satellite remote sensing for biodiversity research and conservation applications: a committee on earth observation satellites (ceos) workshop.

Lek, S., Guégan, J.-F., 1999. Artificial neural networks as a tool in ecological modelling, an introduction. Ecological modelling 120 (2), 65–73.

Lengyel, S., Déri, E., Varga, Z., Horváth, R., Tóthmérész, B., Henry, P.-Y., Kobler, A., Kutnar, L., Babij, V., Seliškar, A., et al., 2008. Habitat monitoring in europe: a description of current practices. Biodiversity and Conservation 17 (14), 3327–3339.

Lentile, L. B., Holden, Z. A., Smith, A. M., Falkowski, M. J., Hudak, A. T., Morgan, P., Lewis, S. A., Gessler, P. E., Benson, N. C., et al., 2006. Remote sensing techniques to assess active fire characteristics and post-fire effects. International Journal of Wildland Fire 15 (3), 319–345.

Leprince, S., Barbot, S., Ayoub, F., Avouac, J.-P., Jun. 2007. Automatic and Precise Orthorectification, Coregistration, and Subpixel Correlation of Satellite Images, Application to Ground Deformation Measurements. IEEE Transactions on Geoscience and Remote Sensing 45 (6), 1529–1558.

Lieth, H., 1971. The phenological viewpoint in productivity studies. In: Productivity of forest ecosystems. Proceedings of the Brussels Symposium by UNESCO. pp. 71–83.

Lillesand, T. M., Kiefer, R. W., Chipman, J. W., 2004. Remote Sensing and Image Interpretation. John Wiley & Sons Ltd.

Listner, C., Niemeyer, I., 2011. Object-based change detection. Photogrammetrie Fernerkundung Geoinformation 2011 (4), 233–245.

Liu, S., Liu, R., Liu, Y., 2010. Spatial and temporal variation of global lai during 1981–2006. Journal of Geographical Sciences 20 (3), 323–332.

Liu, X., Zhang, Z., Peterson, J., Chandra, S., Jan. 2007. LiDAR-Derived High Quality Ground Control Information and DEM for Image Orthorectification. GeoInformatica 11 (1), 37–53.

Loveland, T. R., Reed, B. C., Brown, J. F., Ohlen, D. O., Zhu, Z., Yang, L., Merchant, J. W., 2000. Development of a global land cover characteristics database and igbp dis-

cover from 1 km avhrr data. International Journal of Remote Sensing 21 (6-7), 1303–1330.

Ltd, B. C. G., 2000. Beneficial use of dredged sand, sand from neath estuary used for beach nourishment at sker.

Lu, D., Mausel, P., Brondizio, E., Moran, E., 2004. Change detection techniques. International Journal of Remote Sensing 25 (12), 2365–2401.

Lu, F., De-peng, Y., Xiang, G., 2009. A review on application of normal different vegetation index [j]. Forest Inventory and Planning 2, 014.

Lucas, N. S., Shanmugam, S., Barnsley, M., Jul. 2002. Sub-pixel habitat mapping of a costal dune ecosystem. Applied Geography 22 (3), 253–270.

Lucas, R., Blonda, P., Bunting, P., Jones, G., Inglada, J., Arias, M., Kosmidou, V., Petrou, Z. I., Manakos, I., Adamo, M., 2015. The Earth Observation Data for Habitat Monitoring (EODHaM) system. International Journal of Applied Earth Observation and Geoinformation 37, 17–28.

Lucas, R., Bunting, P., Paterson, M., Chisholm, L., 2008. Classification of australian forest communities using aerial photography, casi and hymap data. Remote Sensing of Environment 112 (5), 2088–2103.

Lucas, R., Medcalf, K., Brown, A., Bunting, P., Breyer, J., Clewley, D., Keyworth, S., Blackmore, P., Jan. 2011. Updating the Phase 1 habitat map of Wales, UK, using satellite sensor data. ISPRS Journal of Photogrammetry and Remote Sensing 66 (1), 81–102.

Lucas, R., OConnor, B., Inglada, J., Mucher, S., Roupioz, L., Nagendra, H., Adamo, M., Tarantino, C., P, B., 2012. Hyper-spectral Remote Sensing. BIOSOS Biodiversity Multisource Monitoring System:from Space TO Species.

Lucas, R., Rowlands, A., Brown, A., Keyworth, S., Bunting, P., 2007. Rule-based classification of multi-temporal satellite imagery for habitat and agricultural land cover mapping. ISPRS Journal of photogrammetry and remote sensing 62 (3), 165–185.

Lymburner, L., Beggs, P. J., Jacobson, C. R., et al., 2000. Estimation of canopy-average surface-specific leaf area using landsat tm data. Photogrammetric Engineering and Remote Sensing 66 (2), 183–192.

MacAlister, C., Mahaxay, M., 2009. Mapping wetlands in the lower mekong basin for

wetland resource and conservation management using landsat etm images and field survey data. Journal of Environmental Management 90 (7), 2130–2137.

Maccioni, A., Agati, G., Mazzinghi, P., 2001. New vegetation indices for remote measurement of chlorophylls based on leaf directional reflectance spectra. Journal of Photochemistry and Photobiology B: Biology 61 (1), 52–61.

Main, R., Cho, M. A., Mathieu, R., OKennedy, M. M., Ramoelo, A., Koch, S., 2011. An investigation into robust spectral indices for leaf chlorophyll estimation. ISPRS Journal of Photogrammetry and Remote Sensing 66 (6), 751–761.

Major, D., Baret, F., Guyot, G., 1990. A ratio vegetation index adjusted for soil brightness. International Journal of Remote Sensing 11 (5), 727–740.

Malthus, T. J., Mumby, P. J., 2003. Remote sensing of the coastal zone: an overview and priorities for future research. International Journal of Remote Sensing 24 (13), 2805–2815.

Mantero, P., Moser, G., Serpico, S. B., 2005. Partially supervised classification of remote sensing images through svm-based probability density estimation. IEEE Transactions on Geoscience and Remote Sensing 43 (3), 559–570.

Marceau, D. J., Howarth, P. J., Gratton, D. J., 1994. Remote sensing and the measurement of geographical entities in a forested environment. 1. the scale and spatial aggregation problem. Remote Sensing of environment 49 (2), 93–104.

Martinuzzi, S., Vierling, L. A., Gould, W. A., Falkowski, M. J., Evans, J. S., Hudak, A. T., Vierling, K. T., 2009. Mapping snags and understory shrubs for a lidar-based assessment of wildlife habitat suitability. Remote Sensing of Environment 113 (12), 2533–2546.

Mas, J. F., Flores, J. J., 2008. The application of artificial neural networks to the analysis of remotely sensed data. International Journal of Remote Sensing 29 (3), 617–663.

Matthews, E., 1983. Global vegetation and land use: New high-resolution data bases for climate studies. Journal of Climate and Applied Meteorology 22 (3), 474–487.

Mayer, A. L., Lopez, R. D., 2011. Use of remote sensing to support forest and wetlands policies in the usa. Remote Sensing 3 (6), 1211–1233.

McCarthy, D. P., Donald, P. F., Scharlemann, J. P., Buchanan, G. M., Balmford, A., Green, J. M., Bennun, L. A., Burgess, N. D., Fishpool, L. D., Garnett, S. T., et al., 2012.

Financial costs of meeting global biodiversity conservation targets: current spending and unmet needs. Science 338 (6109), 946–949.

McDermid, G. J., Franklin, S. E., LeDrew, E. F., Dec. 2005. Remote sensing for large-area habitat mapping. Progress in Physical Geography 29 (4), 449–474.

Medcalf, K. A., Parker, J. A., N, T., C, F., 2011. Making Earth Observation Work for UK Biodiversity Conservation - Phase 1. JNCC.

Melgani, F., Bruzzone, L., 2004. Classification of hyperspectral remote sensing images with support vector machines. IEEE Transactions on geoscience and remote sensing 42 (8), 1778–1790.

Menzel, A., 2002. Phenology: its importance to the global change community. Climatic Change 54 (4), 379–385.

Merzlyak, M., Gitelson, A. A., Chivkunova, O., Solovchenko, A., Pogosyan, S., 2003. Application of reflectance spectroscopy for analysis of higher plant pigments. Russian Journal of Plant Physiology 50 (5), 704–710.

Merzlyak, M. N., Gitelson, A. A., Chivkunova, O. B., Rakitin, V. Y., 1999. Non-destructive optical detection of pigment changes during leaf senescence and fruit ripening. Physiologia Plantarum 106 (1), 135–141.

Met Office, 2013. Met Offie Website. URL: http://www.metoffice.gov.uk/news/in-depth/uk-weather-2012.

Metternicht, G., 2003. Vegetation indices derived from high-resolution airborne videography for precision crop management. International Journal of Remote Sensing 24 (14), 2855–2877.

Michelson, D. B., Liljeberg, B. M., Pilesjö, P., 2000. Comparison of algorithms for classifying swedish landcover using landsat tm and ers-1 sar data. Remote Sensing of Environment 71 (1), 1–15.

Mingers, J., 1989a. An empirical comparison of pruning methods for decision tree induction. Machine Learning 4 (2), 227–243.

Mingers, J., 1989b. An empirical comparison of selection measures for decision-tree induction. Machine learning 3 (4), 319–342.

Mitchell, T. M., 1997. Machine learning. 1997. Burr Ridge, IL: McGraw Hill 45 (37), 870–877.

Mora, B., Tsendbazar, N.-E., Herold, M., Arino, O., 2014. Global land cover mapping: Current status and future trends. In: Land Use and Land Cover Mapping in Europe. Springer, pp. 11–30.

Morán-Ordóñez, A., Suárez-Seoane, S., Elith, J., Calvo, L., de Luis, E., 2012. Satellite surface reflectance improves habitat distribution mapping: a case study on heath and shrub formations in the cantabrian mountains (nw spain). Diversity and Distributions 18 (6), 588–602.

Mountrakis, G., Im, J., Ogole, C., 2011. Support vector machines in remote sensing: A review. ISPRS Journal of Photogrammetry and Remote Sensing 66 (3), 247–259.

Mountrakis, G., Watts, R., Luo, L., Wang, J., 2009. Developing collaborative classifiers using an expert-based model. Photogrammetric Engineering & Remote Sensing 75 (7), 831–843.

Mücher, C., 2011. Monitoring biodiversity using remote sensing and field surveys.

Muldavin, E. H., Neville, P., Harper, G., 2001. Indices of grassland biodiversity in the chihuahuan desert ecoregion derived from remote sensing. Conservation Biology 15 (4), 844–855.

Müller, R., Krauß, T., Lehner, M., Reinartz, P., 2007. Automatic production of a European orthoimage coverage within the GMES land fast track service using SPOT 4/5 and IRS-P6 LISS III data.

Muller, S., Walker, D., Nelson, F., Auerback, N., Bockheim, J., Guyer, S., Sherba, D., 1998. Accuracy assessment of a land-cover map of the kuparuk river basin, alaska: considerations for remote regions. Photogrammetric Engineering and Remote Sensing 64 (6), 619–628.

Mutanga, O., Adam, E., Cho, M. A., 2012. High density biomass estimation for wetland vegetation using worldview-2 imagery and random forest regression algorithm. International Journal of Applied Earth Observation and Geoinformation 18, 399–406.

Nagendra, H., 2001. Using remote sensing to assess biodiversity. International Journal of Remote Sensing 22 (12), 2377–2400.

Nagendra, H., Lucas, R., Honrado, J. P., Jongman, R. H., Tarantino, C., Adamo, M.,

Mairota, P., 2013. Remote sensing for conservation monitoring: Assessing protected areas, habitat extent, habitat condition, species diversity, and threats. Ecological Indicators 33, 45–59.

Nagendra, H., Rocchini, D., 2008. High resolution satellite imagery for tropical biodiversity studies: the devil is in the detail. Biodiversity and Conservation 17 (14), 3431.

Nagendra, H., Rocchini, D., Ghate, R., 2010a. Beyond parks as monoliths: Spatially differentiating park-people relationships in the tadoba andhari tiger reserve in india. Biological Conservation 143 (12), 2900–2908.

Nagendra, H., Rocchini, D., Ghate, R., Sharma, B., Pareeth, S., 2010b. Assessing plant diversity in a dry tropical forest: Comparing the utility of landsat and ikonos satellite images. Remote Sensing 2 (2), 478–496.

NASA Jet Propulsion Laboratory, 2014. Shuttle Radar Topography Mission. URL: http://www2.jpl.nasa.gov/srtm/.

National Assembly for Wales, 2006. Environment Strategy for Wales. URL: http://www.assemblywales.org/07-005.pdf.

Nunes, M. C., Vasconcelos, M. J., Pereira, J. M., Dasgupta, N., Alldredge, R. J., Rego, F. C., 2005. Land cover type and fire in portugal: do fires burn land cover selectively? Landscape Ecology 20 (6), 661–673.

Oldeland, J., Dorigo, W., Lieckfeld, L., Lucieer, A., Jürgens, N., Jun. 2010. Combining vegetation indices, constrained ordination and fuzzy classification for mapping semi-natural vegetation units from hyperspectral imagery. Remote Sensing of Environment 114 (6), 1155–1166.

Olson, J., 1982. Earth's vegetation and atmospheric carbon dioxide. Carbon dioxide review 1982, 388–398.

Ostermann, O. P., Dec. 1998. The Need for Management of Nature Conservation Sites Designated Under Natura 2000. Journal of Applied Ecology 35 (6), 968–973.

Ozdemir, I., Karnieli, A., Oct. 2011. Predicting forest structural parameters using the image texture derived from WorldView-2 multispectral imagery in a dryland forest, Israel. International Journal of Applied Earth Observation and Geoinformation 13 (5), 701–710.

Pacificia, F., Chinib, M., Emeryc, W. J., Jun. 2009. A neural network approach using

multi-scale textural metrics from very high-resolution panchromatic imagery for urban land-use classification. Remote Sensing of Environment 113, 1276–1292.

Pal, M., 2005. Random forest classifier for remote sensing classification. International Journal of Remote Sensing 26 (1), 217–222.

Pal, M., Mather, P., 2005. Support vector machines for classification in remote sensing. International Journal of Remote Sensing 26 (5), 1007–1011.

Pal, M., Mather, P. M., 2003. An assessment of the effectiveness of decision tree methods for land cover classification. Remote sensing of environment 86 (4), 554–565.

Papeş, M., Tupayachi, R., Martinez, P., Peterson, A., Powell, G., 2010. Using hyperspectral satellite imagery for regional inventories: a test with tropical emergent trees in the amazon basin. Journal of Vegetation Science 21 (2), 342–354.

Paul, M. M., Magaly, K., 2011. Computer Processing of Remotely Sensed ImagesAn Introduction. John Wiley & Sons Ltd.

Peddle, D. R., 1995. Knowledge formulation for supervised evidential classification. Photogrammetric Engineering and Remote Sensing 61 (4), 409–417.

Pembrokeshire National Park, 2011. Pembrokeshire coast national park lca 6 - castlemartin/merrion ranges.

Peñuelas, J., Filella, I., Biel, C., Serrano, L., Save, R., 1993. The reflectance at the 950–970 nm region as an indicator of plant water status. International Journal of Remote Sensing 14 (10), 1887–1905.

Petrou, Z., Manakos, I., Stathaki, T., Tarantino, C., Adamo, M., Blonda, P., 2014a. A vegetation height classification approach based on texture analysis of a single vhr image. In: IOP Conference Series: Earth and Environmental Science. Vol. 17. IOP Publishing, p. 012210.

Petrou, Z., Tarantino, C., Adamo, M., Blonda, P., Petrou, M., 2012. Estimation of vegetation height through satellite image texture analysis. In: Proceedings of the International archives of the photogrammetry, remote sensing and spatial information sciences, XXII ISPRS Congress, Melbourne. Vol. 25. pp. 321–326.

Petrou, Z. I., Kosmidou, V., Manakos, I., Stathaki, T., Adamo, M., Tarantino, C., Tomaselli, V., Blonda, P., Petrou, M., 2014b. A rule-based classification methodology

to handle uncertainty in habitat mapping employing evidential reasoning and fuzzy logic. Pattern Recognition Letters 48, 24–33.

Pimm, S. L., Raven, P., Feb. 2000. Biodiversity: Extinction by numbers. Nature 403 (6772), 843–845.

Pinter Jr, P. J., Hatfield, J. L., Schepers, J. S., Barnes, E. M., Moran, M. S., Daughtry, C. S., Upchurch, D. R., 2003. Remote sensing for crop management. Photogrammetric Engineering & Remote Sensing 69 (6), 647–664.

Plieninger, T., 2006. Habitat loss, fragmentation, and alteration–quantifying the impactof land-use changes on a spanish dehesa landscape by use of aerial photography and gis. Landscape Ecology 21 (1), 91–105.

Pôças, I., Cunha, M., Marcal, A. R., Pereira, L. S., 2011. An evaluation of changes in a mountainous rural landscape of northeast portugal using remotely sensed data. Landscape and Urban Planning 101 (3), 253–261.

Price, J. C., 1994. How unique are spectral signatures? Remote Sensing of Environment 49 (3), 181–186.

Price, K. P., Guo, X., Stiles, J. M., 2002. Optimal landsat tm band combinations and vegetation indices for discrimination of six grassland types in eastern kansas. International Journal of Remote Sensing 23 (23), 5031–5042.

Provoost, S., Jones, M. L. M., Edmondson, S. E., 2011. Changes in landscape and vegetation of coastal dunes in northwest europe: a review. Journal of Coastal Conservation 15 (1), 207–226.

Pu, R., Gong, P., 2004. Determination of burnt scars using logistic regression and neural network techniques from a single post-fire landsat 7 etm+ image. Photogrammetric Engineering & Remote Sensing 70 (7), 841–850.

Pu, R., Gong, P., Yu, Q., 2008. Comparative analysis of eo-1 ali and hyperion, and landsat etm+ data for mapping forest crown closure and leaf area index. Sensors 8 (6), 3744–3766.

Pye, K., Blott, S., 2009. Coastal processes and shoreline behaviour of estuary dominated systems in swansea bay and carmarthen bay. Report prepared on behalf of Halcrow Group Ltd., Swindon, by K. Pye Associates, Crowthorne 15.

Pye, K., Blott, S. J., 2011. Kenfig sand dunes - potential for dune reactivation.

Pye, K., Saye, S., 2005. The geomorphological response of welsh sand dunes to sea level rise over the next 100 Years and the management implications for SAC and SSSI sites. Countryside Council for Wales.

Qiu, H.-L., Sanchez-Azofeifa, A., Gamon, J. A., 2007. Ecological applications of remote sensing at multiple scales.

Quinlan, J. R., 1987. Simplifying decision trees. International journal of man-machine studies 27 (3), 221–234.

Quinlan, J. R., 2014. C4. 5: programs for machine learning. Elsevier.

Rahman, M. M., Sumantyo, J. T. S., 2010. Mapping tropical forest cover and deforestation using synthetic aperture radar (sar) images. Applied Geomatics 2 (3), 113–121.

Rama Rao, N., Garg, P., Ghosh, S., 2007. Evaluation of radiometric resolution on land use/land cover mapping in an agricultural area. International Journal of Remote Sensing 28 (2), 443–450.

Ramsey III, E., Rangoonwala, A., Nelson, G., Ehrlich, R., 2005. Mapping the invasive species, chinese tallow, with eo1 satellite hyperion hyperspectral image data and relating tallow occurrences to a classified landsat thematic mapper land cover map. International Journal of Remote Sensing 26 (8), 1637–1657.

Rapinel, S., Clément, B., Magnanon, S., Sellin, V., Hubert-Moy, L., 2014. Identification and mapping of natural vegetation on a coastal site using a worldview-2 satellite image. Journal of environmental management 144, 236–246.

Raunikar, R. P., Forney, W. M., Benjamin, S. P., 2013. What is the economic value of satellite imagery? Tech. rep., US Geological Survey.

Reinartz, P., Müller, R., Schwind, P., Suri, S., Bamler, R., Jan. 2011. Orthorectification of VHR optical satellite data exploiting the geometric accuracy of TerraSAR-X data. ISPRS Journal of Photogrammetry and Remote Sensing 66 (1), 124–132.

Rhind, P., Jones, P., 1999. The floristics and conservation status of sand-dune communities in wales. Journal of Coastal Conservation 5 (1), 31–42.

Richardson, A. D., Duigan, S. P., Berlyn, G. P., 2002. An evaluation of noninvasive methods to estimate foliar chlorophyll content. New phytologist 153 (1), 185–194.

Rodriguez-Galiano, V., Chica-Olmo, M., Abarca-Hernandez, F., Atkinson, P. M., Je-

ganathan, C., 2012a. Random forest classification of mediterranean land cover using multi-seasonal imagery and multi-seasonal texture. Remote Sensing of Environment 121, 93–107.

Rodriguez-Galiano, V. F., Ghimire, B., Rogan, J., Chica-Olmo, M., Rigol-Sanchez, J. P., Jan. 2012b. An assessment of the effectiveness of a random forest classifier for land-cover classification. ISPRS Journal of Photogrammetry and Remote Sensing 67, 93–104.

Rogan, J., Franklin, J., Stow, D., Miller, J., Woodcock, C., Roberts, D., 2008. Mapping land-cover modifications over large areas: A comparison of machine learning algorithms. Remote Sensing of Environment 112 (5), 2272–2283.

Rouget, M., 2003. Measuring conservation value at fine and broad scales: implications for a diverse and fragmented region, the agulhas plain. Biological Conservation 112 (1), 217–232.

Rouget, M., Cowling, R., Vlok, J., Thompson, M., Balmford, A., 2006. Getting the biodiversity intactness index right: the importance of habitat degradation data. Global Change Biology 12 (11), 2032–2036.

Roy, P., Tomar, S., 2000. Biodiversity characterization at landscape level using geospatial modelling technique. Biological conservation 95 (1), 95–109.

Sabins, F. F., 2007. Remote sensing: principles and applications. Waveland Press.

Sarmiento, G., Monasterio, M., 1983. Life forms and phenology. Ecosystems of the World 13, 79–108.

Sawaya, K. E., Olmanson, L. G., Heinert, N. J., Brezonik, P. L., Bauer, M. E., 2003. Extending satellite remote sensing to local scales: land and water resource monitoring using high-resolution imagery. Remote sensing of Environment 88 (1), 144–156.

Scheffe, H., 1959. The analysis of variance.

Schmeller, D. S., 2008. European species and habitat monitoring: where are we now? Biodiversity and Conservation 17 (14), 3321–3326.

Schmidt, K. S., Skidmore, A. K., Apr. 2003. Spectral discrimination of vegetation types in a coastal wetland. Remote Sensing of Environment 85 (1), 92–108.

Schmidtlein, S., Sassin, J., 2004. Mapping of continuous floristic gradients in grasslands using hyperspectral imagery. Remote Sensing of Environment 92 (1), 126–138.

Schneider, A., 2012. Monitoring land cover change in urban and peri-urban areas using dense time stacks of landsat satellite data and a data mining approach. Remote Sensing of Environment 124, 689–704.

scikit learn.org, 2016. scikit-learn website.

Seher, J. S., Tueller, P. T., 1973. Color aerial photos for marshland. Photogrammetric Engineering 9 (5).

Serra, P., Pons, X., Sauri, D., 2003. Post-classification change detection with data from different sensors: some accuracy considerations. International Journal of Remote Sensing 24 (16), 3311–3340.

Serrano, L., Ustin, S. L., Roberts, D. A., Gamon, J. A., Penuelas, J., 2000. Deriving water content of chaparral vegetation from aviris data. Remote Sensing of Environment 74 (3), 570–581.

Sesnie, S. E., Gessler, P. E., Finegan, B., Thessler, S., 2008. Integrating landsat tm and srtm-dem derived variables with decision trees for habitat classification and change detection in complex neotropical environments. Remote Sensing of Environment 112 (5), 2145–2159.

Seto, K. C., Liu, W., 2003. Comparing artmap neural network with the maximum-likelihood classifier for detecting urban change. Photogrammetric Engineering & Remote Sensing 69 (9), 981–990.

Shanmugam, S., Barnsley, M., 2002. Quantifying landscape-ecological succession in a coastal dune system using sequential aerial photography and GIS. Journal of Coastal Conservation 8 (1), 61–68.

Shanmugam, S., Lucas, N., Phipps, P., Richards, A., Barnsley, M., 2003. Assessment of remote sensing techniques for habitat mapping in coastal dune ecosystems. Journal of Coastal Research, 64–75.

Shima, L. J., Anderson, R. R., Carter, V. P., 1976. The use of aerial color infrared photography in mapping the vegetation of a freshwater marsh. Chesapeake Science 17 (2), 74–85.

Shrestha, D. P., Zinck, J. A., 2001. Land use classification in mountainous areas: integration of image processing, digital elevation data and field knowledge (application to nepal). International Journal of Applied Earth Observation and Geoinformation 3 (1), 78–85.

Shupe, S. M., Marsh, S. E., 2004. Cover-and density-based vegetation classifications of the sonoran desert using landsat tm and ers-1 sar imagery. Remote Sensing of Environment 93 (1), 131–149.

Siegert, F., Ruecker, G., Hinrichs, A., Hoffmann, A., 2001. Increased damage from fires in logged forests during droughts caused by el nino. Nature 414 (6862), 437–440.

Sims, D. A., Gamon, J. A., 2002. Relationships between leaf pigment content and spectral reflectance across a wide range of species, leaf structures and developmental stages. Remote Sensing of Environment 81 (2), 337–354.

Sims, D. A., Gamon, J. A., Apr. 2003. Estimation of vegetation water content and photosynthetic tissue area from spectral reflectance: a comparison of indices based on liquid water and chlorophyll absorption features. Remote Sensing of Environment 84 (4), 526–537.

Singh, A., 1989. Review article digital change detection techniques using remotely-sensed data. International Journal of Remote Sensing 10 (6), 989–1003.

Skånes, H., Mäki, A.-H., Andersson, A., 2007. Flygbildstolkningsmanual för basinventeringen natura 2000 version 7.1.

Sluiter, R., Pebesma, E., 2010. Comparing techniques for vegetation classification using multi-and hyperspectral images and ancillary environmental data. International Journal of Remote Sensing 31 (23), 6143–6161.

Smith, G. M., 2014. Land use & land cover mapping in europe: Examples from the uk. In: Land Use and Land Cover Mapping in Europe. Springer, pp. 273–282.

Somers, B., Asner, G. P., Tits, L., Coppin, P., 2011. Endmember variability in spectral mixture analysis: A review. Remote Sensing of Environment 115 (7), 1603–1616.

Somodi, I., Čarni, A., Ribeiro, D., Podobnikar, T., 2012. Recognition of the invasive species robinia pseudacacia from combined remote sensing and gis sources. Biological Conservation 150 (1), 59–67.

Souza, C., Firestone, L., Silva, L. M., Roberts, D., 2003. Mapping forest degradation in

the eastern amazon from spot 4 through spectral mixture models. Remote Sensing of Environment 87 (4), 494–506.

Stamp, L. D., 1934. Land utilization survey of britain. Geographical Review 24 (4), 646–650.

Stanners, D., Bourdeau, P., European Environment Agency, 1995. Europe's environment: the Dobrís assessment.

Statutory Instrument 2716, 1994. The conservation (natural habitats) regulations 1994.

Steele, B. M., 2000. Combining multiple classifiers: An application using spatial and remotely sensed information for land cover type mapping. Remote sensing of environment 74 (3), 545–556.

Steers, J. A., 1946. The Coastline of England and Wales. Cambridge University Press.

Stevens, J., Blackstock, T., Howe, E., Stevens, D., 2004. Repeatability of phase 1 habitat survey. Journal of Environmental Management 73 (1), 53–59.

Stone, T. A., Schlesinger, P., Houghton, R. A., Woodwell, G. M., 1994. A map of the vegetation of south america based on satellite imagery. Photogrammetric Engineering and Remote Sensing 60 (5), 541–551.

Strittholt, J., Steininger, M., Loucks, C., White, B., Wilkie, M. L., Guariguata, M., 2007. Trends in selected biomes, habitats, and ecosystems: forests. In: Sourcebook on Remote Sensing and Biodiversity Indicators. Secretariat of the Convention on Biological Diversity, Montreal Technical Series. Vol. 32. pp. 35–63.

Tao, C. V., Hu, Y., Dec. 2001. A comprehensive study of the rational function model for photogrammetric processing. Photogrammetric Engineering and Remote Sensing 67 (12), 1347–1357.

Taylor Jr, F. G., 1974. Phenodynamics of production in a mesic deciduous forest. In: Phenology and seasonality modeling. Springer, pp. 237–254.

Tewkesbury, A. P., Comber, A. J., Tate, N. J., Lamb, A., Fisher, P. F., 2015. A critical synthesis of remotely sensed optical image change detection techniques. Remote Sensing of Environment 160, 1–14.

Thackrah, G., Rhind, P., Hurford, C., Barnsley, M., 2004. Using earth observation data

from multiple sources to map rare habitats in a coastal conservation area. Journal of Coastal Conservation 10 (1), 53–64.

Théau, J., Peddle, D., Duguay, C., 2005. Mapping lichen in a caribou habitat of northern quebec, canada, using an enhancement_classification method and spectral mixture analysis. Remote Sensing of Environment 94 (2), 232–243.

Thenkabail, P. S., Enclona, E. A., Ashton, M. S., Van Der Meer, B., 2004. Accuracy assessments of hyperspectral waveband performance for vegetation analysis applications. Remote Sensing of Environment 91 (3), 354–376.

Thomas, N. M., 2016. Mapping and monitoring mangrove forest baselines across the globe. Ph.D. thesis, Aberystwyth University.

Tiku, M. L., 1971. Power function of the f-test under non-normal situations. Journal of the American Statistical Association 66 (336), 913–916.

Todd, S. W., Hoffer, R. M., 1998. Responses of spectral indices to variations in vegetation cover and soil background. Photogrammetric Engineering and Remote Sensing 64, 915–922.

Tomaselli, V., Dimopoulos, P., Marangi, C., Kallimanis, A. S., Adamo, M., Tarantino, C., Panitsa, M., Terzi, M., Veronico, G., Lovergine, F., 2013. Translating land cover/land use classifications to habitat taxonomies for landscape monitoring: a Mediterranean assessment. Landscape Ecology 28 (5), 905–930.

Tong, C., Wu, J., Yong, S.-p., Yang, J., Yong, W., 2004. A landscape-scale assessment of steppe degradation in the xilin river basin, inner mongolia, china. Journal of Arid Environments 59 (1), 133–149.

Torres, J., Brito, J., Vasconcelos, M., Catarino, L., Gonçalves, J., Honrado, J., 2010. Ensemble models of habitat suitability relate chimpanzee (pan troglodytes) conservation to forest and landscape dynamics in western africa. Biological Conservation 143 (2), 416–425.

Toutin, T., 2004. Review article: Geometric processing of remote sensing images: models, algorithms and methods. International Journal of Remote Sensing 25 (10), 1893–1924.

Townsend, A. R., Asner, G. P., Cleveland, C. C., 2008. The biogeochemical heterogeneity of tropical forests. Trends in Ecology & Evolution 23 (8), 424–431.

Townshend, J. R., 1994. Global data sets for land applications from the advanced very

high resolution radiometer: an introduction. International Journal of Remote Sensing 15 (17), 3319–3332.

Treuhaft, R. N., Law, B. E., Asner, G. P., 2004. Forest attributes from radar interferometric structure and its fusion with optical remote sensing. BioScience 54 (6), 561–571.

Trullén, V. S., Alonso, J. L. B., 2007. Mapa de hábitats de aragón: la cartografía de hábitats corine como herramienta para la gestión de la biodiversidad y de los espacios naturales protegidos.

Tso, B., Olsen, R. C., 2005. Combining spectral and spatial information into hidden markov models for unsupervised image classification. International Journal of Remote Sensing 26 (10), 2113–2133.

Turner, W., 2014. Sensing biodiversity. Science 346 (6207), 301–302.

Turner, W., Rondinini, C., Pettorelli, N., Mora, B., Leidner, A. K., Szantoi, Z., Buchanan, G., Dech, S., Dwyer, J., Herold, M., et al., 2015. Free and open-access satellite data are key to biodiversity conservation. Biological Conservation 182, 173–176.

Turner, W., Spector, S., Gardiner, N., Fladeland, M., Sterling, E., Steininger, M., Jun. 2003. Remote Sensing for Biodiversity Science and Conservation. Trends in Ecology & Evolution 18 (6), 306–314.

UK Parliament, 1981. Parliament: Wildlife and Countryside Act 1981. URL: http://www.legislation.gov.uk/ukpga/1981/69.

Underwood, E., Ustin, S., DiPietro, D., 2003. Mapping nonnative plants using hyperspectral imagery. Remote Sensing of Environment 86 (2), 150–161.

Unit, E. F., 1990. Handbook for phase 1 habitat survey- a technique for environmental audit. JNCC, Peterborough.

United Nations, 1992. United Nations: 'Convention on biological diversity'. URL: http://www.cbd.int.

Updike, T., Comp, C., 2010. Radiometric Use of WorldView-2 Imagery. Technical Note, 1–17.

USGS, 2016. USGS Landsat Missions. URL: https://www.usgs.gov/.

Vahtmäe, E., Kutser, T., Martin, G., Kotta, J., 2006. Feasibility of hyperspectral remote

sensing for mapping benthic macroalgal cover in turbid coastal watersa baltic sea case study. Remote Sensing of Environment 101 (3), 342–351.

Vapnik, V. N., Vapnik, V., 1998. Statistical learning theory. Vol. 1. Wiley New York.

Varela, R. D., Rego, P. R., Iglesias, S. C., Sobrino, C. M., 2008. Automatic habitat classification methods based on satellite images: A practical assessment in the nw iberia coastal mountains. Environmental Monitoring and Assessment 144 (1-3), 229–250.

Vauhkonen, J., Korpela, I., Maltamo, M., Tokola, T., 2010. Imputation of single-tree attributes using airborne laser scanning-based height, intensity, and alpha shape metrics. Remote Sensing of Environment 114 (6), 1263–1276.

Verburg, P. H., Neumann, K., Nol, L., 2011. Challenges in using land use and land cover data for global change studies. Global Change Biology 17 (2), 974–989.

Vermote, E., Saleous, N., 2007. Ledaps surface reflectance product description. College Park: University of Maryland.

Vermote, E. F., Tanré, D., Deuze, J. L., Herman, M., Morcette, J.-J., 1997. Second simulation of the satellite signal in the solar spectrum, 6s: An overview. IEEE transactions on geoscience and remote sensing 35 (3), 675–686.

Wang, C., Menenti, M., Stoll, M.-P., Belluco, E., Marani, M., 2007a. Mapping mixed vegetation communities in salt marshes using airborne spectral data. Remote Sensing of Environment 107 (4), 559–570.

Wang, F.-M., Huang, J.-F., Tang, Y.-L., Wang, X.-Z., 2007b. New vegetation index and its application in estimating leaf area index of rice. Rice Science 14 (3), 195–203.

Wang, Q., Tenhunen, J. D., 2004. Vegetation mapping with multitemporal ndvi in north eastern china transect (nect). International Journal of Applied Earth Observation and Geoinformation 6 (1), 17–31.

Ward, R., Burnside, N., Joyce, C., Sepp, K., 2013. The use of medium point density lidar data in determining the coverage of plant community types in internationally important baltic seashore indicators. Ecological Indicators 33, 96–104.

Warner, T. A., Almutairi, A., Lee, J. Y., 2009. Remote sensing and land cover change. SAGE: London, UK.

Waser, L., Baltsavias, E., Ecker, K., Eisenbeiss, H., Feldmeyer-Christe, E., Ginzler, C.,

Küchler, M., Zhang, L., 2008. Assessing changes of forest area and shrub encroachment in a mire ecosystem using digital surface models and cir aerial images. Remote Sensing of Environment 112 (5), 1956–1968.

Waske, B., Braun, M., 2009. Classifier ensembles for land cover mapping using multitemporal sar imagery. ISPRS Journal of Photogrammetry and Remote Sensing 64 (5), 450–457.

Webb, A. R., 2003. Statistical pattern recognition. John Wiley & Sons.

Webb, H., Pye, K., Huckle, J., Blott, S., 2010. Beach topographic variability in relation to significant biological.

Weiers, S., Bock, M., Wissen, M., Rossner, G., 2004. Mapping and indicator approaches for the assessment of habitats at different scales using remote sensing and gis methods. Landscape and Urban Planning 67 (1), 43–65.

Williams, A., Davies, P., 2001. Coastal dunes of wales; vulnerability and protection. Journal of Coastal Conservation 7 (2), 145–154.

Williams, J., 2006. Common standards monitoring for designated sites: first six year report. JNCC Peterborough.

Wilson, M., Henderson-Sellers, A., 1985. A global archive of land cover and soils data for use in general circulation climate models. Journal of Climatology 5 (2), 119–143.

Wu, C., Niu, Z., Tang, Q., Huang, W., Rivard, B., Feng, J., 2009. Remote estimation of gross primary production in wheat using chlorophyll-related vegetation indices. Agricultural and Forest Meteorology 149 (6), 1015–1021.

Wulder, M. A., Hall, R. J., Coops, N. C., Franklin, S. E., 2004. High spatial resolution remotely sensed data for ecosystem characterization. BioScience 54 (6), 511–521.

Wulder, M. A., Masek, J. G., Cohen, W. B., Loveland, T. R., Woodcock, C. E., 2012. Opening the archive: How free data has enabled the science and monitoring promise of landsat. Remote Sensing of Environment 122, 2–10.

Xian, G., Homer, C., 2010. Updating the 2001 national land cover database impervious surface products to 2006 using landsat imagery change detection methods. Remote Sensing of Environment 114 (8), 1676–1686.

Xie, Y., Sha, Z., Yu, M., Apr. 2008. Remote sensing imagery in vegetation mapping: a review. Journal of Plant Ecology 1 (1), 9–23.

Yang, C., Everitt, J. H., Bradford, J. M., Murden, D., 2004. Airborne hyperspectral imagery and yield monitor data for mapping cotton yield variability. Precision Agriculture 5 (5), 445–461.

Yang, X., 2007. Integrated use of remote sensing and geographic information systems in riparian vegetation delineation and mapping. International Journal of Remote Sensing 28 (2), 353–370.

Zak, M. R., Cabido, M., 2002. Spatial patterns of the chaco vegetation of central argentina: Integration of remote sensing and phytosociology. Applied Vegetation Science 5 (2), 213–226.

Zarco-Tejada, P. J., Miller, J. R., Noland, T. L., Mohammed, G. H., Sampson, P. H., 2001. Scaling-up and model inversion methods with narrowband optical indices for chlorophyll content estimation in closed forest canopies with hyperspectral data. IEEE Transactions on Geoscience and Remote Sensing 39 (7), 1491–1507.

Zhang, Y., Chen, J. M., Miller, J. R., Noland, T. L., 2008. Leaf chlorophyll content retrieval from airborne hyperspectral remote sensing imagery. Remote Sensing of Environment 112 (7), 3234–3247.

Zharikov, Y., Skilleter, G. A., Loneragan, N. R., Taranto, T., Cameron, B. E., Sep. 2005. Mapping and characterising subtropical estuarine landscapes using aerial photography and GIS for potential application in wildlife conservation and management. Biological Conservation 125 (1), 87–100.

Zhu, Z., Woodcock, C. E., Rogan, J., Kellndorfer, J., 2012. Assessment of spectral, polarimetric, temporal, and spatial dimensions for urban and peri-urban land cover classification using landsat and sar data. Remote Sensing of Environment 117, 72–82.